The development of novel aptamers for the detection of T-2 and HT-2 mycotoxins

Sara Ioana Lock

Doctor of Philosophy

Newcastle University

Faculty of Science, Agriculture and Engineering

July 2022

Abstract

Contamination of food and feed with fungal secondary metabolites, such as the mycotoxins T-2 and HT-2 produced by *Fusarium* spp., poses a significant risk to human and animal health. Rapid and portable detection methods based on the use of biomolecules such as aptamers are highly desirable to ensure food safety. The aim of this study was to develop novel DNA aptamers with specificity for the low molecular weight mycotoxins, T-2 and HT-2. A combination of three experimental approaches were evaluated to achieve this aim. First, selection of aptamers through a modified Capture SELEX protocol using lambda exonuclease for digestion of dsDNA to ssDNA following PCR amplification. Second, application of high throughput sequencing (HTS) for the characterisation of aptamer candidates. Third, assessment of aptamer binding through colorimetric gold nanoparticle (AuNPs) aggregation assays.

Improved ssDNA recovery (>55%) suitable for use in subsequent selection rounds significantly reduced Capture SELEX process time. HTS analysis within the T-2 and HT-2 selections successfully enabled identification of unique sequences as aptamer candidates. Six novel aptamers (three from the T-2 and three from the HT-2 selection rounds), originating from different selection rounds, were obtained. Two of these aptamers were cross-selected between the targets.

Six aptamers (Apta20-01, Apta20-02, Apta20-04, Apta20-57, Apta20-90 and Apta20-100) were found to specifically bind to both targets over a range of concentrations T-2 (0.2µM to 214.3µM) and HT-2 (0.2µM to 235.5 µM), with Apta20-01, Apta20-57 and Apta20-100 showing best performance. Apta20-90 selected from Capture SELEX selection round 1 also demonstrated good performance. Although minimal cross reactivity with non-target mycotoxins (aflatoxin B1 and DON) was observed, the assay proved unsuitable for detection of T-2 and HT-2 in extract derived from one oat sample.

Overall, aptamers with target specificity were obtained significantly more rapidly than previously reported Capture SELEX protocols. The protocol has the potential to be applied successfully to other small molecule targets.

Dedication

To Mum and Dad

Acknowledgements

To paraphrase Gandalf the Grey : ''A PhD does never arrive late, nor does it arrive early, it arrives precisely when it means to.''

Table of Contents

List of Figures

List of Tables

Abbreviations

∞	Infinity
AuNPs	Gold nanoparticles
DNA	Deoxynucleic acid
DON	Deoxynivalenol
dsDNA	Double stranded deoxynucleic acid
EDTA	Ethylenediaminetetraacetic acid
HT-2	Hydroxy trichothecene-2 toxin
HTS	High throughput sequencing
MgCl	Magnesium chloride
NaCl	Sodium chloride
PAGE	Polyacrylamide gel electrophoresis
PCR	Polymerase chain reaction
qPCR	Quantitative polymerase chain reaction
RNA	Ribonucleic acid
ssDNA	Single stranded deoxynucleic acid
T-2	Trichothecene toxin
Tris	Tris(hydroxymethyl)aminomethane
Tris-HCl	Tris(hydroxymethyl)aminomethane hydrochloride

Glossary

Amplicon	Oligonucleotide sequence resulting from PCR amplification
Apta20-xxxx	Label name for a unique aptamer sequence formed using Apta (short for aptamer), 20 (reference to the decade), xxxx (sequential number allocated to label)
Disqualified	Unique oligonucleotide sequence not matching acceptance criteria
Frequency	Rate at which a unique oligonucleotide sequence occurs within a Capture SELEX round or number of reads
Replicate	Capture SELEX protocol of 3 samples per target toxin carried through all the rounds
Sequence Similarity	Sameness of nucleotides at a position within a unique sequence compared to other unique sequences
Total Frequency	Total proportion of a unique sequence found in a sequencing run on the MiSeq, per sample.
Unique Sequence	Oligonucleotide sequence with unique combination of nucleotides across the length of the sequence, labelled as Apta20-xxxx. For consideration as a possible aptamer candidate.

Chapter 1. Introduction

The Earth's population has been steadily increasing in recent years, widely reported as having increasingly negative impacts. Current predictions estimate that the world's human population will rise to 11.2 billion by 2050, requiring an estimated increase in food production of 70%, (Crist, Mora and Engelman, 2017). Additionally, climate change poses many challenges, particularly for the food industry; from farm to fork. The combination of growing populations and pressures on the environment through climate change require increased focus on producing safe food, (Crist, Mora and Engelman, 2017).

It is the responsibility of all parties involved in the food chain to ensure food is safe for consumption. Food safety can be compromised in many ways, of which the four major categories are: biological, physical, chemical and allergenic European Commission (2000). Biological contaminants requiring control are bacteria, viruses, fungi and parasites. Within the group of biological hazards mycotoxin producing fungal organisms are an increasing threat to food and feed commodities. Whilst the fungal organism (mould) is considered a biological hazard, the produced mycotoxins are classed as a chemical hazard. In a recent study by Xia *et al.* (2020), the estimated economic losses due to mycotoxin contamination were around two billion United States Dollars *per annum*. Mycotoxin contamination of food products from farm to fork are of concern as they occur in different agricultural products in varying amounts, (Ekwomadu, Akinola and Mwanza, 2021). The toxin contamination can result in concentrated, localised and inhomogeneous distribution which has the potential to spoil entire batches of agricultural products and their occurrence being almost unavoidable depending on climatic conditions, (Rivas Casado *et al.*, 2009). The most toxic and prevalent mycotoxins are those belonging to the *Fusarium* family (trichothecenes, fumonisins, and zearalenone) and have been linked to multiple human and animal diseases, (Ekwomadu, Akinola and Mwanza, 2021).

Based on the risk posed by mycotoxins, these compounds were chosen as targets and focus of this thesis.

1.1 Trichothecenes Mycotoxins

In the latest report by the RASFF in 2020, 400 incidents of mycotoxin contamination were reported. Although the reported incidence was lower than the occurrence of contamination by pathogenic organisms and pesticide residues, the risk posed by mycotoxins remains considerable, (RASFF, 2021).

Mycotoxins are secondary metabolites produced by *Penicillium*, *Fusarium* and *Aspergillus* species. The most frequently reported mycotoxins found are trichothecenes (T-2, HT-2 and deoxynivalenol), zearalenone and fumonisins B1 and B2 Marin *et al.* (2013) and Ekwomadu, Akinola and Mwanza (2021). The trichothecenes producing fungal organism *Fusarium*, infects predominately wheat and maize crops during their growth. An infection in wheat plants leads to Fusarium Head Blight disease of the plants, causing T-2 and HT-2 accumulation within the kernels, (Morettli, 2019). Fusarium infections on maize crop leads to Gibberella ear rot directly infecting the kernels and causing mycotoxin accumulation, (Dinolfo, 2022).
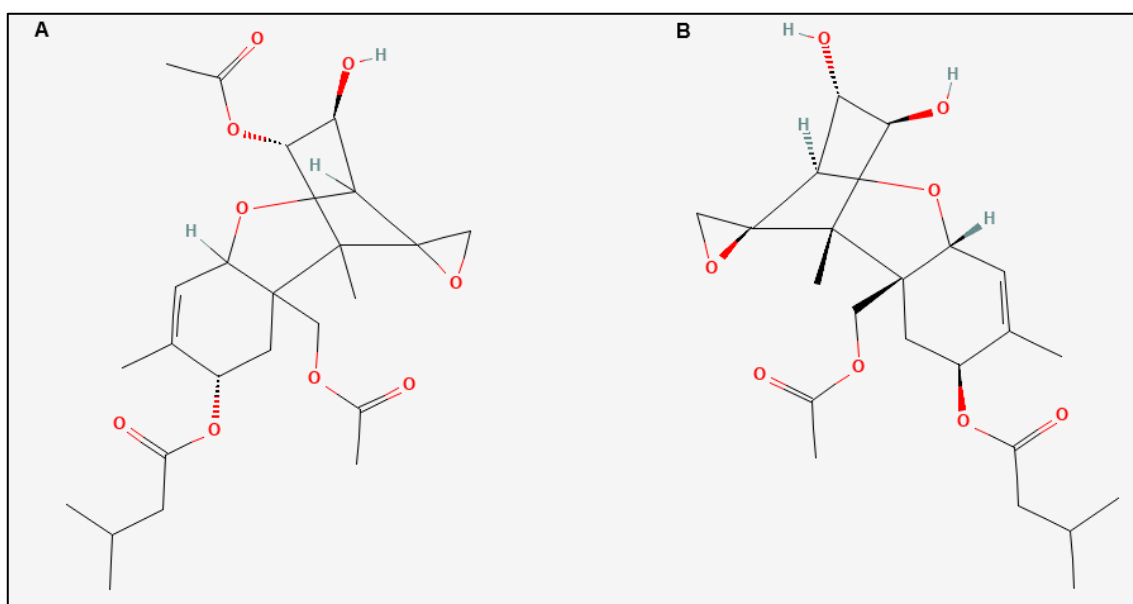
Figure 1 Molecular 2D structures displaying both T-2 (A) and HT-2 (B) molecules retrieved from (PubChem, 2022a; PubChem, 2022b)

Mycotoxin monitoring programs have been established in all Member States of the EU and large data sets allow a realistic assessment of human and animal exposure and accompanying health risk, as evidenced by recent surveys conducted in Europe and other countries, (Fink-Gremmels and van der Merwe, 2019).

The above Figure 1 shows the molecular structures of the type A Trichothecenes T-2 mycotoxin (**A**) and HT-2 mycotoxin (**B**) highlighting the structural similarity in the core structure of the 9-ene (EPT), (Ji *et al.*, 2019).

The T-2 toxin, full chemical name 3-hydroxy-4-15-diacetoxy-8ct-(3-methyl butyryloxy) 12,13 epoxytrichothec-9-ene, contains an epoxy trichothecene loop. HT-2 is a deacetylated form of T-2 and the principal metabolite of T-2. The toxicities of T-2 and HT-2 are similar, both contain the epoxy sesquiterpenoid moiety. Consequently, the toxicity of T-2 may be partly attributable to HT-2 for T-2 is rapidly metabolized to HT-2, (Ndossi *et al.*, 2012). *Fusarium langsethiae* is the major producer of T-2 and HT-2 followed by *Fusarium poae* and *Fusarium sporotrichioides.*T-2 and HT-2 contaminate many grains, such as maize, oat, barley, wheat, rice, and soybeans. Their optimal growth in crops for metabolic production is between 25-28°C with high humidity or water availability, Ji *et al.* (2019), Twarużek *et al.* (2021) and Patriarca and Fernández Pinto (2017).

T-2 toxins are agriculturally among the most important mycotoxins that present a potential hazard to health worldwide, due to the global occurrence of mycotoxigenic moulds, (Raj *et al.*, 2022). The T-2 mycotoxin is distinctive in that systemic toxicity can result from any route of exposure, i.e., dermal, oral, or respiratory, (Polak-Śliwińska and Paszczyk, 2021). Studies investigating mycotoxin contaminations found that T-2 and HT-2 contaminations continued to be high and demand robust and sensitive detection methods. Panasiuk *et al.* (2019) found that HT-2 occurred at a concentration of 43.2µg/kg compared to 5.90µg/kg of T-2 in maize silage samples collected from Poland.

An Italian study by Juan, Ritieni and Mañes (2013) investigating multi mycotoxin occurrence suggested that only 6.5% of samples were contaminated with HT-2 and 2% with T-2 in organic cereal samples in Italy.

As mentioned above, the changing climate impacts on food safety, with a study performed by Verheecke-Vaessen *et al.* (2019) demonstrating that higher temperatures experienced with climate change increase the growth of T-2 and HT-2 producing species and thereby elevating contaminations in oat crops.
The chemical nature of *Fusarium* spp. mycotoxins known as trichothecenes have been known since the 1990s. The trichothecene compounds are a structurally related group with the common 12,13-epoxytrichothec-9-ene ring system. Overall, 170 trichothecenes have been identified and classed into 4 types A-D and their classification depends on their variations in the functional hydroxyl and acetoxy group, type A includes T-2 and HT-2 toxins and Type B deoxynivalenol (DON), (Grove, 1993).

The biosynthesis of Type A which includes T-2 and HT-2 toxins starts with the cyclization of farnesyl pyrophosphate (FPP), which is the intermediate metabolite that forms trichodiene, (Hohn and Vanmiddlesworth, 1986; Hohn and Beremand, 1989). The product trichodiene further undergoes several oxygenations catalysed by cytochrome P450 monooxygenase. Oxygenations are carried out by four molecules of oxygen and two epoxides which form the intermediate isotrichotriol. Isotrichotriol further undergoes isomerization and cyclization forming isotrichodermol, which is possibly non-enzymatic. Isotrichodermol is converted by acetyltransferase encoded by the gene TRI101 to isotrichodermin, (Kimura *et al.*, 1998).

The biosynthesis pathway is illustrated in the Figure 2 below.
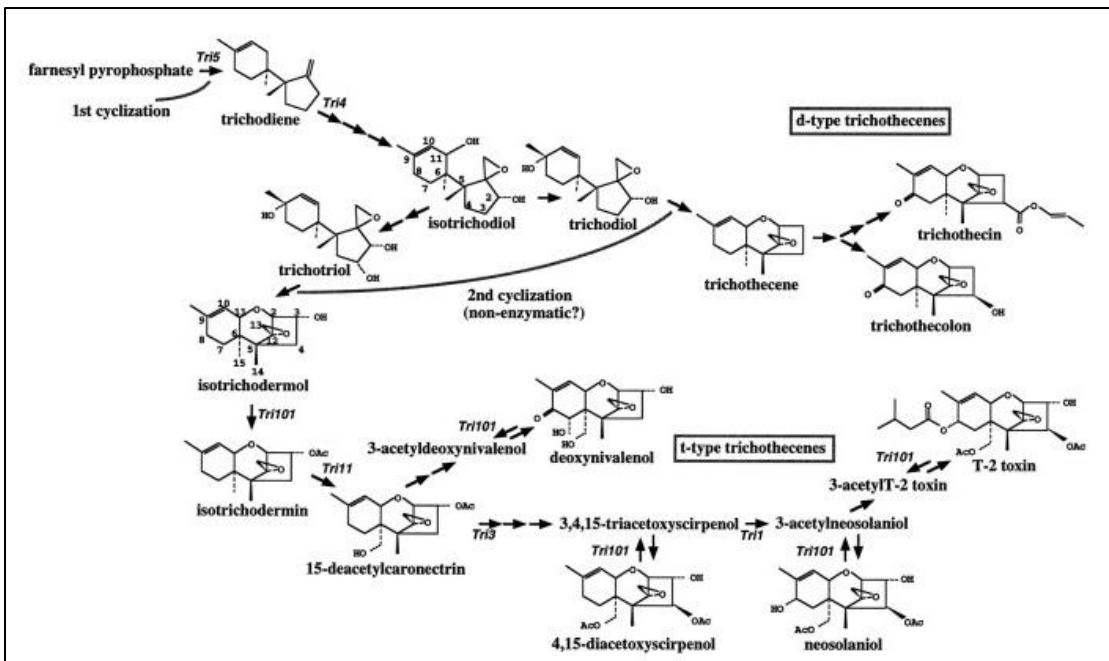
Figure 2 Illustration of the proposed trichothecene biosynthetic pathway, (Kimura et al., 1998)

Trichothecenes have been classified into simple and macrocyclic, type A, B and C are the simple forms and Type D macrocyclic. Investigations into the LD50 values conducted by Ueno (1984) showed an LD50 value for T-2 toxin for adult mice at 10.5mg/kg by mouth which was 10x greater than the toxicity of DON.

In more recent reviews, the toxicity of T-2 and HT-2 was evaluated highlighting the immunotoxic, neurotoxic and reproductive toxicity effects of the parent toxins and modified forms resulting through metabolism. The presence of T-2 within cells has been found to facilitate pathogenic infection through suppression of the immune response, (Wu *et al.*, 2020). T2 and HT-2 are most found to contaminate barley, maize, corn, rice, sorghum, wheat, oats, dried fruits, nuts, coffee, beer, spices, herbs and feed containing wheat, maize and corn. Due to the large variety of raw ingredients contaminated, food products utilising these materials consequently become contaminated with toxins as well, (Chen *et al.*, 2020).

1.2 Toxicity of trichothecenes Mycotoxins

The toxic effects of both mycotoxins have been established with T-2 inhibiting the synthesis of proteins, mitochondrial function, as well as having immunosuppressive and cytotoxic effects. Additionally, T-2 toxin has been reported to have extremely harmful effects on the skin and mucous membranes, (Schuhmacher-Wolz, Heine and Schneider, 2010). In contrast the toxicity of HT-2 has been less investigated, because T-2 is rapidly metabolised into HT-2 and therefore toxicity data is considered comparable, (Schuhmacher-Wolz, Heine and Schneider, 2010). Chronic exposure of T-2 toxin, HT-2 as well as DON can cause a disease known as alimentary toxic aleukia. Patients with this condition require extensive recovery time as it causes gastroenteritis and bronchial pneumonia. In extreme cases it can cause death, (Marin *et al.*, 2013).

In livestock T-2 toxin causes decreased feed intake and weight loss as well as oral lesions. In bovine species a decrease in milk production as well as gastroenteritis and intestinal bleeding have been observed. (Marin *et al.*, 2013)
As well as the toxicity from the original compound, modified mycotoxins need to be considered. Modified mycotoxins can be produced during food processing, through heating or cooking, (Freire and Sant'Ana, 2018). Modified T-2 toxins have shown a reduction in toxicity due to the increased capability to be excreted by the body. However further investigations into the metabolic fate of these compounds needs to be conducted in order to fully understand their toxic potential, (Freire and Sant'Ana, 2018).

Following a report from the European Food Standards Agency (EFSA), in 2011 results from 22 European Countries were analysed for both T-2 and HT-2 toxins,. The results obtained indicated that 65% of the samples had contamination levels below standard detection limits (15µg/kg) and within these quantifiable results most of the contamination was by HT-2. The highest concentrations were found in grain (wheat and maize) and grain milled products (flours, cornflakes and tortillas), (Stadler *et al.*, 2020). The toxins are not destroyed during processing. Steps such as cleaning, sorting, sieving and de-hulling results in a release of the

toxins from the kernels. It has been established that both mycotoxins can be reduced in level in commodities through thermal treatment (cooking, baking etc,). However, degradation products are formed, known as covalent adducts, these restructured mycotoxins may still have a high toxicity and require further research into reliable analytical methods for their detection (Stadler *et al.*, 2020).

It has been estimated that the dietary exposure for both HT-2 and T-2 toxins in adults (≥ 18 to < 65 years old) combined is 3.4 – 18 ng/kg per day for average onsumers (range representing the minimum lower bounds to maximum upper bounds of consumers from the different countries) of grain products and 7.2 – 39 ng/kg per day for high consumers (95th percentile consumers). The average intake in elderly populations (≥ 65 years old) was overall lower compared to adult populations and the toddler population (≥ 12 months to < 36 months old) exposure is estimated to be 12 – 43 ng/kg per day. These figures were calculated from the means from lower bound to upper bound contributions of the reported food groups. The tolerable daily intake limit for T-2 and HT-2 mycotoxins combined was set at 100 ng/kg/day, (EFSA, 2011).

The mycotoxins T-2 and HT-2 are the toxins focused on in this thesis as they have been identified as the most potent of the trichothecenes with an estimated tolerable daily intake for humans of 100 ng/kg body weight/day (Chain, 2011).

1.3 Health Impact of Mycotoxins

An updated report by the EFSA (2011) concluded that although there is a daily exposure of T-2 and HT-2 toxins in humans, the data obtained showed that overall exposure was below the tolerable daily intake of 100ng/kg. Therefore, it is considered unlikely to be an immediate health risk for humans independent of life stage. Investigations into dietary differences between populations have not sufficiently been analysed. Limited data is available on the exposure differences of vegetarians and vegans; however, it is presumed that the health risk is low as with the general population. Similarly, the animal health risk of consuming feedstuff containing T-2 and HT-2 toxins has been identified as low. This is

regarding animal species consumed by humans such as, beef cattle, pigs, poultry, rabbits and fish. For both pigs and poultry, the intake of toxins through grain products has been investigated and concluded that high intake levels pose a health risk, however levels are below limits (EFSA, 2011). Regarding companion animals such as dogs and cats, there is not enough research and data available to conclude if both toxins pose an immediate health risk. However, assumptions have been made for dogs based on the findings based for pigs. Similar assumptions have been made for horses as no data is currently available. The immediate health risk for horses has therefore also been concluded as low. (EFSA, 2014).

Due to their prevalence in a variety of food, ingestion is almost unavoidable and can have serious health effects when chronically exposed. This includes exposure through primary foods, for example maize and maize products as well as secondary contamination through milk produced by livestock, (Leite *et al.*, 2021).

1.4 Risk Impact of Mycotoxins

Climate is a key factor driving the occurrence of mycotoxin producing fungal organisms and thereby the contamination of mycotoxins in pre- and post-harvest crops, (Perrone *et al.*, 2020). Climate change may have different impacts on fungal organisms in their native regions with models predicting a rise in temperatures and reduced rain fall during winter and increased CO_2 atmospheric concentrations, (Pieczka *et al.*, 2018).

Mycotoxin producing fungal organisms have an increased higher likelihood of spreading and contaminating food products due to climate change and global trade. Climate change may trigger a change to crop growth regions resulting in non-native fungal organisms being introduced into the environment and spreading. The COVID-19 pandemic in combination with food supply problems may increase the occurrence of mycotoxins in food products due to the increased

storage times in higher temperature conditions in comparison to previous years, (Magyar *et al.*, 2021).

1.5 Mitigation Strategies

Comprehensive monitoring programs are essential when trying to assess the impact of climate change on agricultural processes and the resulting increase of known safety risks and emerging risks. With regards to mycotoxin contamination of crops, prevention is impossible, however the occurrence and contamination should be assessed and controlled to achieve acceptable levels through the use of effective management systems, (Tirado *et al.*, 2010).

Many management systems, including HACCP (Hazard Analysis and Critical Control points) have been established and used in conjunction with predictive climate change models investigating mycotoxin growth throughout the seasons and in various global regions. Despite extensive modelling and analysis, there is still a high degree of uncertainty surrounding the exact threat levels of mycotoxins for the key production areas in South America, Asia and Africa, (Medina *et al.*, 2017). Advances in predictive modelling techniques incorporating climate change models provide greater insight into regions which may experience increased contamination by fungal organisms and mycotoxins. The predictions support the effective control and management of food processing directly at time of plant growth and subsequent harvest, (Marín *et al.*, 2021). Mycotoxin control continues post-harvest, in storage, distribution and use of raw materials. As mentioned previously, the HACCP principles are a preventative management system focused on the control of and reduction of hazards to acceptable levels, through the implementation of corrective actions in conjunction with other pre-requisite programs, (Gehring and Kirkpatrick, 2020). Traditional control measures include sanitation processes, temperature and humidity controls, chemical additives to reduce pH levels and water activity as well as ventilation with CO_2 controls. These traditional measures may not be adequate to act as successful controls with the

increased pressures of higher yield requirements. Novel strategies which include crop condition control, plant bioengineering and nano-antifungal agents, (Fumagalli *et al.*, 2021).

1.6 Analytical Techniques for Detection of Mycotoxins

Established analytical techniques have been used for the detection of all mycotoxin species. This includes chromatographic techniques as well as antibody based techniques; such as ELISA (Enzyme-linked immunosorbent assay), Busman, Poling and Maragos (2011), De Angelis *et al.* (2013), Meneely *et al.* (2010a), Roseanu *et al.* (2010) and Meneely *et al.* (2011).

A great variety of instrumentations and methodologies are available to detect mycotoxins in food products which are either general screening or multi-targeted methods. The multi-targeted approach is most desirable due to the fast turnaround of results and application possibilities. Berthiller *et al.*, (2018) published a review on the development in the field of mycotoxin analysis, covering the past two years and providing a comprehensive overview of the various analytical methodologies available to detect mycotoxins in various food commodities. Most common chromatographic techniques require expensive equipment and trained laboratory personal to operate and interpret results. Liquid Chromatography – Mass Spectrometry (LC-MS) requires pre-cleaning of the target analyte, concentrating and suspending into a solvent prior to analysis. LC-MS allows for low concentration recovery as well as multiple target analysis in one sample, (Di Marco Pisciottano *et al.*, 2020). Most desirable are detection methods that do not require expensive equipment to analyse for contaminates.

Advances in sample clean-up techniques using nanomaterials have been developed and commercialised, simplifying the analysis of multiple mycotoxins *via* HPLC instrumentation, (Polak-Śliwińska and Paszczyk, 2021). The economical loss to food manufacturers and suppliers is substantial when considering the time required for sampling, analysis and reporting. A fast response is desirable to reduce the time of stock holding and subsequent release and therefore a need for analytical handheld devices which are cost-effective and fast are in growing demand. The use of nanotechnology has gained increasing interest for use in food safety protocols as they can also provide rapid, real-time and cost-effective methods to determine contaminants in food. Research needs to focus on incorporating some of the available technologies into commercial biosensors to produce portable and simple devices which can be used in situ, (Krishna *et al.*, 2018).

1.7 Biosensors

A biosensor is basically defined as an analytical device which consists of two parts, a molecular biologically relevant recognition element and a component that is capable of transferring a signal, (Navani and Li, 2006). Nanostructured biosensors may be developed and utilised at various stages in the food chain. At the pre-harvest stage they could be developed to support the monitoring of crop diseases and thereby contribute to smart agricultural practices, (Antonacci *et al.*, 2018). Biosensors can provide a fast, sensitive and efficient option for the on-site analysis of food products, avoiding the issues arising from traditional time consuming laboratory based methods which require trained personnel whom are able to use the expensive equipment required and interpret the resulting data, (Lv *et al.*, 2018). In commercially available biosensors; antibodies (monoclonal and polyclonal), are still considered the gold standard method of choice. The use of antibodies as a diagnostic tool have been investigated and frequently used since the 20th century. For a long period of time antibodies have been considered as a standard for molecular recognition, (Hock, 1997). Through the COVID-19 pandemic the use of biosensors gained refreshed traction described as quick and

accurate tool to detect the SARS-CoV-2 virus through antibody-antigen interactions, (Drobysh *et al.*, 2022).

Antibodies with specificity for food and environmental contaminants such as polyaromatic hydrocarbons, pesticides, dioxins, PCBs, bacteria and pathogens have been produced and form the basis of commercial immunoaffinity and immunoassay methods for contaminants and adulterants., (Birch and Racher, 2006; Kotsiri, Vidic and Vantarakis, 2022). Despite the utility of antibodies, there are clear moral and ethical reasons why alternative biomolecules are desirable. Antibodies are primarily prepared in animals, or in cell culture systems derived from the tissues of sacrificed animals, (Amaya-González *et al.*, 2013).The production of antibodies in large quantities requires immunization and purification techniques which are time consuming and can lead to batch to batch variation due to changes in temperature and pH, (Li *et al.*, 2021a). It can therefore be challenging to develop antibodies with specificity to small molecules such as mycotoxins, nonetheless antibodies specific to T-2 and HT-2 are commercially available and form the basis of many available antibody-based test kits, (Oplatowska-Stachowiak *et al.*, 2017). The origin of the methodology for the development of antibodies specific to small molecules was described by Köhler and Milstein (1975) in which monoclonal antibodies were raised through a fusion of mouse myeloma and spleen cells harvested from the immunised donor animal. Although the authors did not specifically describe the methodology dedicated to these mycotoxins, the methodology forms the basis of subsequent methodologies specifically describing antibodies raised against T-2 and HT-2 mycotoxins and their applications in assays, (Molinelli *et al.*, 2008; Meneely *et al.*, 2010b and Oplatowska-Stachowiak *et al.*, 2017). In the publication by Molinelli *et al.* (2008) the authors described the use of their produced antibodies in the development of a qualitative test strip based on gold nanoparticles capable of detecting T-2 mycotoxin, with minimal cross-reactivity to HT-2. The developed lateral flow biosensor device demonstrated suitability for rapid on-site sample analysis (what and oat foodstuff), producing results in 4min with minimal sample preparation required with a limit of detection of 100µg/kg.

A surface plasmon resonance (SPR) screening assay described by Meneely *et al.* (2010a) allowed for the detection of HT-2 mycotoxin in cereals and infant food. The described assay showed high cross-reactivity to T-2 and resulted in the determination of a limit of detection between 25µg/kg and 26 µg/kg depending on the commodity. The other applied use of the raised antibodies described by Oplatowska-Stachowiak *et al.* (2017) was an improved enzyme-linked immunosorbent assay (ELISA) capable of combined detection of T-2 and HT-2 in cereals and infant food. The ELISA was able to detect the mycotoxins in combination to the screening target concentrations between 12.5µg/kg and 7.5µg/kg depending on commodity being analysed. The main drawbacks on novel and established biosensors using antibody technologies are matrix interferences and antibody cross-reactivity. Thereby requiring validation against each food commodity being tested, (Janik *et al.*, 2021).

An alternative to antibodies, often referred to as artificial antibodies, are molecularly imprinted polymers (MIPs). MIPs are synthetic materials with the capability to be recognise target molecules, similar to antibodies, (Apetrei *et al.*, 2018). The synthetic materials are produced using a template molecule with a similar structure to the target molecule, a crosslinker, a functional monomer and an initiator through polymerisation techniques, (Apetrei *et al.*, 2018; Gómez-Caballero *et al.*, 2021). MIPs can be targeted and used in different polymerisations mechanisms and methods for the controlled adsorption or desorption of target analytes and active substances and therefore can provide a wide range of application possibilities, (Villa *et al.*, 2021). MIPs can be used within biosensors for contaminants, nutrients or trace substances in food samples, (Filipe-Ribeiro, Cosme and Nunes, 2020). However, the use of MIPs may be limited in the case of complex or highly processed food samples, (Ashley, Feng and Sun, 2018). A further limitation are the polymerisation temperatures at which MIPs are produced which is between 36°C and 42°C which makes biomacromolecules and microorganisms as synthesising bases challenging, (BelBruno, 2018). Additionally, the production of MIPs is expensive, requires specialised equipment and reagents and has a long processing time. Some MIPs

have been proposed based on food grade polymers which can lower the production cost, (Cao *et al.*, 2019). MIPs technologies have seen most advances recently in their application as biosensors for medical and forensic diagnostics as part of electrochemical and optical sensors. However commercially available diagnostic MIPs are not yet available on the market for routine use, (Ahmad *et al.*, 2019). One major drawback of MIPs are their unspecific interactions with small target molecules making their application to mycotoxin detection very complex. They require modification to non-imprinted polymers to overcome the nonspecific binding, resulting in limited application of MIPs to the detection of mycotoxins, (Li *et al.*, 2021b).

Short peptides, up to 50 amino acids, have also been reported to be used in biosensors. The peptides are formed through two methodologies, bacteriophage display cycle or combinatorial synthesis. Peptides developed through the phage display cycle method are incubated with phages and specific antigens to the target molecule. Following several cycles nonspecific phages are removed and only the specific peptides remain. The limitation to this method is the non-applicability to small molecules and the method has not yet been described with mycotoxin detection, (Wang *et al.*, 2022) Combinatorial synthesis was applied in the peptide biosensor targeting aflatoxin B1 mycotoxin described by Liu *et al.*, (2022a). The team constructed a library of aflatoxin B1 specific peptides through combination of key amino acids, amino acid mutations and molecular docking. The peptides were attached to porous gold nanoparticles bound to a glassy carbon electrode to form the sensor and trialled on contaminated cereal samples, achieving a LOD of 9.4×10^{-4}. The main drawbacks on novel and established biosensors using antibody technologies are matrix interferences and antibody cross-reactivity. Thereby requiring validation against each food commodity undergoing testing, (Janik *et al.*, 2021).

To summarise, a variety of biosensors based on antibodies, MIP or peptides are available in a variety of formats for specific target analysis purposes and can either be bought commercially and developed based on specific target and matrix needs, (Bonwick and Smith, 2004). Aptamer based bioassays (aptasensors) are an alternative to established biosensors and have shown to be a rapid and reliable technique for the detection of harmful substances, (Liu *et al.*, 2022c)

1.8 Aptamers

Aptamers are short strands of nucleic acids which are chemically produced molecular recognition tools, first described by Tuerk and Gold (1990), the first aptamer was developed for the pharmaceutical industry for therapeutic purposes, developed through an in vivo selection procedure reported through a SELEX protocol They are either DNA or RNA based, single stranded oligonucleotides, which link together by a hydrogen bond. The first aptamers described were initially synthetic RNA molecules developed specifically to bind to molecular targets, (Ellington and Szostak, 1990). They have the capability, like proteins, to fold themselves into intricate tertiary structures. This characteristic allows them to perform a large variety of functions, such as gene-regulation, catalytic activity and ligand-binding. Originally the functions of aptamers were discovered through investigations into non-coding ribonucleic acids, (Weigand and Suess, 2009). Aptamers have gained a lot of interest in recent years with the number of peer review publications increasing steadily as can be seen in Figure 3.
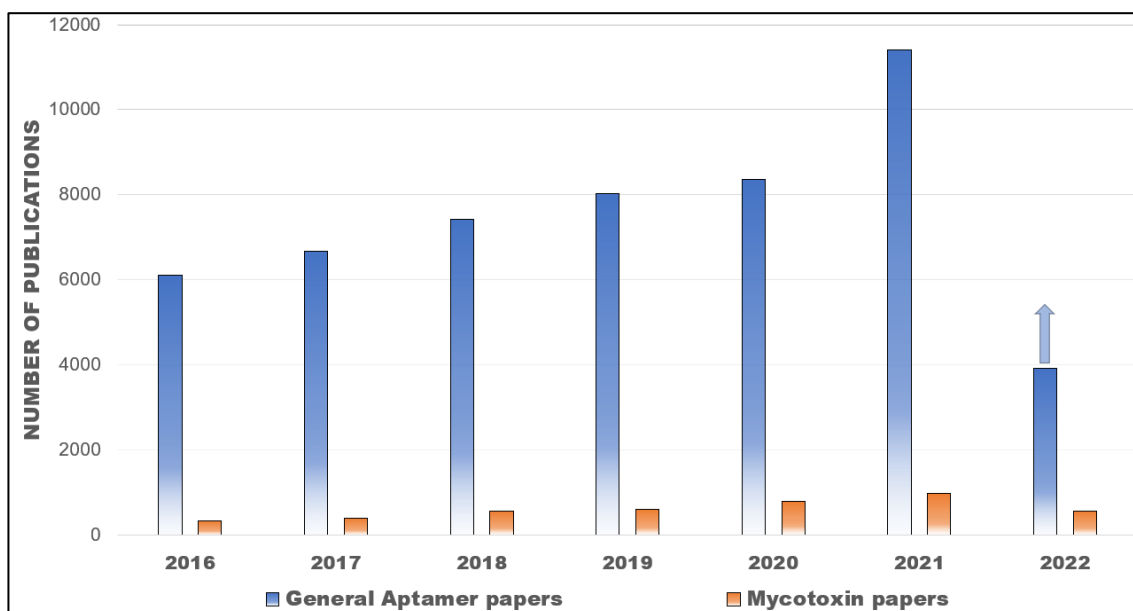
Figure 3 Overview of the number of publications comparing the general aptamer (blue) and mycotoxin papers (orange). Data retrieved from publications available on Google Scholar.

The overview of number of publications shown in the above figure 3 highlight the upward trend of aptamer related papers published from 2016 to March 2022, with an upwards trend expected throughout the year 2022. In comparison the published number relating to mycotoxins has remained relatively low across the reviewed time.

Aptamers have a range of advantages over the commonly used antibodies. Their cost of bulk production is considerably lower (selected sequences), they are smaller in size and can be synthesised to bind to almost all targets, including small molecules, which gives aptamers the ability to be used in a variety of sensor structures and not requiring cold storage when incorporated into assays. Like antibodies, aptamers have the capability to bind to a target molecule with high affinity, (Toh *et al.*, 2015).In addition, the development of aptamers does not require the immunisation of animals and purification techniques for synthesis, (Li *et al.*, 2021a).

Properties	Antibody	Aptamers
Synthesis	*In Vivo* selection through animal immunisation	*In Vitro* selection
	Selection process cannot be modified	Selection process modifiable and controllable
	Targets with non-immunogenic properties not applicable	Targets of any type applicable
	High production cost	Low production cost
	Batch to batch variation	Negligible batch to batch variation
Stability	Cold Storage essential	Ambient storage applicable
	Short shelf life	Long shelf life
	Highly susceptible to changes in pH, temperatures and ionic concentrations	Negligible susceptibility to changes in pH, temperatures and ionic concentrations
	Stability cannot be increased	Stability increased through chemical modifications
Modification, specificity and affinity	Comparable affinities	
	Comparable specificities	
	Modifications can lead to changes in binding affinities	Modifications can enhance binding affinity if desired
	Immobilisation challenging	Immobilisation easier
Structural changes	Upon binding no structural changes	Structural changes upon binding favouring sensitivity

Table 1 Comparison of aptamers to antibodies, based on summarisation table by Reid et al. (2020).

Aptamers are an excellent alternative to antibodies and have been selected as focus of the thesis, particularly as the adaptability of their synthesis method allows for the development of aptamers specific to small molecules such as mycotoxins T-2 and HT-2.

Aptamers remain largely used within research fields with 28% of peer reviewed publications on biosensors based on aptamer technologies published. However, commercial aptamer based analysis kits are not yet available, despite many commercial companies dedicated to the commercialisation of aptamers, (Villalonga, Pérez-Calabuig and Villalonga, 2020). Recently, a combined aptamer-antibody biosensor has been reported by (Gao *et al.*, 2022) for the detection of tumour necrosis factor alpha (TNFα), an indicator for cancer, Alzheimer's disease, rheumatoid arthritis and diabetic eye disease. The reported aptamer-antibody receptor had a limit of detection of 0.0625nM and demonstrates the application of cross application biosensors as analytical tools.

In addition to their use in biosensors, aptamers can be applied to Lateral Flow Assays and devices (LFA and LFD). This is of particular advantage for fast detection *in situ* in the food and diagnostic industry, as samples can be taken and screened quickly prior to waiting for a lengthy laboratory turnaround time, (Majdinasab, Badea and Marty, 2022). The chemical production of aptamers has further advantages as it reduces batch to batch variability and enhanced function (stability, affinity) due to aptamer modification. Aptamer based biosensors have shown to be more resistant to denaturation when compared to antibody based sensors and have a longer shelf life, (Tombelli, Minunni and Mascini, 2005). Prior to commencing aptamer development, consideration needs to be given to the selection of a DNA or RNA based aptamer. RNA aptamers in particular, have shown to undergo significant structural changes during the binding process which leads to nuclease sensitivity, impacting negatively on the binding affinity, (Famulok, Mayer and Blind, 2000).

Additionally, the development of RNA aptamers required additional steps with in the SELEX process allowing for reverse transcription PCR prior to amplification PCR, (Kang and Lee, 2013). DNA based aptamers were chosen as the structure for the aptamers in this thesis, due to their ease of use and applicability to small molecules.

1.9 SELEX protocol

Additionally, the SELEX protocols for the development of RNA based aptamers require additional steps to convert the RNA to DNA, through reverse transcriptase via bacteriophage transcriptase prior to PCR amplification, (Osborne and Ellington, 1997). The production of aptamers relies on a technique called Systematic Evolution of Ligands by Exponential Enrichment (SELEX). This technique became possible after the advances in polymerase chain reaction (PCR) techniques, which enabled the isolation of reverse transcriptase as well as the possibility of producing long strands of oligonucleotides comprising random nucleotide regions. The technique has since been developed further to include a variety of functions, (McKeague *et al.*, 2010).

The SELEX process starts with a large random library pool of oligonucleotides, DNA or RNA based, which is incubated with the target of selection. The oligonucleotides will fold around the target and unbound nucleotides are removed through buffer washing steps. The binding nucleotides are amplified through PCR and used as the basis pool for further selection rounds. This process is repeated, for as many selection rounds as necessary to achieve the required selectivity. The SELEX process of binding, separation, amplification and conditioning are repeated until an enriched pool of aptamers is achieved, (Komarova and Kuznetsov, 2019). It is of particular importance to understand the chemical nature of the nucleotides which form the aptamer. This is with reference to their possibilities of folding in 3D structures which have an impact on the stability and

degradation of the aptamer. In order to overcome possible aptamer instability, modification to the nucleotide bases as well as phosphodiester backbone can be made, (Sampson, 2003). Furthermore, the SELEX process relies on combinatorial chemistry techniques where the oligonucleotides randomly selected can be produced inexpensively and rapidly by the duplication of the natural 3'-5' linkages. Due to the complexity of the aptamer library during the selection and enrichment steps mutations of the oligonucleotides may occur, (Sampson, 2003). Choosing a SELEX protocol will also depend on the time and cost efficiencies of the protocol and required post-SELEX protocols supporting the aptamer selection. An ideal SELEX protocol does not yet exist hence the plethora of SELEX methodologies and variations, (Darmostuk *et al.*, 2015b). To select an appropriate SELEX protocol, it is of importance to understand the process and the variables within it.
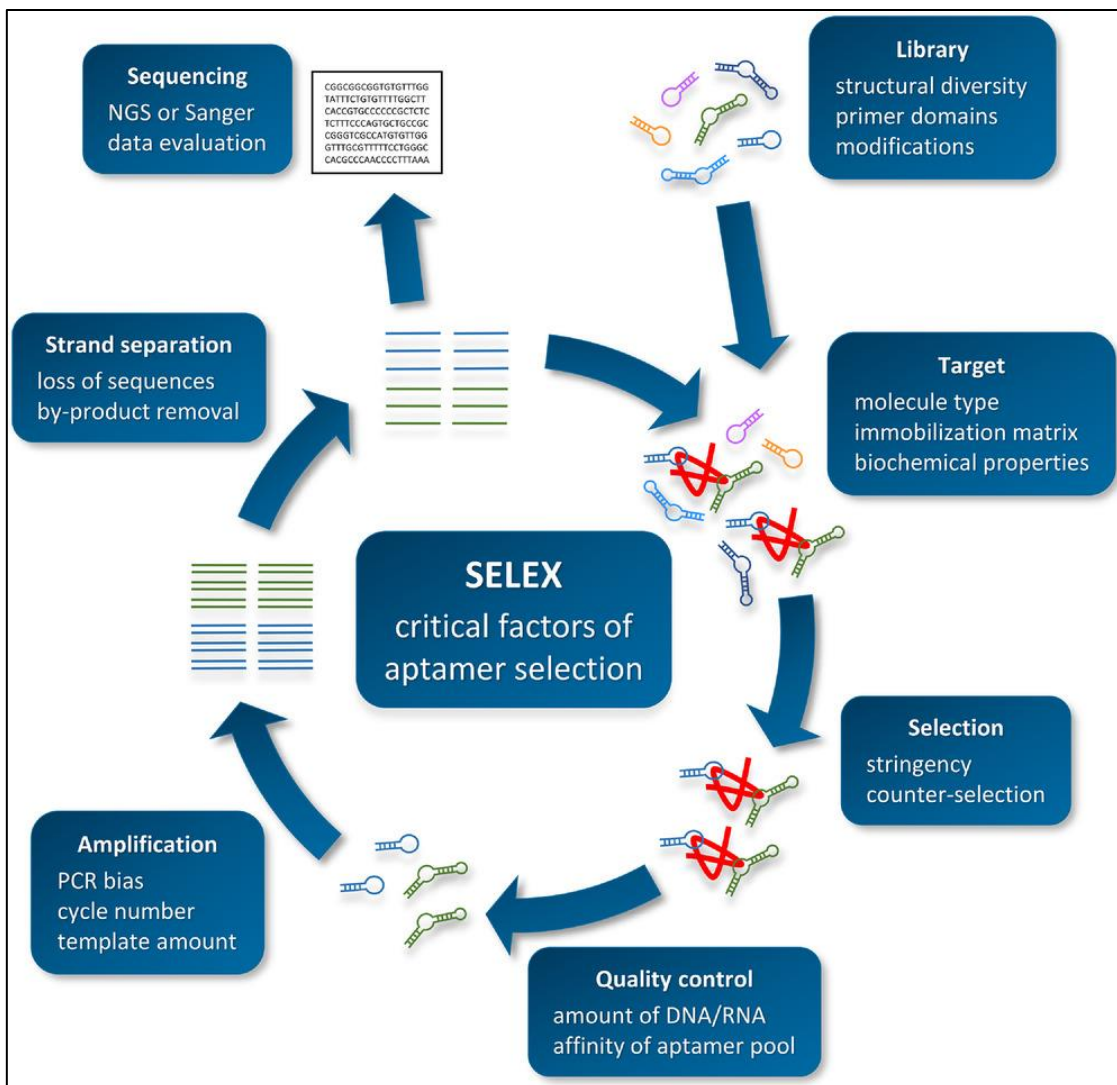
Figure 4 Schematic overview of the variables within a SELEX protocol,
(Kohlberger and Gadermaier, 2021)

Figure 4 published by Kohlberger and Gadermaier (2021) highlights the various important variables which occur with a SELEX protocol ranging from the selection of starting library, target, selection process and duration as well as subsequent sequence identifications. Considerations should be given to the oligonucleotide library, their length and diversity, modifications (for example fluorescence tags) as well as the length and structure of the primer sites. The target structure, chemical properties should be considered, and a selection process chosen accordingly: selection in solution or immobilised depending on likely oligonucleotide interactions and target conformations.

Of importance are the amplifications of the selected oligonucleotides and understanding of possible PCR bias when undergoing many SELEX rounds as well as methodology of recovering sequences post amplifications. The use of high throughput sequencing supports the evaluation of the selected sequences and provides information of sequence changes as well as aiding in the understanding of the selected aptamer pools.

1.10 SELEX protocols for small molecules

Several variations of SELEX have been developed, these modifications are either based on improving existing protocols or combination of existing strategies, (Stoltenburg, Nikolaus and Strehlitz, 2012a) (Sun and Zu, 2015). The correct initial selection of a SELEX model is important and requires an understanding of the final aptamer's use and the designated target, (Aquino-Jarquin and Toscano-Garibay, 2011). The key concept for the successful development of a specific aptamer lies in the adaptation of the SELEX method, (Toh *et al.*, 2015)

SELEX modifications allow for high sensitivity during the screening process as well as adapting to the target molecules. Selecting for small molecules comes with many challenges and may be the reason why the development of aptamers targeting these has been slowed. Even selecting the most appropriate SELEX method may not result in an aptamer with complete affinity, due to the difficulty of eliminating and separating non-target bound oligonucleotides, (McKeague and DeRosa, 2012).To overcome the problem encountered by small molecule detection several specific SELEX modifications and protocols have been suggested (Flumag / Capture or Structure-switching) and described. Small molecule detection poses particular issues due to the non-target binding and solutions require an immobilisation of target or oligonucleotide library, (Ruscito and DeRosa, 2016).

Flumag SELEX has been described by Stoltenburg, Reinemann and Strehlitz (2005) and basically involves the immobilisation of the target molecule, in this case streptavidin , to magnetic beads before the introduction of the oligonucleotide library. The proposed SELEX protocol was reported to produce aptamers with low binding affinity as the selection to the target occurs on a conjugate rather than the target alone, thereby increasing the probability of cross-reactivity.

A technique called Capture-SELEX or Structure-Switching SELEX has been described that is specific for small molecules, which does not rely on the immobilisation of the target and therefore reduces cross-reactivity probability, (Nutiu and Li, 2003). During Capture-SELEX the oligonucleotide library is immobilized instead of the target molecule. This allows for an efficient way of separating the target bound nucleotides and the non-bound nucleotides, (Stoltenburg, Nikolaus and Strehlitz, 2012a). Furthermore, the technique is described as highly flexible allowing for additional steps to be added to increase the specificity of the aptamer developed, (Stoltenburg, Nikolaus and Strehlitz, 2012b). The Capture-SELEX technique has been used in pharmaceutical development predominantly and has shown to produce a selective aptamer. However, further investigation of the technique is necessary to apply the protocol to targets of interest in food safety, (Stoltenburg, Nikolaus and Strehlitz, 2012a).

Traditionally, aptamers have been selected in the final round of the SELEX process through cloning and Sanger Sequencing technologies. This approach has several shortcomings as it only identifies sequences produced in the final stage and omits the full sequence information produced during the full SELEX process. Crucial sequences and possibly more adequate aptamer candidates may be missed through the traditional approach, (Sun and Zu, 2015).

Although the SELEX method is routinely used, it has been suggested that it can be difficult to identify the optimal sequences from the library pool of oligonucleotides and that possibly high-throughput sequencing for the screening of aptamers might be more suitable technique for the aptamer identification, (Cho *et al.*, 2010). High throughput sequencing has been proposed for the use in aptamer developments as the technologies allow for short reads of the oligonucleotides, (Goodwin, McPherson and McCombie, 2016). High throughput sequencing analysis is mainly performed through the Illumina, 454 Roche® and IonTorrent platforms® of which the Illumina sequencing platform is the most commonly used, (Sharma, Bruno and Dhiman, 2017). Spiga, Maietta and Guiducci (2015) utilised high throughput sequencing in combination with Capture SELEX and were able to identify aptamers with high affinity after 8 rounds of selection compared to the previously described 15 rounds. In recent years, high throughput sequencing technologies have become more affordable and widespread and can be applied efficiently to aptamer sequence screening prior to their binding affinity evaluation, (Ferreira *et al.*, 2021).

1.11 Aptasensors

Selected aptamers can be developed to act as biosensor, known as aptasensors, which is a combination of a sample or target, a biological recognition element and physical transducer to give a measurable outcome. The recognition element in the example of a biosensor must be selective towards the target analyte. Furthermore, the transducer is of importance as it creates a signal which is measurable in relation to the target analyte, (McKeague *et al.*, 2010). Aptamers based on DNA are more suited for applications into biosensors for environmental monitoring and therapy as they are more stable compared to RNA based aptamers as well as showing better specificity to small molecule targets. However RNA based aptamers have shown higher binding affinities due to their ability to fold in a variety of conformations not possible with DNA, (Hamula *et al.*, 2006).

A simple very rapid methodology exists for screening for aptamer affinity and aptasensor suitability on a large scale. An example is the HAPIscreen® method, which utilises AlphaScreen® technology produced by Perkin Elmer, (https://resources.perkinelmer.com/lab-solutions/resources/docs/APP_AlphaScreen_Principles.pdf). The technology is based on the conjugation of the designated target molecule and the selected aptamer through donor and acceptor microbeads. During the assay, the aptamer binds to the target and is detected through a fluorescence reader through the fluorescence signal produced by the microbeads, (Yasgar *et al.*, 2016). Another more complex screening method, requires the encapsulation of ssDNA into single agarose droplets using a flow-focusing microfluid device. Performing single-molecule emulsion PCR has resulted in monoclonal DNA in each agarose bead, which are subsequently detected through fluorescence staining and evaluated *via* flow cytometry, identifying the target binding ability of each bead, (Darmostuk *et al.*, 2015a). Aptamers have been applied to a variety of sensors and research fields.

Area of Research	Type of Sensor	Analytical performance	Target	Reference
Medical, Diagnostic	Electrochemical aptasensor based on two-dimensional nanocomposite of graphitic carbon nitride, nanosheets and MoS_2 quantum dots with chitosan stabilised gold nanoparticles	LOD 0.71 pgmL^{-1}	Prostate specific antigen	Duan *et al.* (2018)
Medical, Diagnostic	Label-free surface plasmon resonance aptasensor utilising thiol-modified niobium carbide MXene quantum dots	LOD 4.9 pgmL^{-1}	SARS-CoV-2	Chen *et al.* (2021)
Food, Adulteration	Single strand DNA utilising biotinylated reporter and streptavidin functionalised gold nanostars	LLOQ 1.0 nM	Donkey Meat	Mansouri *et al.* (2020)
Food, Food Safety	Biotin modified aptamer immobilised onto $ZnFe_2O_4$ reduced graphene oxide nanostructures	LOD 11 cfu/mL	*Salmonella enterica servar typhimurium*	Wu *et al.* (2017)
Food, Food Safety	Sandwich type aptamer based capillary colorimetric platform	LOD 10^3 cfu/mL	*Salmonella enteritidis*	Bayraç, Eyidoğan and Avni Öktem (2017)
Food, Food Safety	Nanoparticle based aptasensor based on fluorescence resonance energy transfer with black phosphorus sheets	LOD 0.028 ng/mL	Aflatoxin B1	Wu *et al.* (2021)
Food, Food Safety	Fluorescent turn-off aptasensor	LOD 2.7×10^2 cfu/mL	*Cronobacter sakazakii*	Liu *et al.* (2021)
Food, Food Safety	Lateral flow nucleotide biosensor based on aptamer magnetic nanoparticles and hybridization chain reaction	LOD 2.6×10^3 cfu	*Vibrio parahaemolyticus*	Ying *et al.* (2021)
Medical, Diagnostic	Label-free graphene oxide modified aptasensor	LOD 0.032 µg mL^{-1}	Glycated albumin (diabetes monitoring)	Aye *et al.* (2021)
Food, Food Safety	Aptamer based fluorescent biosensor with ribonuclease H assisted cycle response	LOD 0.08 ng/mL	Ochratoxin A	Wu *et al.* (2019)
Food, Crop Safety	Electrode modified screen-printed gold with thiolated aptamers immobilised on gold nanoparticles	LOD 0.0169nM	Diazinon	Hassani *et al.* (2018)
Food, Food Safety	Microfluid aptasensor through sequential folding of chromatography paper substrate patterned with microchannel and screen-printed electrodes	LOD 21.6 ng/mL	Peanut allergen Ara H1	Jiang *et al.* (2021)
Medical, Diagnostic	Label-free electrochemiluminescence aptasensor based on nano material composition of reduced graphene oxide /tris(2,2-bipyridyl) ruthenium(II) complex-cerium oxide nanoparticles- chitosan platform	25pM	Cytochrome c (cell apoptosis monitoring)	Karimi Pur *et al.* (2018)
Medical & Food, Diagnostic, Food Safety	Impedance aptasensor based on interdigital array microelectrode immobilised on multi-walled carbon nanotubes	Quantification 10^{-9} to 10^{-3}	Tetracycline	Hou *et al.* (2017)

Table 2. Research applications of aptamers.

Table 2 highlights the various application possibilities of aptamers in the fields of medicine and food, demonstrating their versatility and continuous research carried out on the application potential. Aptamer applications have been seen in a variety of fields; chemical hazard detection, forensics, food safety applications, analytical reagents, bioimaging, drug delivery systems, therapeutics and diagnostics, (Darmostuk *et al.*, 2015b).

In recent years there has been an increase in the development of aptamers specific to mycotoxins and their use this is mainly due to their highly selective advantages. The majority of the developments have been focused on aptamers used as medication delivery systems Lee *et al.* (2005) and Bates *et al.* (2009) as well as diagnostic tools, (Wang *et al.*, 2013). Guo *et al.* (2014) describing a specific aptamer for the detection of aflatoxin B1 developed by Sangon Biotechnology Co. Ltd. in China comprised of a 3'-terminal biotin group and a complementary DNA fragment. The aptamer was used as a molecular recognition probe with a complementary DNA strand to act as signal in real time PCR amplification. A colorimetric bioassay was developed based on a DNAzyme aptamer for the detection of ochratoxin A (OTA). The DNA structure included the OTA specific aptamer as well as a G-rich sequence of nucleotides which imitate peroxidase activity. During binding of OTA to the aptamer a reduction of the hybridization efficiency occurs and as a result the DNAzyme activity is increased. Within the detection process an optimal concentration of Mg2+ is needed to assure highest possible sensitivity. Data analysis showed a good correlation between DNAzyme and OTA concentration in a linear range, (Yang *et al.*, 2013). A DNA based aptamer has been developed for the identification of fumonisin B1 toxin. The developed aptamer showed a dissociation constant in the nanomolar range and displayed its use in fumonisin biosensors and solid phase extraction columns, (McKeague *et al.*, 2010).

The very first aptamer for aflatoxin B1 has been reported which is based on a chemiluminescence competitive aptamer assay using aptamer-linked HRP-DNAzyme. Furthermore, the biosensor-based aptamer was applied to real corn samples. The sensitivity was found to be sufficient to detect the toxin, although cross reactivity has been shown with aflatoxin G1 and zearalenone, (Shim *et al.*, 2014). A Fe3O4/PANi-based electrochemical label-free aptasensor for the aflatoxin M1 detection had also been developed. Additionally, magnetic nanoparticles were used for signal amplification within the sensing platform and showed good sensitivity with an LOD of 1.98ng/L, (Nguyen *et al.*, 2013).

Aptamers have the potential to be incorporated into rapid detection assays. One example for which aptamers are very well suited are lateral-flow assays. These assays are representative of on-site detection technologies and are generally based on a membrane containing a detector and a capture reagent. Lateral-flow assays are very useful as they are straightforward to use by minimally trained personnel, compact in size and cost-effective. A specific lateral-flow assay using aptamers targeting the mycotoxin aflatoxin B1 has been reported. The results indicated a LOD of 0.3ng/g. Although the lateral-flow assay required fluorescence light for analysis of the aptamer, results were available after 30 minutes without any separation or washing of sample, (Shim *et al.*, 2014). Rapid detection assays have previously suffered from issues with false positive results, however with the use of specific aptamers designed for highly specific targets, confidence in aptamer technology development has increased. Although many specific aptamers have been reported in the peer reviewed literature, they are still not available in commercial formats. Nonetheless, the commercial potential remains significant as development technologies are becoming increasingly sophisticated for mass production. As mentioned above the selection of an aptamer against a small molecule can be difficult, however, the ability to adapt the SELEX protocol can facilitate the process, (Toh *et al.*, 2015). Despite of all the research and advances carried out on the development of aptamers to small molecules such as mycotoxins their application remains limited to laboratory settings.

The development of high quality/affinity aptamers requires effort and is inherently trial and error. To overcome these problems and allow aptasensors to become commercially available robust SELEX protocols, high throughput sequencing streamlined evaluations and rapid post selection binding assessment techniques are key, (Yu *et al.*, 2021). Most popular biosensor technologies utilising aptamers are colorimetric assays based on gold nanoparticles (AuNPs) as the protective effect of the DNA or RNA against salt-induced aggregation of AuNPs. They have the additional benefit of being label free and require, in comparison, relatively cheap analytical equipment for evaluation and can be evaluated by eye, (Zhang and Liu, 2021).

The use and benefits of colorimetric biosensors using aptamers and AuNPs for the detection of food contaminants have been described and have shown to be of particular benefit in targeting small molecules as they can diffuse quickly in assay conditions and are less likely to interact with the AuNPs if aptamers are added in excess, (Zhang and Liu, 2021).

In a publication by Zhu *et al.* (2020), the authors describe the application of a colorimetric aptamer-based biosensor for the detection of aflatoxin B1 and Ochratoxin A. The biosensor was combination of Fe_3O_4 and AuNPs as the platform. The observed detection ranges were between 5-250ng/mL for aflatoxin B1 and 0.5-80 ng/mL for Ochratoxin A detected through an UV–vis spectrophotometer. An example of a colorimetric assay which can be evaluated by eye has been described by Sun *et al.* (2018). The assay is based on the inhibition of the peroxidase-mimicking activity of AuNPs by the zearalenone mycotoxin aptamer. The aptamer binding to the target can no longer inhibit the AuNPs and a colour change occurs. The results were compared to commercially available ELISA antibody-based kits and the LOD was found to be 10 ng/mL. Due to the relative low cost of AuNPs and their application possibilities with aptamer and small molecules such as mycotoxins the colorimetric principle was selected as an evaluation tool of the proposed aptamers in this thesis.

1.12 Aims and Objectives

The food safety risks posed by T-2 and HT-2 *Fusarium spp.* mycotoxins remain present, despite mitigation strategies and reliable analytical analysis. To address the threat of increased prevalence in the food supply chain, there is a need for cheap, rapid, sensitive assays with specificity for T-2 and HT-2 mycotoxins. The use of assays based on biomolecules with binding specificity such as aptamers will provide the basis of a range of analytical platforms including portable formats suitable for field use.

The aim of this study is to develop aptamers with specificity for T-2 and HT-2 mycotoxin.

The objective workflow of aptamer development follows a set path and is comprised by three stages: selection of aptamers, identification and characterization of aptamers and functional validation, (McKeague *et al.*, 2015).

1. The development of DNA aptamers through sequence selection using a modified Capture SELEX protocol.
2. Identification of the DNA sequences found within the selection protocol to be determined through high-throughput sequencing for structural characteristics.
3. Trialling of the aptamer sequences in assays to identify and determine binding specificity.

The methodology to achieve these aims and objectives included the use of a modified Capture SELEX protocol (Chapter 3), followed by using High Throughput Sequencing methods (Chapter 4). Once suitable candidate aptamers are selected, evaluation in a colorimetric assay (Chapter 5).

This project aimed at supporting the analytical capabilities of these mycotoxins in the field of biosensors by developing an aptamer or multiple aptamers capable of their detection as there is an established increased risk posed by mycotoxin contamination, T-2 and HT-2. Analysis strategies which can be applied are crucial in controlling the identified hazard. To achieve this aim, the selection of aptamers is made using the Capture-SELEX protocol as it has been reported to be very suitable to the application to small molecules. To enhance the selection and contribute to the understanding of the aptamer development across selection rounds high throughput sequencing has been deployed. To evaluate the proposed aptamers developed, a colorimetric assay has been selected in combination with AuNPs due to their low cost and the natural ability of nucleotides to inhibit AuNP aggregation. To the best of current knowledge aptamers selected through the Capture-SELEX in combination with high throughput sequencing targeting T-2 and HT-2 mycotoxins have not yet been reported in peer reviewed publications.

Chapter 2. Equipment and Materials

2.1 Equipment and Software

DynaMag™ -2 Magnet, Magnetic rack

> ThermoFisher Scientific, United Kingdom

Epoch 3, Spectrophotometer

> Biotech, Ltd, United Kingdom

Gen 5, Spectrophotometer Software

> Biotech Ltd, United Kingdom

Membrane Filter, 0.2µm pore dimension

> Merck, United Kingdom

MEME, Multiple Em for Motif Elicitation, Version 5.5.0
> https://meme-suite.org/meme/index.html

MEGA, Molecular Evolutionary Genetics Analysis, Version 11
> https://www.megasoftware.net

MiSeq

> Illumina, United States of America

Mini-Sub® Cell GT Cell

> Bio-Rad Laboratories, Inc, United Kingdom

Molecular Imager, ChemiDoc XRS+, Image Lab Software

> BioRad, Ltd, United Kingdom

Nanodrop

> ThermoFisher Scientific Ltd, United Kingdom

PowerPac™ Basic Power Supply

Bio-Rad Laboratories, Inc, United Kingdom

Wide Mini-Sub Cell GT Cell

Bio-Rad Laboratories, Inc, United Kingdom

ThermoMixer

Eppendorf Ltd, United Kingdom

2.2 Materials

Agarose, BioReagent for molecular biology, low EEO

Merck, KGaE, Germany

Boric acid, BioReagent, for molecular biology, ≥99.5%

Merck, KGaE, Germany

Calcium chloride, anhydrous, granular, ≤7.0 mm, ≥93.0%

Merck, KGaA, Germany

Deoxyribonucleic acid oligonucleotides

Integrated DNA Technologies, BVBA, Belgium

DNA Ladder, 100 bp

Thermo Fisher Scientific, Ltd, United Kingdom

Dynabeads™ MyOne™ Streptavidin C1

Thermo Fisher Scientific, Ltd, United Kingdom

Ethylenediaminetetraacetic acid (EDTA), Ultrapure

ThermoFisher, United Kingdom

Ethanol, 99.8%, for analysis, absolute

Thermo Fisher Scientific, Ltd, United Kingdom

Gel Loading Dye, DNA, 6x

Thermo Fisher Scientific, Ltd, United Kingdom

GelRed® Nucleic Acid Gel Stain, 10,000X in water

Biotium, Inc, United States of America

Gold nanoparticles, 20nm diameter, OD 1

Sigma Aldrich, United Kingdom

Lambda Exonuclease, (10U/µL)

ThermoFisher Scientific, United Kingdom

Magnesium Chloride, anhydrous, ≥98%

Merck, KGaA, Germany

Mycotoxin, Aflatoxin B1, in acetonitrile, 100ppm

R-Biopharm, Belgium

Mycotoxin, Deoxynivalenol, in acetonitrile, 100ppm

R-Biopharm, Belgium

Mycotoxin, HT-2, in acetonitrile, 100ppm

Romer Labs, United Kingdom

Mycotoxin, T-2, in acetonitrile, 100ppm

Romer Labs, United Kingdom

RIDASCREEN®, T-2/HT-2 Toxin

R-Biopharm, United Kingdom

Sodium Chloride, BioXtra, ≥99.5% (AT)

Merck, KGaA, Germany

Tris Base, Molecular Biology Grade ≥99.8%

Severn Biotech Ltd, United Kingdom

Tris-HCl, 1M Solution, pH 8.0, Molecular Grade, Ultrapure

Fisher Scientific, United Kingdom

UltraPure™ 0.5M EDTA, pH 8.0

Thermo Fisher Scientific, Ltd, United Kingdom

UltraPure™ 1 M Tris-HCl Buffer, pH 7.5

Thermo Fisher Scientific, Ltd, United Kingdom

Potassium Chloride, BioXtra, ≥99.0%

Merck, KGaE, Germany

QIAquick Gel Extraction Kit, DNA extraction

Qiagen, United Kingdom

Standard laboratory consumables used included: glass and plastic wear, manual and automatic pipettes with fitting filter tip pipette tips, holding racks, storage containers for freezing, deionized water and glassware sterilised through autoclaving at 121°C for 15min.

Chapter 3. Evaluation and use of SELEX protocols for the development of aptamers

3.1 Introduction

Systematic evolution of ligands through exponential enrichment (SELEX) protocols are key to developing aptamers with target binding specificity. Various approaches to the SELEX principle have been described since the original methodology was published by Tuerk and Gold (1990).
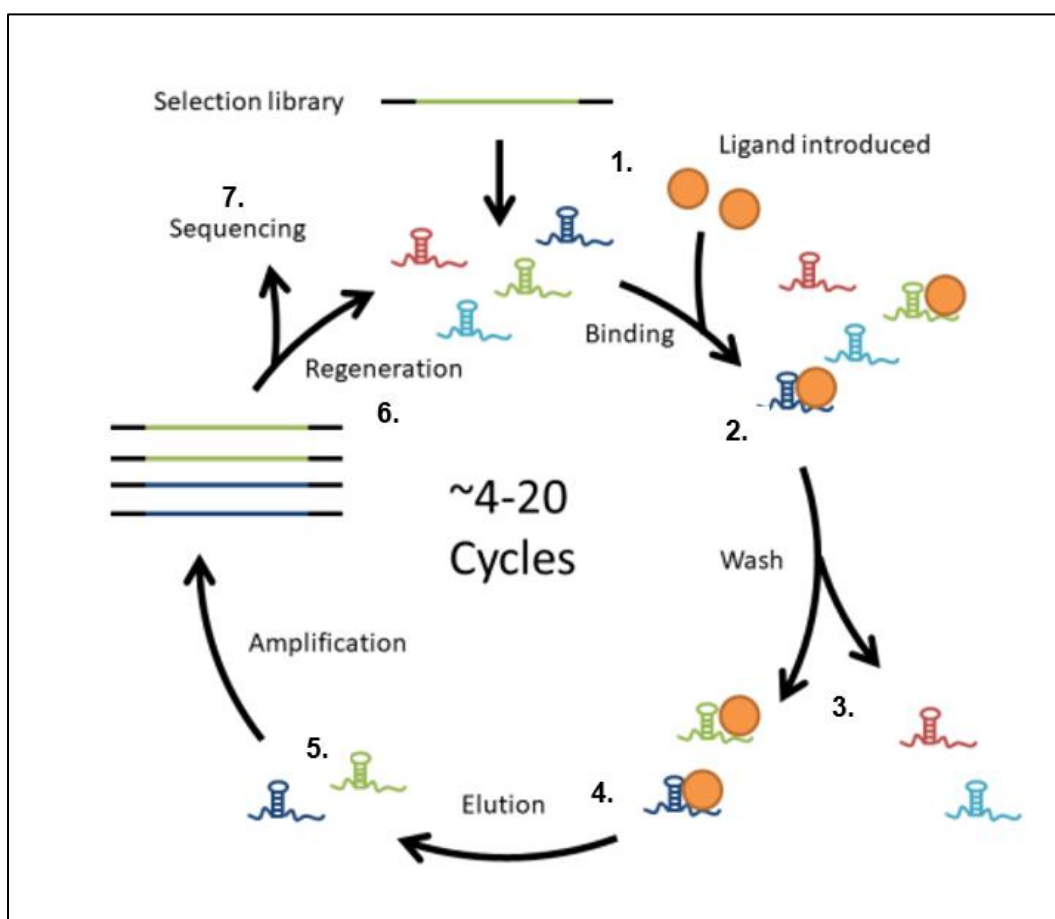
Figure 5 Diagram showing the traditional SELEX protocol principle, (Piccolo, 2021).

The key principles of the original heterogenous SELEX protocol are illustrated in Figure 5. An oligonucleotide library pool is combined with a target molecule for binding (**1.**). Following binding (**2.**), unbound oligonucleotides are removed (**3.**), and the binding oligonucleotides are eluted (**4.**). These selected oligonucleotides are retained for PCR amplification (**5.**) The amplified PCR products are used in subsequent SELEX rounds (**6.**) and the selection process is repeated. Following the final stage of selection, the oligonucleotides are sequenced (**7.**).

Separation of the single stranded DNA (ssDNA) oligomers that have bound to the target from the unbound ssDNA oligomers is essential to ensure that only those with target specificity are amplified in the subsequent PCR step. Where the targets are significantly larger than the ssDNA oligomers (e.g. cells, microorganisms, large polypeptides), separation can be achieved through use of techniques such as filtration or gel permeation chromatography, (Vivekananda and Kiel, 2006). These techniques are of limited use for low molecular weight targets such as mycotoxins (typically <1000Da) because the size differences between ssDNA (typically >30 kDa) and the resulting ssDNA-target complexes are too small, (Yu *et al.*, 2021). In these cases, alternative methods for the separation of binding and nonbinding sequences can be applied.

Immobilisation of low molecular weight targets on to solid supports such as magnetic beads or Sepharose gel have been reported for aptamer production (Yu *et al.*, 2021). Binding of the target to a support requires chemical conjugation through appropriate functional groups (e.g. hydroxyl, carboxyl or amine) present on the molecule. However, low molecular weight targets generally possess few functional groups, limiting their amenability for conjugation and impeding interactions between the ssDNA and the immobilized target. Chemical spacing groups between the target and the support may also be introduced to reduce steric hindrance and improve ssDNA binding, however, the attachment of linkers or moieties for conjugation can greatly change the chemical properties of the small-molecule target, and it has been reported that aptamers isolated against

conjugated small-molecule targets exhibit greatly reduced or no affinity for the free target relative to the conjugated target, (Ohsawa *et al.*, 2008).

The traditional SELEX methodology was labour intensive and expensive, leading to extensive experimental work to adapt and modify the protocols, (Wang *et al.*, 2019). Depending on the nature of the targets, protocols have been developed to address differences in size, structure and chemical or physical properties (Ruscito and DeRosa, 2016). Consequently, aptamer technologies have been reported for various applications, ranging from therapy, drug delivery, diagnostics, functional genomics and biosensing, based on different SELEX approaches, (Wang *et al.*, 2019). More than 32 variations to SELEX have been reported, with only a few differentiating greatly from the originally proposed protocol, (Darmostuk *et al.*, 2015b). These modifications include target preparations (Cell SELEX), library immobilisation (Capture SELEX) and introduction of bioinformatics, (Wang *et al.*, 2019).

For these reasons, the traditional SELEX approach as described by Vivekananda and Kiel (2006) in which target-ssDNA complexes were separated from unbound ssDNA by filtration are likely to be unsuitable for the development of aptamers with T-2 or HT-2 binding specificity. Consequently, it was considered that a different approach to the SELEX protocol should be evaluated.

The Capture-SELEX procedure allows for the development of deoxyribonucleic acid (DNA) aptamers targeting small organic molecules, without the need to immobilise the target onto a surface. Instead, a capture sequence is used which is bound to a surface and attaches to a corresponding capture sequence within the random DNA oligomer library. The first reported use of the technique was described by Stoltenburg, Nikolaus and Strehlitz (2012b)The capture sequence is immobilised on streptavidin coated magnetic beads via the biotin-streptavidin bond. The magnetic beads can be held in place using magnets and thereby allowing for a structural framework for the library sequence to bind around the targets. Stoltenburg (2012b) and colleagues concluded that the use of the capture

sequence was better suited to allowing for binding and removing non-specific nucleotides than conventional SELEX methods, as well as being better suited to targeting small molecules.

The Capture SELEX protocol presented in this chapter was based upon the methodology described by Paniel *et al.* (2017). The modified protocol presented herein started with the immobilisation of the defined 12 base pair docking sequence to magnetic beads, followed by binding of the DNA oligonucleotide library sequences to the defined and complimentary 12 base pair docking sequence through the defined capture region on the library sequence. The targets (T-2 or HT-2) were added and allowed to bind. Following binding, the target bound sequences were recovered from the binding mixture and amplified through polymerase chain reaction (PCR). In contrast to the approach described by Paniel *et al.* (2017) of gel electrophoresis followed by band excision for recovery of the double stranded DNA (dsDNA) PCR products from the electrophoresis gels, the resulting dsDNA was separated into ssDNA using lambda exonuclease enzymatic digestion. The resulting ssDNA obtained following digestion was then used in further selection rounds.
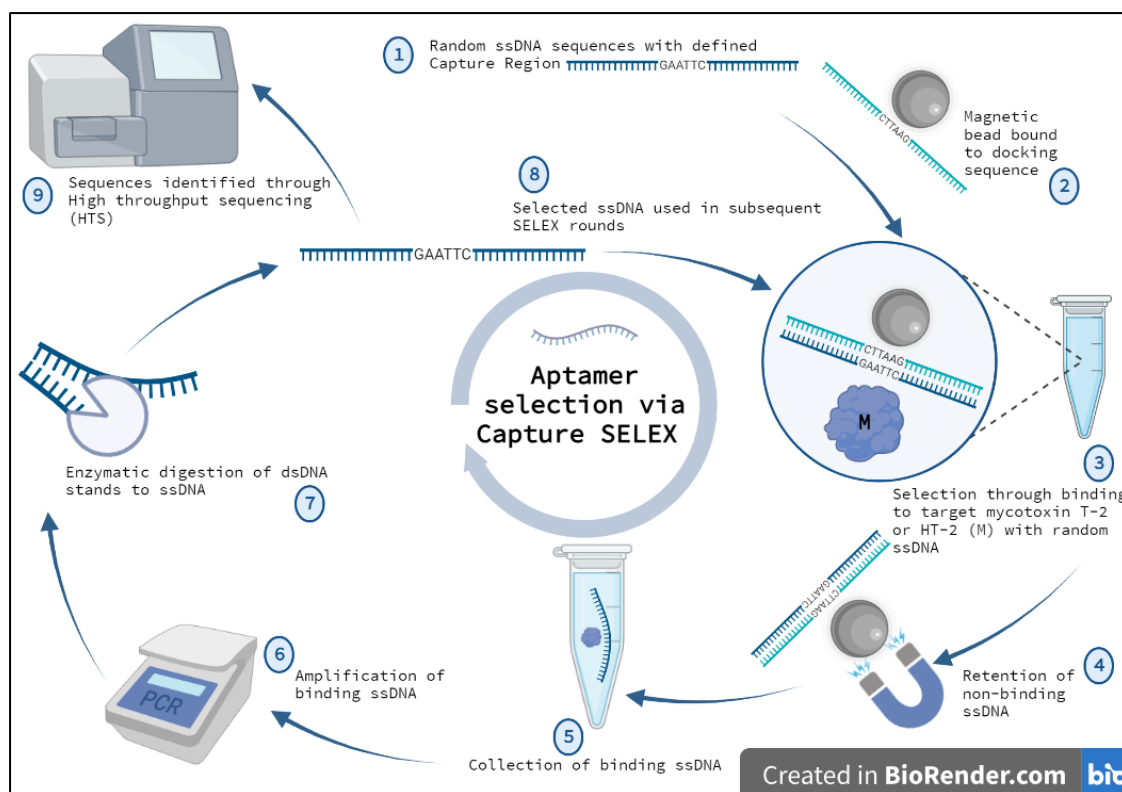
Figure 6 Diagram showing the Capture SELEX protocol principle

The modified Capture-SELEX protocol is summarised in Figure 6. In the initial phase the defined docking sequence is immobilised onto magnetic beads as support structure (**2.**). The oligonucleotide library with the defined capture region (**1.**) is added to the immobilised beads allowing for the binding of the capture regions of the docking sequence and oligonucleotide library. The oligonucleotide library binds around the target molecule introduced (**3.**). Following binding, the bound oligonucleotide library and targets are removed from the support structure, leaving the nonbinding sequences (**4. & 5.**). The binding oligonucleotide sequences are amplified using PCR (**6.**) and the resulting double stranded DNA sequences are separated into single strands using lambda exonuclease enzyme. (**7.**). The separation includes a heat inactivation step of the enzymes. The single strands are used in the next selection rounds (**8.**). Sequences identified following each Capture SELEX selection round are identified using High throughput sequencing (**9.**).

The objective of the work presented in this chapter was the application of a Capture SELEX protocol for the development of DNA aptamers targeting T-2 and HT-2 mycotoxins and comparison with the traditional SELEX procedure. Evaluation of the lambda exonuclease method for ssDNA recovery instead of the use of gel electrophoresis and band excision was also performed.

3.2 Methods

3.2.1 Deoxyribonucleic acid oligonucleotides (DNA) preparation from stock solutions; Traditional SELEX protocol sequences

The DNA oligonucleotide stocks used to perform the traditional SELEX method were synthesised by Integrated DNA Technologies (IDT), the sequences obtained were described by Vivekananda and Kiel (2003)

Sequence description	Sequences 5' – 3'	Base Pair length
DNA random library	ACC CCT GCA GGA TCC TTT GCT GGT ACC NNNN (N=42) AGT ATC GCT AAT CAG TCT AGA GGG CCC CAG AAT	102
Forward primer	ACC CCT GCA GGA TCC TTT GCT GGT ACC	27
Reverse primer	ATT CTG GGG CCC TCT AGA CTG ATT AGC GAT ACT	33

Table 3 Sequences used for the traditional SELEX method as described by Vivekananda and Kiel (2006) and Vivekananda and Kiel (2003)

The DNA random library sequence (30712.9g/mol), forward primer (8187.3g/mol) and reverse primer (10119.6g/mol) were supplied on a 1µmol scale and reconstituted in the vials to 100µM with sterile deionised water (Table 3).

3.2.2 Deoxyribonucleic acid oligonucleotides (DNA) preparation from stock solutions; Capture SELEX protocol sequences

The DNA oligonucleotide stock used to perform the Capture-SELEX method was synthesised by Integrated DNA Technologies (IDT) the sequences obtained were as described by Paniel *et al.* (2017). Modifications were made to the reverse primer, phosphorylation of the 5', to allow for lambda exonuclease digestion.

Sequence description	Sequences 5' – 3' and modifications	Base Pair length
DNA oligonucleotide library with capture region	GGG AGG ACG AAG CGG AAC-N10-TGA GGC TCG ATC-N40-CAG AAG ACA CGC CCG ACA	98
Forward primer	GGG AGG ACG AAG CGG AAC	18
Reverse primer	Phos-TGT CGG GCG TGT CTT CTG	18
Docking sequence	Biot-CTG-HEGL-GAT CGA GCC TCA	12

Table 4 Sequences and modifications of the oligonucleotides used for the Capture-SELEX methodology.

The DNA oligonucleotide library with capture region sequence was supplied on a 0.25µmol scale. The docking sequence (5301.8g/mol), forward primer (5647.7g/mol) and reverse primer (5608.6g/mol) were supplied on a 1 µmol scale and reconstituted in sterile deionised water to 100µM (Table 4).

3.2.3 Traditional SELEX protocol: Selection procedure

The initial pool of DNA oligonucleotides was lineralised (90°C for 8min) immediately prior to use. A 1µM concentration dilution was prepared of DNA oligonucleotide pool in Binding Buffer (0.2M Tris HCl, 0.045M NaCl, 0.03M MgCl, 0.001M EDTA to 1L of deionised sterile water). The mycotoxins T-2 (0.2µM) and HT-2 (0.2µM) were prepared in BB. Both solutions were mixed, 3 replications per mycotoxin, and incubated for 1 hour at room temperature with mild shaking, 500rpm in the thermomixer.

Following incubation, the oligonucleotide/target mix was filtered through a 0.2µm membrane filter using a vacuum manifold at low pressure. The membranes were washed 3x to remove unbound oligonucleotides. The binding sequences retained on the filter, due to the size of the oligonucleotide and target complex, were extracted using preprepared Elution buffer (Qiagen). A negative control was included in the selection procedure which underwent the same protocol apart from no target added.

3.2.4 Traditional SELEX protocol: PCR amplification of selected oligonucleotides

The extracted oligonucleotides (20µL) were added to 1µL forward primer and 1µL reverse primer with 3µL sterile deionised water in a pre-prepared Ready-to-Go PCR bead tube (GE Healthcare). A positive control was included consisting of original oligonucleotide library sequence, forward and reverse primers. The mix was vortexed briefly and the tube was placed in the thermocycler after the bead had dissolved fully, indicated by the settling of foam inside the tube.

The PCR cycle conditions utilised were:

  Denaturation, 1 x 95°C for 5min
  Followed by 30 cycles of;
  Denaturation, 1 x 95°C for 1min
  Annealing, 1 x 51°C for 1min
  Extension, 1 x 72°C for 1min
  Followed by;
  Final Extension, 1 x 72°C for 10min
  Final Holding Temperature, ∞4°C

Following PCR amplification, 5µL of the product was mixed with 2µL of loading dye. The mix was pipetted into the wells of the prepared 2% agarose gel, (24g of agarose powder dissolved in 120mL of 1xTBE buffer (0.89M Tris-borate, 0.89M Boric acid, 0.02M EDTA with 5µL gel red), heated to dissolve and set in a wide mini sub cell GT gel tray at room temperature). A 100bp DNA ladder was added for reference. The loaded agarose gel was placed in a wide mini-sub cell GT cell gel tank filled with 1xTBE buffer and run at 85V for 35min using a PowerPac. The agarose gel was visualised under the transilluminator to identify band locations.

3.2.5 Traditional SELEX protocol: QIAquick gel extraction (Qiagen)

The DNA segment was cut from the agarose gel using a sterile scalpel and transferred into a 1.5mL tube. An equal volume of ready to use Buffer QG was added to the tube. The volume to gel ratio varied depending on the weight of the cut gel sample. The tube was incubated in a 50°C water bath for 10min followed by addition of Isopropanol to the tube in equal volumes (50:50) followed by vortex to mix. The solution was transferred into a kit provided spin column tube and centrifuged for 1min at 13000 rpm, the filtrate was discarded. The retentate was washed using ready to use kit provided Buffer PE and incubated for 5min at room temperature.

The spin column tube was centrifuged for 1min at 13000 rpm and the filtrate discarded. The column insert containing the filter was placed into a clean 1.5mL tube and 50µL of ready to use kit provided Elution buffer was added and incubated for 4min at room temperature. The tube was centrifuged for 1min at 13000 rpm and the flow through with the eluted DNA collected for nanodrop analysis.

3.2.6 Traditional SELEX protocol: DNA concentration measurement

The sample (1µL) was loaded into the nanodrop and the concentration measured in ng/µL. Samples were analysed both post-PCR amplification and post- gel extraction dsDNA separation.

3.2.7 Capture SELEX protocol

The Capture SELEX methodology was performed as described by Paniel *et al.* (2017) with changes detailed below.

3.2.8 Capture SELEX protocol: Magnetic bead preparation

The Dynabeads MyOne Streptavidin C1 were vortexed to re-suspend the beads in stock solution. Dynabeads stock (100µL) was added to a sterile tube to which 1mL of 1 x Binding & Washing Buffer (1 x B&W; 0.01M Tris-HCl, 0.1M EDTA, 2M NaCl) was added and vortexed. The tube was placed on the magnetic rack for 1min and the supernatant discarded. The washing cycle was repeated 3 times and the beads remained on the magnet during the wash. Following the final washing step, 100µL of 0.2µ docking sequence was added to the tube and vortexed to mix.

3.2.9 Capture SELEX protocol: Immobilisation phase

The dynabead/docking sequence mix was incubated in the thermomixer for 1h at 21°C at 500rpm. Following incubation, the tube was placed on the magnet for 3 x washing cycles with 500µL of 1x B&W buffer. A further 3 x washing cycles were carried out with 500µL of Selection Buffer, (SLB; 0.02M Tris HCl, 0.1M NaCl, 0.002M $MgCl_2$, 0.005M KCl, 0.001M $CaCl_2$). Following the final wash, the mix was resuspended in 200µL of SLB. To prepare the working complex for the Capture SELEX protocol, 2µL were removed and added 198µL of SLB.

3.2.10 Capture SELEX protocol: Target solution preparation

The target solutions were prepared fresh before each Capture SELEX round. The mycotoxins T-2 and HT-2 were mixed with SLB to 0.2µM.

3.2.11 Capture SELEX protocol: 1st round of selection

The first round of selection started with a linearisation of the DNA oligonucleotide library with capture region. The library (1µM) was incubated in the thermomixer for 8min at 90°C and 10min at 4°C and left to come to room temperature (~18°C) before use.

The previously prepared working complex (Section 3.2.9) was added to the oligonucleotide library and incubated in the Thermomixer for 18-20h at 21°C at 500rpm. Following incubation, the mixture was placed on the magnetic rack and a 9x washing cycles with 500µL of SLB were performed. After the final wash, the mix was incubated again in the Thermomixer for 15min at 28°C. Following incubation, the tube was placed on the magnetic rack and 7x washing cycles with 500µL SLB were performed. Each target solution, T-2 and HT-2 was added to the respective oligonucleotide library/working complex solutions. A negative control was included prepared as above without target molecule to identify non-specific binding in the absence of target. The solutions were incubated in the Thermomixer for 45min at 28°C at 500rpm. Following incubation, the solutions were placed on the magnetic rack for 5min and the supernatant was collected to be used in the amplification stage (Section 3.2.12). The remaining non-binding sequences and magnetic beads in solution were discarded.

3.2.12 Capture SELEX protocol: PCR amplification and agarose gel visualisation

The binding oligonucleotide library sequences collected (20µL) was added to 1µL forward primer and 1µL reverse with 3µL sterile distilled water in a pre-prepared Ready-to-Go PCR bead tube. A positive control was included consisting of original library sequence, forward and reverse primers prepared as described above. The mix was vortexed briefly and the tube was placed in the thermocycler after the bead had dissolved fully, indicated by the settling of foam inside the tube.

The PCR cycle conditions were:

Denaturation, 1 x 95°C for 5min
Followed by 30 cycles of;
Denaturation, 1 x 95°C for 1min
Annealing, 1 x 51°C for 1min
Extension, 1 x 72°C for 1min
Followed by;
Final Extension, 1 x 72°C for 10min
Final Holding Temperature, ∞4°C

Following PCR amplification, 5µL of the product was mixed with 2µL of loading dye. The 7µL mix was pipetted into the wells of the prepared 2% agarose gel, heated to dissolve and set in a wide mini sub cell GT gel tray at room temperature. A 100bp DNA ladder was added for reference. The loaded agarose gel was placed in a wide mini-sub cell GT cell gel tank filled with 1xTBE buffer and run at 85V for 35min using a PowerPac. The agarose gel was visualised under the transilluminator to identify band locations.

3.2.13 Capture SELEX protocol: Double stranded DNA (dsDNA) separation post PCR

The dsDNA post PCR amplification was separated using lambda exonuclease enzymatic reaction. 5 µL of 10x supplied reaction buffer was added to the PCR product (20µL) with 2µL of lambda exonuclease. The mix was incubated in the Thermomixer for 30min at 37°C and 10min at 80°C and then immediately cooled by placing on ice. The resulting ssDNA is subsequently referred to as working oligonucleotide library to be used in the following Capture SELEX rounds.

3.2.14 Capture SELEX protocol: DNA concentration measurement

The sample (1µL) was loaded into the nanodrop and the concentration measured in ng/µL. Samples were analysed both post-PCR amplification and post-Lambda Exonuclease dsDNA separation.

3.2.15 Capture SELEX rounds: 2nd to 15th

All selection rounds following the first round (round 2 to 15) were performed following the same protocol as described above utilising the working oligonucleotide library.

3.3 Results

3.3.1 Traditional SELEX protocol

The methodology previously described by Vivekananda and Kiel (2006) to produce oligomers for a traditional SELEX was followed as described in Sections 3.2.3 to 3.2.6. Following PCR of the of the oligonucleotide library, agarose gel electrophoresis demonstrated the presence of 100bp amplicons and successful working of the conditions (Figure 7).
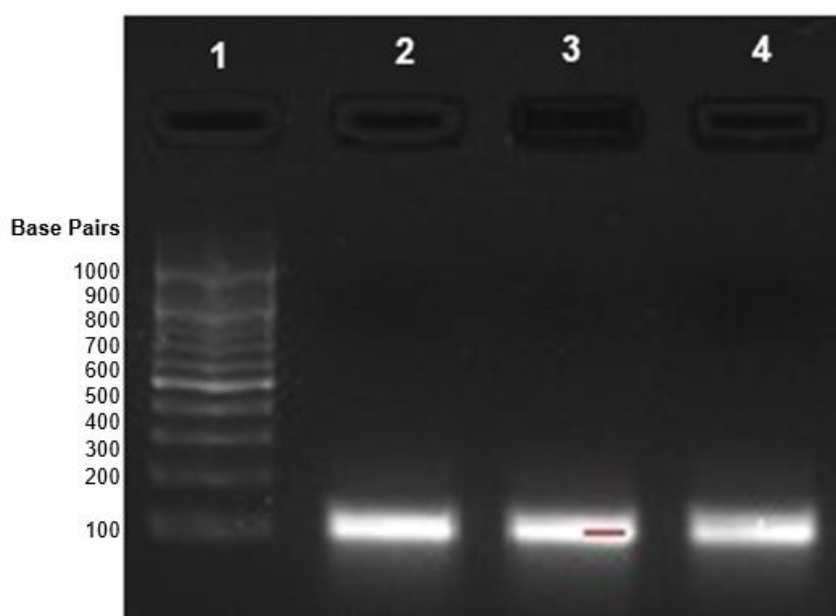
Figure 7 Agarose gel electrophoresis of PCR products. **Lane 1,** 100bp DNA ladder for reference; **Lanes 2** to **4,** random oligonucleotide library amplifications post PCR.

Following the addition of T-2 to the oligonucleotide library, subsequent PCR amplification of recovered ssDNA-target complexes was performed and examined by agarose gel electrophoresis (Figure 8). PCR products approximately 100 bp were observed for the oligonucleotide library control and the oligonucleotide library without the target molecule. A very faint band of 100bp

size was observed for oligonucleotide library bound to the target (T-2), showing that the traditional method was not applicable to the small molecule target.
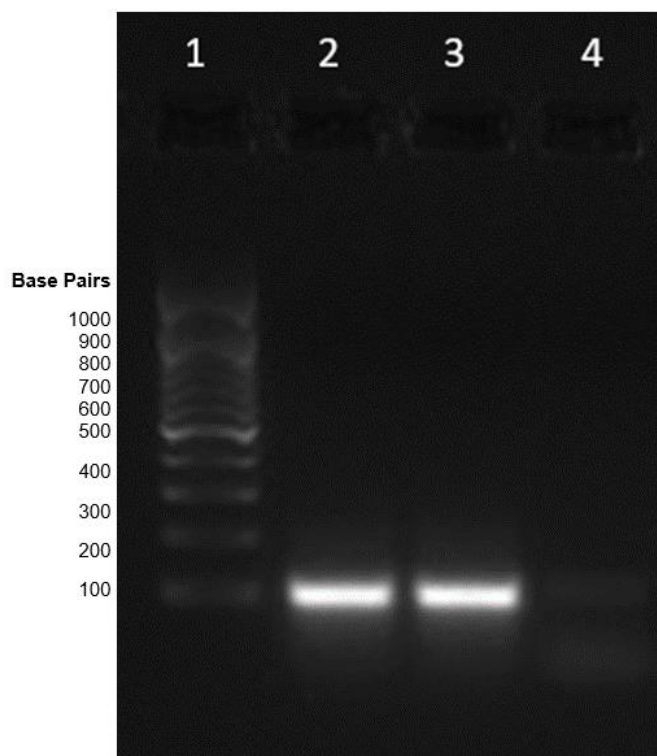
Figure 8 Agarose gel electrophoresis of PCR products following T-2 incubation. **Lane 1.** 100bp DNA ladder for reference, **Lane 2.** Control of DNA oligonucleotide library and primer amplification. **Lane 3.** DNA oligonucleotide library and primers in traditional SELEX without addition of target. **Lane 4.** DNA oligonucleotide library and T-2 mycotoxin target in traditional SELEX protocol.

Further analysis of PCR products following incubation with HT-2 are shown in Figure 9. PCR products of approximately 100 bp were only observed for the oligonucleotide library control. No amplification was observed following the application of the protocol to HT-2, further demonstrating the unsuitability of the traditional method for small target aptamer selection.
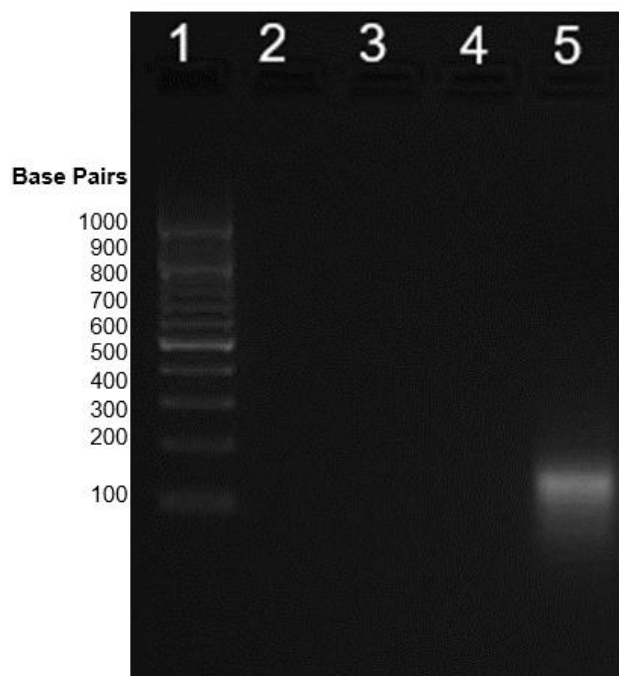
Figure 9 Agarose gel electrophoresis of PCR products following HT-2 incubation. **Lane 2** to **Lane 4** DNA oligonucleotide library with HT-2 target during traditional SELEX protocol. **Lane 5.** DNA oligonucleotide library control.

3.3.2 Oligonucleotide concentration results

The traditional SELEX protocol included extraction of the amplified PCR product from the agarose gel to receive the oligonucleotide library with binding characteristics to the target molecule. In total of 15 replications were performed of the PCR control. Prior to PCR amplification the concentration of the oligonucleotide library was measured through nanodrop and ranged between 612ng/µL to 681ng/µL, with a mean (± standard deviation; s.d.) of 647 ± 21ng/µL. In comparison, the recovery seen post elution ranged from 6ng/µL to 18 ng/µL, with mean (±s.d.) of 12 ± 4ng/µL. The percentage recovery values recorded for each replication are shown in Figure 10.
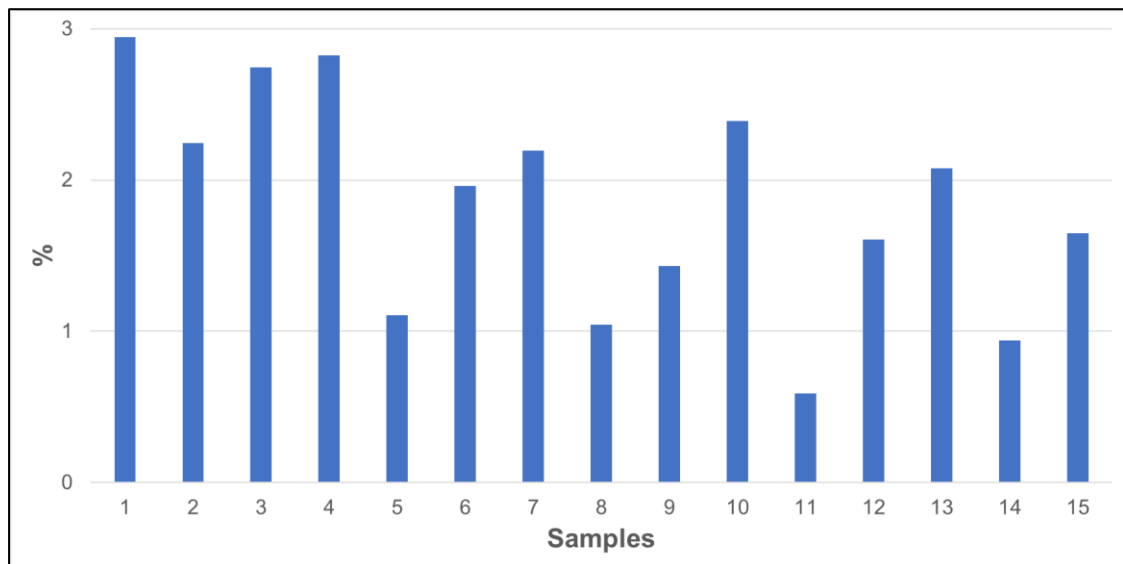
Figure 10 Recovery of DNA eluted from agarose gel post PCR amplification. Percentage recovery was determined from the concentration of DNA post elution as a proportion of the concentration of the random library pre-PCR.

The results from the PCR amplification and elution methodology showed poor recovery of oligonucleotides from the agarose gel using the Qiagen extraction kit. Percentage recovery values ranged from 0.6 to 3% across the replications with a mean percentage recovery (±s.d.) of 1.86 ± 0.76%.

3.3.3 Capture SELEX protocol

Each Capture SELEX round for each toxin was evaluated in triplicate. Three separate reaction tubes were set up for T-2 and HT-2 respectively, with one negative control without target included to evaluate the process. Prior to the PCR step, a positive control was included to evaluate the amplification and performance of negative control. This resulted in 7 reaction tubes per SELEX round, a total of 105 SELEX reactions with an additional 15 per round for positive controls. The pool of sequences was retained at the end of each round allowing for staged recovery.
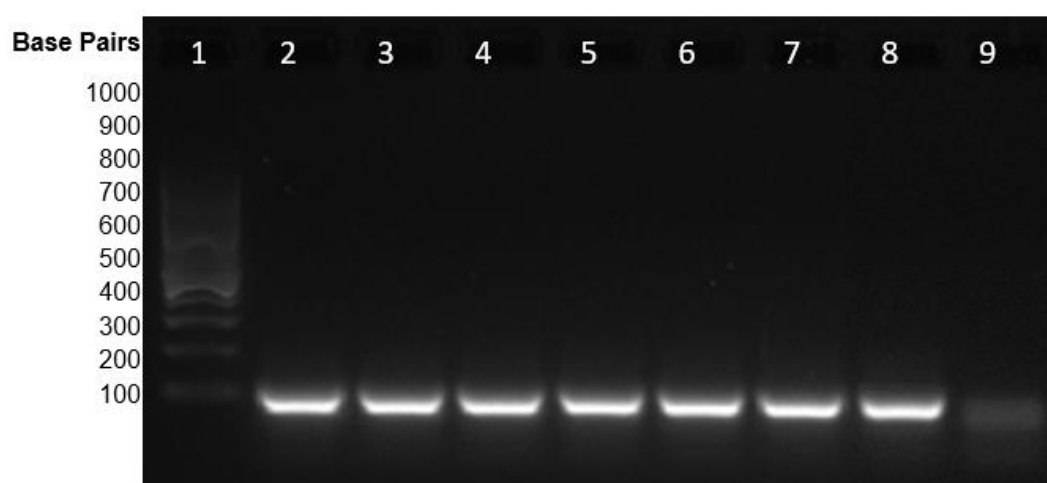
Figure 11 Agarose gel electrophoresis of the PCR products from Capture SELEX round 1. **Lane 1,** 100bp DNA ladder for reference; **Lanes 2-4,** DNA oligonucleotide library targeting T-2; **Lanes 5-7,** DNA oligonucleotide library targeting HT-2; **Lane 8,** Positive control; **Lane 9,** Negative control.

Agarose gel electrophoresis of the amplified oligonucleotide library targeting T-2 and HT-2 mycotoxins from the Capture SELEX protocol (Round 1) are shown in Figure 11. Amplification can be seen in lanes 2 to 4 which contained the oligonucleotide library targeting T-2. Lanes 5 to 7 demonstrated amplification of the oligonucleotide library targeting HT-2. Lane 8 showed amplification of the positive control and Lane 9 showed very much reduced amplification of the negative control.

The oligonucleotides generated during the Capture SELEX process and their identification codes are detailed in Table 5, below.

Round	Description	CS ID	NGS ID	Round	Description	CS ID	NGS ID	Round	Description	CS ID	NGS ID
1	(-) Control	1	10	6	(-) Control	1	60	11	(-) Control	1	110
	T-2	2	11		T-2	2	61		T-2	2	111
	T-2	3	12		T-2	3	62		T-2	3	112
	T-2	4	13		T-2	4	63		T-2	4	113
	HT-2	5	14		HT-2	5	64		HT-2	5	114
	HT-2	6	15		HT-2	6	65		HT-2	6	115
	HT-2	7	16		HT-2	7	66		HT-2	7	116
2	(-) Control	1	20	7	(-) Control	1	70	12	(-) Control	1	120
	T-2	2	21		T-2	2	71		T-2	2	121
	T-2	3	22		T-2	3	72		T-2	3	122
	T-2	4	23		T-2	4	73		T-2	4	123
	HT-2	5	24		HT-2	5	74		HT-2	5	124
	HT-2	6	25		HT-2	6	75		HT-2	6	125
	HT-2	7	26		HT-2	7	76		HT-2	7	126
3	(-) Control	1	30	8	(-) Control	1	80	13	(-) Control	1	130
	T-2	2	31		T-2	2	81		T-2	2	131
	T-2	3	32		T-2	3	82		T-2	3	132
	T-2	4	33		T-2	4	83		T-2	4	133
	HT-2	5	34		HT-2	5	84		HT-2	5	134
	HT-2	6	35		HT-2	6	85		HT-2	6	135
	HT-2	7	36		HT-2	7	86		HT-2	7	136
4	(-) Control	1	40	9	(-) Control	1	90	14	(-) Control	1	140
	T-2	2	41		T-2	2	91		T-2	2	141
	T-2	3	42		T-2	3	92		T-2	3	142
	T-2	4	43		T-2	4	93		T-2	4	143
	HT-2	5	44		HT-2	5	94		HT-2	5	144
	HT-2	6	45		HT-2	6	95		HT-2	6	145
	HT-2	7	46		HT-2	7	96		HT-2	7	146
5	(-) Control	1	50	10	(-) Control	1	100	15	(-) Control	1	150
	T-2	2	51		T-2	2	101		T-2	2	151
	T-2	3	52		T-2	3	102		T-2	3	152
	T-2	4	53		T-2	4	103		T-2	4	153
	HT-2	5	54		HT-2	5	104		HT-2	5	154
	HT-2	6	55		HT-2	6	105		HT-2	6	155
	HT-2	7	56		HT-2	7	106		HT-2	7	156
N/A	(+) Control	N/A	8								

Table 5 Identification list of all samples during the Capture SELEX process listing with identification (ID) numbers for each round and for samples analysed by high throughput sequencing (Chapter 4). CS describes Capture SELEX and NGS describes High Throughput sequencing sample ID.

3.3.4 Lambda exonuclease oligonucleotide strand separation during Capture SELEX protocol

The amplified PCR products were separated using enzymatic digestion with lambda exonuclease. Nucleotide concentrations measured throughout the 15 rounds of selection are recorded in Table 6.

Capture SELEX round	Average oligonucleotide concentrations		Average percentage degradation of oligonucleotide
	dsDNA ng/µL	ssDNA ng/µL	
1	434.0	262.9	50
2	522.6	234.5	47
3	477.0	249.6	53
4	646.1	340.7	55
5	478.3	264.1	55
6	467.1	242.0	55
7	417.5	216.3	46
8	478.7	250.4	53
9	472.9	248.6	53
10	482.0	250.0	52
11	442.7	239.1	54
12	477.9	245.9	52
13	522.1	242.0	47
14	529.3	242.4	47
15	519.7	262.9	51

Table 6 Oligonucleotide concentrations following enzymatic separation using lambda exonuclease pre- and post-oligonucleotide strand separation.

The average concentrations of all the oligonucleotide pools within each Capture SELEX round were recorded. The data (Table 6) includes the controls, positive and negative and all 6 target mixes, 3 replications of T-2 toxin and 3 replications of HT-2 toxin. From the average concentrations the percentage degradation of the double stranded oligonucleotides to single strands was measured and this ranged from 46% to 55% with mean (±s.d.) of 51 ± 3.1%.

The percentage degradation as result of the enzymatic digestion process is further illustrated in Figure 12. The three replications of samples containing the target toxin were pooled providing average values for the Capture SELEX round. The results show an average degradation across all the selection rounds between 40% and 60%. The negative control is the library sequence without addition of a target and the positive control used as verification of the PCR amplification. The degradation of the negative control is more varied in comparison to the positive, ranging between 30% and 70%, whereas the positive control is between 50% and 60%.
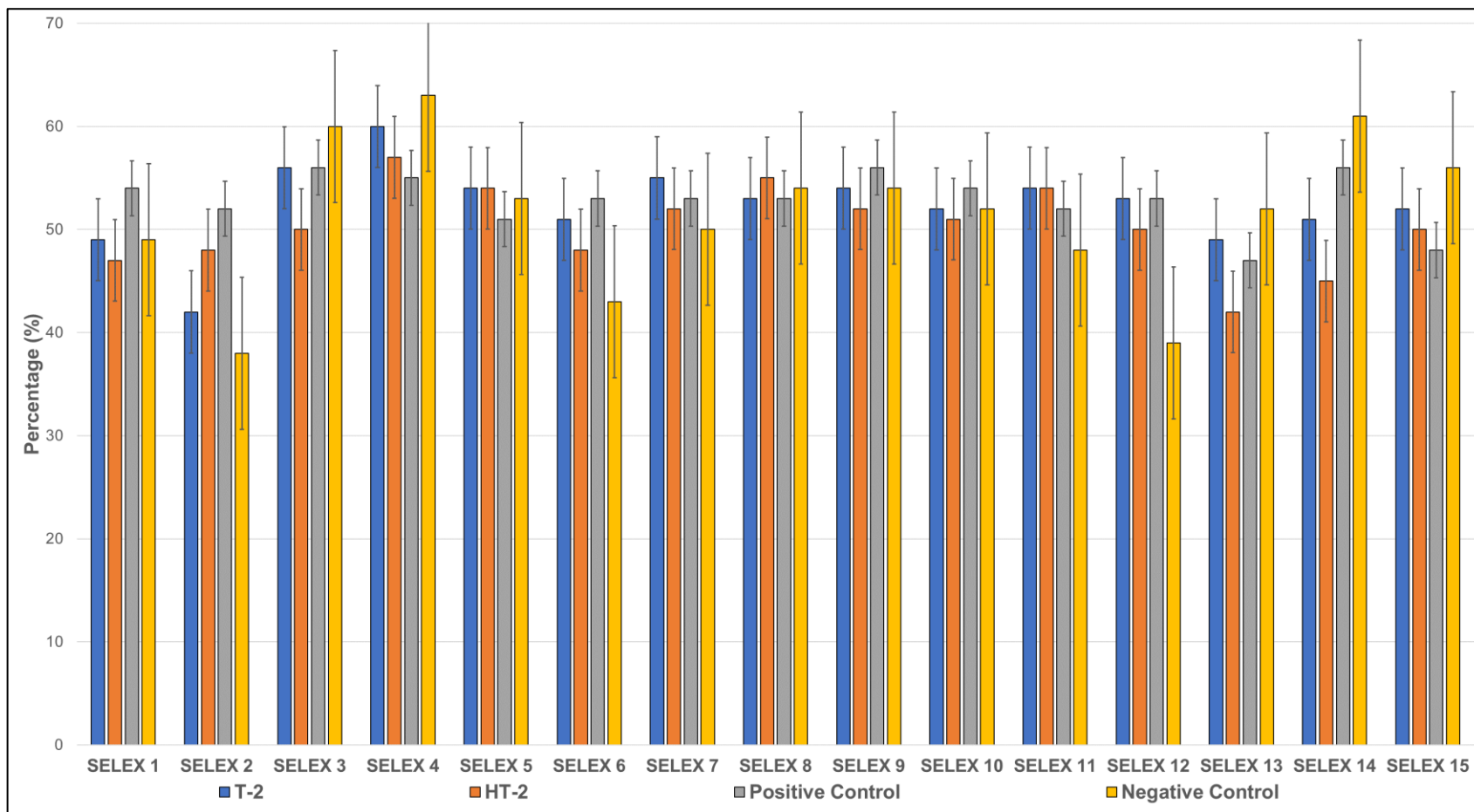
Figure 12 Percentage degradation of the oligonucleotides per Capture SELEX round, showing the replications of T-2 and HT-2, positive and negative controls. Values shown are averages (±s.d.), n=3

3.4 Discussion

The use of the traditional SELEX protocol aimed to develop aptamer sequences specific to T-2 and HT-2 mycotoxin. The results in Figure 7 demonstrated the suitability of the PCR conditions to amplify the sequences as anticipated, verifying the conditions described by Vivekananda and Kiel (2006). However, the results seen of the combination of T-2 and HT-2 with the oligonucleotide library (Figure 8 and Figure 9) demonstrate the unsuitability of the traditional SELEX protocol. Although a small amount of DNA was amplified in connection with T-2 target (Figure 8) it is unlikely that this would present as successfully bound oligonucleotides. This result is more likely to be an artefact of possible nonspecific binding of the nucleotides to the filter material. As expected, the target / oligonucleotide complexes passed through the filter and recovery of successful binding sequences was not possible. Subsequent evaluation of the dsDNA recovery from agarose gel with elution showed poor performance. With a calculated average recovery of 1.86 ± 0.76% (Figure 10). The poor performance of the DNA recovery causes issues as insufficient DNA available for selection rounds limits the diversity of possible aptamers. Alternative methodologies have been proposed, lambda exonuclease digestion, asymmetric PCR, biotin-streptavidin separation and denaturing urea-PAGE, (Kohlberger and Gadermaier, 2021).

The method published by Paniel *et al.* (2017) describes the use of Capture SELEX for the development of aptamers targeting penicillin G. Their methodology was closely aligned to the one described by Stoltenburg, Nikolaus and Strehlitz (2012a). The library sequence was immobilised through the defined complementary capture sequence to the complementary docking sequence onto streptavidin coated magnetic beads through the biotin label attached to the docking sequence. The strong binding capabilities of biotin and streptavidin allowed for the immobilisation to take place. The methodologies used gel purification and elution techniques to recover the PCR amplified sequences and

separation. Following the final round of SELEX, the sequences were cloned and amplified before sequencing.

The Capture SELEX protocol was also described in a study published by Boussebayle *et al.* (2019) describing it's use to develop an RNA based aptamer for the identification of a synthetic riboswitch for drug delivery. The RNA library was immobilised through a complimentary capture sequence onto streptavidin coated magnetic beads. The Capture SELEX protocol has been described for many different applications, but recently has been described more frequently in connection with food safety applications, as many contaminants of concern are comprised of small molecules (≤1000 Daltons), (Alshannaq and Yu, 2017). A similar SELEX protocol to Capture SELEX has been described by Duan *et al.* (2017). In this study, the oligonucleotide library was immobilised directly onto Fe_3O_4 magnetic beads coated in avidin. The library bound directly to the beads through a biotin link coupled to the primer sequence. The target molecule, ractopamine, was introduced to the mix for selection. Following selection and PCR amplification, lambda exonuclease was used to digest and separate the DNA stands. For the identification of suitable aptamer candidates, the team utilised traditional cloning and sequencing after the 16th round of selection, resulted in 40 possible aptamer candidates.

The Capture methodology was chosen as an alternative to the traditional method as it provided peer reviewed evidence of successful selection of aptamer candidates against a small molecule. As both T-2 and HT-2 mycotoxins are defined as small molecules Alshannaq and Yu (2017), it was selected as a more suitable approach. Additionally, as suggest in the reviews by Frutiger *et al.* (2021) and Lyu, Khan and Wang (2021), to reduce the non-binding proneness of oligonucleotide sequences a rigid structure provided by the capture and docking elements would increase the specific binding capabilities of the structures. The Capture SELEX protocol does not require immobilisation of the target to a support structure. This is advantageous as immobilisation is complex and can change the chemical structure of a target, thereby impeding the oligonucleotide binding as well as creating aptamers unable to bind to a free molecule, (Lyu, Khan and

Wang, 2021). The results seen in Figure 11 demonstrate the ability of the Capture SELEX protocol to successfully retain and amplify binding oligonucleotide sequences. The negative control seen in Figure 11 shows amplification, although the sample did not contain a target for the oligonucleotides to interact with. This demonstrates a problem described in literature with the Capture SELEX methodology, (Lyu, Khan and Wang, 2021). Due to the immobilised library possibly dissociating from the support structure during washing, unbound sequences are retained and amplified resulting in a partial positive, (Lyu, Khan and Wang, 2021). These unbound sequences can occur within the target-library complexes, however, can be screened out following high throughput sequencing analysis as they would appear most likely at low frequency.

Modifications to the original Capture SELEX protocol by Paniel *et al.* (2017) were applied to allow for changes to the gel elution and purification methods. To enable the use of lambda exonuclease as a mechanism to separate dsDNA into ssDNA, the reverse primer was modified to a phosphorylated 5' end. Lambda exonuclease is a highly processive enzyme derived from *E. coli* which digests from the 5' end phosphorylated strand of double stranded DNA. During the digestion the phosphorylated labelled strand is removed, and a single strand of DNA retained. Additional benefits of the use of enzyme digestion during SELEX protocol is the low cost of the enzyme and time efficacy compared to PAGE gel separation techniques, (Avci-Adali *et al.*, 2010). Additionally, enzymatic digestion does not require gel extraction stages, minimising the loss of gel based methods such as PAGE, (Kohlberger and Gadermaier, 2021).

The results seen in Table 6 and Figure 12 demonstrated the suitability of the lambda exonuclease to separate the double stranded DNA into single strands. The use of the enzyme digestion provides for a robust recovery of single stranded DNA for the use in SELEX. The quantification of the oligonucleotides (Table 6) showed that it was possible to recover on average over 50% of the ssDNA from the PCR products. This can be seen in more detail in Figure 12, showing degradation in each Capture SELEX round.

In general, the recovery of the oligonucleotides for T-2 and HT-2 ranged between 40% and 60%. In addition, the use of the enzyme was cost effective and time efficient, allowing for the SELEX process to be completed faster (~45 min) with less equipment and resources when compared to traditional gel elution and separation techniques (~3 days).

At the time of completing this thesis, the use of lambda exonuclease enzyme was the first to be used in the described format within a Capture SELEX process, instead of gel separation and elution. The Capture SELEX protocol described by Paniel *et al.* (2017) did not include next generation sequencing of aptamer candidates through the selection rounds, instead they used a traditional cloning and sequencing method at the final selection round. The cloning and sequencing stages involved several overnight incubations to generate plasmids containing the sequences generated with subsequent extraction and preparation for sequencing. Their method resulted in 20 aptamer candidates which were subsequently trialled in binding assays.

The volume of the retrieved supernatant containing the bound oligonucleotides and target was greater than that required for the use with the PCR ready to go beads (Section 3.2.12). The use of PCR beads had the distinct advantage of reducing the risk of variability during PCR and across rounds as in house prepared master mixes can suffer from high variability and instability. A further reason for not amplifying the full possible pool generated after each selection round was time and cost as a part of the generated sequence pool had to be retained to allow for high throughput sequencing of the individual SELEX rounds. Whilst a necessity of the Capture SELEX methodology is to retain PCR product for further selection rounds it could cause successfully binding aptamer sequences to be left behind in the process. The complete impact of this as well as the success of a SELEX process can only be decided upon evaluation of obtained sequences and binding assessments.

3.5 Conclusion

Chapter 3 of this thesis describes the initial evaluation and use of a traditional SELEX protocol to develop aptamers targeting T-2 and HT-2 mycotoxins. Following the results obtained from the traditional SELEX protocol (no amplification of binding oligonucleotides), the Capture SELEX protocol was chosen for the use and 15 rounds of selection were completed with the aim to develop aptamers with specific binding properties to T-2 and HT-2. Although the sequences of the aptamers generated in each selection round are analysed and discussed in Chapter 4. the results obtained from this part of the thesis highlighted the importance of careful SELEX protocol selection and understanding of their applications.

In addition to the evaluation and use of Capture SELEX as described by Paniel *et al.* (2017), modifications were made to the protocol. Lambda exonuclease was used for enzymatic separation of the dsDNA to ssDNA, instead of the traditional gel elution techniques, providing a faster, simpler, and better performing solution to traditional gel elution methods. Additionally, sequences obtained from the last selection round (round 15) were not cloned and amplified to produce aptamer candidates, instead sequence pools from all rounds were retained for evaluation by high throughput sequencing. At the time of completing this thesis, this was the first reported use of lambda exonuclease in combination with Capture SELEX and retention of sequence pools for next generation sequencing.

Chapter 4. High throughput sequencing for the identification of aptamers

4.1 Introduction

High Throughput Sequencing (HTS) is a DNA sequencing technology allowing for genomic research and most commonly used in clinical and microbiological sciences (Behjati and Tarpey, 2013). The use of HTS in combination with bioinformatic techniques, which have the objective of obtaining fully integrated systems that allow for automated sequencing and characterisation, has become prominent in the development of aptamers (Blind and Blank, 2015). HTS gives the ability to identify a greater number of unique sequences produced through SELEX protocols and allows for more precise aptamer candidate identification, (Komarova, Barkova and Kuznetsov, 2020). Additionally, through the application of HTS to each selection round of the SELEX process, aptamer candidates can be screened more effectively and provide insight into the selection process, (Komarova, Barkova and Kuznetsov, 2020).

Upon completion of the 15 Capture SELEX rounds, described in Chapter 3, HTS of the oligonucleotides was performed, allowing for the identification of each unique oligonucleotide sequence produced and identification of suitable aptamer candidates for application in binding assays. The approach utilised for the characterisation of the sequences described in this chapter was through amplicon sequencing on an Illumina MiSeq sequencer and different bioinformatic analysis approaches.

The specific use of HTS analysis in combination with Capture SELEX has been infrequently described in the literature. Spiga (2015) and colleagues describe the use of HTS and surface plasmon resonance to obtain a DNA-based aptamer for tobramycin. Lu *et al.* (2020) proposed an aptamer selection, targeting Di(2-ethylhexyl) phthalate (DEHP, a food packaging additive) based on a combination of HTS of the SELEX rounds, as well as monitoring of each round through qPCR.

HTS has been used more frequently for a wider range of targets, partly due to the reduction in cost of the technique, as well as the efficacy of aptamer screening, (Komarova, Barkova and Kuznetsov, 2020). Whilst the focus of HTS has been on the selection of DNA aptamers, Mukherjee *et al.* (2022) demonstrated its application to the identification of RNA aptamers binding to CMBL3aL (cyclic mismatch binding ligand).

The combined use of Capture SELEX and HTS to obtain aptamers that target mycotoxins, specifically T-2 and HT-2, has not yet been reported in the literature. The aim of the HTS was the identification of unique sequences developed within each Capture SELEX round, thereby identifying aptamer candidates. This allowed for an in-depth analysis of the unique sequences developed throughout the Capture SELEX protocol.

4.2 Methods

4.2.1 Capture SELEX generated sequence preparation for high throughput sequencing

The forward primer (747.1nmol) and reverse primer (876.5nmol) sequences used during MiSeq sequencing were supplied on a 1µmol scale. The forward primer and reverse primer were reconstituted in deionised water to 100µM.

The supernatant collected during the Capture SELEX rounds (20µL) was added to 1µL forward primer and 1µL reverse primer with 3µL sterile deionised water in a pre-prepared Ready-to-Go PCR bead tube (GE Healthcare). A positive control was included consisting of original oligonucleotide library sequence, forward and reverse primers. The mix was vortexed briefly and the tube was placed in the thermocycler after the bead had dissolved fully, indicated by the settling of foam inside the tube.

The PCR cycle conditions were:

Denaturation, 1 x 95°C for 5min
Followed by 30 cycles of;
Denaturation, 1 x 95°C for 1min
Annealing, 1 x 51°C for 1min
Extension, 1 x 72°C for 1min
Followed by;
Final Extension, 1 x 72°C for 10min
Final Holding Temperature, ∞4°C

Following PCR amplification, 5µL of the product was mixed with 2µL of loading dye. The mix was pipetted into the wells of the prepared 2% agarose gel, 2.4g of agarose powder dissolved in 120mL of 1xTBE buffer (0.89M Tris-borate, 0.89M Boric acid, 0.02M EDTA with 5µL gel red), heated to dissolve and set in a wide mini sub cell GT gel tray at room temperature. A 100bp DNA ladder was added for reference. The agarose gel was placed in a wide mini-sub cell GT cell gel tank filled with 1xTBE buffer and run at 85V for 35min using a PowerPac. The agarose gel was visualised under the transilluminator to identify band locations.

4.2.2 High throughput sequencing of the generated sequences for the selection of aptamer candidates

The oligonucleotides obtained from the Capture SELEX protocol were utilised by Chris Conyers at Fera Science Ltd following internal standard operating procedures. The methodology was performed by Fera Science Ltd member of staff, due to the specialised facilities, training and equipment required. The preparation of the obtained PCR amplicons for sequencing required a clean-up and indexing stage. Clean-up of the PCR product was performed utilising AMPure XP beads to remove any contamination arising from the PCR amplification process.

Following the clean-up step, the process required the utilisation of the Illumina Nextera® DNA (now Illumina DNA Prep) Unique Dual Indexes set. The dual indexed workflow adds two distinct Index oligonucleotide sequences which allows for the generation of uniquely tagged libraries which can be read during the sequence run of the MiSeq instrument. Following indexing, PCR amplicons were again cleaned with magnetic beads. Cleaned, indexed PCR products were then run on an Illumina MiSeq sequencer using Reagent Kit V3.

4.2.3. Bioinformatic analysis of sequences generated for the selection of aptamer candidates

The initial analysis of the sequence data using the bioinformatics packages was performed by Fera Science member of staff Sam McGreig, because specialist training and software were required. The sequence data obtained from the MiSeq sequence run was analysed using the Qiime2® bioinformatics package. The primers were trimmed with cutadapt (a software function), before the sequences were de-noised with DADA2 program, Martin (2011) and Callahan *et al.* (2016). The unique sequences were extracted into an Excel spreadsheet, together with information concerning their frequency of occurrence, Capture SELEX round and replication. The extracted sequencing data presented in this chapter was provided by Sam McGreig in two formats on Excel spreadsheets. The first format was the combined data set (Section 4.2.4) of all sequences generated during the MiSeq sequencing run consolidated across Capture SELEX rounds. The second format was a filtered data set (Section 4.2.5), composed of all sequences generated within each replication (A, B and C), for each Capture SELEX round, after application of the aptamer acceptability criteria described in Section 4.2.4.

4.2.4 Combined Format sequence categorisation and evaluation

In the first stage of the data categorisation and evaluation, all unique sequences were labelled with a name to allow for easy identification. The labelling was from the top of the first unique sequence to the last, starting with Apta20-01 and ending at Apta20-21978.

The combined data set provided by Sam McGreig was further separated into Excel spreadsheets based on Capture SELEX protocols specific to T-2 and HT-2 and specific sheets for each round of selection.

Once the data had been categorised, the cell containing the oligonucleotide sequence was split into individual cells, displaying each nucleotide in order per cell. This was performed by selecting the Text to Column button in the Data ribbon and following the on-screen instructions. Each individual nucleotide was assigned the sequential position starting from 1 to 62 and a filter was applied to the labels allowing for evaluation of the fixed capture region (position 11 to 22).

In the evaluation stage, all sequences with more than 62 base pairs overall were disqualified, as were any sequences with more than 10 base pairs before the fixed capture region. The fixed capture region (nucleotide positions 11 to 22) was evaluated, and sequences showing variation from the fixed capture region at the base pair position were disqualified. The accepted unique sequences were within the acceptability criteria of sequence length of 62 base pairs and no variation to the capture region.

Following the evaluation, the non-disqualified unique sequences (accepted unique sequences) were sorted by total frequencies starting from highest to lowest using the Excel feature in the Data ribbon. The aim was to identify the unique sequences that occurred most frequently or at highest abundance within a selection round. The percentage abundance of each unique sequence within the round was calculated by dividing the total frequency value of a unique sequence by the total sum frequency of all unique sequences and multiplying by 100. From these calculations, the unique sequences which comprised the top 50% most abundant sequences in each round could be identified and were designated aptamer candidates and were within the acceptability criteria set.

Further evaluation was conducted on the separated A, C, T and G cells of the unique sequences. The Excel COUNTIF function was used to identify each base pair at each sequence position. This allowed for the calculation of percentage similarity of the aptamer candidates.

4.2.5 Filtered Format sequence categorisation and evaluation

The filtered data sets in the Excel spreadsheets provided by Sam McGreig had the three acceptability criteria pre-applied bioinformatically. Subsequently, the sequences found in each replicate (A, B and C) had to be matched manually to the label assigned in Section 4.2.4. The search and find function in Excel was used to match the sequence to the label. This was an important step to allow for identification and cross-referencing of the unique sequences. Following the matching of the labels, the data was separated into sets per replication (A, B and C) across the Capture SELEX rounds.

4.2.6 Phylogenetic tree construction using MEGA software

The phylogenetic trees of the aptamer sequences obtained from the filtered data format were constructed using the MEGA 11 software, (Tamura, Stecher and Kumar, 2021). The sequences were automatically aligned through the Muscle function and the trees constructed using the option for Neighbor-Joining (NJ) Tree, (Saitou and Nei, 1987). The percentage of replicate trees in which the associated taxa clustered together in the bootstrap test (1000 replicates) are shown next to the branches, (Felsenstein, 1985). The tree is drawn to scale, with branch lengths in the same units as those of the evolutionary distances used to infer the phylogenetic tree. The evolutionary distances were computed using the p-distance method and are in the units of the number of base differences per site, (Nei and Kumar, 2000).

4.3 Results

All the unique sequences identified during the MiSeq run and subsequent bioinformatic data analysis were evaluated using three acceptability criteria as described in Section 4.2.4 and Section 4.2.5, with the aim of identifying aptamer candidates to be trialled in a binding assay (Chapter 5). Additionally, the evaluation of the unique sequences obtained through the HTS method provided information on the evolution and selection of sequences that occurred during the Capture SELEX protocol, allowing for an improved insight into the selection process.

4.3.1 Evaluation of combined T-2 sequences

The total number of unique sequences found in each Capture SELEX round targeting T-2 mycotoxin, before and after application of the two acceptability criteria (Section 4.2.4), are shown in Table 7.

Capture SELEX Round	Total Number of unique sequences	Sequence length more than 62 base pairs	Variation in capture region	Total number of unique sequences retained	Percentage of sequences excluded
1	2	0	1	1	50
2	4609	162	22	4425	3
3	10	4	1	5	50
4	53	10	7	36	32
5	50	8	8	34	32
6	138	22	13	103	25
7	117	25	10	81	30
8	88	6	13	69	21
9	113	9	14	90	20
10	86	11	10	65	24
11	51	9	2	40	21
12	38	5	1	32	15
13	41	4	2	35	14
14	36	5	0	31	13
15	42	5	2	35	16
				Average exclusion	24

Table 7 The unique sequences identified during the MiSeq run on the Capture SELEX round samples targeting T-2 mycotoxin, and the number of unique sequences discarded due to each acceptability criterion.

The application of the two acceptability criteria resulted in a reduction of the total number of unique sequences seen within each Capture SELEX round. The process showed that in each round of the Capture SELEX protocol unique sequences had undergone structural changes to the defined capture region and were longer than the defined 62 base pairs. The exception being Capture SELEX round 1, in which one sequence was excluded due to capture region variation and not a length beyond 62 base pairs.

These unique sequences were further evaluated to identify their percent abundance within each selection round (Section 4.2.4) and establish which unique sequences formed the top 50% most abundant sequences within a selection round and were thus suitable for consideration as aptamer candidates.

4.3.2 Frequency of combined T-2 sequences

The unique sequences with a percentage abundance greater than 50% (aptamer candidates) found across the 15 rounds of Capture SELEX targeting the T-2 mycotoxin are recorded in Table 8. A total of 12 aptamer candidates were identified: Apta20-89, Apta20-21974, Apta20-21975, Apta20-91, Apta20-02, Apta20-05, Apta20-04, Apta20-56, Apta20-01, Apta20-03, Apta20-06 and Apta20-15.

Aptamer Label	Sequence
Apta20-01	ACCCAATATA**TGAGGCTCGATC**AACAGTGTTCTTGATATCACGTCCCTTAACTGGTAGGGTC
Apta20-02	CTAAGCATCT**TGAGGCTCGATC**TATTTTATTTCCCCGAATTCGGGATAACTATAATCCGACA
Apta20-03	GACAAGTTAT**TGAGGCTCGATC**TTTCGTTCGCGCGCGTGCTTCGTCGCATTGACGTCTATCA
Apta20-04	CATCCGACCA**TGAGGCTCGATC**CAGCATGTTTTATCAATGGGACATCGGGTCCTTTTGTGAA
Apta20-05	GACGGGCCAC**TGAGGCTCGATC**CTTGCTTTGTTCAGCGGCCAACATTAATCATTGCCTTGTA
Apta20-06	ACAGATTTGC**TGAGGCTCGATC**TCATCTGGTCTGAATAGGTAATAGCGGTTATTGTTTAAGA
Apta20-15	TAAGGTTCCG**TGAGGCTCGATC**AACTGTACACATCAACATCACACAATTATTCATATCACAA
Apta20-21974	AAACTATCCA**TGAGGCTCGATC**ACATCCTTGGTATAAGATAGAATATTAATCACCGTCGTAT
Apta20-21975	GATACAACAG**TGAGGCTCGATC**AACTAACTATGTTGATCGATTTCCATAGTTTAATTTTAGA
Apta20-56	AAGTGGTATA**TGAGGCTCGATC**TCAACAGGAGTCTTTTCAGAAGAAGAAGAAAATTCAATAT
Apta20-89	CTAAGCATCT**TGAGGCTCGATC**TATTTTATTTCCCCGAATTCGGGATAACTATAATCCGGCA
Apta20-91	TATTAATGGT**TGAGGCTCGATC**CCTTGATGCTAATCCAGGCTAATCACGAGTTAAAGTCTCG

Table 8 Candidate aptamers from the T-2 selection process. The capture regions are highlighted in bold.

Apta20-01 was seen within the 50% most abundant unique sequences in rounds 9, 10, 11, 12, 13, 14 and 15. The unique sequence was not seen in rounds 1 to 8 either within or outside of the 50% most abundant unique sequences cut-off criterion.

Apta20-02 was seen within the 50% most abundant unique sequences in rounds 4,5, 6, 7, 9, 10, 11, 12, 13, 14 and 15. The unique sequence was not seen in rounds 1 to 3 either within or outside of the 50% most abundant unique sequences cut-off criterion. The unique sequence was seen within round 8 outside of the cut-off criterion.

Apta20-03 was seen within the 50% most abundant unique sequences in round 10. The unique sequence was not seen in rounds 1 to 8 either within or outside of the 50% most abundant unique sequences cut-off criterion. The unique sequence was seen within rounds 9, 11, 12, 13, 14 and 15 outside of the cut-off criterion.

Apta20-04 was seen within the 50% most abundant unique sequences in rounds 6 to 14. The unique sequence was not seen in rounds 1, 2, 3, 5 and 15 either within or outside of the 50% most abundant unique sequences cut-off criterion. The unique sequence was seen within round 4 outside of the cut-off criterion.

Apta20-05 was seen within the 50% most abundant unique sequences in rounds 4, 5, 10 and 11. The unique sequence was not seen in rounds 1 to 3 either within or outside of the 50% most abundant unique sequences cut-off criterion. The unique sequence was seen within rounds 6, 7, 8, 9, 12, 13, 14 and 15 outside of the cut-off criterion.

Apta20-06 was seen within the 50% most abundant unique sequences in rounds 11 and 12. The unique sequence was not seen in rounds 1 to 8 either within or outside of the 50% most abundant unique sequences cut-off criterion. The unique sequence was seen within rounds 9, 10, 13, 14 and 15 outside of the cut-off criterion.

Apta20-15 was seen within the 50% most abundant unique sequences in round 13. The unique sequence was not seen in rounds 1 to 8 either within or outside of the 50% most abundant unique sequences cut-off criterion. The unique sequence was seen within rounds 9, 10, 11, 12, 14 and 15 outside of the cut-off criterion.

Both Apta20-21974 and Apta20-21975 were seen within the 50% most abundant unique sequences in round 3. The unique sequences were not seen in rounds 1 to 2 and 4 to 15 either within or outside of the 50% most abundant unique sequences cut-off criterion.

Apta20-56 was seen within the 50% most abundant unique sequences in rounds 8, 12 and 15. The unique sequence was not seen in rounds 1 to 3 either within or outside of the 50% most abundant unique sequences cut-off criterion. The unique sequence was seen within rounds 4, 5, 6, 7, 9, 10, 11, 13, 14 and 15 outside of the cut-off criterion.

Apta20-89 was seen within the 50% most abundant unique sequences in round 1. The unique sequence was not seen in rounds 2 to 3 and 11 to 15 either within or outside of the 50% most abundant unique sequences cut-off criterion. The unique sequence was seen within rounds 4, 5, 6, 7, 8, 9 and 10 outside of the cut-off criterion.

Apta20-91 was seen within the 50% most abundant unique sequences in rounds 4, 6 and 7. The unique sequence was not seen in rounds 1, 2, 3, 8, 10, 11, 12, 13 and 14 either within or outside of the 50% most abundant unique sequences cut-off criterion. The unique sequence was seen within rounds 5, 9 and 15 outside of the cut-off criterion.

The evaluation of the unique sequences and their appearance across the Capture SELEX rounds (within the 50% most abundant sequence cut-off criterion and outside of the criterion), allowed for further understanding and evaluation of their distribution. Figure 13 shows this distribution or appearance pattern of the 50% most abundant sequences. Additionally, in contribution to the population tracing, the unique sequences appearing outside of the 50% cut-off criteria have been included.
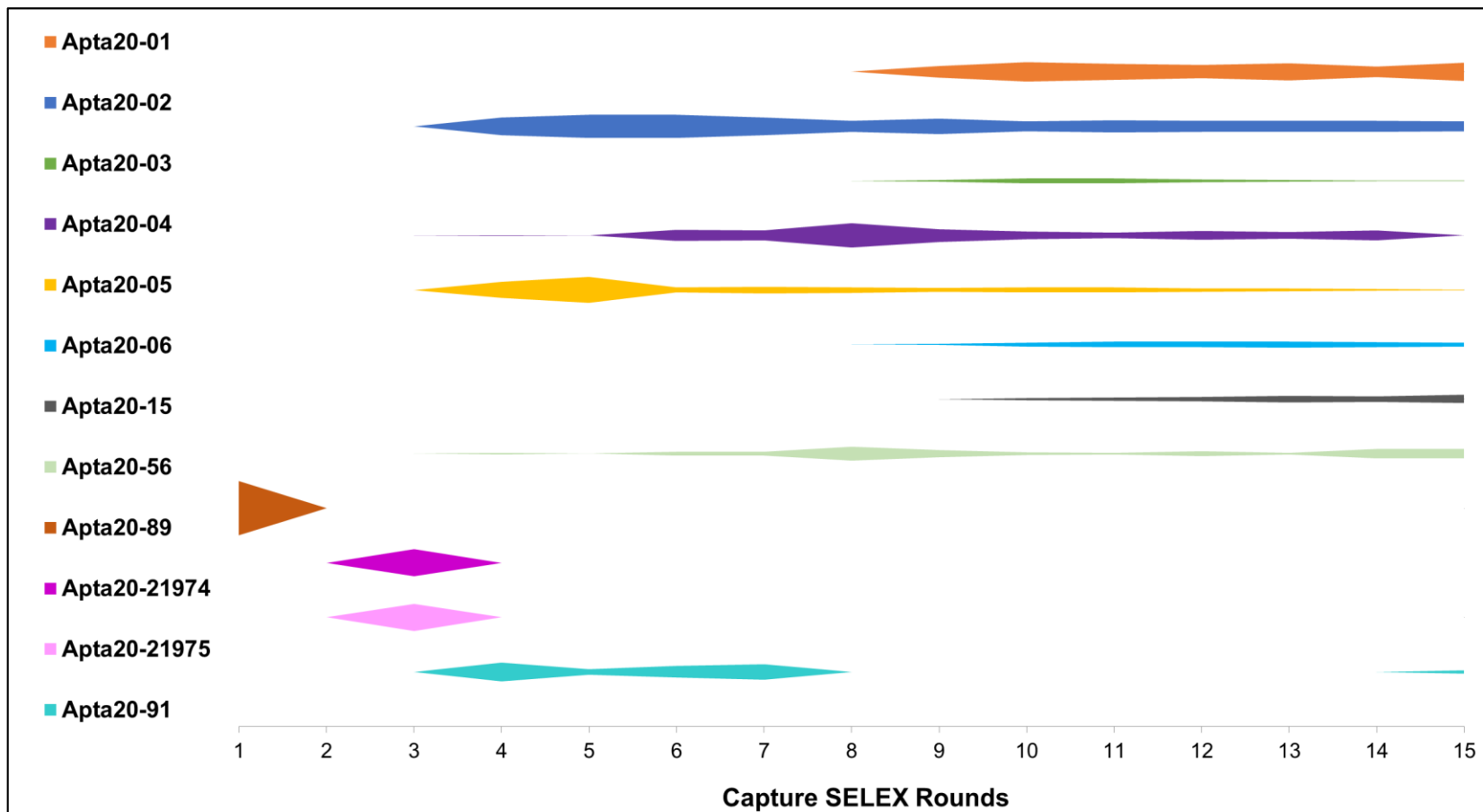
Figure 13 Aptamer population tracing of the 12 aptamer candidates identified through the application of the 50% most abundant acceptability criteria. The unique sequence distribution is shown across all rounds of the Capture SELEX process including their appearance within and outside of the 50% cut-off.

Figure 13 shows the distribution or appearance pattern of the 12 aptamer candidates identified using high throughput sequencing and subsequent evaluation. The size of the diagram bar represents the frequency. Apta20-01, Apta20-02, Apta20-03, Apta20-04, Apta20-05, Apta20-06, Apta20-15 and Apta20-56 can be seen to be most prominent throughout the majority of the Capture SELEX rounds, whereas Apta20-21974 and Apta20-21975 were exclusively seen in single rounds of the selection process. Apta20-91 can be observed to populate the middle selection rounds of the process, as well as the final round. It needs to be highlighted that due to the nature of the kite diagram presented above, Apta20-89 appears to be observed in Capture SELEX round 1 only however the raw data shows a very low frequency occurrence in other rounds which cannot be represented on the graphic.

4.3.3 Evaluation of combined HT-2 sequences

The total number of unique sequences found in each Capture SELEX round targeting HT-2 mycotoxin, before and after application of two acceptability criteria (sequence length beyond 62 base pairs and variation in capture region) are shown in Table 9.

Capture SELEX Round	Total Number of unique sequences	Sequence length more than 62 base pairs	Variation in capture region	Total number of unique sequences retained	Percentage value of sequences excluded
1	2	1	0	1	50
2	16315	444	209	15662	4
3	3	1	2	0	100
4	53	0	2	51	3
5	23	4	2	17	26
6	153	4	19	130	15
7	97	4	16	83	14
8	597	25	46	526	11
9	227	8	219	205	9
10	212	16	30	166	21
11	219	17	25	177	19
12	151	4	13	124	17
13	57	5	5	47	17
14	66	9	4	53	19
15	93	14	5	74	20
				Average exclusion	23

Table 9 The unique sequences identified during the MiSeq run on the Capture SELEX round samples targeting HT-2 mycotoxin, and the number of unique sequences discarded due to each acceptability criterion.

The application of the two acceptability criteria resulted in a reduction of the total number of unique sequences seen within each Capture SELEX round. The process showed that in each round of the Capture SELEX protocol, the unique sequences had undergone structural changes to the defined capture region and were longer than the defined 62 base pairs, as seen in the evaluation of the T-2 data (Section 4.3.2). The exception was Capture SELEX round 1, in which one sequence was excluded due to a length beyond 62 base pairs and not for a variation in the capture region. In SELEX round 3, all the 3 unique sequences seen were excluded due to changes in the capture region and differences in length, resulting in no sequence being accepted in that round from the application of the acceptability criteria.

These unique sequences were further evaluated to identify their percent abundance within each selection round (Section 4.2.4) and establish which unique sequences (aptamer candidates) formed the top 50% most abundant sequences within a selection round.

Table 10 summarises the unique sequences that exhibited an abundance of greater than 50% across the 15 rounds of Capture SELEX targeting HT-2 mycotoxin, along with the sequence description. In total, 9 aptamer candidates were identified which matched the 3 acceptability criteria: Apta20-100, Apta20-106, Apta20-107, Apta20-108, Apta20-23, Apta20-49, Apta20-57, Apta20-90 and Apta20-93.

Aptamer Label	Sequence
Apta20-100	TCCCTCCCTT**TGAGGCTCGATC**GTCAAGCCACCTGGCAATTTCATAACTCTCATGTTTTACG
Apta20-106	TCCCCAAAAA**TGAGGCTCGATC**ACTATATAAACTAGCACTACACTGCCAGGTCCCTGAGGTC
Apta20-107	GCGATATCCT**TGAGGCTCGATC**AGATCGGTAGATCTTCTTTTTATCTCTAAATCCTTCATTG
Apta20-108	GCGAACATCC**TGAGGCTCGATC**TACTAACTATTCTTTTTACGCAACTGTTCGTATGTGCAAT
Apta20-23	AGCGTATTTT**TGAGGCTCGATC**TGTAAACCACTAACATTGTCAATCTACTATTCTCGGGCAA
Apta20-49	GACTCACACC**TGAGGCTCGATC**ATCCCATAGTGGCACTTTGTTGTCTATACTATAATATAAA
Apta20-57	AACATTACGG**TGAGGCTCGATC**GCCTACAATATCCAAAATACACTTTCATATCTATCGGATC
Apta20-90	GCTTCTTCAT**TGAGGCTCGATC**GTTTTATCGAAACAAATTTAGCTAGGGCATTACGCGCTCA
Apta20-93	CATAAGAATG**TGAGGCTCGATC**CCACAGATTATATGATTCTAGGCTGTCGTTGTAAGATTGT

Table 10 Candidate aptamers from the HT-2 selection process. The capture regions are highlighted in bold.

Apta20-100 was seen within the 50% most abundant unique sequences in rounds 6 and 7. The unique sequence was not seen in rounds 1 to 3 and 15 either within or outside of the 50% most abundant unique sequences cut-off criterion. The unique sequence was seen within rounds 4, 5, 8, 9, 10, 11, 12, 13 and 14 outside of the cut-off criterion.

Apta20-106, Apta20-107 and Apta20-108 were seen within the 50% most abundant unique sequences in round 15. The unique sequence was not seen in rounds 1 to 7 either within or outside of the 50% most abundant unique sequences cut-off criterion. The unique sequence was seen within rounds 8 to 14 outside of the cut-off criterion.

Apta20-23 was seen within the 50% most abundant unique sequences in rounds 9, 12 and 13. The unique sequence was not seen in rounds 1 to 3 either within or outside of the 50% most abundant unique sequences cut-off criterion. The unique sequence was seen within rounds 4, 5, 6, 7, 8, 10, 11, 14 and 15 outside of the cut-off criterion.

Apta20-49 was seen within the 50% most abundant unique sequences in rounds 4, 9, 11, 12 and 13. The unique sequence was not seen in rounds 1 to 3 either within or outside of the 50% most abundant unique sequences cut-off criterion. The unique sequence was seen within rounds 5, 6, 7, 8, 10, 14 and 15 outside of the cut-off criterion.

Apta20-57 was seen within the 50% most abundant unique sequences in rounds 10 to 15. The unique sequence was not seen in rounds 1 to 3 either within or outside of the 50% most abundant unique sequences cut-off criterion. The unique sequence was seen within rounds 4 to 9 outside of the cut-off criterion.

Apta20-90 was seen within the 50% most abundant unique sequences in rounds 1, 8, 9, 10 and 14. The unique sequence was not seen in rounds 2 to 4 either within or outside of the 50% most abundant unique sequences cut-off criterion. The unique sequence was seen within rounds 5, 6, 7, 11, 12, 13 and 15 outside of the cut-off criterion.

Apta20-93 was seen within the 50% most abundant unique sequences in round 5. The unique sequence was not seen in rounds 1 to 3 either within or outside of the 50% most abundant unique sequences cut-off criterion. The unique sequence was seen within rounds 4 and 6 to 15 outside of the cut-off criterion.
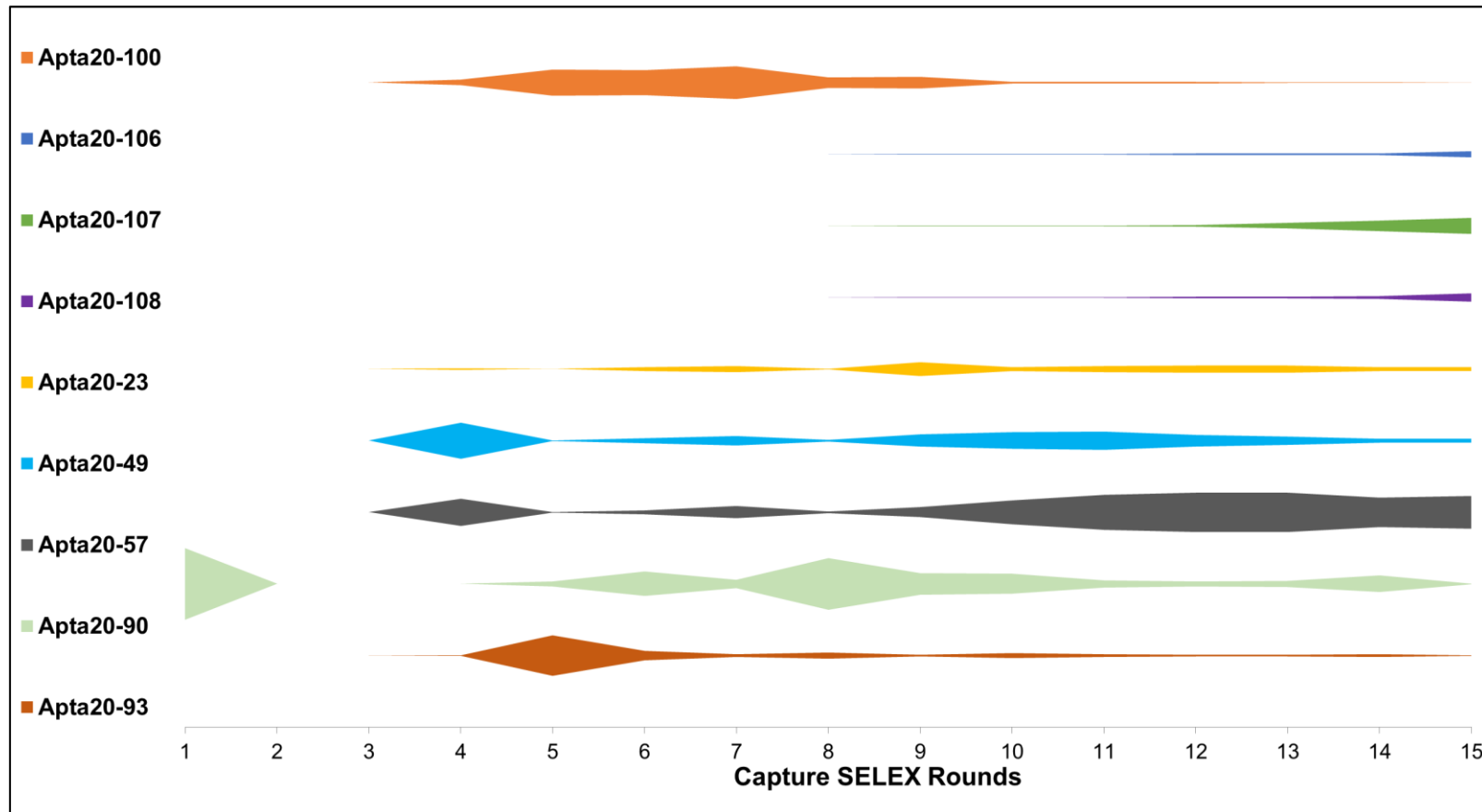
Figure 14 Aptamer population tracing of the 9 unique sequences identified through the application of the 50% most abundant acceptability criteria. The unique sequence distribution is shows across all rounds of the Capture SELEX process including their appearance within and outside of the 50% cut-off.

The evaluation of the HT-2 related aptamer candidates and their appearance across the Capture SELEX rounds (both within the 50% most abundant sequence cut-off criterion and outside), allowed for further understanding and evaluation of their distribution or appearances across the selection process. Figure 14 shows the population tracing of the 50% most abundant sequences. As with the T-2 related unique sequences data, information of the HT-2 unique sequences appearing outside of the 50% cut-off criteria have been included. The size of the diagram bar representing the frequency.

The unique sequences can be seen appearing throughout the Capture SELEX process with the exceptions of rounds 1 to 3. Only Apta20-90 appears in selection round 1, it does however occur throughout the middle and later stages of selection. Apta20-106, Apta20-107 and Apta20-108 appear most prominently in selection round 15. Apta20-100 appears within the middle rounds, like Apta20-23, Apta20-49, Apta20-57 and Apta20-93.

4.3.4 Filtered Format sequence evaluation of T-2 sequences

The above-described evaluation (Section 4.3.3) for combined sequences for both T-2 and HT-2 related unique sequences looked at the three replications per target mycotoxin per round in a combined pool of sequences. Whilst this provided an overview of the unique sequences for each target, the approach could not show evaluation of the sequences within replications (A, B and C).

Within each Capture SELEX round, each replication was as a sample carried through the 15 rounds. Therefore, an analysis was carried out to review the sequences within replicates based on the methodology described in Section 4.2.5. The results provide information of the unique sequences found within each replication, their distribution or appearance across the selection rounds as well as across replications.

SELEX Round	Replicates		
	T-2 mycotoxin NGS ID		
	A	B	C
1	11	12	13
2	21	22	23
3	31	32	33
4	41	42	43
5	51	52	53
6	61	62	63
7	71	72	73
8	81	82	83
9	91	92	93
10	101	102	103
11	111	112	113
12	121	122	123
13	131	132	133
14	141	142	143
15	151	152	153

Table 11 Summary of the naming convention used for replicates and their identification numbers used for the filtered analysis.
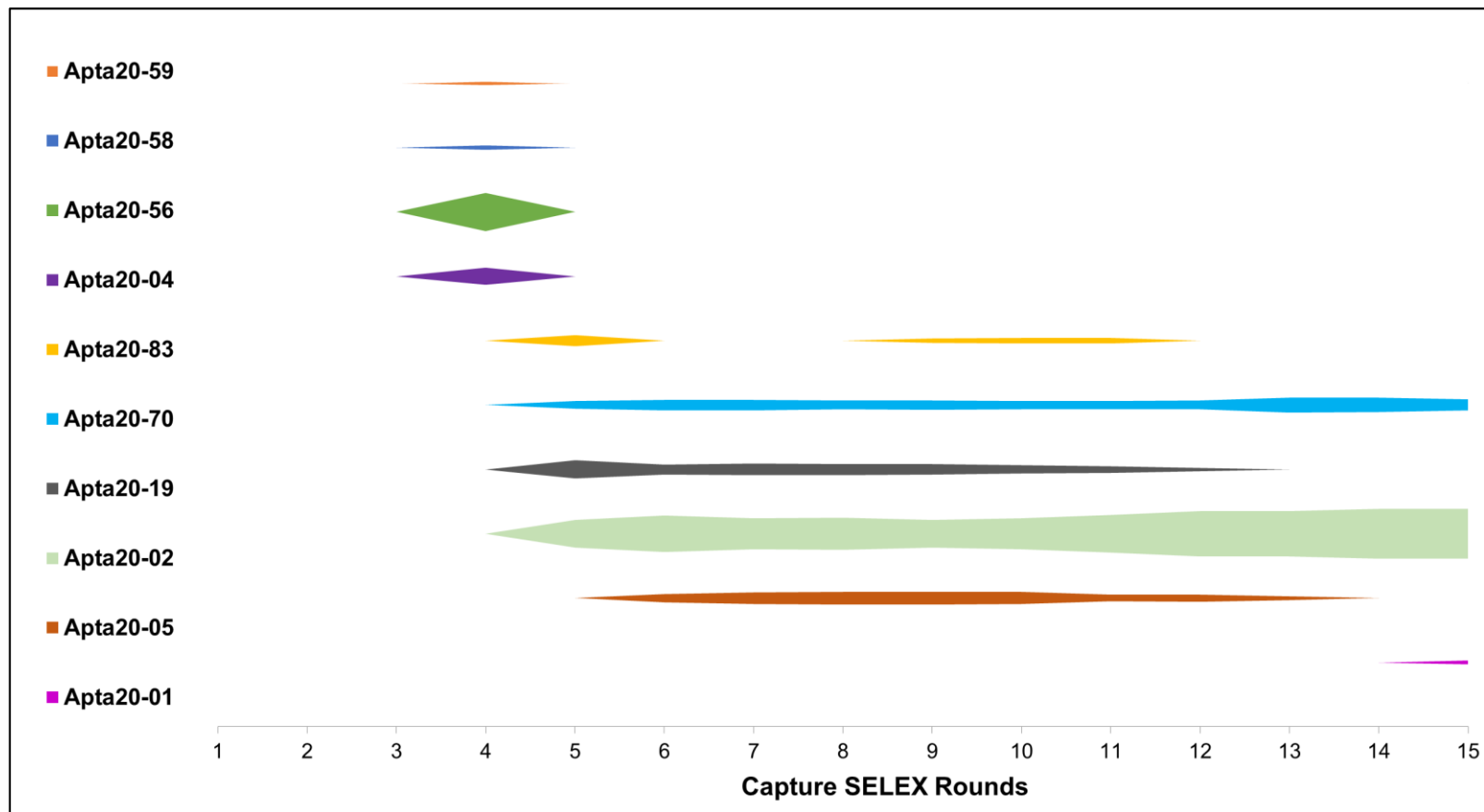
Figure 15 Aptamer population tracing of the 10 unique sequences identified through the evaluation of the filtered format data obtained through replication A of the T-2 Capture SELEX process.
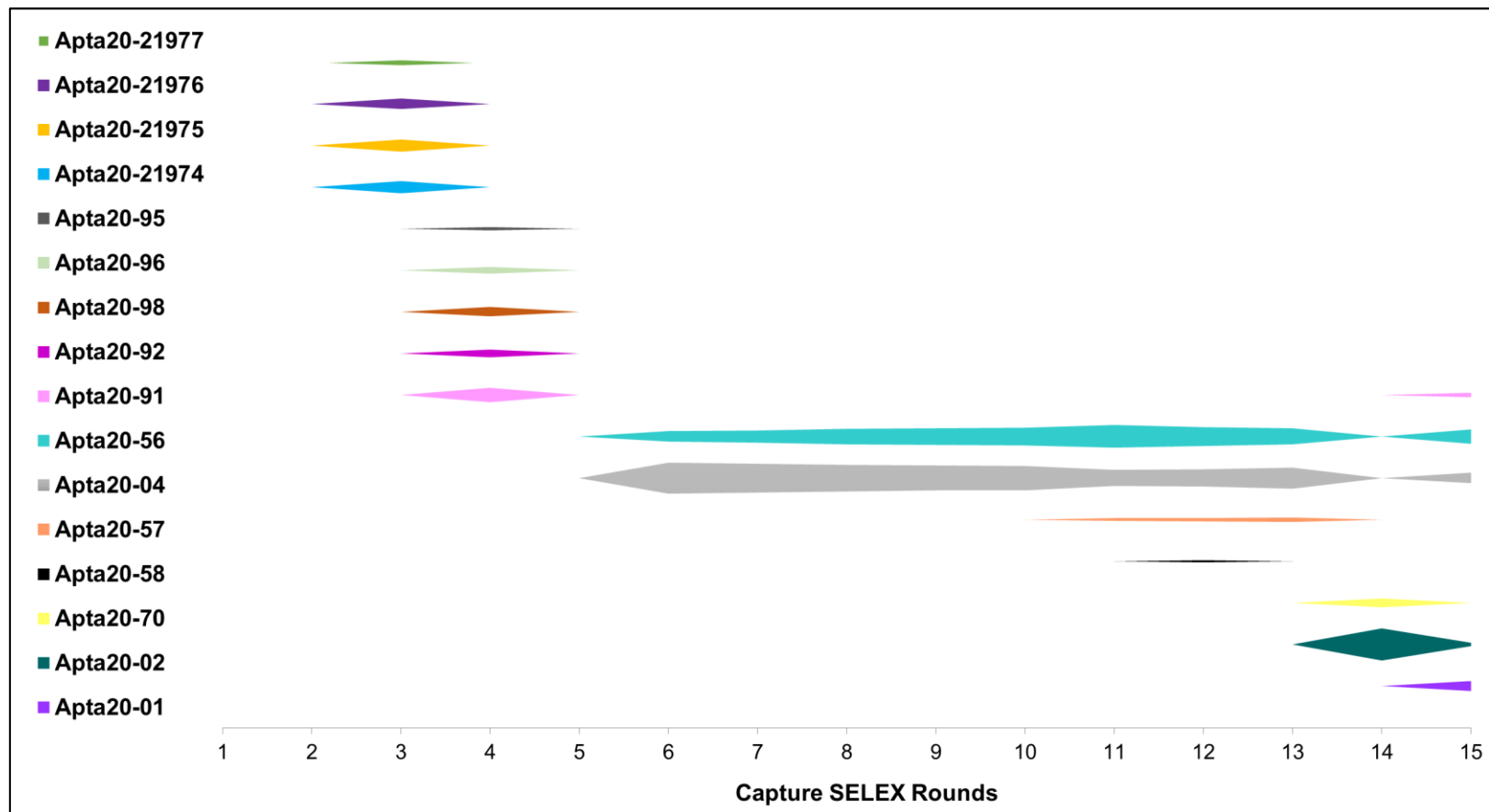
Figure 16 Aptamer population tracing of the 16 unique sequences identified through the evaluation of the filtered format data obtained through replication B of the T-2 Capture SELEX process.
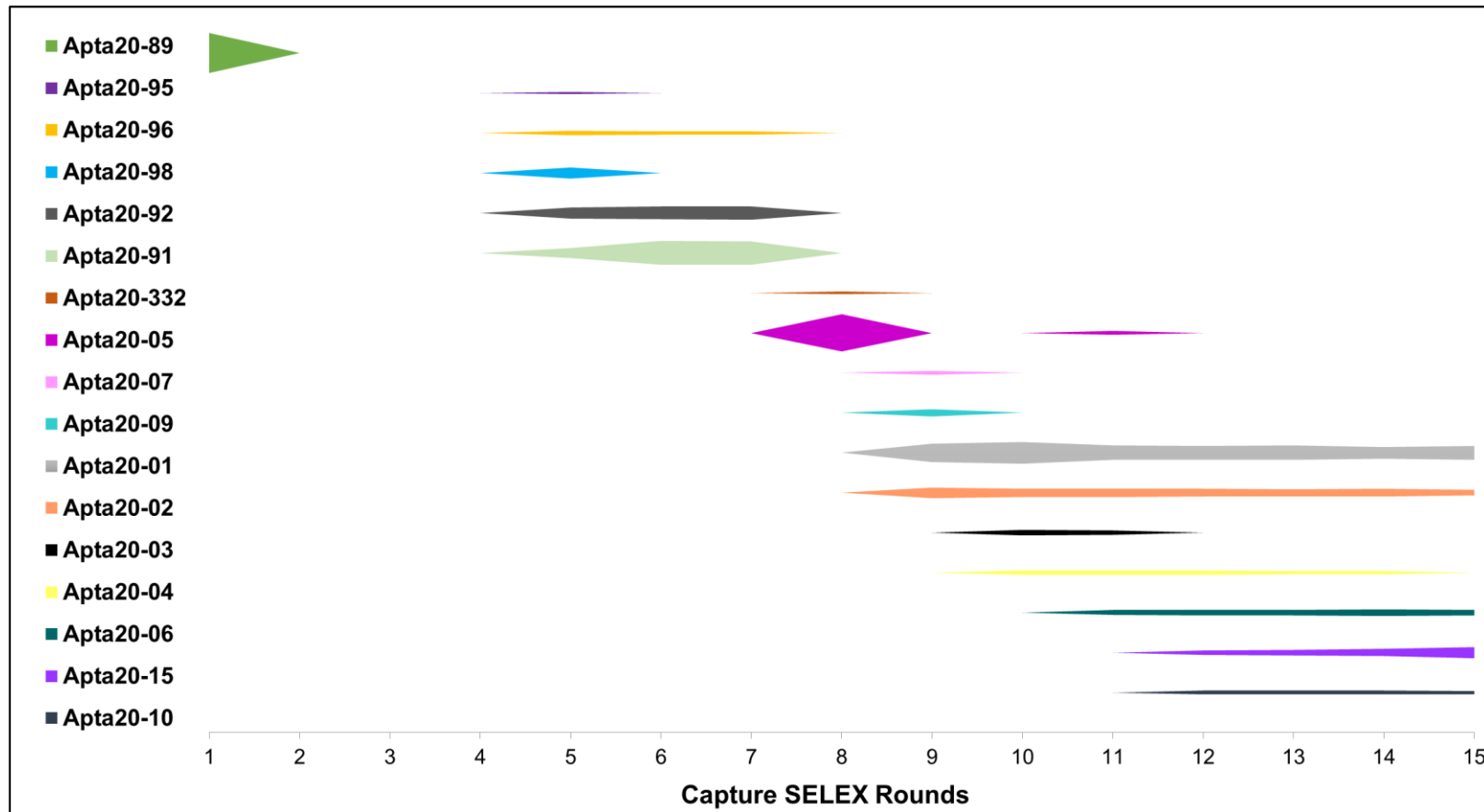
Figure 17 Aptamer population tracing of the 17 unique sequences identified through the evaluation of the filtered format data obtained through replication C of the T-2 Capture SELEX process.

The evaluation of the filtered format data (Figures 15, 16 and 17) shows the aptamer candidates within each replication (A, B and C) obtained through the application of the three acceptability criteria and their appearance across the Capture SELEX selection rounds. Through the evaluation 14 unique sequences were found which were not found within the combined data set analysis. These unique sequences are described below in Table 12. The unique sequences observed in the combined data set can be linked to a particular replication or several replications.

Figure 15 showing replication A, 10 unique sequences were found of which Apta20-59, Apta20-58, Apta20-56 and Apta20-04 can be seen to be present in single rounds (round 4 only) as well as Apta20-01 seen in round 15 only. Apta20-83, Apta20-70, Apta20-19, Apta20-02 and Apta20-05 can be seen distributed across the Capture SELEX rounds. Of the unique sequences seen within the figure Apta20-01 and Apta20-02 and Apta20-56 can also be seen in the combined format data evaluation.

Figure 16 showing replication B, 16 unique sequences were found of which Apta20-21977, Apta20-21976, Apta20-21975, Apta20-21974 and Apta20-95, Apta20-96, Apta20-98, Apta20-92 can be seen to appear in single rounds only, rounds 3 and 4 respectively. Apta20-91 can be seen distributed in rounds 4 and 15. Apta20-56 and Apta20-04 can be seen to be distributed or appear across the selection rounds starting from round 5. Apta20-57, Apta20-58, Apta20-70, Apta20-02 and Apta20-01 can be seen in the later stages of the selection process in either single or couple of rounds. Apta20-21974, Apta20-21975, Apta20-01, Apta20-02, Apta20-91, Apta20-56 and Apta20-04 can be seen in both the combined format data and in the replication B.

Figure 17 showing the replication C, 17 unique sequences were found of which Apta20-89 can be seen exclusively in round 1. Apta20-95, Apta20-96, Apta20-98, Apta20-92, Apta20-91 can be seen to be distributed or appear in the rounds 4 to 7. Apta20-322 can be seen in selection round 8 only as Apta20-07 and Apta20-09 in round 9 only. Apta20-05 and Apta20- 03 can be seen within two rounds, 8 and 11 and 10 and 11 respectively. Apta20-01, Apta20-02, Apta20-04, Apta20-06, Apta20-15 and Apta20-10 can be seen distributed across the later selection rounds. Apta20-89, Apta20-01, Apta20-02, Apta20-03, Apta20-04, Apta20-05, Apta20-06, Apta20-15 and Apta20-91 can be seen in both the combined format and in replication C.

Cross-reviewing the replications A, B and C, several of the unique sequences are present across the replications and others do not appear. Apta20-59 and Apta20-83 are solely observed in replication A. Apta20-21977, Apta20-21976 are solely seen in replication B and Apta20-332, Apta20-07, Apta20-10 and Apta20-09 can be seen in replication C. However, these unique sequences can be found in the combined format data outside of the 50% most abundant unique sequence acceptability criterion. Apta20-58, Apta20-56, Apta20-04, Apta20-70, Apta20-02 and Apta20-01 can be observed in replication A and B. Apta20-04, Apta20-02, Apta20-05 and Apta20-01 can be seen in replications A and C. Apta20-95, Apta20-96, Apta20-98, Apta20-92, Apta20-91, Apta20-04, Apta20-02 and Apta20-01 can be seen in replications B and C.

Aptamer Label	Sequence
Apta20-59	CTGCTACTGA**TGAGGCTCGATC**CTACGATCGTCCCTCTCCTAAATGTCACTTCCGTCCTACG
Apta20-58	TCTTTGACGG**TGAGGCTCGATC**CTTAGTCCCCTTACAGACCGGTTTATAGAACATGGGTAAG
Apta20-83	CTCGTTTCTT**TGAGGCTCGATC**ACTAGTTCTTTTTATAAGTGTTACAATACGCATTGGGGCT
Apta20-70	AACTAAAATT**TGAGGCTCGATC**TACACACTTGGGTTTTCCATCACAAAACAATTGGCTATTT
Apta20-19	GAGGTACTTT**TGAGGCTCGATC**AGACATTTACTTGTCACAAGGACATCCGGTTCGGGCCCTT
Apta20-21977	AAATATCGCT**TGAGGCTCGATC**TCTCTTGGGAATTGCATCGGCTCCCTAGCAAGGAAATATA
Apta20-21976	TTTATCTTTA**TGAGGCTCGATC**TCAAAATGCCCCGACGAAGGCGCGCATAATCCTAACGAGC
Apta20-95	ATTTCGCTAT**TGAGGCTCGATC**ACTACACCCCCTCTTAAAGGTTTCCTGGGGACTGTGGAAG
Apta20-96	ATTTTTACAT**TGAGGCTCGATC**GTGAAAGACAAGGCGCCCGAAATTTATCACCTTATTACCT
Apta20-98	TCACATGACT**TGAGGCTCGATC**TTTAGTAAAAGCCGAGTAGCATTCCCCGTAGTTCTAGATG
Apta20-92	GATGACAATT**TGAGGCTCGATC**AACTTTATACCGTTACGGATCACATAAGTACTCAGGCTTC
Apta20-322	GACGGGCCAC**TGAGGCTCGATC**CTTGCCTTGTTCAGCGGCCAACATTAATCATTGCCTTGTA
Apta20-07	TAAGACAATT**TGAGGCTCGATC**TAATGTTTTCCTAATGGGAGCCACAGGCATTCACAAGGGT
Apta20-09	TTCCTTACCT**TGAGGCTCGATC**TTCCTTACATAGCGAAATTTTCCAGTCGTCCCAAAACAG

Table 12 Candidate aptamers from the T-2 selection process. The capture regions are highlighted in bold.

4.3.5 Filtered Format sequence evaluation of HT-2 sequences

As described for HT-2 mycotoxin sequences, within each Capture SELEX round each replication was carried through as a sample through the 15 rounds. Therefore, a separate analysis was carried out to review the sequences within replicates based on the methodology described in Section 4.2.5. The results are described in the below Figures 18, 19 and 20.

SELEX Round	Replicates		
	HT-2 mycotoxin NGS ID		
	A	B	C
1	14	15	16
2	24	25	26
3	32	35	36
4	44	45	46
5	54	55	56
6	64	65	66
7	74	75	76
8	84	85	86
9	94	95	96
10	104	105	106
11	114	115	116
12	124	125	126
13	134	135	136
14	144	145	146
15	154	155	156

Table 13 Summary of the naming convention used for replicates and their identification numbers used for the filtered analysis.
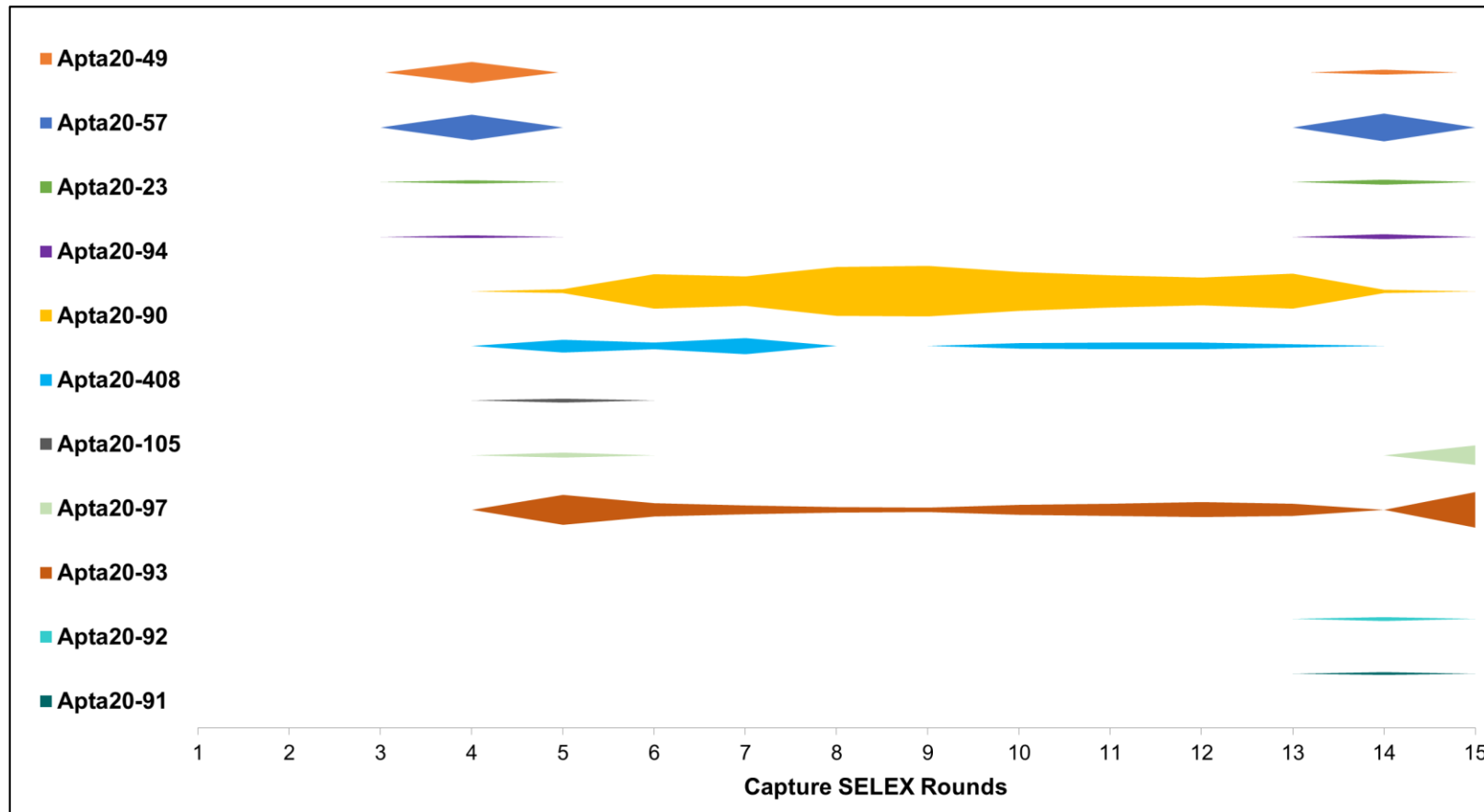
Figure 18 Aptamer population tracing of the 11 unique sequences identified through the evaluation of the filtered format data obtained through replication A of the HT-2 Capture SELEX process.
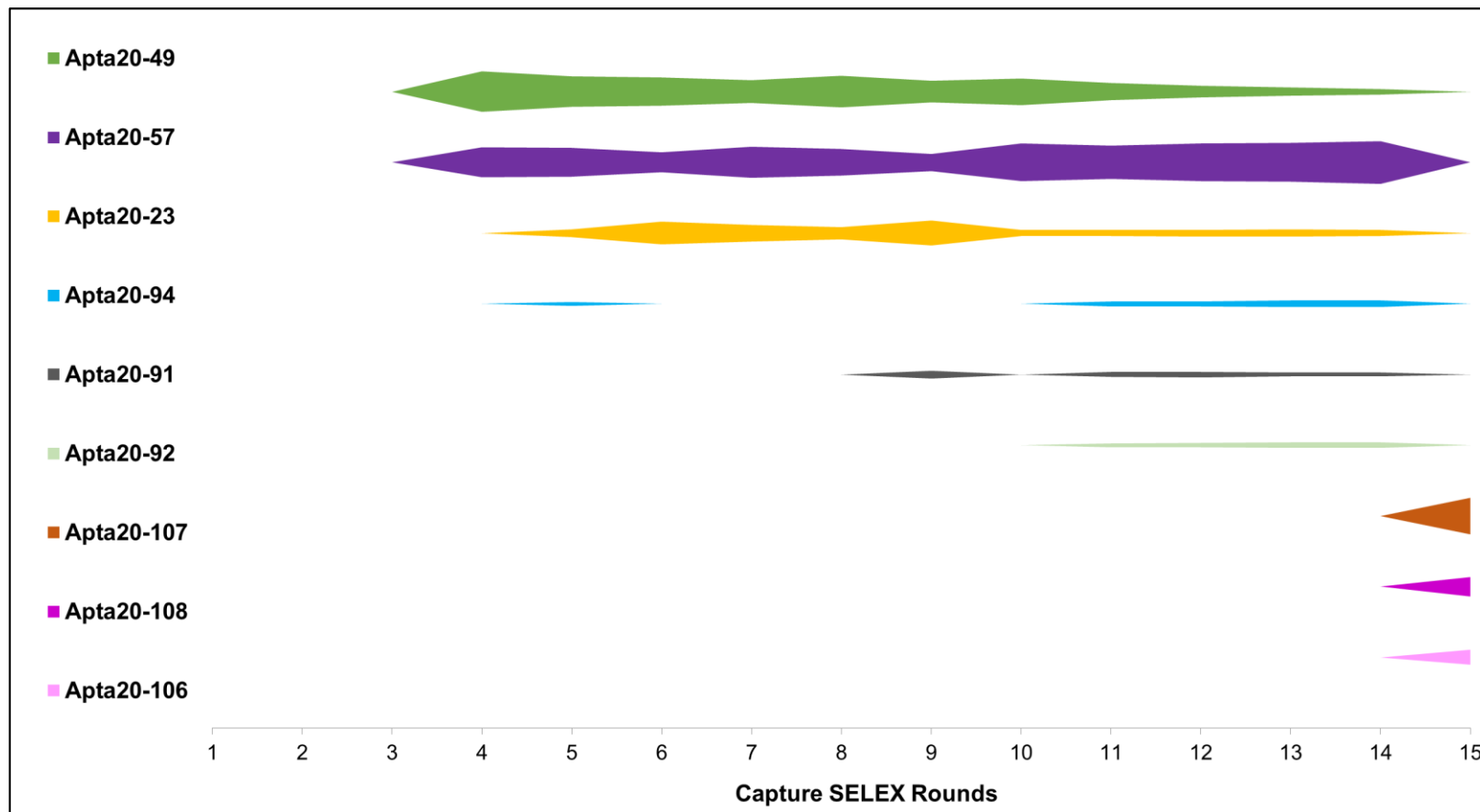
Figure 19 Aptamer population tracing of the 9 unique sequences identified through the evaluation of the filtered format data obtained through replication B of the HT-2 Capture SELEX process.
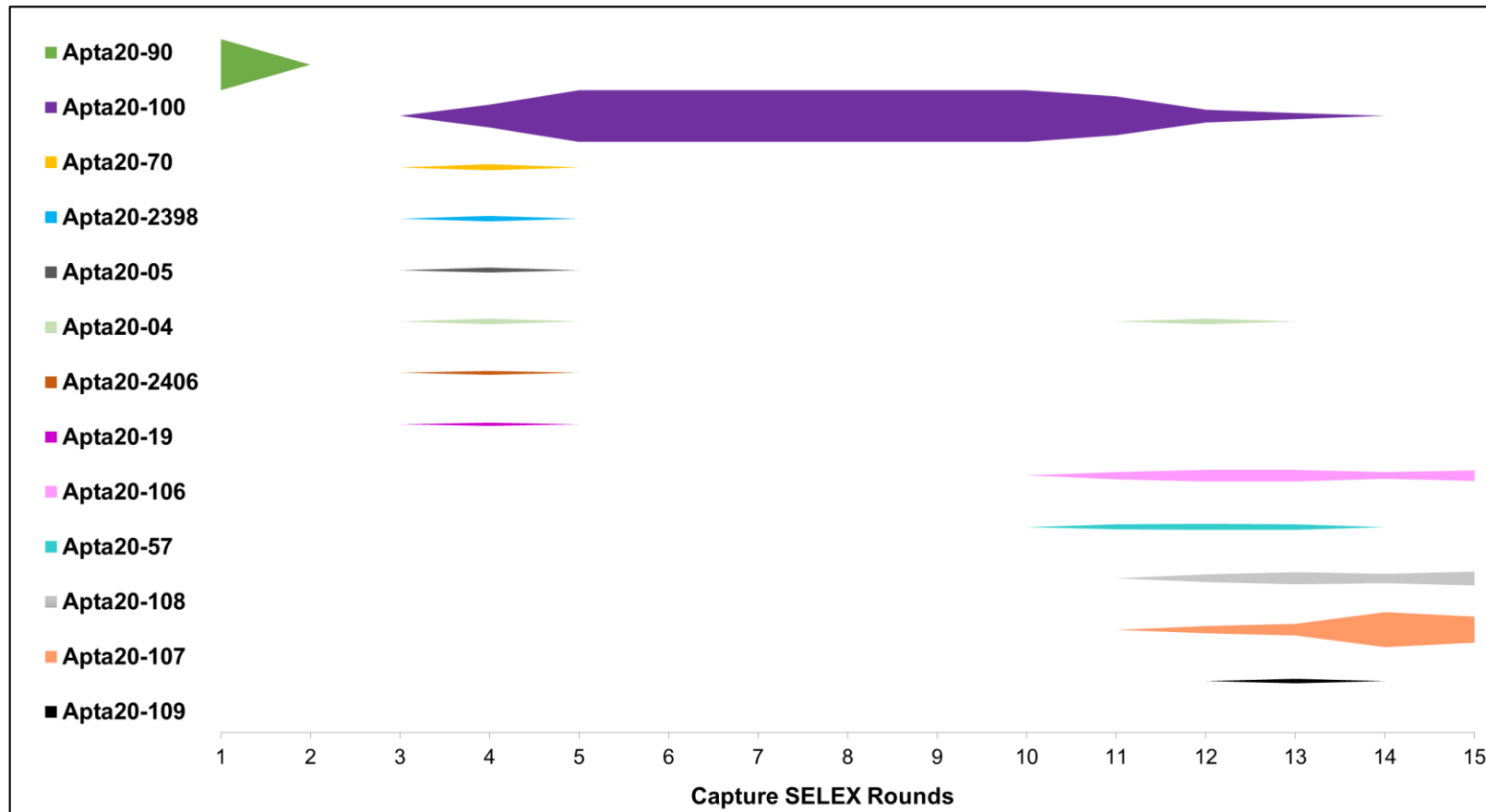
Figure 20 Aptamer population tracing of the 13 unique sequences identified through the evaluation of the filtered format data obtained through replication C of the HT-2 Capture SELEX process.

The evaluation of the filtered format data (Figures 18, 19 and 20) shows the unique sequences within each replication (A, B and C) obtained through the application of the three acceptability criteria and their appearance across the Capture SELEX rounds. Through the evaluation, 6 unique sequences were identified, which had not been found within the combined data set analysis. These unique sequences are described below in Table 14. The unique sequences observed in the combined data set can be linked to a particular replication or several replications.

Figure 18 showing replication A, 11 unique sequences were found of which Apta20-49, Apta20-57, Apta20-23, Apta20-94 can be observed in two rounds 4 and 14. Apta20-90, Apta20-408 and Apta20-93 can be seen distributed across most rounds. Apta20-105, Apta20-92 and Apta20-91 can be seen in single rounds 5 and 14 respectively. Apta20-97 can be seen in rounds 5 and 15 only as well as Apta20-93 across 1 to 13 only. Of the unique sequences seen within the figure Apta20- 57, Apta20-90, Apta20-23, Apta20-49 and Apta20-93 can also be seen in the combined format data evaluation.

Figure 19 showing the replication B, 9 unique sequences were found of which Apta20-49, Apta20-57 and Apta20-23 can be seen across most of the Capture SELEX selection rounds. Apta20-94 can be seen in early round 5 followed by later rounds. Similar distribution pattern can be observed for Apta20-91 and Apta20-92 seen in round 9 and later stages. Apta20-107, Apta20-108 and Apta20-106 can be observed in round 15 of the replication. Of the unique sequences seen within the figure Apta20-49, Apta20-57 and Apta20-23 can be found in the combined format data set.

Figure 20 showing the replication C, 13 unique sequences were found of which Apta20-89 was seen in round 1 of the selection process whereas Apta20-100 can be seen through the majority of the rounds. Apta20-70, Apta20-2398, Apta20-05, Apta20-2406 and Apta20-19 can be seen in single round 4. Apta20-04 can be seen in round 4 and 12. Apta20-106, Apta20-57, Apta20-108, Apta20-107 can be observed in the last rounds. Apta20-109 can be observed in the later round 13. Of these unique sequences seen in the figure Apta20-90, Apta20-100, Apta20-106, Apta20-57, Apta20-108 and Apta20-107 can be seen in the combined format data set as well.

Cross-reviewing the replications A, B and C, several of the unique sequences are present across the replications and others do not appear. Apta20-408, Apta20-105 can be found in replication A only and Apta20-2398, Apta20-2406 and Apta20-109 in replication C only. These unique sequences can be found in the combined format data outside of the 50% most abundant unique sequence acceptability criterion. Apta20-49, Apta20-57, Apta20-23, Apta20-94, Apta20-91 and Apta20-92 can be observed in replication A and B. Apta20-90 and Apta20-57 can be seen in replications A and C. Apta20-106 and Apta20-107 can be seen in replications B and C.

From the evaluation of both filtered data sets obtained from T-2 and HT-2 related sequences, several unique sequences found in HT-2 data set can be seen in the T-2 data set as well. These unique sequences are Apta20-04, Apta20-05, Apta20-57, Apta20-91, Apta20-19, Apta20-70 and Apta20-92.

Aptamer Label	Sequence
Apta20-2398	TATTTTATCC**TGAGGCTCGATC**ACACTTATTCATAGGTGTAAACCCCTTTATGTGAGGTTTT
Apta20-2406	AACGTTCGCG**TGAGGCTCGATC**TTTTTAGCAGAGACTTGTTCTGCGTCCATCGCCTCTGATT
Apta20-109	TCCCTTTTAA**TGAGGCTCGATC**AAAATTACGATTACCAACCTCGGATCTTCATGGGTCCATT
Apta20-408	TATAGGCGAG**TGAGGCTCGATC**ATTCGATGGGCTGAGACCTGCAATAAGAGTGCGATCCCC
Apta20-105	CCGGCCACGA**TGAGGCTCGATC**CGTCTTTCACAAGCAGGTCAAGAGCCGCTCATGTGGTTTA
Apta20-97	TCATTTCCTC**TGAGGCTCGATC**TCGCCTCTCATCACTGGATGTTATAGCATGATGGCCATGC

Table 14 Candidate aptamers from the HT-2 selection process. The capture regions are highlighted in bold

4.3.6 Oligonucleotide homology evaluation of T-2 and HT-2 sequences

The phylogenetic trees illustrated in the Figures 21 and 22 below highlight the homology between the aptamer sequences evaluated through the filtered format. The phylogenetic trees were generated through MEGA 11 as described in Section 4.2.6. The assigned bootstrap (BS) values are shown at the start of branch junctions. Each cluster of aptamers shown on the phylogenetic tree have common nucleotide sequences and show their sequence homology. The scale of 0.02 indicates the probability of substitution per nucleotide position.

The phylogenetic tree of the unique sequences observed during the Capture SELEX protocol targeting the T-2 mycotoxin is shown in Figure 21. Three main clusters are shown from origin which further branch off into individual clusters. Within the first cluster (top) contains Apta20-04, Apta20-02, Apta20-21975, Apta20-92, Apta20-19, Apta20-21974. Apta20-57, Apta20-15, Apta20-09, Apta20-21977 and Apta20-10. The bootstrap values range within the cluster between 22% and 64%, in which the subcluster of Apta20-15 and Apta20-09 show the highest homology of 64%. The second cluster (middle) contains Apta20-70, Apta20-56, Apta20-96, Apta20-91, Apta20-89, Apta20-322, Apta20-05, Apta20-59 and Apta20-03. The bootstrap values range within the cluster between 18% and 100%, in which the subcluster of Apta20-322 and Apta20-05 show the highest homology of 100%. The third cluster (bottom) contains Apta20-58, Apta20-95, Apta20-06, Apta20-98, Apta20-21976, Apta20-07, Apta20-83 and Apta20-01. The bootstrap values range within the cluster between 18% and 48%, in which the subcluster of Apta20-58 and Apta20-95 show the highest homology of 48%.
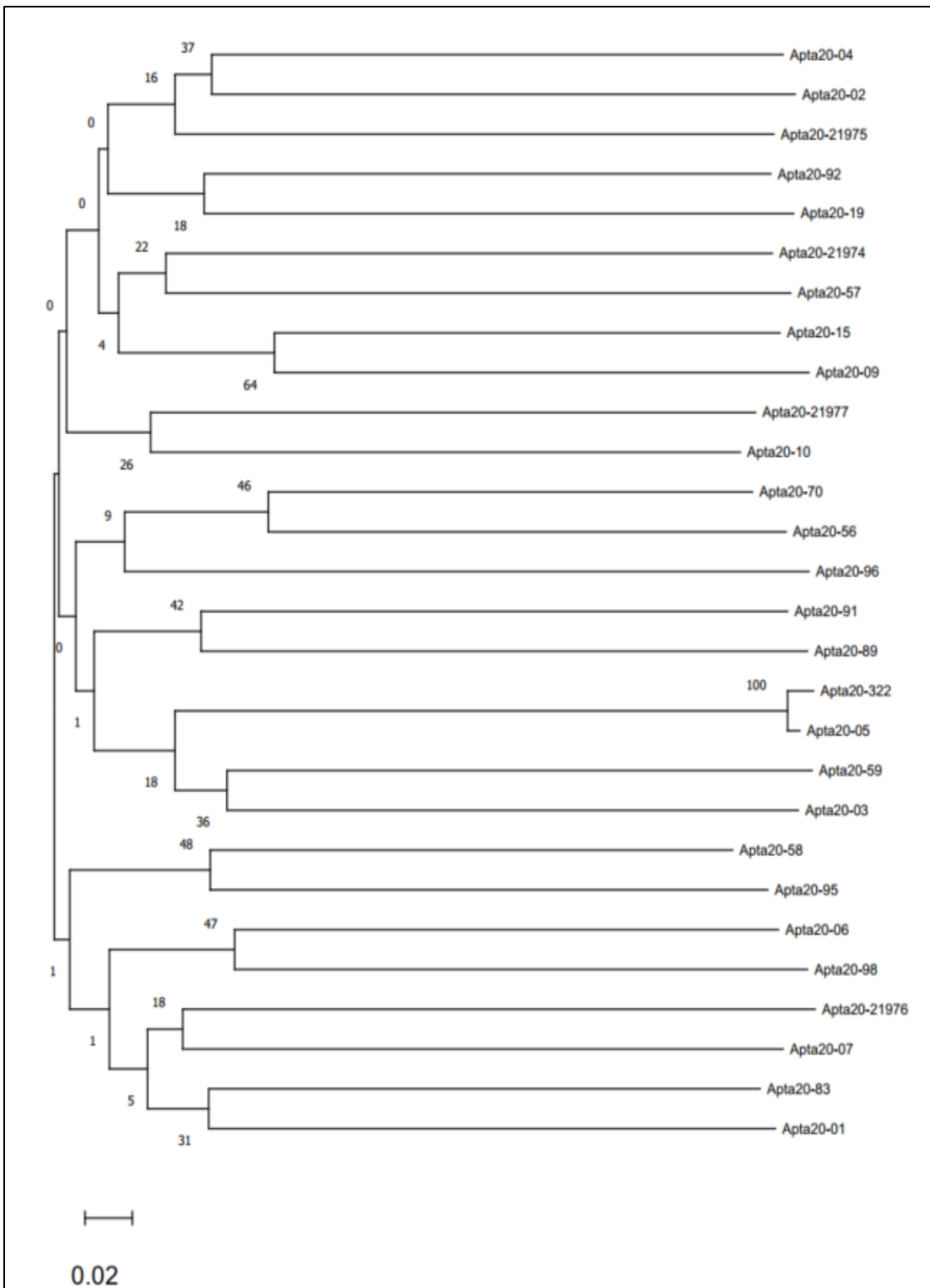
Figure 21 Phylogenetic tree of the unique sequences seen in the filtered format of the T-2 data.
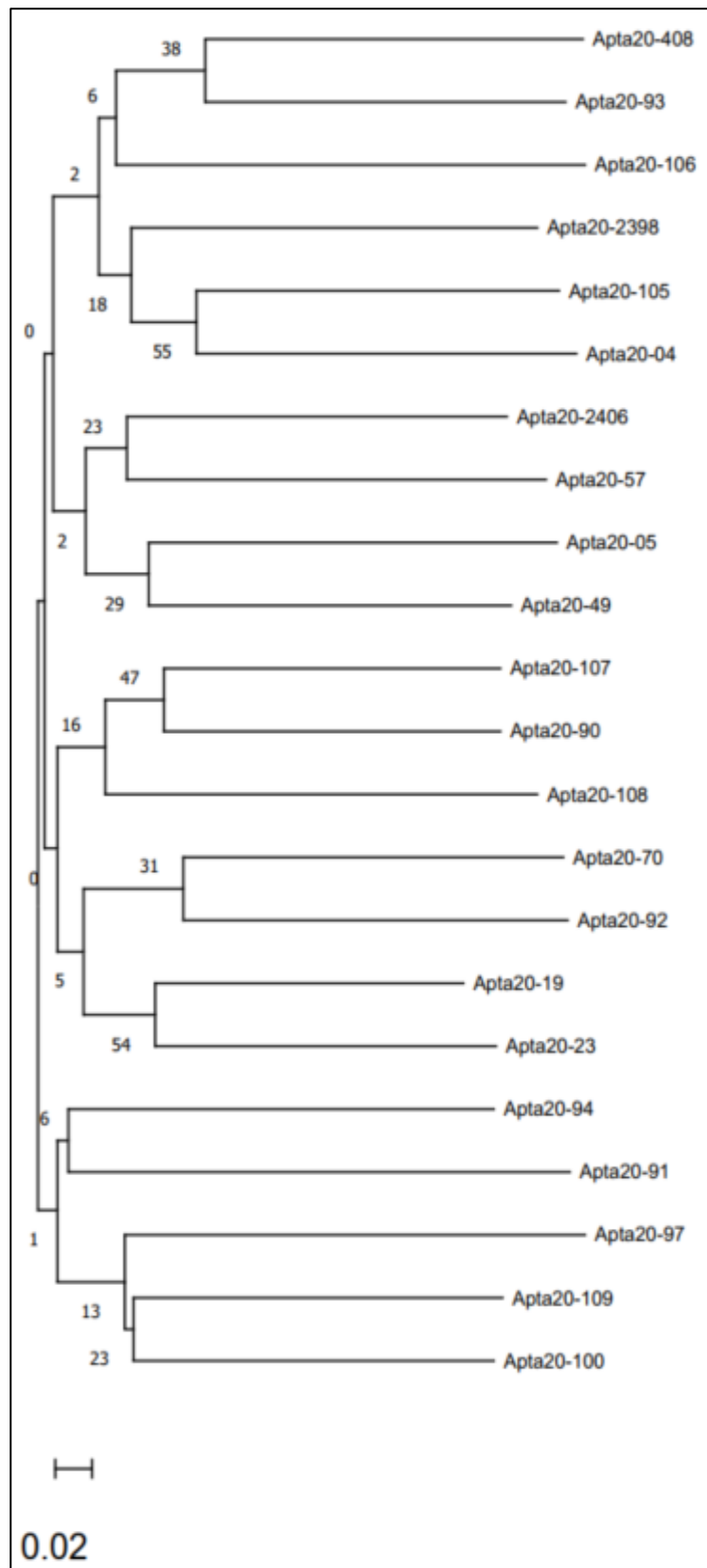
Figure 22 Phylogenetic tree of the unique sequences seen in the filtered format of the HT-2 data.

The phylogenetic tree of the unique sequences observed during the Capture SELEX protocol targeting HT-2 mycotoxin is shown in Figure 22. Three main clusters are shown from origin which further branch off into individual clusters. Within the first cluster (top) contains Apta20-408, Apta20-93, Apta20-106, Apta20-2398, Apta20-105, Apta20-04, Apta20-2406, Apta20-57, Apta20-05 and Apta20-49. The bootstrap values range within the cluster between 18% and 55%, in which the subcluster of Apta20-105 and Apta20-04 show the highest homology of 55%. The second cluster (middle) contains Apta20-107, Apta20-90, Apta20-108, Apta20-70, Apta20-92, Apta20-19 and Apta20-23. The bootstrap values range within the cluster between 47% and 54%, in which the subcluster of Apta20-19 and Apta20-23 show the highest homology of 54%. The third cluster (bottom) contains Apta20-94, Apta20-91, Apta20-97, Apta20-109 and Apta20-100. The bootstrap values range within the cluster between 6% and 23%, in which the subcluster of Apta20-109 and Apta20-100 show the highest homology of 23%.

4.3.7 Sequences not evaluated

Many sequences were found in the Capture SELEX selection rounds for both mycotoxin targets which did not fall within the 50% of most abundant sequences criterion but did pass the acceptance criteria of no more than a total length of 62 base pairs and no changes to the capture sequence. To evaluate the sequences not matching the 50% acceptability criterion for both T-2 and HT-2 selection rounds, they were analysed to evaluate the sequence similarity of the oligonucleotides A, C, G and T at each position within the 62 base pair sequence. Figures 23 and 24 (below) show the similarity of the sequences found within the T-2 and HT-2 sequencing pools compared to the pool of the 50% most frequent or abundant sequences.
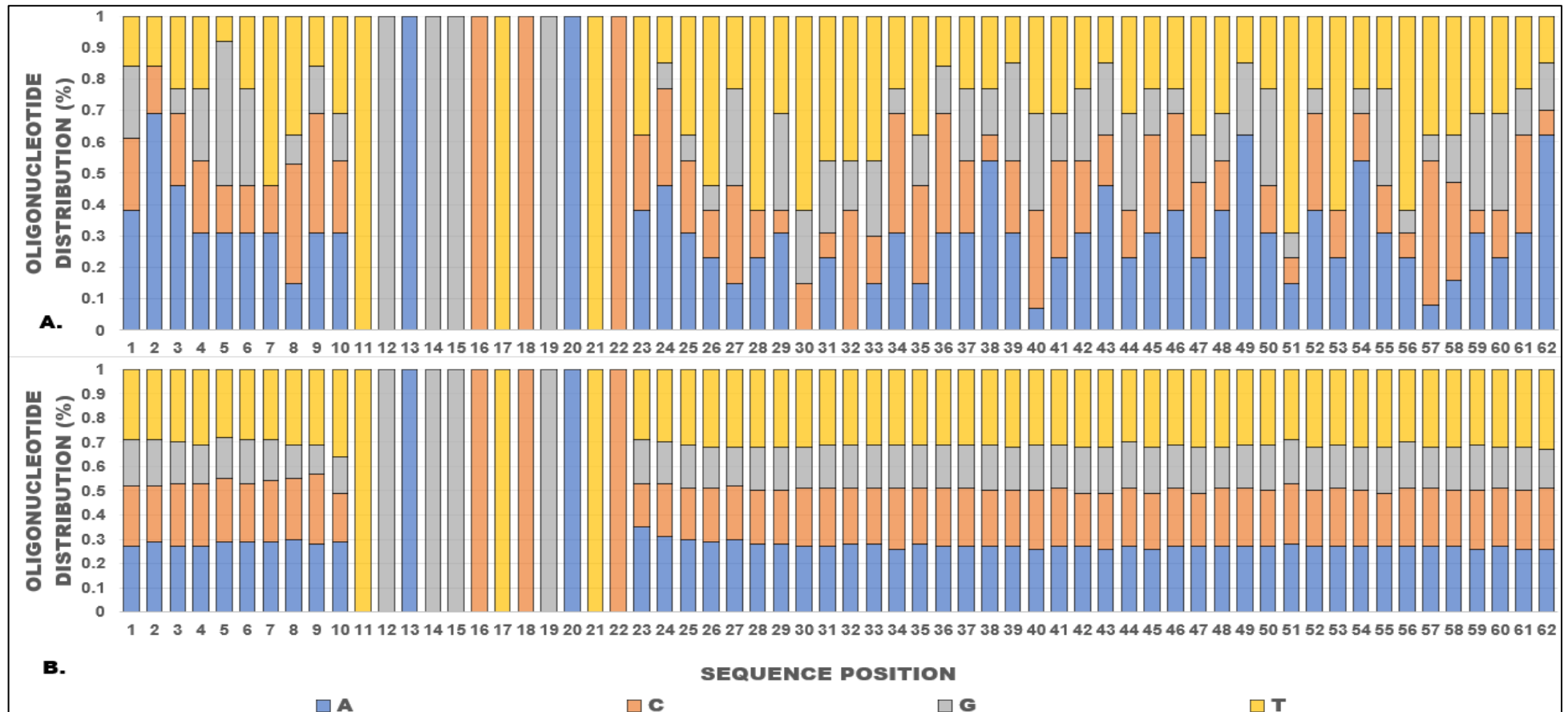
Figure 23 Oligonucleotide distribution (A, C, G and T) expressed as percent at position of the unique sequences in Capture SELEX rounds 2 to 15 targeting T-2 not seen in the top 50% most frequent unique sequences. **A.** Showing the unique sequences seen within the pool of 50% most abundant sequences. **B.** Showing the pool of the unique sequences not evaluated.
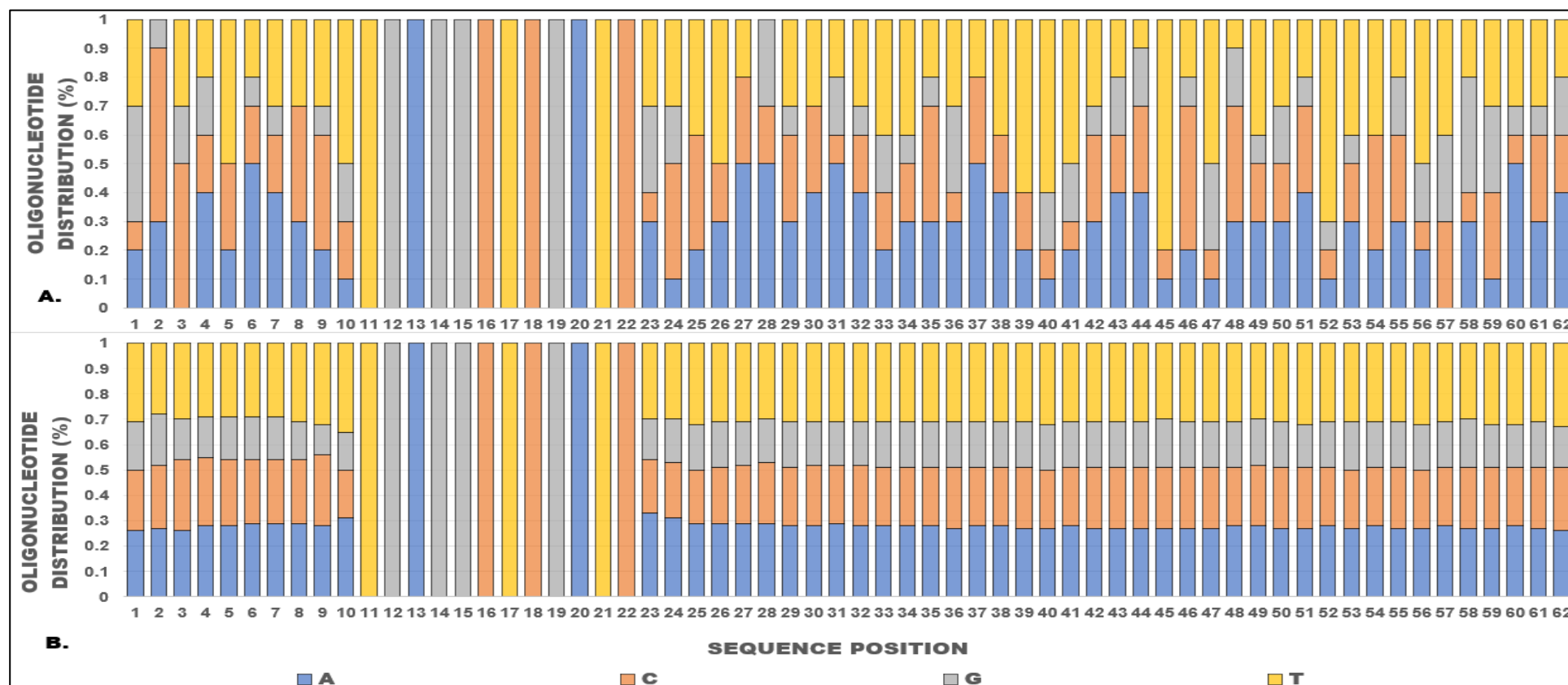
Figure 24 Oligonucleotide distribution (A, C, G and T) expressed as percent at position of the unique sequences in Capture SELEX rounds 2 to 15 targeting HT-2 not seen in the top 50% most frequent unique sequences. **A.** Showing the unique sequences seen within the pool of 50% most abundant sequences. **B.** Showing the pool of the unique sequences not evaluated.

The results from Figure 23 A of the similarity calculations of the unique sequences found within the pool of 50% most abundant unique sequences within the T-2 selection, showed that T was most common through the sequence positions and on positions 7, 26, 28, 30,51 and 56 most dominant. The nucleotide A was not present at all in position 30, although it was a commonly appearing nucleotide throughout the unique sequences. The nucleotide C occurred throughout the unique sequence positions with largest distributions at positions 8, 40, 52 and 57. G can be seen to be absent at positions 2, 7, 23, 28 and 53. In comparison, in Figure 23 B all four nucleotides can be observed at all positions, T being the most frequent and G having the smallest distribution. All the nucleotides were present in the unique sequences.

The results from Figure 24 A of the similarity calculations of the unique sequences found within the pool of the 50% most abundant unique sequences within the HT-2 selection, showed that T was had the highest frequency across the sequence positions, however, it was found absent in position 2. The nucleotide A was seen to be absent at positions 3 and 57. Nucleotide C was found throughout the sequences with highest frequency at positions 2, 3 and 46. Nucleotide G had the overall lowest frequency except for the first position in the sequences and was absent from the 5th, 8th, 25th, 26th, 27th, 30th, 37th, 38th, 39th and 45th position. Comparing the findings to Figure 24 B all nucleotides can be observed at each sequence position with none being absent. The nucleotides T and A have the highest distributions followed by C and G.

4.4 Discussion

The DNA sequences selected through the Capture SELEX process described in Chapter 3 were identified through HTS and further evaluated through combined and filtered format data set analysis. The aim of the evaluation was to identify suitable aptamer candidates to trial in subsequent binding assays, as well as to obtain information of the evolution and selection of the unique sequences that occurred during the Capture SELEX process.

The Capture SELEX protocol described by Paniel *et al.* (2017) was followed by an E. coli-based cloning procedure, in which the sequences generated in the last round of selection were used. Following ligation into a suitable plasmid, transformation of competent cells and colony selection, the extracted plasmid DNA was digested and subjected to Sanger sequencing to identify the sequences generated. The authors did not evaluate any other of their selection rounds to identify aptamer candidates.

SELEX protocols in principle follow the same methodology, an oligonucleotide library (DNA or RNA) is incubated with a target of interest. At the end of a selection round the lower affinity sequences are removed and the binding sequences are retained, these are then amplified to continue selection. Sequences from the final round of selection are considered aptamers with binding specificity, (Hoinka *et al.*, 2015). The use of HTS allows for the identification of a large number of potential aptamer candidates across the selection rounds based on the abundance or frequency of unique sequences, distribution of each oligonucleotide within sequence and evolution of the enriched sequences across selection, (Ferreira *et al.*, 2021). In the recent study published by Ferreira *et al.* (2021), HTS was used to support the development of aptamers for the detection of metastatic breast cancer cells. The team utilised modified Cell-SELEX applying sequencing and bioinformatic analysis following each round of selection. After 8 rounds of selection, 25 unique sequences had been identified matching the set

acceptability criteria of most frequent across the selection rounds and showing the defined core region. The core region was described as a fixed region within the sequences, like the capture region described within this thesis. From the 25 unique sequences, 2 were selected to be used in their subsequent detection assays.

The results obtained from the high throughput sequencing of available sequences within each Capture SELEX round, in this thesis, identified an overall total of 21,978 unique sequences across both T-2 and HT-2 15 rounds of selection. Acceptability criteria were applied, similar to those described by Ferreira *et al.* (2021), to reduce the number of unique sequences and aid in the identification of best suited aptamer candidates for binding assays. The criteria of removing unique sequences with base pair length beyond 62 and modification to the capture sequences were ideal criteria, as they allowed for the removal of sequences having undergone changes during the Capture SELEX protocol, possibly introduced during the PCR amplifications.

Hoinka (2015) and colleagues describe the problems caused through PCR bias in SELEX protocols with many PCR amplification stages (>10 amplification stages). PCR bias can occur due to differences in the amplification efficiency or through inhibition of amplification by self-annealing. They describe the use of high throughput sequencing and evaluation of the sequences at each stage as a checking system for possible bias, as well as for the evaluation of most frequent sequences being consistent with defined parameters. Starting oligonucleotide sequences with defined regions are advantageous as they can be used as a form of fixed reference point during evaluation. The Capture SELEX oligonucleotide library used within the experimental design has a defined capture region and modification to the region suggests undesired sequence structure modifications. During the Capture SELEX protocol, the capture region provided the support structure attached to the docking sequence and magnetic beads around which the oligonucleotides bind to the target molecule.

Therefore, being critical to the functioning of the selection process and unique sequences with an unmodified capture region. The application of both acceptability criteria reduced the overall pools throughout the selection rounds by 24% in the T-2 selection and 23% in the HT-2 selection. Most notable exclusions occurred in the T-2 selections in rounds 1 and 3 (50%), like HT-2 selections in the same rounds with 1 (50%) and 3 (100%) exclusion. In both selections, round 2 saw the least exclusion of unique sequences due to the acceptability criteria being applied, 3% (Table 7) and 4% (Table 9).

Through the evaluation of the combined data (Section 4.3.2 and Section 4.3.3), obtained from both T-2 and HT-2 data sets, 12 unique sequences within the Capture SELEX protocol were identified targeting T-2 and 9 unique sequences targeting HT-2; all matching the three acceptability criteria. To summarise, these were: Apta20-89, Apta20-21974, Apta20-21975, Apta20-91, Apta20-02, Apta20-05, Apta20-04, Apta20-56, Apta20-01, Apta20-03, Apta20-06 and Apta20-15. within the T-2 selection pool and Apta20-100, Apta20-106, Apta20-107, Apta20-108, Apta20-23, Apta20-49, Apta20-57, Apta20-90 and Apta20-93 within the HT-2 selection pool. This provided a pool of unique sequences as aptamer candidates to be used within binding assays targeting T-2 and HT-2 mycotoxins.

Within the combined format data all unique sequences observed could not be cross-referenced between the selection pools. However, during the analysis of the filtered format data set unique sequences were found within both selection pools. These unique sequences were Apta20-04, Apta20-05, Apta20-57, Apta20-91, Apta20-19, Apta20-70 and Apta20-92. Of these unique sequences, Apta20-04 and Apta20-57 stand out as they were within the groups of unique sequences identified above as possible top aptamer candidates for T-2 and HT-2 targets during binding assays.

The evaluation of the distribution or appearance patterns completed shows that Apta20-04 in the combined T-2 selection pool was found throughout the Capture SELEX rounds starting at round 4, either within the 50% cut-off criterion or outside (Figure 12). Further in-depth review of the appearance pattern of the unique sequences within the filtered data of the T-2 selections showed that Apta20-04 occurred in all three replications.

Given that the replications A, B and C correspond to selections which have been followed through the process without mixing of pools (Figures 14, 15 and 16). the unique sequence configuration of the oligonucleotides appears to be favourable in binding to the target mycotoxin. Apta20-04 appears in replication C of the filtered data of the HT-2 selection pools, suggesting that the sequence configuration has cross-selected to both mycotoxins. These observations contribute to Apta20-04 being a prime candidate for use in binding assays. Apta20-57 shows a similar distribution or appearance pattern in the combined format of the HT-2 pools, starting at selection round 4 (Figure 13) with highest abundance within the latter rounds. Reviewing the replications, A, B and C of the filtered format data of the HT-2 selections shows the appearance of the unique sequence within all three replications. as well as appearance in replication B of the T-2 selection. These observations, like Apta20-04, make Apta20-57 a further prime candidate to trial during binding assays. Furthermore, the observations highlight the interest to trial the unique sequences in binding assays for both mycotoxins to establish their performance.

An additional benefit of sequencing the pool of all the selection rounds was that this provided an opportunity to identify at which point unique sequences were becoming most abundant or frequent within the round. Schütze *et al.* (2011) describe the use of HTS to aid in the identification of unique sequence appearance patterns.

The team suggested in their findings that unique sequences seen in early selection rounds have a higher likelihood of being better binders, when compared to unique sequences found in latter stages. In addition, they state that the appearance and distribution of unique sequences should be compared to their frequency or abundance within the selection rounds as these are important factors to identify aptamer candidates.

A review of the combined and filtered data of selection rounds 1 to 3 for T-2 selection pools showed unexpected distributions and appearances of unique sequences. In round 1, Apta20-89 was most abundant and the only unique sequence passing the acceptability criteria. Although the sequence does re-occur in latter stages, the frequency is very low. Following on in round 2, a total of 4425 unique sequences were seen, however, their calculated percentage abundance excluded the unique sequences from consideration as aptamer binding candidates. It should also be highlighted that in contrast, none of the 21 unique sequences described above were found within round 2 of the selection process. In round 3 of the selection, 5 unique sequences were found of which 4 passed the 50% acceptability cut off criterion: Apta20-21977, Apta20-21976, Apta20-21975 and Apta20-21974.

Similar observations can be made in the combined and filtered data of selection rounds 1 to 3 for the HT-2 selection pools. In selection round 1, Apta20-90 was the only unique sequence out of 2 passing the acceptability criteria, however, the unique sequence does re-occur again in middle and later rounds at abundance outside of the 50% cut-off criteria. In the following round 2, a total of 15662 unique sequences were identified, however, their frequency calculations excluded these sequences from further consideration as aptamer candidates.

Although as stated above, a large proportion of the unique sequences passed the first two acceptability criteria. None of the above identified top aptamer candidates were found within this selection round. In selection round 3, a total of 3 unique sequences were identified, however, all were excluded due to variation in sequence length and capture region. In the subsequent selection round 4, a total number of 51 unique sequences were identified.

The change from one unique sequence (round 1) to several thousands (round 2) back to less than 5 or even none (round 3) is a pattern not described by Paniel *et al.* (2017) or Stoltenburg, Nikolaus and Strehlitz (2012a) in their development of aptamers using the Capture SELEX protocol. The main reason for this is their focus on the final selection round to identify aptamer candidates. Within the SELEX-related literature utilising HTS for the identification of aptamer candidates a similar pattern could not be identified.

The HTS process described within this chapter was carried out once on each of the selection rounds, however, this limited sampling could have impacted on identification and characterisation of unique sequences. Whilst the likelihood of most abundant sequences not occurring within the sampled pool are low, unique sequences with lower abundance may have not been captured within the sequencing. The limited sampling and sequencing could cause a misrepresentation of the selection landscape of Capture SELEX. Many SELEX protocols, including Capture SELEX require the generated pool of selection to be carried into the next selection round which complicates full sequencing of selection rounds.

El-Husseini (2022) and colleagues described a combinational use of real-time-PCR (qPCR) and high throughput sequencing during Cell SELEX, to monitor the selection of the aptamers in real time during the protocol.

The authors concluded that the combined approach led to the identification of all possible aptamer sequences, compared to standard SELEX strategies. A similar approach can be applied to a Capture SELEX protocol; through the addition of qPCR monitoring the complete landscape of selection can be explored. Future work would be required to include qPCR within the methodology of selection using the Capture SELEX protocol. Applying it to the selection of aptamers targeting T-2 and HT-2 mycotoxins giving complete insight into the selection process.

A review of the data presented by El-Husseini *et al.* (2022) further shows that the Cell SELEX demonstrated a decreasing diversity of unique sequences. This happened most notably after their first round of selection, where a very low diversity of unique sequences compared to the library pool control suggested a removal of many unsuitable aptamers. They observed a decreasing diversity of unique sequences throughout the following 8 selection rounds and completed their selection at round 8. They applied three acceptability criteria to their unique sequences for selection: unique sequence frequency, appearance in early selection rounds and increasing frequency during the selection process. Through this methodology they identified 10 aptamer candidates matching their criteria. The combinational use of qPCR and Cell SELEX was described by Kolm *et al.* (2020). They utilised qPCR as a monitoring tool of the selection and identified a decrease in unique sequences diversity from selection round 9 to 11, in previous selection rounds a distinct reduction of unique sequences could not be observed. Following the qPCR analysis, HTS was applied to identify aptamer candidates and the unique sequences were grouped based upon their frequency or abundance. This analysis showed that the frequency of unique sequences increased from selection round 7 onwards and peaked at rounds 10 and 11. A total of 11 rounds of Cell SELEX were performed to reduce the effect of possible PCR bias.

They applied acceptability criteria of removing unique sequences beyond the sequence length (40bp), variation to the primer regions and grouping of all unique sequences based upon their frequency. Through the methodology they identified 16 aptamer candidates.

Summarising the work by El-Husseini *et al.* (2022), the evaluation of the Cell SELEX for the development of aptamers targeting *Brucella* spp. showed decreasing unique sequence diversity after the first round of selection. In contrast, the work by (Kolm *et al.*, 2020) evaluating Cell SELEX for the aptamer development targeting *Enterococcus faecalis* indicated that decreased diversity was seen starting at selection round 8. Both research approaches applied Cell SELEX to bacterial targets and found different unique sequence diversity trends. Although qPCR was not a methodology applied to the Capture SELEX used in this thesis, a trend can be observed that differs from that described above. In both T-2 and HT-2 selections, the first round resulted in one unique sequence accepted, followed by thousands and dropping off again in selection round 3. The exact cause for the distribution pattern remains unclear and further highlights the insight gained by applying qPCR to the Capture SELEX protocol, allowing in detail identification of the selections occurring in the rounds 1 to 3.

Following the application of the acceptability criteria and identifying aptamer candidates, the unique sequences were further evaluated for their sequence homology. The comparison of homology can support the choice of suitable aptamer candidates for trialling in binding assays.

The work carried out by Yang *et al.* (2021) suggested that homology analysis is best carried out on unique sequences with the highest abundance found in the selection.

Liu *et al.* (2022b) suggest a similar approach to the selection of aptamer candidates; following filtering of the obtained unique sequences by frequency, the selected unique sequences should be aligned and grouped by similarity using appropriate software. Xie *et al.* (2022) propose the use of MEGA software to compare homology and construct evolutionary trees. The homological comparison allows for the determination of familiarity and grouping of aptamer candidates, giving initial predictions about which unique sequences could show similar binding based upon their alignment within the evolutionary tree.

Within this chapter, MEGA 11 was utilised to construct the evolutionary trees (Figure 21 and 22) based on the filtered format data set for T-2 and HT-2 selections. The phylogenetic tree of the unique sequences found within the T-2 selection (Figure 21) showed three clusters with subclusters with bootstrap (BS) values applied. Phylogenetic bootstrapping is a standard analysis technique to assess the confidence of the phylogenetic trees, (Pattengale *et al.*, 2010). Typically a BS value above 70% or 75% is considered inferring high value of confidence within the calculated phylogenetic tree, (Lemoine *et al.*, 2018). The results obtained from Figure 21, T-2 selection, suggest that the Apta20-322 and Apta20-05 (100%) are the only group which can be supported with confidence. All other BS values are below the confidence value of 70%. The results obtained from Figure 22, HT-2 selection, suggest very low confidence in all the proposed clusters with BS values below 55%.

In a publication by Pereira *et al.* (2022), phylogenetic trees were constructed and the tree length inferred similarity of the aptamer sequences. Branches distinctly longer than others (observed through their scale of 6.0) were considered different to those branches with matching lengths. Based upon their findings, the branch length in Figures 21 and 22 are to a 0.02 scale and show minimal length differences between the clusters, the exception being the candidates Apta20-322 and Apta20-05.

For T-2, the aptamer candidates identified from the application of the three acceptability criteria are Apta20-01, Apta20-02 and Apta20-04 and Apta20-57, Apta20-90 and Apta20-100 from the HT-2 selection. Analysis of the phylogenetic tree of the T-2 selection groups Apta20-04 and Apta20-02 with the same cluster (top) and Apta20-01 in a separate cluster (bottom). This suggests that Apta20-02 and Apta20-04 are likely to have similar target binding performance. Within the tree Apta20-57 can be seen within the same cluster as Apta20-04 and Apta20-02 and may also demonstrate similar binding.

Analysis of the phylogenetic tree of the HT-2 selection indicates that the unique sequences are clustered in different groups, suggesting that they could exhibit differences in target binding. Apta20-57 is clustered in the top within the same region as Apta20-04, showing similar grouping difference as in the T-2 specific tree. Apta20-90 is clustered in the middle and Apta20-100 is clustered in the bottom. Based upon conclusion by Xie *et al.* (2022), aptamer candidates should be selected from different subgroups as this provides a broader overview of unique sequences in binding trials as well as providing alternative aptamer candidates. This can be achieved from the selected six aptamer sequences as well as giving comparison of binding for similar sequences (Apta20-04 and Apta20-02).

Through the evaluation of the phytogenic trees, it was possible to understand the homology between the top aptamer candidates. However, many unique sequences were identified during the evaluation of the combined format data which did not match the 50% most frequent or abundant sequence criterion.

To understand the similarity between these non-selected unique sequences, the distribution of the oligonucleotides at each position within the 62 base pair sequence was evaluated.

The analysis of the unique sequences from the T-2 selection (Figure 23) and the unique sequences from the HT-2 selection (Figure 24) show similar distribution patterns across the sequence length. The base pairs A and T are most frequently observed, followed by G and C. The evaluation highlights the generally even distribution of the base pairs across the sequence length. With the exception of positions 11 to 22 comprising the defined capture region, no oligonucleotide specifically dominates at a given position. The comparison to the similarities of the 50% most abundant unique sequences shows that at many positions various nucleotides are either absent or dominate.

Similar analysis was carried out by Kolm *et al.* (2020) in which they found their selected aptamer candidates to be rich in nucleotide A as well as T, with lowest proportion of C and G nucleotides. Based upon the differences observed between the selected and non-selected unique sequences, further investigations would be required to assess the binding of non-selected aptamer candidates. Whilst the current literature suggest that unique sequences found abundantly are best suited as aptamers, Hoinka *et al.* (2015) suggest the opposite; that unique sequences with relatively low frequency would be equally good aptamer candidates as those at high frequencies. Future work comparing unique sequences for binding would provide additional information on the selection of aptamer candidates from a Capture SELEX protocol.

The use of high throughput sequencing provided an insight into the development of the pool of sequences during the Capture SELEX process and gave additional information of the workings of the selection process. The aim of the presented work in this chapter was to identify suitable aptamer candidates to be used in binding assays. Based upon the most frequent or abundant unique sequences and their appearance pattern a total of 6 aptamer candidates were selected for trialling in the binding assays presented in Chapter 6 of this thesis. 3 aptamer sequences from the T-2 selection pool and 3 from the HT-2 selection pool.

Apta20-01 and Apta20-57 were selected due to their prominence and abundance in later stages of selection thereby providing data on the binding capabilities of aptamers selected in later stages of the process. Additionally, Apta20-57 was found within both mycotoxin selection pools. Through the homological analysis both unique sequences were found within separate groups of the phylogenetic tree and provide selection diversity.

Apta20-02, Apta20-04 and Apta20-100 were selected due to their appearance pattern observed throughout the Capture SELEX process thereby providing evidence of the binding capabilities of a sequence selected in early and later stages of the process and being most frequent or abundant within the selection pools throughout the rounds as well as the last round. Additionally, Apta20-04 is another example of a unique sequence found across both mycotoxin selections. Through the homological evaluations Apta20-02 and Apta20-04 aligned to different unique sequences within different groups providing selection diversity.

Apta20-90 was selected due to its abundance in selection round 1, and subsequent later rounds, possibly providing evidence through the binding assays if a sequence selected after the first round can be an aptamer with high binding affinities and providing evidence on how many SELEX rounds would be required to generate suitable aptamer candidates. Furthermore, Apta20-90 showed no homology between other unique sequences selected.

4.5 Conclusion

The application and analysis of HTS data allowed for the identification and characterisation of unique sequences as aptamer candidates. The application of these acceptability criteria to aptamer HTS data is the first to be reported in a Capture SELEX protocol targeting T-2 and HT-2 mycotoxins.

The aim of the evaluations was to identify aptamer candidates to be used in binding assays. The HTS analysis showed that the Capture SELEX protocol developed unique sequences originating from both the T-2 and HT-2 selections. Apta20-04 and Apta20-57 are examples of unique sequences which can be found in both selection pools showing cross-selection between the target mycotoxins. The evaluation of population tracing of the unique sequences across the selection rounds based on their frequency highlighted their development path. The first three rounds of selection demonstrated different aptamer occurrences. One unique sequence (round 1), several thousands (round 2) and couple or none (round 3). It is possible that the limited sampling of the selection pools contributed to this occurrence pattern. To fully understand the occurrences of unique sequences obtained from a Capture SELEX protocol qPCR would need to be applied. This will allow for real time monitoring of the selection process.

Further evaluation of the homogeneity of the unique sequences through phylogenetic trees enabled observation of the clustering of the unique sequences and further select aptamer candidates. Subsequent evaluation of non-selected unique sequences through similarity calculations concluded that further investigations of non-selected sequences would be required. This would clarify whether less abundant aptamers would be suitable candidates.

Through the evaluation of the HTS data six aptamer candidates were selected for binding assays (Chapter 5), Apta20-01, Apta20-02 and Apta20-04 from the T-2 selection. Apta20-57, Apta20-90 and Apta20-100 from the HT-2 selection. These aptamers are novel unique sequences and the first to be reported targeting T-2 and HT-2 mycotoxins.

Chapter 5. Aptamer binding performance

5.1 Introduction

The aptamer candidates selected using HTS, presented in (Chapter 4) required assessment to determine their binding to both target mycotoxins, T-2 and HT-2. The Capture SELEX protocol described by Paniel *et al.* (2017) used an affinity chromatography assay with immunoenzymatic detection for the assessment of their selected aptamer candidates. The authors concluded that the aptamers were capable of binding between 0% and 46.5% to the penicillin G target.

Gold nanoparticles (AuNPs) are readily available commercially and can form the basis of various assay formats. A colorimetric assay based on gold nanoparticles is suitable for use with aptamers and can provide results that are both visual and measurable by instrumentation, allowing for both qualitative and quantitative analysis. A colorimetric assay for T-2 and HT-2 was evaluated, based on the methodology described by Mondal *et al.* (2018) in which the aptamers were targeting Staphylococcal enterotoxin B demonstrated binding to the toxin over the concentration range of 0.5ng/mL to 50µg/mL.

Similarly, the use of high throughput sequencing for the evaluation of aptamer candidates followed by a detection assay based on AuNPs was described by Jing *et al.* (2021) targeting the illegal food additive borax. They utilised a column SELEX protocol for the development of aptamer candidates followed by sequencing and selection of one aptamer sequence to trial in colorimetric detection assays. The aptamer used within the assay was able to detect borax with an LOD range of 0.30-0.50µg/mL.
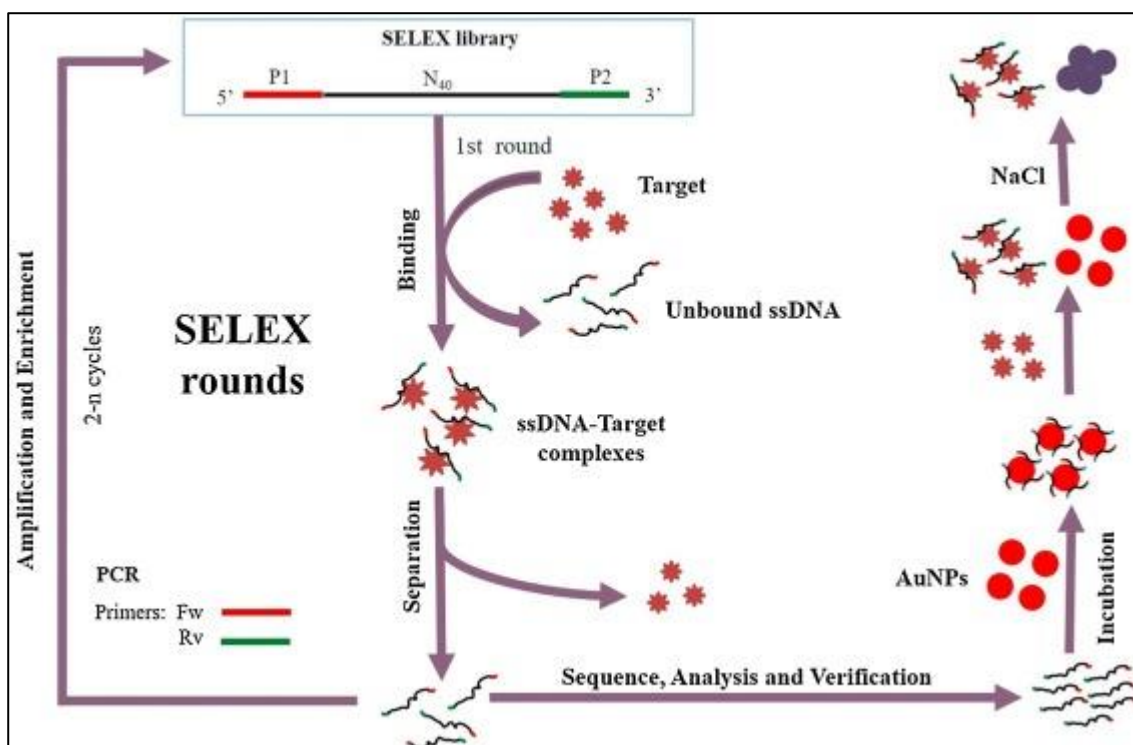
Figure 25 Schematic overview of the column SELEX protocol with sequencing and AuNPs colorimetric detection of borax as proposed by Jing *et al.* (2021).

The methodology pathway followed by Jing *et al.* (2021) for the development of novel aptamers, detailed in Figure 25 above, has similarities to the experimental methodologies used within this thesis. They use Capture SELEX followed by high throughput sequencing for the evaluation of the aptamer pools, in combination with an AuNPs colorimetric assay for the investigation of the binding capabilities of the selected aptamer sequences.

The use of AuNPs in a label-free colorimetric assay allows for a direct visual evaluation of aptamer binding capability. The assay principle is based upon the colour changes observed through the aptamer interacting with the AuNPs preventing aggregation (red colour) or aptamer binding to the target enabling aggregation of the AuNPs (blue/purple colour of aggregation), (Zhang and Liu, 2021).

The main objective of the colorimetric assays was to evaluate the binding capabilities of the selected aptamer sequences against the mycotoxins T-2 and HT-2. This included the cross-binding of all aptamers to all targets. Using high throughput sequencing described in Chapter 4 of this thesis, six aptamer candidates were selected for the use in binding assays, Apta20-01, Apta20-02, Apta20-04, Apta20-57, Apta20-90 and Apta20-100. The aim of this chapter was to explore the binding of the sequences to the targets (T-2 and HT-2) and to identify if the most abundant unique sequences selected had the ability to bind to them.

5.2 Methods

5.2.1 Aptamer sequence preparation from stock solutions

The aptamer sequences, Apta20-01 (19042.4g/mol), Apta20-02 (18976.3g/mol), Apta20-04 (19074.4g/mol), Apta20-57 (18963.4 g/mol), Apta20-90 (19048.4 g/mol) and Apta20-100 (18856.2 g/mol) manufactured on a 0.25μM scale by IDT Technologies. The aptamers were reconstituted in the original vials in sterile deionised water to give final stock concentrations of 100μM. Dilutions of the stock solutions were prepared to give the following range of aptamer concentrations, 50μM, 10μM, 1μM and 0.1μM in sterile deionised water. Each aptamer was linearised at 90°C for 8min in a water bath followed by ~4°C for 10min on ice prior to use. The aptamers used and their sequences are summarised in Table 15.

Identification	Sequence 5' to 3'
Apta20-01	ACC CAA TAT ATG AGG CTC GAT CAA CAG TGT TCT TGA TAT CAC GTC CCT TAA CTG GTA GGG TC
Apta20-02	CTA AGC ATC TTG AGG CTC GAT CTA TTT TAT TTC CCC GAA TTC GGG ATA ACT ATA ATC CGA CA
Apta20-04	CAT CCG ACC ATG AGG CTC GAT CCA GCA TGT TTT ATC AAT GGG ACA TCG GGT CCT TTT GTG AA
Apta20-56	AAC ATT ACG GTG AGG CTC GAT CGC CTA CAA TAT CCA AAA TAC ACT TTC ATA TCT ATC GGA TC
Apta20-90	GCT TCT TCA TTG AGG CTC GAT CGT TTT ATC GAA ACA AAT TTA GCT AGG GCA TTA CGC GCT CA
Apta20-100	TCC CTC CCT TTG AGG CTC GAT CGT CAA GCC ACC TGG CAA TTT CAT AAC TCT CAT GTT TTA CG

Table 15 Summary of aptamers and their sequence used during the colorimetric binding assay

5.2.2 Colorimetric assay – Proof of concept

The T-2 mycotoxin was diluted from a stock concentration of 100ppm (214.3µM) to 107.1µM, 21.4µM, 2.1µM and 0.2µM immediately before use in sterile deionised water. The HT-2 mycotoxin was diluted from a stock concentration of 100ppm (235.5µM) to 117.7µM, 23.5µM, 2.3µM and 0.2µM immediately before use in sterile deionised water.

The aptamer binding performance evaluation assays were based on the colorimetric approach described by Mondal *et al.* (2018). The assay format is illustrated in Figure 26, with modifications as described below. Selection buffer (SLB) pH 7.5 was used as salt buffer. In total three controls were used throughout all the assays. The controls were set up identically through all assays performed. The first control (CA) was prepared by adding 20µL of AuNPs to 20µL of sterile deionized water. The second control (CB) was prepared by adding 20µL AuNPs to 20µL SLB. The third control (CC) was prepared by adding 20µL AuNPs to 20µL of 100µM of oligonucleotide library (ILS2) utilized as starting library during the Capture SELEX protocol.

The samples containing the aptamer sequences (Apta20-01, Apta20-02, Apta20-04, Apta20-57, Apta20-90 and Apta20-100) and target were set up in the same volumes as described for the controls, 20µL of 10µM aptamer and 20µL of 21.4µM T-2 and 23.5µM HT-2 respectively. Aptamer and target solutions were added to a 1.5mL tube with 20µL of AuNPs added. Incubation was carried out in the thermomixer at 37°C for 12min at 500rpm. After completion of the initial incubation, the tubes were removed and 20µL of SLB was added to each sample. A further incubation of 15min 37°C for 12min in the thermomixer was carried out.
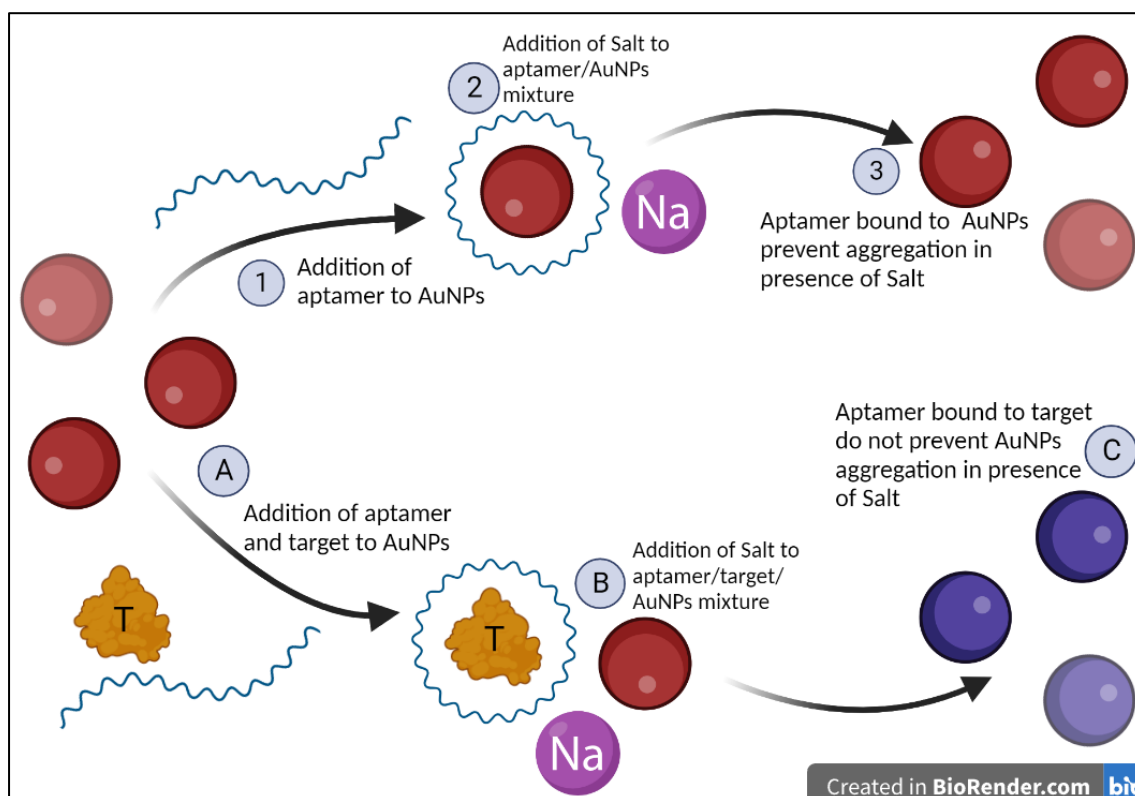
Figure 26 The basic principle of the colorimetric format. AuNPs protected by the oligonucleotides in presence of salt will keep their original red colour. Colour change or aggregation is forced when the aptamers bind to their target instead of the AuNPs present. This colour change can be seen by eye and the intensity measured by spectrophotometry.

5.2.3 Possible aptamer sequence folding in assay

The Mfold software Zuker (2003) was used, **http://www.unafold.org/**, to understand the possible aptamer folding which could be occurring under the assay conditions. The software input details were set without constraints on folding and the ionic conditions set to 100mM for the salt value.

5.2.4 Motif discovery of selected aptamer sequences

Motif comparison of the selected aptamer sequences was completed using the MEME (Multiple Em for Motif Elicitation) software V 5.5.0 (Bailey and Elkan, 1994).

MEME was used to discover novel and ungapped motifs (fixed length patterns) within the sequences. The MEME suite utilised the standard command line : meme sequences.fa -dna -oc . -nostatus -time 14400 -mod zoops -nmotifs 20 - minw 6 -maxw 50 -objfun classic -revcomp -markov_order 0, with maximum number of motifs set to 20 at a minimum width of 6 maximum width of 50. Threshold of p-value was defined as 0.05.

5.2.5 Colorimetric Checkerboard Assays

The 6 aptamers were evaluated using the AuNPs colorimetric assay and in total 12 colorimetric assays were performed based on the checkerboard principle on a 96-well plate. Each aptamer was evaluated against each target, distributing the aptamer dilutions vertically and the toxin dilutions horizontally obtaining the checkerboard dilution principle, (Crowther, 2009).

Each checkerboard assay followed the same format, including the controls (CA, CB and CC) and aptamer/toxin concentration mixes. The analysis parameters of the Epoch 2 were set to wavelength readings at 580nm, 600nm, 620nm, 640nm, 680nm and 700nm at 40°C for a 1min interval duration of 35min, during experimental set up with controls only to determine the optimum wavelength to be used during assay analysis. No shaking was applied. The Gen5 software was used for raw data retrieval.

In the initial stage of the assay, aptamers (100µM,50µM, 10µM, 1µM and 0.1µM) and mycotoxins (T-2 at 214.3µM, 107.1µM, 21.4µM, 2.1µM and 0.2µM and HT-2 at 235.5µM, 117.7µM, 23.5µM, 2.3µM and 0.2µM) were added to designated wells on the plate at 20µL volume respectively. Following, 20µL of AuNPs were added to all of the assay wells. A disposable plate seal was placed onto the plate for incubation. Initial incubation was carried out in the thermomixer at 37°C for 12min at 500rpm. After completion of the initial incubation, the seal was removed and 20µL of SLB was added to each of the assay wells.

The plate was transferred to the Epoch 2 plate reader for spectrophotometric analysis. No shaking was applied. The analysis parameters of the Epoch 2 were set to wavelength reading at 640nm, at 40°C for a 1min interval duration of 30min. The Gen5 software was used for raw data retrieval.

5.2.6 Aptamer binding specificity to non-targets and negative controls

In addition to the checkerboard assays, control assays were performed to evaluate aptamer binding to non-targets and additional negative controls of mycotoxin interference in the colorimetric assay. Aflatoxin B1 and Deoxynivalenol (DON) were selected as non-targets; trialling cross-reactivity. Aflatoxin B1 (320.2μM) and DON (337.5μM) were added to separate solution and with each aptamer at 100μM.

Aptamers, Aflatoxin B1 and DON mixes, as well as T-2 (214.3μM) and HT-2 (235.5μM) without aptamer addition, were added to designated wells on the plate at 20μL volume respectively. 20μL of AuNPs were added to all the assay wells. Controls (CA, CB and CC) were added as described. A disposable plate seal was placed onto the plate for initial incubation. Following initial incubation 20μL of SLB was added except for the T-2 and HT-2 to which water was added. The plate was transferred to the Epoch 2 plate reader for spectrophotometric analysis. The analysis parameters of the Epoch 2 were set to wavelength reading at 640nm, at 40°C for a 1min interval duration of 30min. No shaking was applied. The Gen5 software was used for raw data retrieval.

5.2.7 Benchmark setting utilising Ridascreen® T-2/HT-2 Toxin analysis

An antibody-based ELISA assay was run on proficiency testing materials (oat-based flour) provided by Fera Science Ltd to set a benchmark for the aptamer performance on toxins in the matrix. The ELISA assay was run with 3 samples of finely milled flour containing T-2 mycotoxin spiked at 646.4µg/kg and HT-2 mycotoxin spiked at 218µg/kg. One sample matrix blank of finely milled oat flour was also included.

The samples contained other mycotoxins as part of the proficiency testing scheme. Samples (5g) were weighed out and 25mL of ready-to-use extraction buffer was added. The samples were shaken for 10min and centrifuged for 10min at 3000g at room temperature. The supernatant was used in the ELISA assay. Standard (50µL) were added to the designated assay wells. 50µL of sample was added to the designated assay wells and 70% methanol (50µL) as control were added. To each well 50µL of ready-to-use antibody and 50µL of ready-to-use conjugate were added. The wells were incubated for 30min at room temperature and then washed three times with ready-to-use PBS-Tween wash buffer. Following the wash, 100µL of ready-to-use substrate/chromogen was added and the plate was incubated in the dark for 15min. Following incubation, 100µL of ready-to-use stop solution was added and the plate read using the Epoch 2 plate reader at 450nm. The Gen5 software was used for raw data retrieval.

5.2.8 Aptamer colorimetric assay on proficiency testing oat flour samples

Based upon the results received from the checkerboard assays 50µM of each aptamer was used. The assay was set up as described in Section 5.2.4. The matrix blank and matrix samples, described in Section 5.2.6 were applied to each aptamer, diluted in 70% methanol. The Ridascreen® T-2/HT-2 kit standards were also applied to each aptamer. Additional controls were added to identify cross-reactivity with the 70% methanol between the aptamers, AuNPs and SLB. These controls were applied in the same format as controls CA, CB and CC. Additional controls included the combination of aptamers and 70% methanol and AuNPs and 70% methanol.

The assays were read at 640nm using the Epoch 2 plate reader at 40°C for a 1min interval sweep reading of wells for a duration of 30min. No shaking was applied, The Gen5 software was used for raw data retrieval.

5.3 Results

5.3.1 Possible aptamer folding under assay conditions

The proposed folding structures of the aptamer sequences was predicted using the Mfold web server Zuker (2003). These are illustrated in Figure 27.

An observation made for all the proposed folding structures of the aptamer sequences is that the capture region is part of the main folding body of the structure and does not self-fold. A hairpin region of varying length is also observed in all the aptamer structures. The location of the hairpin varies but closest observed to the 3'.
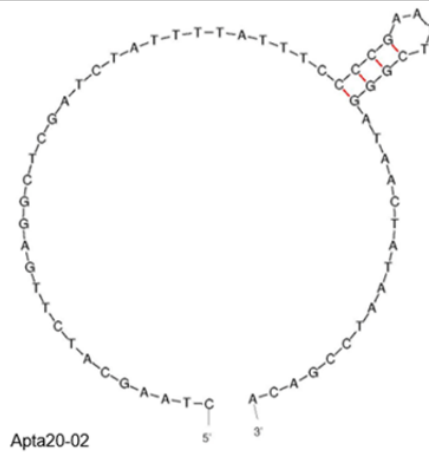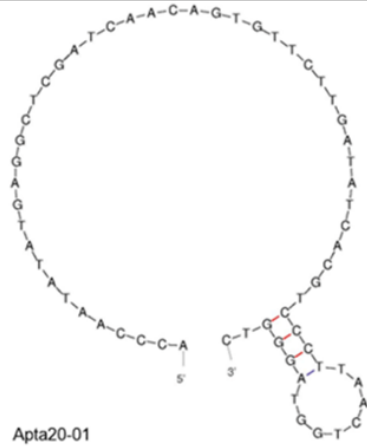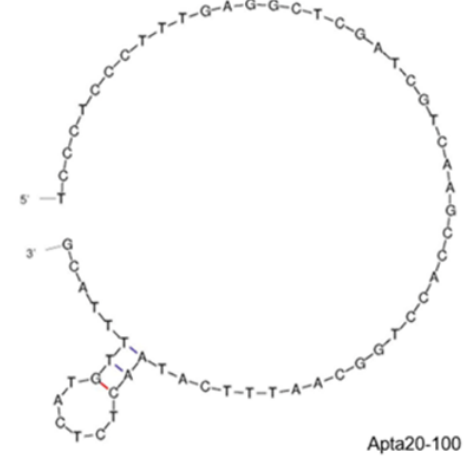
Figure 27 Possible folding structures of the 6 selected aptamer sequences by Mfold web server.

5.3.2 Motif discovery of selected aptamer sequences

Table 16 (page 136 to 138) shows the motif discovery results received from the MEME analysis. The discovery resulted in 15 identified motifs. The table shows the starting position of each motif located on each aptamer sequence as well as the *p*-value of each motif.

Motif	Logo	Aptamer	Motif Start Position	*p*-value
1		Apta20-01 Apta20-02 Apta20-04 Apta20-57 Apta20-90 Apta20-100	11	4.41e-8
2		Apta20-02 Apta20-04	56 3	1.88e-4
3		Apta20-01 Apta20-02 Apta20-04 Apta20-57 Apta20-90 Apta20-100	33 43 29 46 23 41	2.81e-6 2.21e-4 1.41e-5 1.25e-4 6.15e-5 1.70e-5
4		Apta20-01 Apta20-90 Apta20-100	54 43 2	4.17e-5 1.17e-4 7.50e-5
5		Apta20-57 Apta20-90	3 50	6.53e-5

6		Apta20-02 Apta20-04	33 46	1.50e-4 3.38e-4
7		Apta20-01 Apta20-04	43 39	3.75e-4
8		Apta20-02 Apta20-90	5 1	4.70e-4
9		Apta20-57 Apta20-100	23 28	6.75e-4 3.00e-4
10		Apta20-01 Apta20-57	3 34	4.55e-5

11		Apta20-04 Apta20-90	55 33	2.94e-4 6.63e-4
12		Apta20-01 Apta20-04	25 23	6.58e-4
13		Apta20-02 Apta20-100	23 54	2.31e-4 1.02e-4
14		Apta20-57 Apta20-100	56 34	1.88e-3
15		Apta20-90 Apta20-100	57 24	5.70e-3 1.13e-2

Table 16 Motif discovery performed on the 6 aptamer candidates showing 15 motifs found, the sequence logo showing the frequencies scaled relative to the measure of conservation at each position, the aptamer associated to the motif and starting point on the unique sequence with associated combined *p*-values.

138

The MEME analysis identified 15 motifs within the tested 6 aptamer sequences.

Motif 1 was identified to be present across all 6 candidates, showing complete conservation and starting uniformly at position 11. The calculated p-value of the motif was less than 0.05, showing statistical significance. Further evaluation of the motif identifies it as the defined capture region within the aptamer sequence.

Motif 2 was identified on Apta20-02 and Apta20-04, starting before and after the defined capture region within the sequences respectively and showing complete conservation. The calculated p-value of the motif was less than 0.05, showing statistical significance.

Motif 3 was identified to be present across all 6 aptamer candidates. However, the motif was found at different starting positions across the sequences after the defined capture region. Full conservation was seen at motif positions 1, 5 and 6, relating to base pairs T and A. The calculated p-value of the motif was less than 0.05, showing statistical significance.

Motif 4 was identified to be present on Apta20-01, Apta20-90 and Apta20-100. The motif started before the defined capture region on Apta20-100 and post capture region on Apta20-01 and Apta20-90. Full conservation was observed on motif positions 1, 4, 5, 6 and 7 relating to base pairs G and A. The calculated p-value of the motif was less than 0.05, showing statistical significance.

Motif 5 was identified on Apta20-57 and Apta20-90, starting at positions prior to the capture region and post respectively. Full conservation was seen across the motif. The calculated p-value of the motif was less than 0.05, showing statistical significance.

Motif 6 was identified on Apta20-02 and Apta20-04, starting at positions post capture region. Full conservation was seen within the motif with exception of position 1 relating to base pairs A and C. The calculated p-value of the motif was less than 0.05, showing statistical significance.

Motif 7 was identified on Apta20-01 and Apta20-04, starting at positions post capture region. Full conservation was seen within the motif with exception of position 6 relating to base pairs A and T. The calculated p-value of the motif was less than 0.05, showing statistical significance.

Motif 8 was identified on Apta20-02 and Apta20-90, starting at positions prior capture region. Full conservation was seen within the motif with exception of position 3 relating to base pairs A and T. The calculated p-value of the motif was less than 0.05, showing statistical significance.

Motif 9 was identified on Apta20-57 and Apta20-100, starting at positions prior capture region. Full conservation was seen within the motif with exception of positions 4 and 5 relating to base pairs A / T and A / C respectively. The calculated p-value of the motif was less than 0.05, showing statistical significance.

Motif 10 was identified on Apta20-01 and Apta20-57, starting at positions prior (Apta20-01) and post (Apta20-57) capture region. Full conservation was seen within the motif with exception of position 5 relating to base pairs A and T. The calculated p-value of the motif was less than 0.05, showing statistical significance.

Motif 11 was identified on Apta20-04 and Apta20-90, starting at positions post capture region. Full conservation was seen within the motif with exception of position 6 relating to base pairs G and T. The calculated p-value of the motif was less than 0.05, showing statistical significance.

Motif 12 was identified on Apta20-01 and Apta20-04, starting at positions post capture region. Full conservation was seen within the motif with exception of position 6 relating to base pairs G and T. The calculated p-value of the motif was less than 0.05, showing statistical significance.

Motif 13 was identified on Apta20-02 and Apta20-100, starting at positions post capture region. Full conservation was seen within the motif with exception of position 2 relating to base pairs G and A. The calculated p-value of the motif was less than 0.05, showing statistical significance.

Motif 14 was identified on Apta20-57 and Apta20-100, starting at positions post capture region. Full conservation was seen within the motif with exception of positions 2, 4 and 6 relating to base pairs G / C and A / T. The calculated *p*-value of the motif was less than 0.05, showing statistical significance.

Motif 15 was identified on Apta20-90 and Apta20-100, starting at positions post capture region. This is the only motif found with no base pair conservation. The calculated *p*-value of the motif was less than 0.05, showing statistical significance.

5.3.3 Proof of concept colorimetric assay

In the initial stages of the assay development the basic principle of the colorimetric and binding capabilities of the aptamers were investigated. The methodology was based on the procedure described by Mondal *et al.* (2018) with modifications of the salt (sodium chloride) solution used to drive AuNP aggregation. In the publication a recommendation was made to use a pH buffered salt solution, ideally one used during aptamer selection. Consequently, the Selection buffer (SLB) was used because it contained salt at a concentration of 100mM and was used during the Capture SELEX protocol to provide a favourable medium for aptamer- target binding.

Figure 28 shows the principle of AuNPs aggregation. The initial pink colour of un-aggregated AuNPs changes to a purple colour when aggregation occurs. The addition of oligonucleotides does not cause aggregation and slows the process when salt is added subsequently.
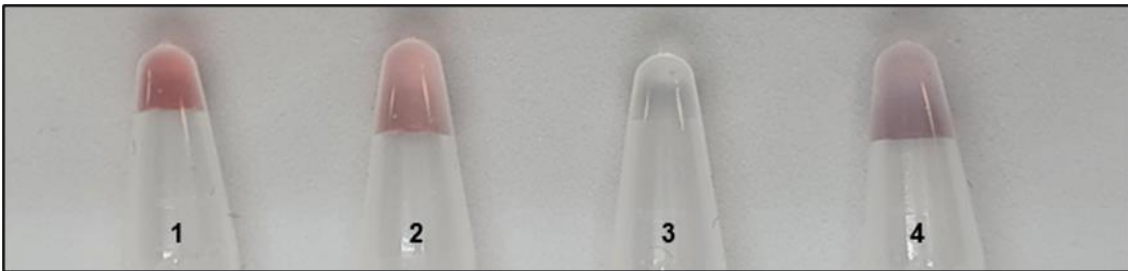
Figure 28 AuNP aggregation assay. **Tube 1** shows the typical AuNPs red colour in their stock form without the addition of any diluents. **Tube 2** shows the AuNPs with the addition of sterile deionised water, displaying a diluted red but no aggregation post incubation. **Tube 3** shows deionised water as neutral colour control. **Tube 4** shows the AuNPs with the addition of SLB showing purple colouration of aggregation

Figure 29 shows the results seen from the colorimetric proof of concept assay testing the aptamer binding capabilities on the target T-2 and HT-2 mycotoxins.

Figure 29 Proof of concept colorimetric assay. (**1.**) show the aggregation controls; **a.** salt buffer control, **b.** AuNPs control (**2.** to **7.**) Aptamer candidates and target toxin mix with control of aptamer sequence and AuNPs; **a.** aptamer and T-2, **b.** aptamer and HT-2, **c.** aptamer and AuNPs

In Figure 29, the first two tubes (**1.**) show the aggregation controls. **a.** AuNPs in presence of SLB show colour change to blue, **b.** AuNPs in presence of sterile deionised water remain in their original red. The lighter shade of red is associated to the dilution of the particles.

Tubes labelled **2.** show binding of Apta20-01 (10µM). **3.** show binding of Apta20-02 (10µM). **4.** show binding of Apta20-04 (10µM). **5.** show Apta20-57 (10µM). **6.** Show binding of Apta20-90 (10µM) and **7.** show binding Apta20-100 (10µM).

The tubes within each series labelled as (**a.**) demonstrate the aggregation of AuNPs (purple colour) as binding of the respective aptamer occurs with the T-2 mycotoxin target (21.4µM). The Tubes labelled as (**b.**) also demonstrate aggregation of AuNPs and binding of the respective aptamer with HT-2 mycotoxin (23.5µM).

The tubes labelled as (**c.**) demonstrate the prevention of aggregation of the AuNPs in presence of the respective aptamer.

5.3.4 Colorimetric checkboard assays

Following the results obtained from the proof-of-concept work a colorimetric checkerboard assay was prepared to assess a limit of detection of the aptamer binding and provide possible quantitative data. Figure 30 shows a representative result of a checkerboard assay, seen after 30 minutes of incubation in the spectrophotometer.
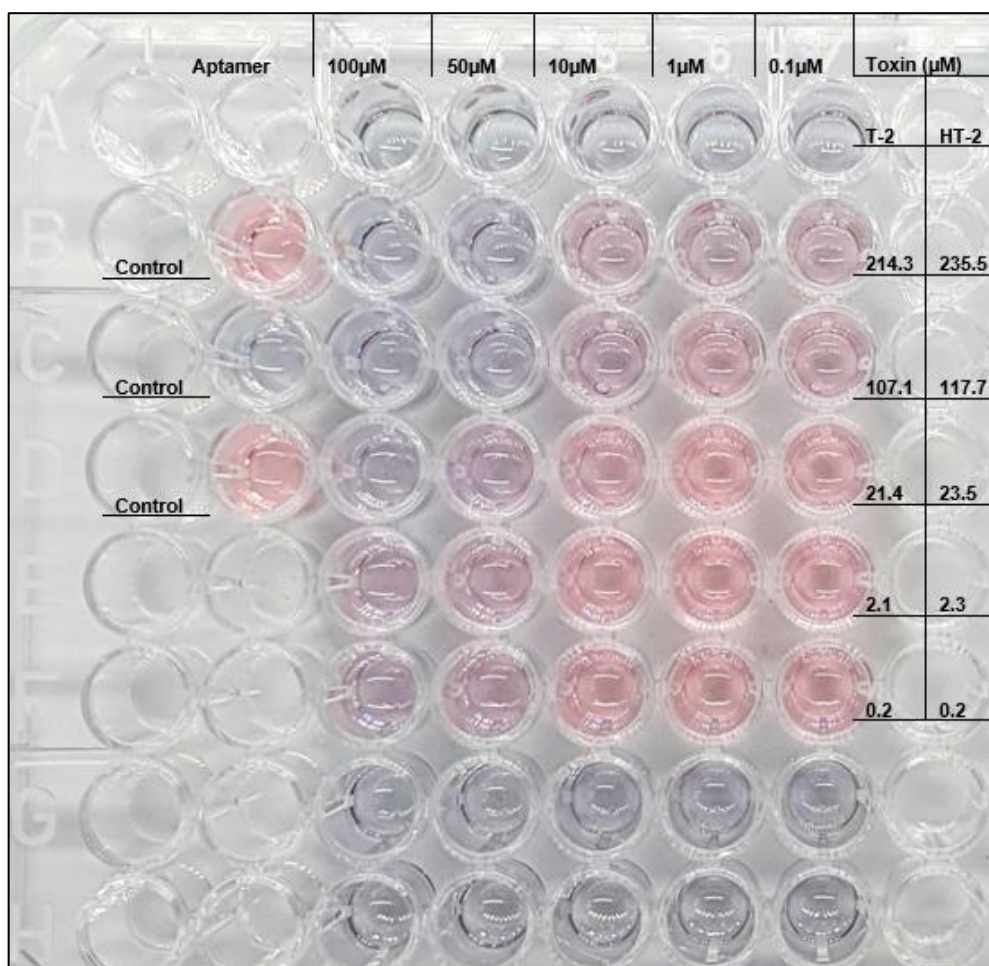
Figure 30 AuNP checkerboard assay. The wells A3 to A7 and G3 to G7 as well as H3 to H7 shall be ignored as these are the result of the filling of the AuNPS and salt buffer (SLB) through a multichannel pipette. Wells B2, C2 and D2 are the controls, CA, CB and CC respectively. The wells B3 to F7 contain the aptamer and toxin mixes.

The wells show distinct colour differences dependant on the aggregation of AuNPs (purple) and non-aggregation of AuNPs (pink). Visually a gradient can be seen, down the aptamer and mycotoxin concentrations, indicating that the binding capabilities of the aptamers at different concentrations to toxins at different concentrations varies. The checkerboard assay was applied to all aptamers trialled, Apta20-01, Apta20-02, Apta20-04, Apta20-57, Apta20-90 and Apta20-100 with similar aggregation patterns observed.
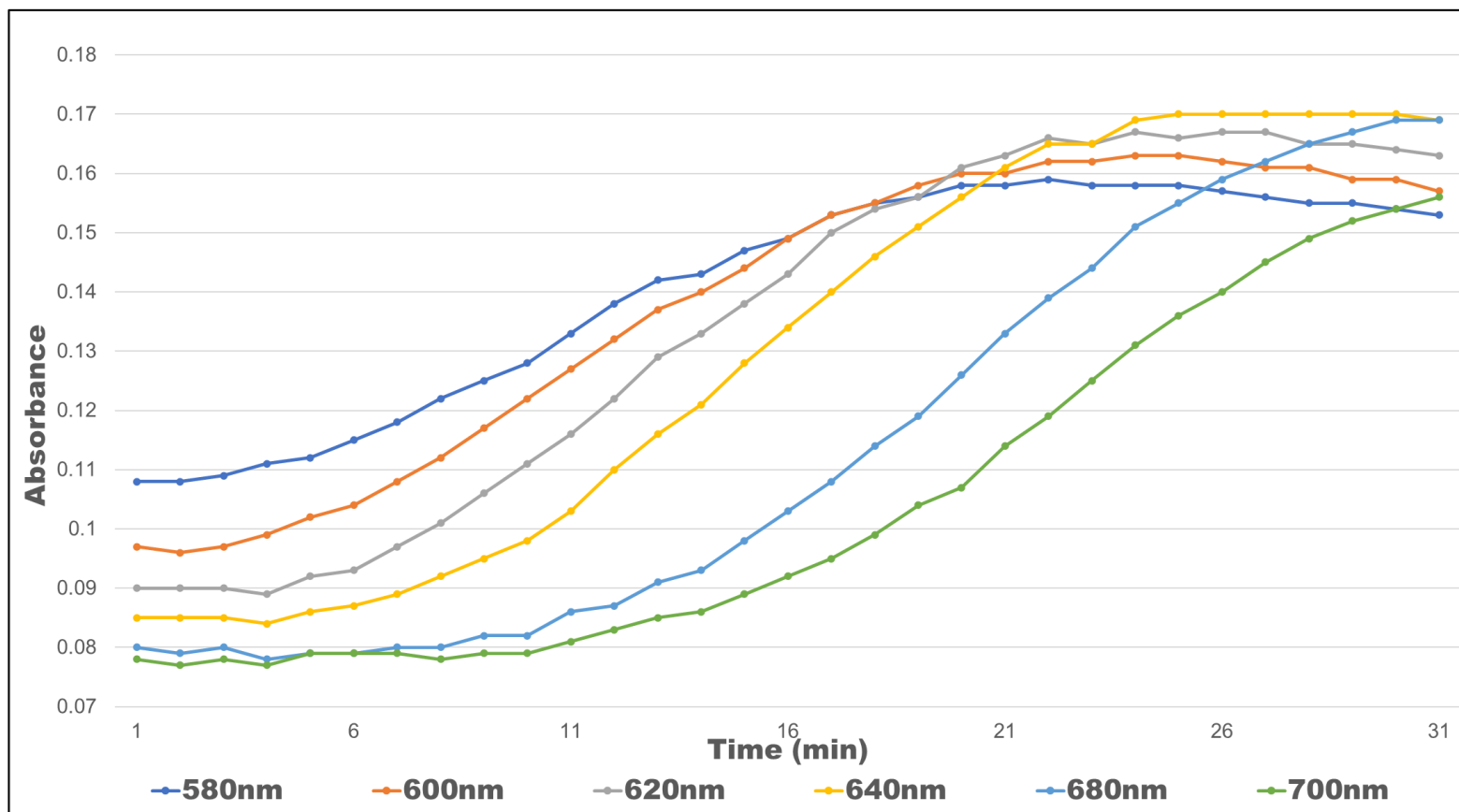
Figure 31 Absorbance curves of the salt buffer control (SLB) with AuNPs showing curve profiles at 580nm, 600nm, 620nm, 640nm, 680nm and 700nm.

Figure 31 shows the changes in absorbance that occurred during the 30min assay run time when measured at various wavelengths. From this the most appropriate wavelength was selected. The highest absorbance was observed at 640nm and this wavelength was selected to evaluate the aptamer performance in all assays.

5.3.5 Aptamer checkerboard assay evaluations of mycotoxins

The checkerboard assay results were evaluated in the same way for all 6 aptamers trialled. The results followed a first step of reviewing the absorbance curves of the aptamer at 100µM at highest and lowest concentration of mycotoxin T-2 and HT-2. The results gave a first indication of the differences in absorbance values measured, which related to the binding of the aptamer to the mycotoxin. The next step included the evaluation of the absorbance values obtained from the aptamer at 100µM across all trialled mycotoxin concentrations. Following the review of the results of the aptamers at 100µM, the aptamer absorbance curves were evaluated across the remaining aptamer and mycotoxin concentrations. From the results, the optimal aptamer concentration was identified. The evaluation allowed for creation of calibration curves as percentage (%) of maximum absorbances with baseline corrections. Baseline correction was applied through the subtraction of the AuNPs control maximum absorbance value. The control consisted of AuNPs with oligonucleotide library (100µM), demonstrating no aggregation.
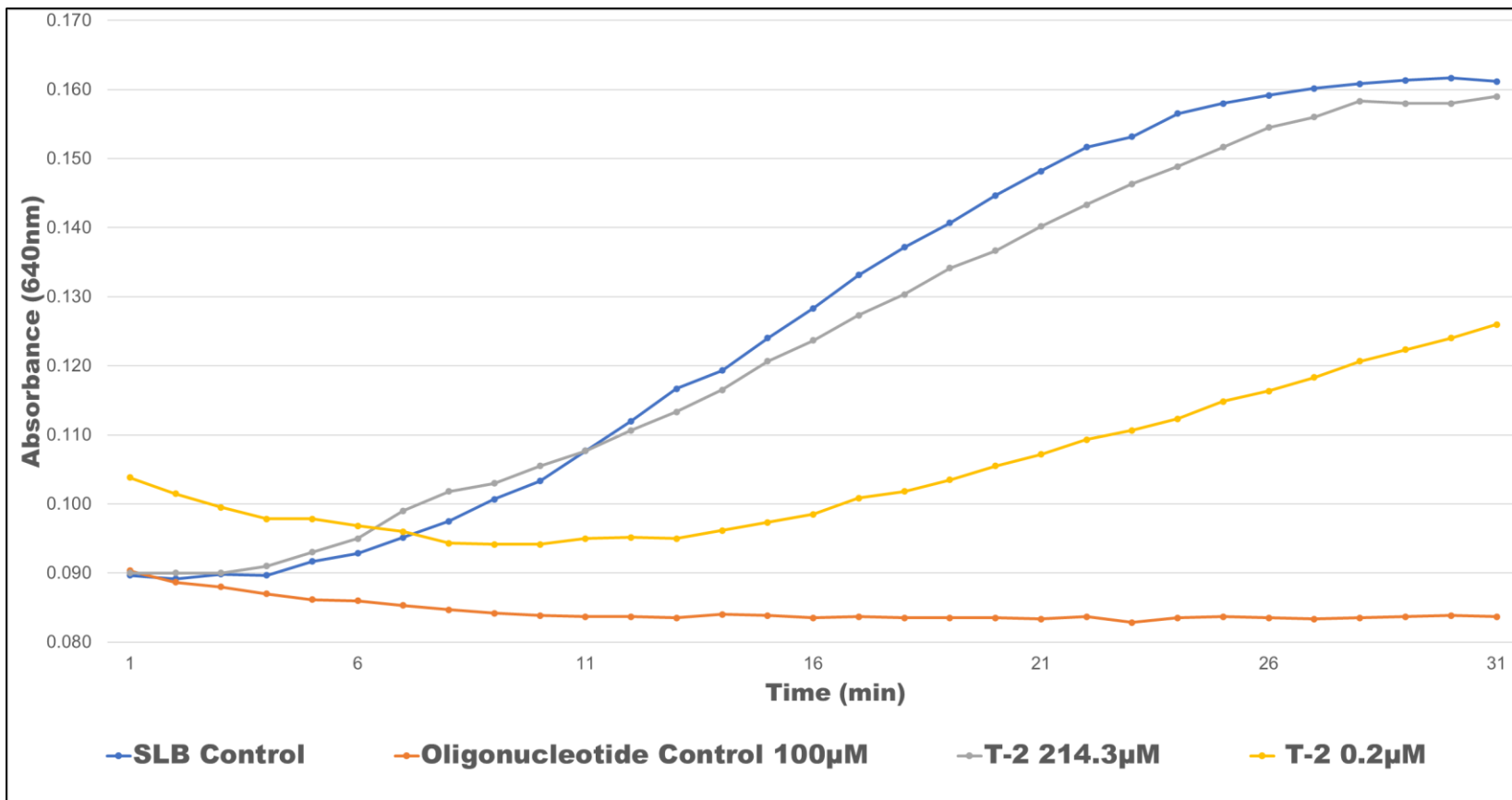
Figure 32 Absorbance curves (640nm) over time. Including SLB and oligonucleotide controls. Samples of Apta20-01 (100µM) incubated with 214.3µM and 0.2µM T-2.

The absorbance values obtained from the incubation of Apta20-01 (100µM) with T-2 mycotoxin at 214.3µM and 0.2µM are shown in Figure 32. Aptamer incubated with 214.3µM T-2 showed a maximum absorbance value of 0.160; demonstrating full binding to target and complete aggregation of AuNPs present. Incubation of Apta20-01 with 0.2µM T-2 demonstrated a maximum absorbance value of between 0.120 and 0.130, indicating partial binding to target and partial aggregation of AuNPs. The SLB control demonstrated full aggregation of the AuNPs with a maximum absorbance value of 0.160. The oligonucleotide control shows no aggregation of the AuNPs with a maximum absorbance value between 0.080 and 0.090.
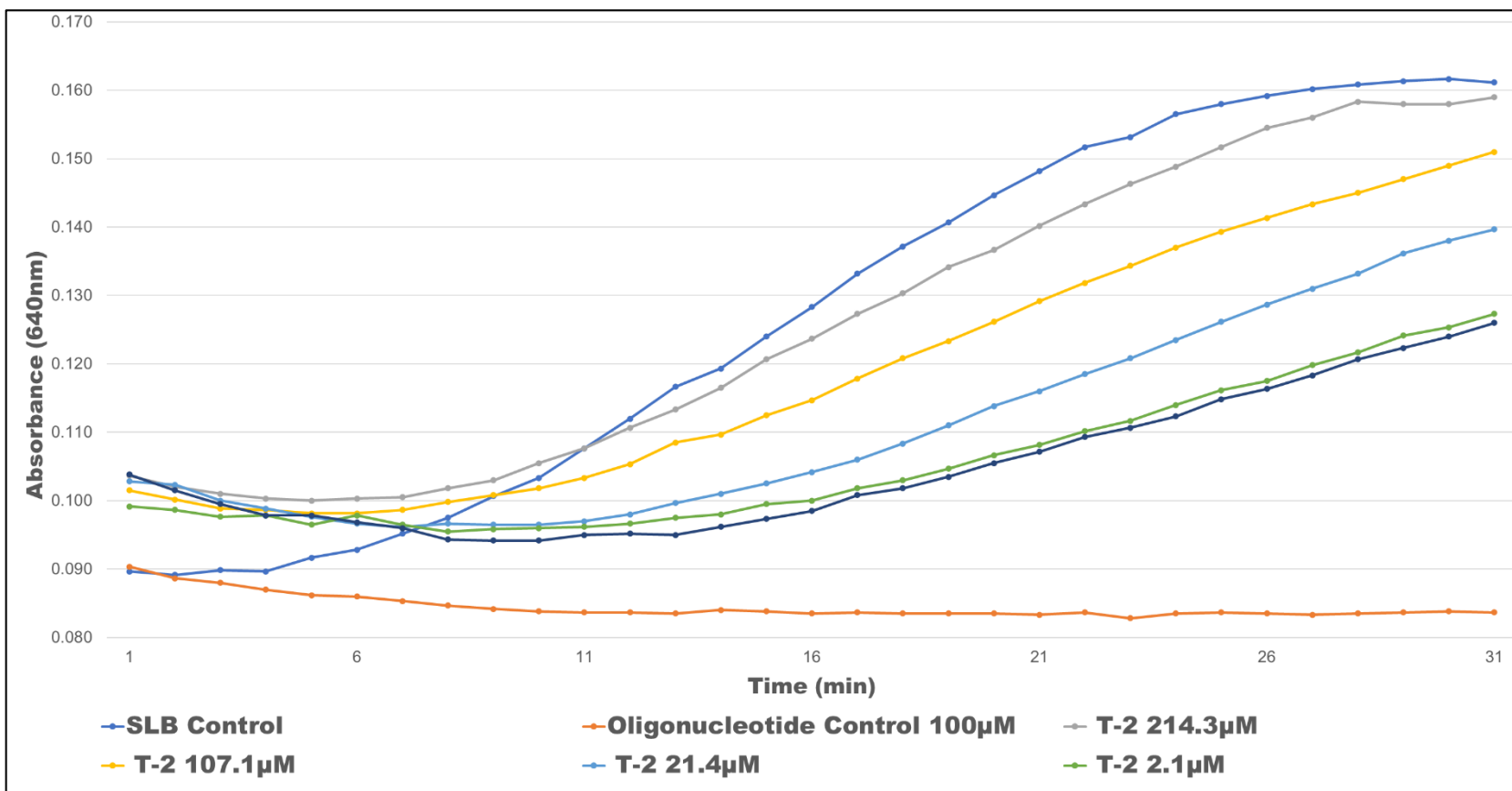
Figure 33 Absorbance curves (640nm) over time. Including SLB and oligonucleotide controls. Samples of Apta20-01(100µM) incubated with 214.3µM, 107.1µM, 21.4µM, 2.1µM and 0.2µM T-2.

The absorbance values obtained from the incubation of Apta20-01 (100µM) with T-2 mycotoxin at 214.3µM, 107.1µM, 21.4µM, 2.1µM and 0.2µM are shown in Figure 33. Aptamer incubated with 214.3µM showed a maximum absorbance value of 0.160; demonstrating full binding to target and complete aggregation of AuNPs present. Apta20-01 incubated with 107.1µM, 21.4µM, 2.1µM and 0.2µM showed a maximum absorbance value of between 0.150 and 0.120; indicating partial binding to target and partial aggregation of AuNPs. The binding of the aptamer can be seen to decrease with the reducing concentrations of mycotoxin, causing the decreasing aggregation of AuNPs. The SLB control demonstrated full aggregation of the AuNPs with a maximum absorbance value of 0.160. The oligonucleotide control shows no aggregation of the AuNPs with a maximum absorbance value between 0.080 and 0.090.
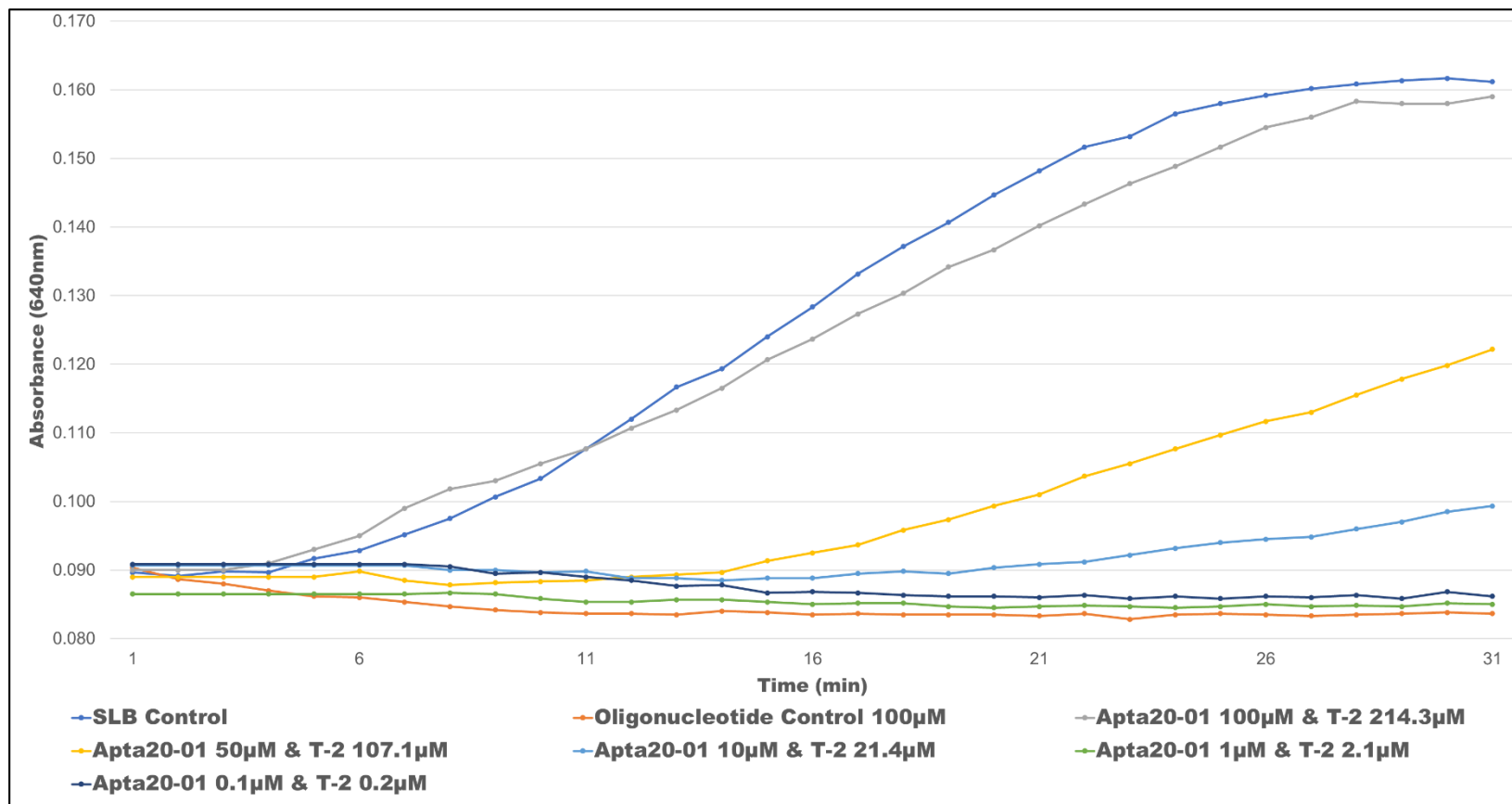
Figure 34 Absorbance curves (640nm) over time. Including SLB and oligonucleotide controls Samples of Apta20-01(100µM, 50µM, 10µM, 1µM, 0.1µM) incubated with 214.3µM, 107.1µM, 21.4µM, 2.1µM and 0.2µM T-2 showing varying aggregation of AuNPs.

The absorbance values obtained from the incubation of Apta20-01 (100µM, 50µM, 10µM, 1µM, 0.1µM) with T-2 mycotoxin at 214.3µM, 107.1µM, 21.4µM, 2.1µM and 0.2µM are shown in Figure 34. Aptamer (100µM) incubated with 214.3µM mycotoxin showed a maximum absorbance value reached at 0.160; demonstrating full binding to target and complete aggregation of AuNPs. Aptamer (50µM) incubated with 107.1µM mycotoxin and 10µM aptamer incubated with 21.4µM T-2 showed a maximum absorbance value of between 0.130 and 0.100; indicating partial binding to target and partial aggregation of AuNPs. The binding of small aptamer concentrations can be seen to decrease with the reducing concentrations of mycotoxins causing the decreasing aggregation of AuNPs. Aptamers (1µM, 0.1µM) incubated with 2.1µM and 0.2µM of T-2 mycotoxin did not demonstrate aggregation of the AuNPs and therefore no binding. A maximum absorbance value of between 0.180 and 0.190 was observed; indicating that the aptamer concentrations are too low to enable target binding. The SLB control demonstrated full aggregation of the AuNPs with a maximum absorbance value of 0.160. The oligonucleotide control shows no aggregation of the AuNPs with a maximum absorbance value between 0.080 and 0.090.
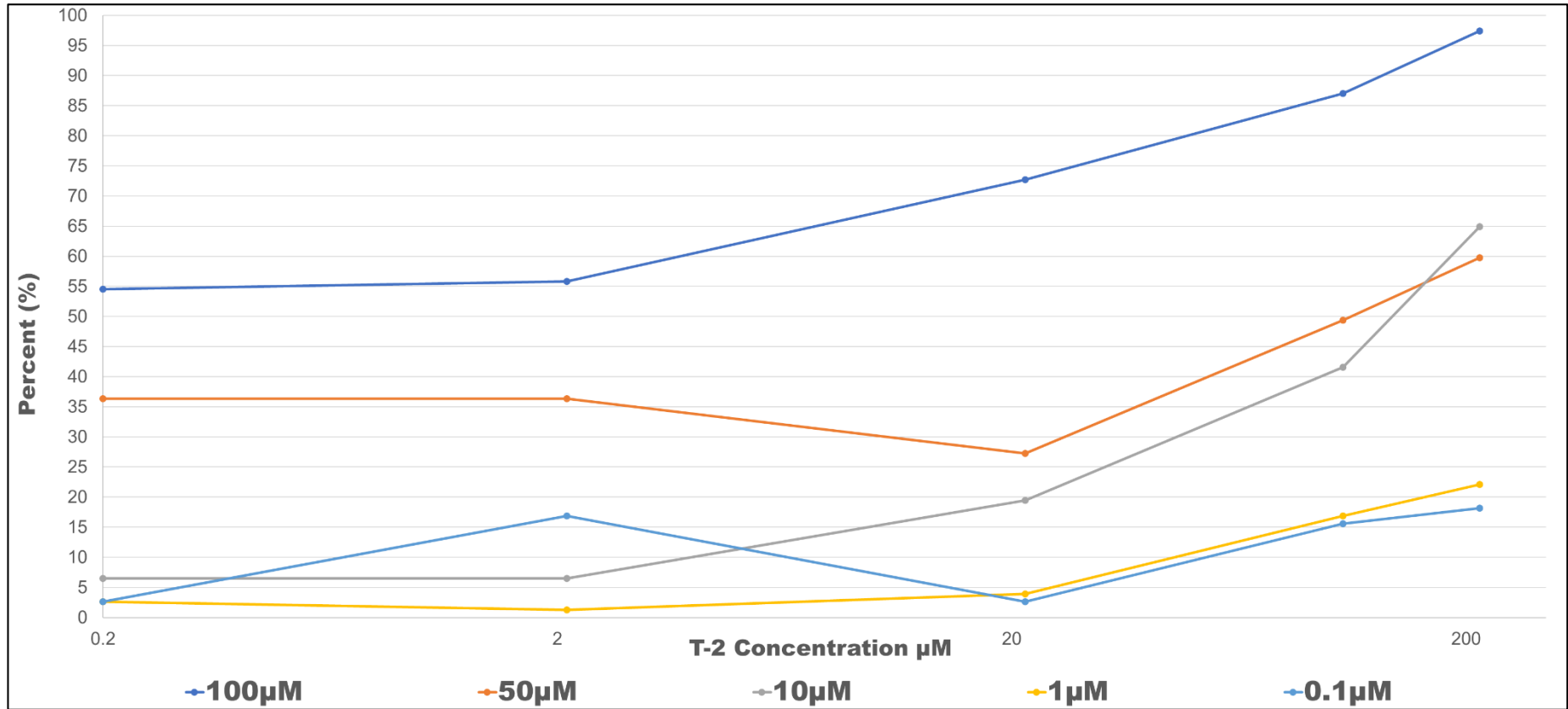
Figure 35 Calibration curve of % maximum absorbance values with baseline corrections on logarithmic scale, of Apta20-01 at 100µM, 50µM, 10µM, 1µM and 0.1µM incubated with 214.3µM, 107.1µM, 21.4µM, 2.1µM and 0.2µM T-2.

Figure 35 showed calibration curves (on a logarithmic scale) for Apta20-01 at various concentrations. The calibration curves showed that increasing toxin concentration raised the maximum absorbance values. In contrast, with reduction in aptamer concentrations the absorbance values decreased. From this data, the optimal concentration of the aptamer binding is 100μM.

5.3.6 Aptamer checkerboard assay evaluations of T-2 and HT-2 mycotoxin

Following the identification of the optimal aptamer concentration (100µM) the calibration curves were compared between Apta20-01, Apta20-02, Apta20-04, Apta20-57, Apta20-90 and Apta20-100 incubated with HT-2 (Figure 36) and T-2 (Figure 37). The aptamer checkerboard evaluations of Apta20-01 with HT-2 and Apta20-02, Apta20-04, Apta20-57, Apta20-90 and Apta20-100 are included in the Appendices (Appendix A to Appendix K).

In Figure 36 the aptamers showed best binding to HT-2 mycotoxin was seen above 117.7µM. Apta20-100 and Apta20-57 showed better binding across a wider target concentration range. Apta20-04 showed good binding, comparable to Apta20-100 and Apta20-57, at 235.5µM and 117.7µM target concentrations. Lower responses were observed for Apta20-01, Apta20-02and Apta20-90 incubated with the mycotoxin.

In Figure 37 the aptamers showed best binding to T-2 mycotoxin target above 107.1µM. Apta20-01 and Apta20-100 show best binding across the mycotoxin concentration ranges. Apta20-57, Apta20-02, Apta20-90 and Apta20-04 bind equally well across the T-2 mycotoxin concentrations, comparably lower than Apta20-01 and Apta20-100.
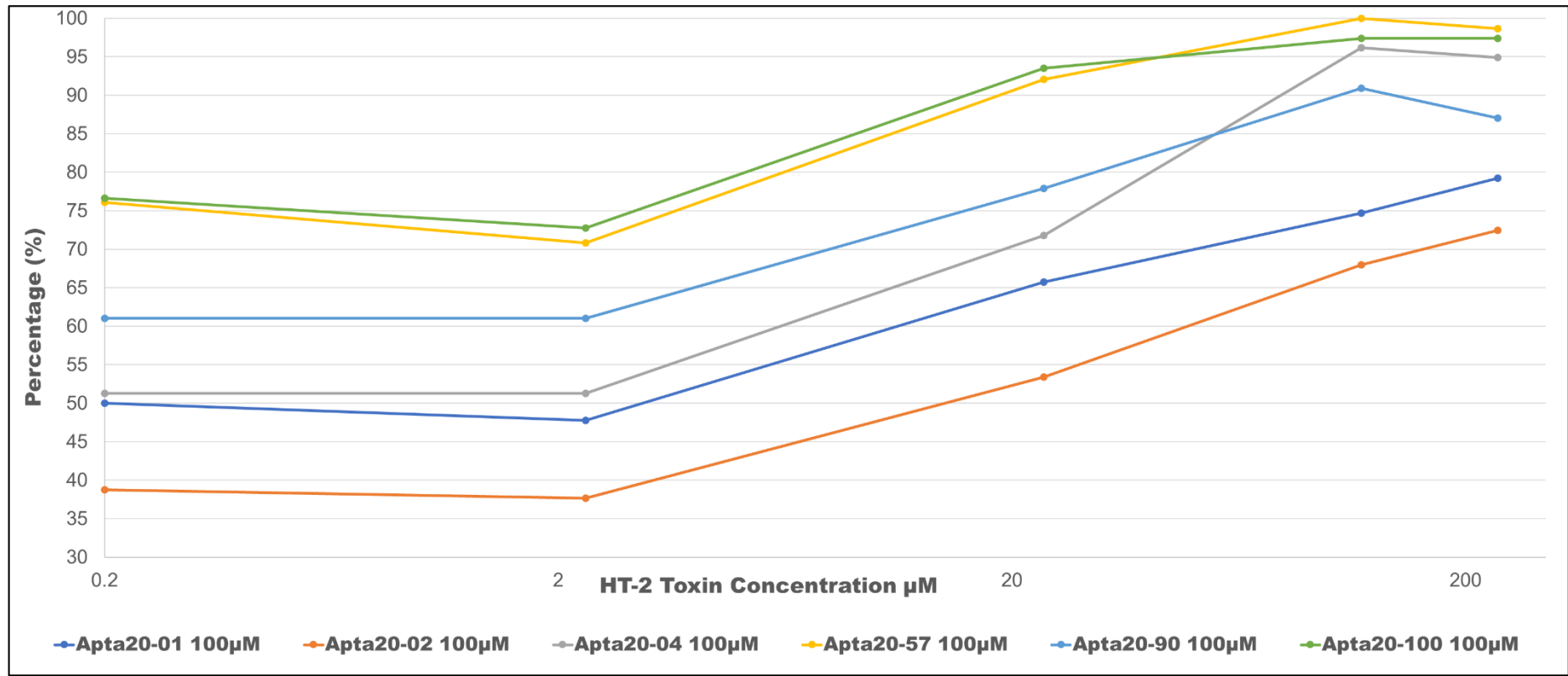
Figure 36 Calibration curve of % maximum absorbance values with baseline corrections, on logarithmic scale of Apta20-01, Apta20-02, Apta20-04, Apta20-57, Apta20-90 and Apta20-100 at 100μM with HT-2 at 235.5μM, 117.7μM, 23.5μM, 2.3μM and 0.2μM.

157
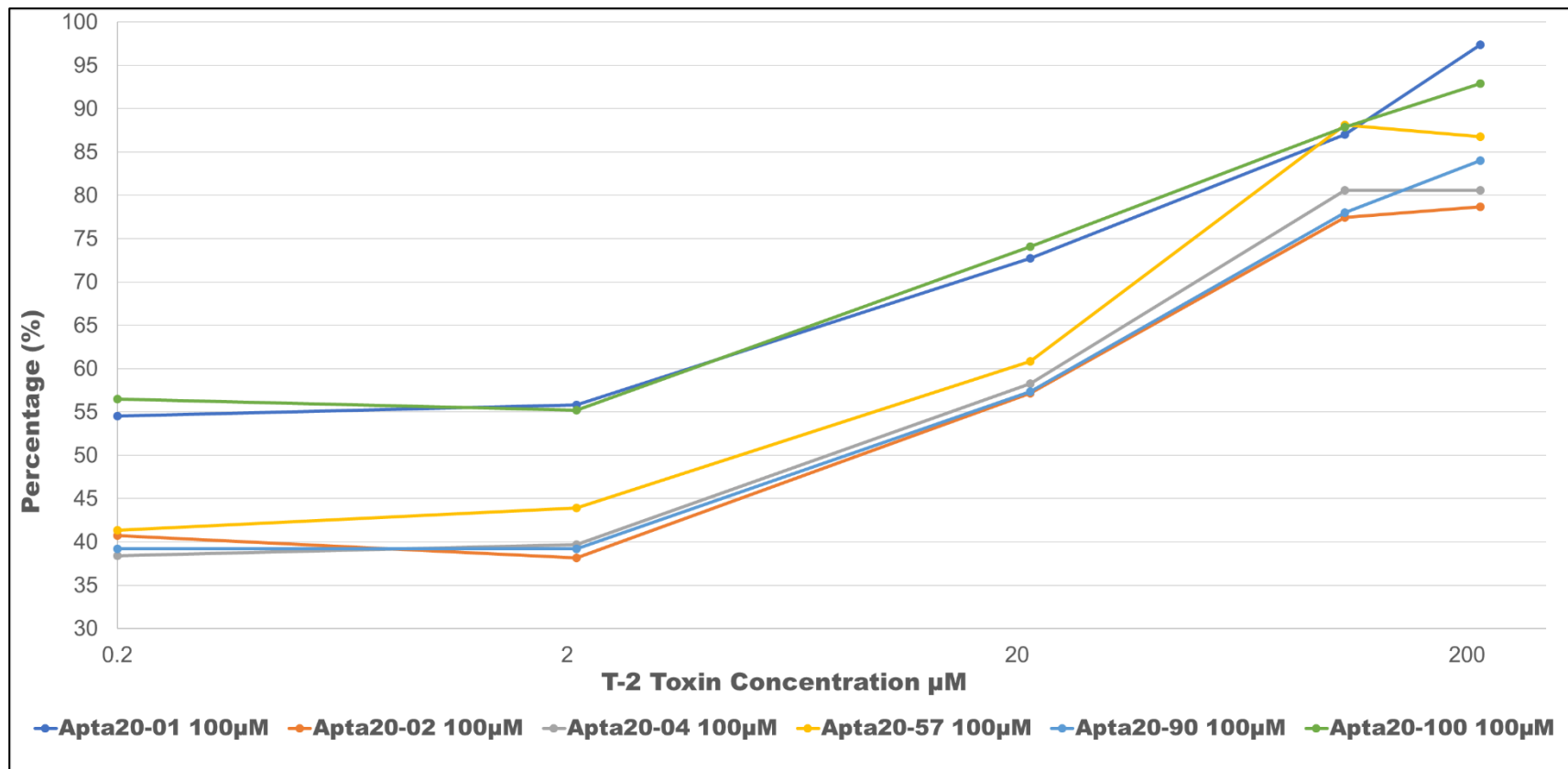
Figure 37 Calibration curve of % maximum absorbance values with baseline corrections, on logarithmic scale of Apta20-01, Apta20-02, Apta20-04, Apta20-57, Apta20-90 and Apta20-100 at 100μM withT-2 at 214.3μM, 107.1μM, 21.4μM, 2.1μM and 0.2μM.
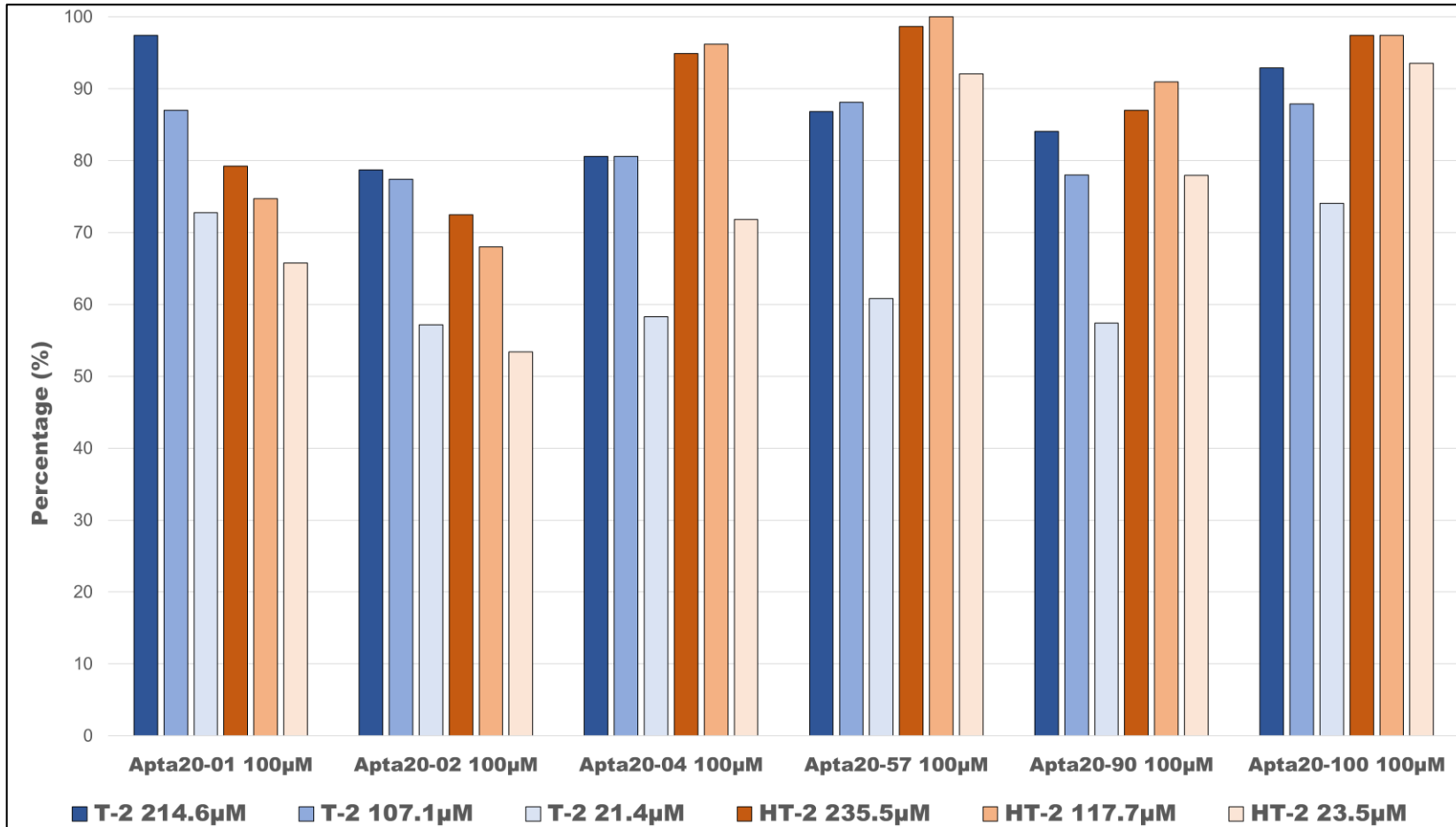
Figure 38 Summary of % maximum absorbance values with baseline corrections of Apta20-01, Apta20-02, Apta20-04, Apta20-57, Apta20-90 and Apta20-100 plotted against T-2 and HT-2 concentrations.

The results in Figure 38 show that under the performed assay conditions, Apta20-100, Apta20-57 and Apta20-04 demonstrated best binding to HT-2 mycotoxin. Apta20-01 demonstrated best binding to T-2 mycotoxin.

5.3.7 Aptamer cross-reactivity

Figure 39 shows a comparison of the 6 aptamers at 100µM with Aflatoxin B1 at 320.2µM, DON at 337.5µM compared to the T-2 at 214.3µM and HT-2 at 235.5µM. Included are the negative controls of T-2 and HT-2 with AuNPs.
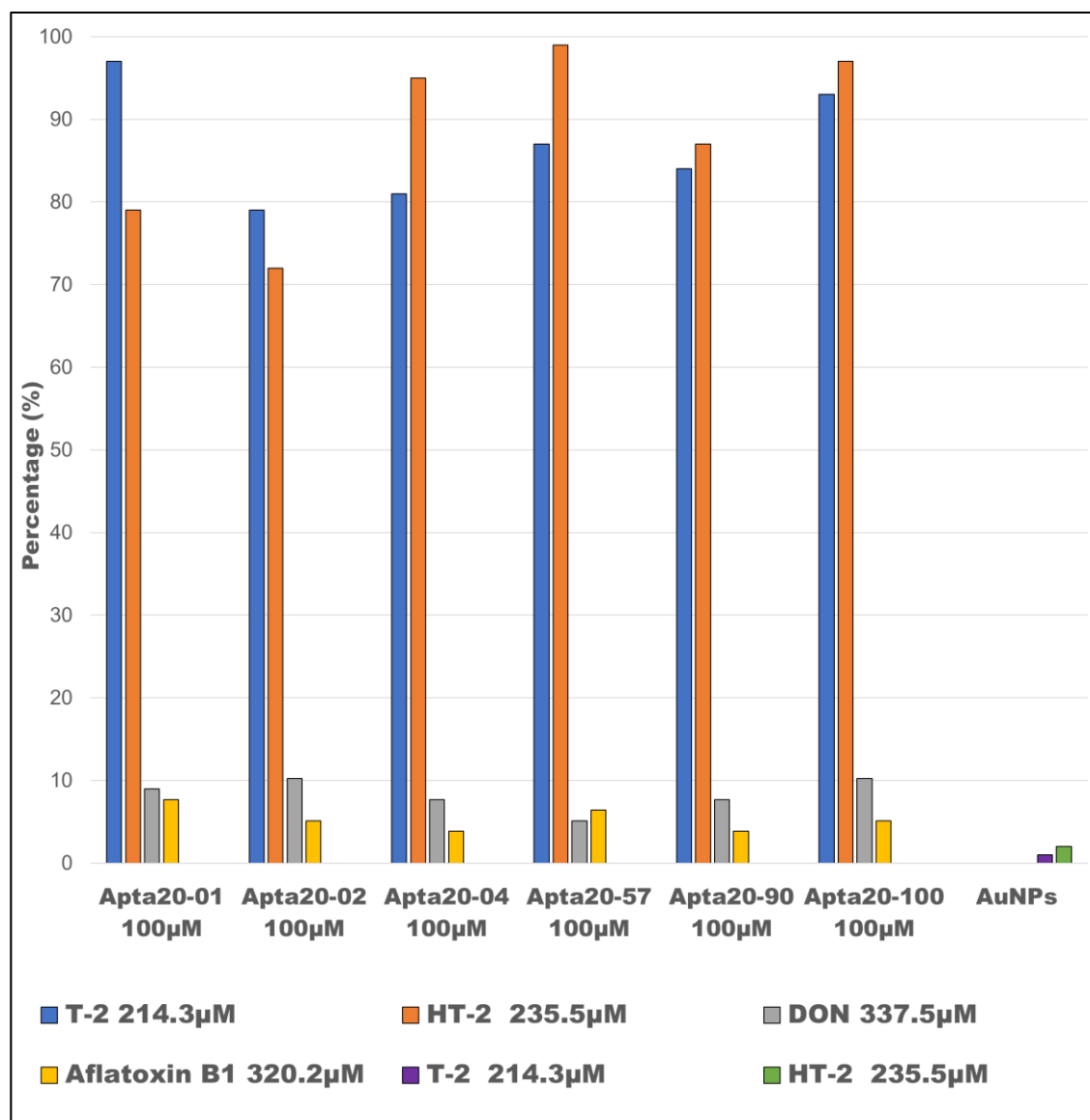
Figure 39 Cross reactivity of aptamers to non-targets DON and aflatoxin B1 in comparison to binding expressed in % maximum absorbance values with baseline correction to the aptamers and the target mycotoxins, T-2 and HT-2. Negative controls of T-2 and HT-2 with AuNPs included.

All aptamers showed low cross-creativity to the non-target mycotoxins DON and aflatoxin B1 with percentage maximum absorbance values below 10% across all aptamer sequences. In comparison the maximum percentage absorbance to the targets, above 70%. No aggregation was observed with the control wells of both T-2 and HT-2 indicating no cross-reaction between mycotoxin and AuNPs.

5.3.8 Ridascreen® T-2/HT-2 Toxin analysis

Figure 40 shows the combined concentration results obtained through the analysis of the oat flour samples through the Ridascreen antibody assay kit.
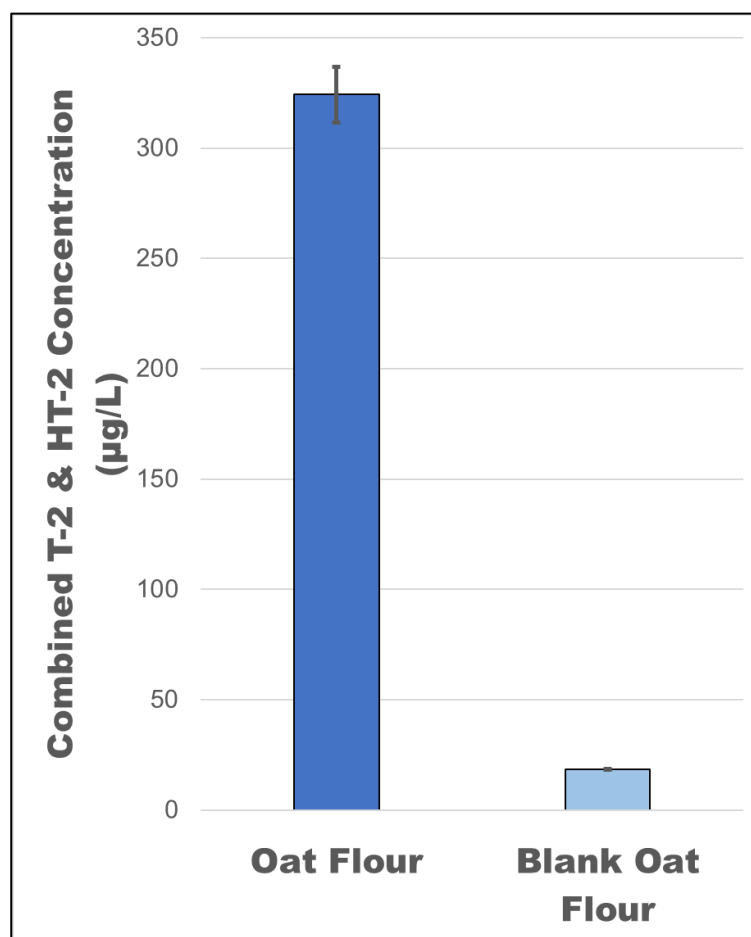
Figure 40 Combined concentrations of T-2 and HT-2 mycotoxins in oat flour samples and blank oat flour samples obtained through the Ridascreen antibody assay. Values shown are averages (±s.d.), n=3.

The results from the antibody assay showed an average (±s.d.) T-2 and HT-2 combined concentration of 324.2µg/L, (±s.d.12). The blank oat flour showed an average concentration of 18.3µg/L, (±s.d.0.2).

5.3.9 Aptamer colorimetric format assay on proficiency testing oat flour samples

Figure 41 shows the results obtained from the analysis of the oat flour samples using Apta20-01. Absorbance measured at 640nm.
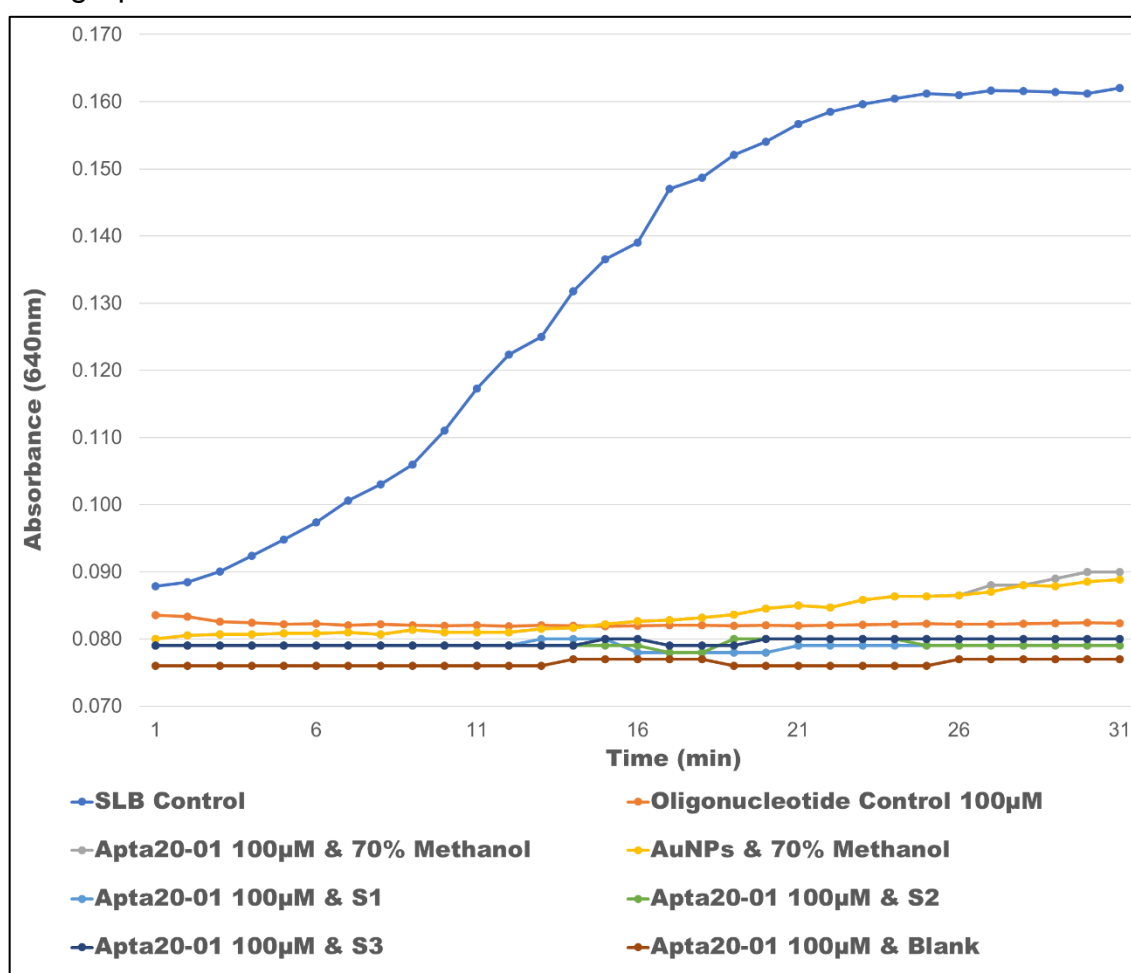
Figure 41 Absorbance curves (640nm) over time. Apta20-01 (100µM) AuNP assay of oat flour samples (S1, S2 and S3). Salt buffer (SLB), oligonuceotides and 70% Methanol as controls.

The results of the colorimetric assay showed that maximum absorbance values were obtained after 30min for the aptamer and sample and blank mixes, comparable to the maximum absorbances values of the oligonucleotide control (0.080). This suggested that no binding to target occurred as the aptamer sequence protected the AuNPs from aggregation. The same results were observed for all the other aptamers tested and highlight the need for future work to understand the cause of the non-binding of the aptamers in matrix.

5.4 Discussion

AuNPs colorimetric assays were successfully developed to investigate the binding of the 6 aptamer candidates: Apta20-01, Apta20-02, Apta20-04, Apta20-57, Apta20-90 and Apta20-100 to the T-2 and HT-2 mycotoxin targets. From the first proof of concept work, the difference between aggregated and non-aggregated AuNPs was visible, showing that the oligonucleotides were able to protect the AuNPs from aggregation (pink colour). Whereas in solution with aptamers and target molecules the aptamers bound to the target instead of protecting the nanoparticles from aggregation (purple colour). The initial results of the colorimetric assay demonstrated that the aptamers also bound to both mycotoxins, independent of the Capture SELEX selection from which the aptamer sequences originated. These aptamers were unique sequences most abundant within the selection pools demonstrated good binding. This confirmed that the application of the acceptability criteria was appropriate. The use of AuNPs was easy to use, cost-effective and don't necessarily require complex analytical equipment to observe a qualitative result.

The data established that aptamer candidates that were most abundant unique sequences within the HTS analysis were good aptamer candidates. Through the evaluation of the high throughput sequencing data in Chapter 4, the unique sequences trialled as aptamer candidates all originated from within the pool of 50% most abundant or frequent sequences. Apta20-01 was observed in the later rounds of selection 9 to 15 within the T-2 specific selection and was not found in the HT-2 selection pool. Apta20-02 was observed across most of the T-2 selection pool, rounds 4 to 15, and like Apta20-01 was not observed within the HT-2 selection pool. Apta20-04 was found in selection rounds 6 to 14 of the T-2 pool as well as within the HT-2 pool, rounds 4 and 12. Apta20-57 was seen across multiple rounds of HT-2 selection however only within the pool of most abundant sequences in the later rounds, 10 to 15.

Furthermore, the sequence was observed within the T-2 selection pool in rounds 11 to 13. Apta20-90 was the only unique sequence seen within the first round of HT-2 selection as well as later rounds, of which the majority of occurrence was outside of the 50% most frequent cut-off criteria. Finally, Apta20-100 was seen in rounds 6 and 7 however most of the occurrence was within rounds 4 to 14 outside of the cut-off criteria.

Similar observations were made by Ferreira *et al.* (2021) and Liu *et al.* (2022b), who reported that aptamer candidates that were most abundant within the selection have the highest binding. The findings from the colorimetric assays presented herein further demonstrate that unique sequences found within early selection rounds and continue to present in later rounds, have strong binding towards their target. Schütze *et al.* (2011) made similar conclusions based upon their evaluation of high throughput sequencing data and subsequent binding assays. For example, in this study Apta20-90 showed good binding to both targets, having been observed within the first round of Capture SELEX.

Hoinka *et al.* (2015) however, made contrary conclusions. Aptamer candidates originating from the most abundant or frequent pool of unique sequences may not have been the best candidates and they highlighted the importance of the structure and length of an aptamer sequence as contributing factors to good binding.

To determine which of these conclusions is most applicable to the aptamers developed in this study, future work would need to include assessment of unique sequences found outside of the 50% cut-off acceptability criteria and at low abundance within a round. The results presented in Chapter 4 of this thesis show the unique sequences observed in selection round 2 for both mycotoxins passed two out of the three acceptability criteria (length of 62 base pairs and capture region).

They were excluded from the 50% most abundant sequences acceptability criteria due to their low abundance within round. Selecting unique sequences from round 2 for binding assessment would provide additional information to understand performance of these unique sequences and allow for comparison of binding between most abundant and least abundant. The results obtained would allow for the understanding if low abundance aptamers have potential use as aptamers.

The findings of the proof-of-concept colorimetric assays were solely based on the observed colour changes induced by aggregation of the AuNPs. Visual evaluation was not entirely suitable as interpretation is subjective with regards to colour intensity and tones of blue, purple, pink and red. Further refinement of the assay required the use of more quantitative methods such as spectrophotometry, especially to evaluate the binding of aptamer to toxin. The checkerboard assay format was successfully utilised allowing for a semi-quantification analysis of aptamer binding. The AuNPs and SLB control acted as a standard for the full aggregation potential of the AuNPs from the salt. Calibration curves containing the aptamers as well as the oligonucleotide control demonstrated successful binding to the T-2 and HT-2 targets, shown by the aggregation of AuNPs. Aggregation curves similar in profile to the AuNPs and oligonucleotide control demonstrated non-binding to the targets. The AuNPs and SLB control reached full aggregation after 30min of assay run time. In comparison the AuNPs and oligonucleotide control did not display aggregation which suggested that the temperatures and time of the assay run did not have an adverse effect. The control curves and values provide a baseline against which the aptamer binding could be evaluated. The application of baseline correction to these absorbance curves allowed for the removal of the background effects, in this instance the removal of the blank AuNPs absorbance values, (Liland *et al.*, 2011).

Overall, a tool was developed successfully enabling subsequent evaluation of aptamer binding. The calibration curves indicated that the aptamers performed optimally at highest concentration (100µM) across the T-2 and HT-2 toxin concentrations (Figures 36 and Figure 37). The 10µM concentration of the aptamers as well as the 1µM concentration were observed to have good binding to the highest toxin concentrations, 214.3µM and 107.1µM for T-2 and 235.5µM and 117.7µM for HT-2. The lowest concentration 0.1µM, showed the lowest % maximum absorbance values to the target nonetheless binding was observed. The findings demonstrated that at the lowest aptamer concentration, target binding occurred. From the target binding calibration curves, it could be concluded that each aptamer at the optimal 100µM concentration enabled a limit of detection of approximately 2.1µM T-2 and 2.3µM HT-2. However, it should be highlighted that even at these lowest toxin concentrations Apta20-100 and Apta20-01 showed a percentage maximum absorbance above 55% binding to T-2. Apta20-100 and Apta20-57 show a percentage maximum absorbance above 75% binding to HT-2 and Apta20-90 showing above 60%. This suggest that the detection limit of both assays could be lower.

Based upon the selection of the optimal aptamer concentration, the binding performance of the 6 aptamers was compared against each other over a range of toxin concentrations (Figure 36 and Figure 37) The 6 aptamers tested with T-2 mycotoxin at different concentrations were observed to have similar calibration curve profiles, suggesting comparable binding. However, Apta20-100 and Apta20-01 exhibited the highest % maximum absorbance values over the range of 21.4µM, 107.1µM and 214.3µM of T-2, ranging between 70% and 100%. Apta20-57, Apta20-02, Apta20-04 and Apta20-90 have comparably lower binding between 50% and 90%. Apta20-57 matched the binding of Apta20-100 and Apta20-01 at 107.1µM of toxin. The observations made for Apta20-100 and Apta20-01 in relation to their occurrence within the 50% most abundant sequences during the Capture SELEX selection, demonstrated that unique sequences observed during the later and middle rounds of selection show good binding. Apta20-01 was specifically selected from the T-2 selection pool and

Apta20-100 from the HT-2 selection pool, however, it showed cross-reactivity to the T-2 toxin molecule. Cross-reactivity was observed with Apta20-90 having originated from the HT-2 selection pool. Apta20-02 and Apta-04, observed across most of the T-2 selection rounds, with Apta20-04 occurring within the HT-2 selection as well. Apta20-57 showed the highest binding at 107.1µM and 214.3µM of T-2 toxin, the unique sequences observed within the T-2 and HT-2 selection rounds.

The 6 aptamers tested with HT-2 mycotoxin at different concentrations showed variability of binding to the target molecule. Apta20-57 and Apta20-100 exhibited the highest binding to the target molecule throughout the range of toxin concentrations. Apta20-100 occurred within the most abundant pool in HT-2 selection rounds 6 and 7 but for the majority below the 50% most abundant cut of criterion. Apta20-57 occurred within the most abundant pool in later rounds and outside of the cut off criterion in multiple rounds as well. Whilst Apta20-57 was observed within the T-2 selection pool, Apta20-100 did not occur in the T-2 selection pool. Apta20-90 showed highest binding at 117.7µM of HT-2 toxin, which demonstrated that an unique sequence seen within the first round of Capture SELEX had good binding to the target toxin. Apta20-04 showed good binding as well, although predominantly seen within the abundance pool of T-2. However, it was also observed within the HT-2 most abundant pool in rounds 4 and 12, which demonstrated that cross-selection can lead to cross-reactivity of aptamers. Apta20-02 and Apta20-01 in comparison have the lowest binding to the HT-2 target and neither unique sequence was seen within the HT-2 selection pools. Despite this, their % maximum binding at 235.5µM of HT-2 toxin ranged between 70% and 80%.

Overall, each of the 6 aptamer candidates demonstrated good binding to T-2 and HT-2 targets. The similarity of the aptamer structures could explain the observed cross-reactivity of the aptamers to both mycotoxins. Through the evaluation of the possible folding of the unique sequences through the Mfold program (Figure 26), all 6 aptamer candidates were modelled with similar structures each with a single hairpin. The Mfold web server is a combination of different related software

applications freely available providing a platform in which RNA and DNA structures can be modelled and folded under different conditions which can be modified by the user, (Zuker, 2003). Overall, the proposed folding of the aptamers was circular with no self-folding on the capture region TGA GGC TCG ATC. The capture region remains part of the main body of the proposed folding structure and can be considered as the important 'anchor' within the Capture SELEX process and the AuNPs colorimetric binding assay. In combination with analysis of folding structures, the use of aptamer sequence motif discovery has been highlighted as a useful characterisation tool, enabling identification of aptamers likely to show highest binding affinity without laboriously testing each identified aptamer individually through binding assays, (Cole and Lupták, 2019). The motif analysis presented in Table 16 within this Chapter shows 15 motifs discovered across the 6 aptamer sequences. None of the discovered motifs were unique to an aptamer sequence and each aptamer sequence presented with multiple motifs. 14 of the motifs showed full or partial conservation except for 1 motif (motif 15). Furthermore, each motif was located at different starting positions within the aptamer sequences, except for motif 1, identified as the capture region. In a recent publication by Zhang and colleagues (2023) motif analysis was used to establish a link between motifs and binding affinity. Briefly, the team used a novel capillary electrophoresis SELEX (CE-SELEX) to develop aptamers targeting the fibroblast activation protein (FAP). Using high throughput sequencing and aptamer structure analysis (folding structure and motif discovery), they concluded that the number of motifs presented on an individual aptamer is not as essential for binding capabilities as the location of the motif and conservation of the motif identified. Within the study, the aptamer sequence with highest binding affinity (tested through gold nanoparticle assay) to the target was a sequence with a full motif conservation and not located within possible hairpin structures. However, all their identified aptamers showed good binding to the FAP target. Their findings align with the motif discovery findings presented in this chapter, most of the discovered motifs presented with full or partial conservation and did not form part of hairpin structures. In combination with calculated p-values below 0.05 the motifs found are significant and likely to be an integral part of the binding capability of the aptamer.

Analysis of the aptamer binding towards non-target mycotoxins, DON and Aflatoxin B1, to assess cross-reactivity further. The mycotoxin DON was selected as it is structurally very similar to T-2 and HT-2 and originated from the same *Fusarium* species. Aflatoxin B1 was selected as it was structurally unrelated.

Type	Trichothecenes	Region 1	Region 2	Region 3	Region 4	Region 5
A	T-2	OH	OAc	OAc	H	OCOCH2CH(CH3)2
A	HT-2	OH	OH	OAc	H	OCOCH2CH(CH3)2
B	Deoxynivalenol	OH	H	OH	H	=O

Table 17 Basic chemical structure comparison of T-2, HT-2 and DON highlighting the region of difference (R2) between T-2 and HT-2, (Thipe *et al.*, 2020).

Given the very close structural similarities between T-2 and HT-2 toxin, differing in the acetyl region between a OAc (T-2) and OH (HT-2) group the cross-reactivity between the aptamers and both molecules can be explained. Structurally, DON differs from both type A mycotoxins at regions 2, 3, 4 and 5 which explains the lack of cross-reactivity. This is further confirmed in the case of aflatoxin B1 which is even more structurally dissimilar.

This observation is confirmed by the results seen in Figure 38 the 6 tested aptamers had very low, almost negligeable, cross-reactivity in comparison to the binding towards the targets.

Having evaluated the aptamer binding performance to the targets when present in very simple matrices the work was extended to evaluate more complex matrices. In a one-off experimental design, the aptamer performance was tested

to bind to the targets extracted from oat flour matrix. Unfortunately, the assay was unable to detect the presence of T-2 and HT-2 in the oat flour extract. The extract from the oat flour samples were tested by the ELISA (according to manufacturers instructions). The results of the antibody assay showed a combined concentration of T-2 and HT-2, over 300µg/L (0.3µg/mL). However, the expected spiked concentrations were above 650µg/mL, (646µg/mL T-2 and 218µg/mL HT-2, suggesting that a degradation of the toxins occurred possibly during sample storage and repeated freezing/thawing. Nonetheless, the calibration curves of the aptamer based assays indicated that they should have been able to detect the concentrations present in the extract (0.6µM and 0.7µM of targets). Apta20-100, Apta20-90 and Apta20-57 demonstrated binding to 0.2µM of HT-2 target at 100µM aptamer concentration (Figure 36). From the calibration curve it appears unlikely that Apta20-01, Apta20-02 and Apta20-04 would be able to bind to HT-2 target at 0.2µM. The limit of detection for these aptamers was shown to be 23.5µM of HT-2. Both Apta20-01 and Apta20-100 demonstrated binding to T-2 at 0.2µM at 100µM aptamer concentration (Figure 37). Apta20-02, Apta20-04, Apta20-57 and Apta20-90 show not to bind to 0.2µM of T-2, having a possible limit of detection of 21.4µM T-2 toxin based. Therefore, Apta20-100, Apta20-90 and Apta20-57 had the potential to detect the HT-2 targets within the oat flour matrix and Apta20-01 and Apta20-100 had the potential to detect the T-2 target. Other factors may have contributed to the assay failure, include the presence of methanol or other components extracted from the sample.

The sample extracts were stored in 70% methanol and several additional controls were performed during the colorimetric assay to establish any adverse effects of the 70% methanol and aptamer combination as well as the ability of the aptamers to protect the AuNPs from aggregation in combination with 70% methanol. The results of the controls indicated that the presence of methanol did inhibit the ability of the oligonucleotide control slightly to protect the aggregation of the AuNPs.

However, in comparison to the full aggregation of the AuNPs in the presence of SLB and methanol the observed inhibition was almost negligible as the maximum absorbance value recorded was 0.089. The combination of matrix blanks and aptamers indicated that aggregation of the AuNPs in presence with the methanol and SLB was prevented. The oat flour sample spiked with T-2 and HT-2 mycotoxin showed the same curve profile as the blank.

Although mixtures of T-2 and HT-2 mycotoxins were not tested during the assay development, it is considered highly unlikely to have interfered with assay performance due to their structural similarities. It would need to be noted that upon further investigation of the components of the proficiency testing material it contained more target analytes (spiked materials) than T-2 and HT-2 mycotoxins, it is therefore possible that these co-extracted materials interfered with the assay performance. These materials could include proteins, lipids, carbohydrates which may have inhibited target binding. Further work would be required to understand the impact of co-extracted components on aptamer binding.

In a recent paper by Zhang *et al.* (2021) the authors describe the use of a colorimetric aptasensor based on AuNPs for the detection of T-2 mycotoxin. The tested aptamer sequence had a length of 41 base pairs and had been previously described by Chen *et al.* (2014) and Zhong *et al.* (2019). The approach to the colorimetric assay was applied to real life wheat and corn samples. The aptamer at 0.1µM concentration was able to bind successfully to T-2 mycotoxin, detecting low concentrations of 0.1µM. In contrast, the aptamers identified within this thesis were found to bind at optimal concentrations of 100µM with target concentrations of 0.2µM. Whilst the investigated aptamers achieved comparable binding concentrations of toxins, the aptamer concentration was 200% greater than reported by Zhang *et al.* (2021).

The authors extracted the T-2 mycotoxin through application of methanol and found within their validation that methanol did not have an adverse effect on the AuNPs aggregation or aptamer performance, which was consistent with the results of this study. Neither was the aptamer sequence found to cross-bind with other mycotoxins. Their findings demonstrate the potential of the colorimetric format for the use of aptamer binding assessment. The authors further noted that extensive validation of the assay conditions was required to allow for the binding of the aptamers. The colorimetric assay described within this thesis has similar potential to function with further investigation and validation of the assay conditions beyond the brief investigation carried out as described. Future work would be required to validate the assay parameters, evaluating the effect of multi-mycotoxin containing samples, non-target containing samples, target concentrations and extract solution effects. Spiking food samples with high levels of mycotoxins and basing the assay development on a larger process of assay optimisation would be required to establish a functional detection assay.

5.5 Conclusion

In total 6 aptamer candidates, obtained through high throughput sequencing and the application of acceptability criteria, were tested with an AuNPs colorimetric assay for their ability to bind T-2 and HT-2. The proof-of-concept assays and the checkboard assays successfully demonstrated the binding of the aptamers and allowed for a qualitative and quantitative assessment. All the candidate aptamers when used at a concentration of 100µM exhibited good binding to both mycotoxin targets, as well as showing no cross-reactivity to other less structurally related mycotoxins (DON and aflatoxin B1). Analysis of T-2 and HT-2 spiked oat extracts showed that the aptamer binding was impeded in the complex matrix, potentially due to the presence of co-extracted matrix components. However, the results provided an insight into the potential strategy required for creating a functional aptamer binding assay for use in food samples utilising the aptamer sequences presented within this thesis.

The overall results of the colorimetric binding assays suggest that aptamers selected from the pool of most abundant sequences as well as occurring towards the later stages of the selection rounds (6 to 15) have good binding towards the target. Based upon the occurrences of Apta20-90, the first round of selection may be sufficient to identify a good performing aptamer. This finding is particularly useful to future application of the Capture SELEX protocol for the development of aptamers targeting small molecules in which a fast methodology is required. The proposed capture SELEX protocol in this thesis in combination with high throughput sequences has demonstrated the ability to select novel aptamers with good binding to the targeted T-2 and HT-2 mycotoxin molecules.

Chapter 6. Conclusion

T-2 and HT-2 mycotoxin contamination through fungal growth is almost unavoidable in a variety of crops and their presence is of concern due to the health hazard they pose, (Ekwomadu, Akinola and Mwanza, 2021). The economic loss associated with mycotoxin contamination has been estimated to be around two billion USD per year, (Xia *et al.*, 2020). Established analytical techniques are available for the detection of the small molecules such as T-2 and HT-2 (chromatographic and antibody techniques), however detection methods not requiring expensive analytical equipment are most desirable for direct on-site applications to manage the food safety risk.

Aptamers present a good alternative to established analytical tools due to advantages in their synthesis, stability, and specificity. They can be selected *in vitro* to specifically target compounds and are easily modifiable enhancing the binding affinity and sensitivity, (Reid *et al.*, 2020). Aptamers have been incorporated into different sensing platforms for the detection of a variety of targets, such as: pathogens, toxins, allergens, and proteins, in food safety and medical diagnosis, (Wu *et al.*, 2017; Wu *et al.*, 2021; Aye *et al.*, 2021; Jiang *et al.*, 2021). The demand for reliable detection of small molecules in food safety grows with aptamers being investigated as alternative to conventional methods. Although the selection of aptamers towards small molecules can be technically challenging, advances to the development protocols have led to successful selections, (Ruscito and DeRosa, 2016).

The primary aim of this study was to develop novel aptamers with specificity for T-2 and HT-2 mycotoxins. To achieve this aim three main stages were completed: a DNA sequence selection process (Capture SELEX), followed by evaluation of selected DNA sequences (High Throughput Sequencing) and finally binding assessment of selected sequences (colorimetric assay format).

In the first stage, (Chapter 3) a Capture SELEX protocol was utilised to select single stranded DNA aptamers from an initial random pool of oligonucleotides. A Capture SELEX protocol previously described by Paniel *et al.* (2017) was modified and used. The modification included the use of lambda exonuclease as a means of preparing ssDNA following PCR amplification. The use of the lambda exonuclease proved to be an efficient method for recovery of ssDNA, with between 40% and 60% success, which could be used for subsequent selection. At the time of completion of this thesis, the Capture SELEX protocol based on enzymatic digestion is the first to be described in the context of selecting DNA aptamers targeting T-2 and HT-2 mycotoxins. The Capture SELEX protocols appears to be a promising alternative allowing for a faster completion of a selection round. The success of the Capture SELEX protocol in selecting aptamer candidates, could only be determined through further work of identifying and evaluating the selected unique sequences.

In the second stage of this study, high throughput sequencing was used (Chapter 4) to identify the unique sequences present in the oligonucleotide pools produced by each selection. This allowed for the identification of suitable aptamer candidates, as well as giving further understanding of the oligonucleotide sequence selection. The sequencing results were presented in two data formats; combined and filtered (Sections 4.4.1 to Section 4.4.5). The unique sequences in both formats were subjected to three acceptability criteria to determine the best suited aptamer candidates for T-2 and HT-2 binding. The acceptability criteria included the presence of unique sequences with 62 base pair lengths, presence of an unmodified capture region in the unique sequences and inclusion of the unique sequences with the 50% most abundant or frequent cut-off pool. The evaluation of the available data provided information of the occurrence of unique sequences throughout the selection process and supported the choice of aptamer candidates. 6 aptamer candidates were selected to test in binding assays: Apta20-01, Apta20-02, Apta20-04, Apta20-57, Apta20-90 and Apta20-100. The unique sequences were selected due to the abundance and occurrence at different selection rounds.

This is the first reported use of this approach to enable successful selection of candidate aptamers targeting T-2 and HT-2 mycotoxins. The evaluation of the HTS data showed gaps within the methodology requiring future work. The variable occurrence pattern of unique sequences within the first three selection rounds could indicate that limited sampling led to unique sequences not being found. The application of qPCR to a SELEX protocol enables real time monitoring of the selection process and amplification of the complete sequence pool. Within each selection round, unique sequences not passing the 50% most abundant unique sequences cut off criterion were not considered as aptamer candidates. Comparison of unique sequences with low abundance should be explored in future assays. The work would provide results determining if low abundance aptamers can show good binding comparable to high abundancy aptamers.

Binding assays were the final step in the achievement of the aim to determine if the selected aptamers bind to the T-2 and HT-2 mycotoxins. A colorimetric assay (Chapter 5) based on the aggregation of gold nanoparticles (AuNPs) and their aggregation through salt was used. Once optimised, the assay format proved useful as a means for the reliable screening of aptamer binding to targets. Although the initial assessment could be done easily through visual result evaluation, microplate-based spectrophotometry enabled more precise comparison of aptamer binding. The results of both visual and spectrophotometric analysis showed that the selected 6 aptamers bound successfully to both T-2 and HT-2 targets. Optimal aptamer binding concentration of 100μM was observed. Apta20-01 and Apta20-100 bound best to 214.3μM and 107.1μM of T-2 mycotoxin target and Apta20-100 and Apta20-57 bound best to 235.5μM and 117.7μM of mycotoxin target. Apta20-01 was found within the T-2 selection pool with abundance in later stages, whereas Apta20-100 was observed in abundance across the HT-2 selection rounds. Apta20-57 was observed in both T-2 and HT-2 selections, abundant in later stages of the rounds. Apta20-02 was seen in abundance from selection round 4 onwards in the T-2 selection.

The sequence showed good binding to both T-2 and HT-2 targets, however, in comparison to the better binding aptamers it showed the lowest binding. Apta20-90, most abundant in the first round of the HT-2 selection, showed good binding to both targets. In comparison to the better binding aptamers, it showed lower binding. Apta20-04 found within the pool of most abundant sequences within both T-2 and HT-2 selection demonstrated better binding to HT-2. The aptamers selected from the Capture SELEX protocol indicate that best binding sequences were found within the later stages of selection, yet the aptamer selected from the first selection round showed binding to the target. This finding provides valuable information for rapid aptamer selection targeting small molecules.

In the Capture SELEX protocol described by Paniel *et al.* (2017), 20 aptamers were identified as candidates following cloning and sequencing of the final selection round oligonucleotide pool. In comparison, the application of HTS to oligonucleotide sequences generated during this study demonstrated the possibility of identifying aptamer candidates throughout the selection process. This increased the number potential aptamer candidates to several hundreds. Although the selection process was focused on the best candidates as defined by the acceptability criteria, a considerable number of unique sequences that were rejected remained with future application possibilities. Use of the AuNPs assay would enable rapid screening of large numbers of candidates.

Additional, one-off experimental work was carried out to investigate the binding of the aptamers when applied to real life samples. Oat Flour materials were used to provide an initial insight into the performance of the aptamers in complex matrices. The results showed the aptamers were unable to bind to their targets in matrix. Zhang *et al.* (2021) demonstrated within their work an aptasensor based on AuNPs aggregation, capable of binding to T-2 mycotoxin in real life samples. The authors highlighting the importance of extensive validation that may be necessary for a functioning assay based on AuNPs. Future extensive work could enable the inclusion of the identified 6 aptamers in a functioning detection assay,

based upon AuNPs or other assay formats once optimisation has been completed.

Through the completion of the final stage described in this thesis, the aim of the research study was successfully achieved, and novel aptamers were efficiently selected with the ability to bind to the T-2 and HT-2 mycotoxin. The ability to accelerate the development of aptamers with specificity to small molecules is highly desirable because many of them have an important role in food safety. This study has contributed to the development of aptamers beneficial to the use in food safety.

References

Ahmad, O. S., Bedwell, T. S., Esen, C., Garcia-Cruz, A. and Piletsky, S. A. (2019) 'Molecularly Imprinted Polymers in Electrochemical and Optical Sensors', *Trends in Biotechnology,* 37(3), pp. 294-309.

Alshannaq, A. and Yu, J.-H. (2017) 'Occurrence, Toxicity, and Analysis of Major Mycotoxins in Food', *International Journal of Environmental Research and Public Health,* 14(6).

Amaya-González, S., De-los-Santos-Álvarez, N., Miranda-Ordieres, A. J. and Lobo-Castañón, M. J. (2013) 'Aptamer-based analysis: A promising alternative for food safety control', *Sensors,* 13(12), pp. 16292-16311.

Antonacci, A., Arduini, F., Moscone, D., Palleschi, G. and Scognamiglio, V. (2018) 'Nanostructured (Bio)sensors for smart agriculture', *TrAC Trends in Analytical Chemistry,* 98, pp. 95-103.

Apetrei, C., Maximino, M. D., Martin, C. S. and Alessio, P. (2018) 'Sensors based on conducting polymers for the analysis of food products', *Polymers for food applications*: Springer, pp. 757-792.

Aquino-Jarquin, G. and Toscano-Garibay, J. D. (2011) 'RNA aptamer evolution: two decades of SELEction', *International journal of molecular sciences,* 12(12), pp. 9155-9171.

Ashley, J., Feng, X. and Sun, Y. (2018) 'A multifunctional molecularly imprinted polymer-based biosensor for direct detection of doxycycline in food samples', *Talanta,* 182, pp. 49-54.

Avci-Adali, M., Paul, A., Wilhelm, N., Ziemer, G. and Wendel, H. P. (2010) 'Upgrading SELEX Technology by Using Lambda Exonuclease Digestion for Single-Stranded DNA Generation', *Molecules,* 15(1).

Aye, N. N. S., Maraming, P., Tavichakorntrakool, R., Chaibunruang, A., Boonsiri, P., Daduang, S., Teawtrakul, N., Prasongdee, P., Amornkitbamrung, V. and Daduang, J. (2021) 'A Simple Graphene Functionalized Electrochemical Aptasensor for the Sensitive and Selective Detection of Glycated Albumin', *Applied Sciences,* 11(21), pp. 10315.

Bates, P. J., Laber, D. A., Miller, D. M., Thomas, S. D. and Trent, J. O. (2009) 'Discovery and development of the G-rich oligonucleotide AS1411 as a novel treatment for cancer', *Experimental and Molecular Pathology,* 86(3), pp. 151-164.

Bailey, T.L. and Elkan, C. (1994) 'Fitting a mixture model by expectation maximisation to discover motifs in biopolymers', Proceedings of the Second International Conference on Intelligent Systems for Molecular Biology, pp.28-36.

Bayraç, C., Eyidoğan, F. and Avni Öktem, H. (2017) 'DNA aptamer-based colorimetric detection platform for Salmonella Enteritidis', *Biosensors and Bioelectronics,* 98, pp. 22-28.

Behjati, S. and Tarpey, P. S. (2013) 'What is next generation sequencing?', *Archives of Disease in Childhood. Education and Practice Edition,* 98(6), pp. 236-238.

BelBruno, J. J. (2018) 'Molecularly imprinted polymers', *Chemical reviews,* 119(1), pp. 94-119.

Berthiller, F., Cramer, B., Iha, M. H., Krska, R., Lattanzio, V. M. T., MacDonald, S., Malone, R. J., Maragos, C., Solfrizzo, M., Stranska-Zachariasova, M., Stroka, J. and Tittlemier, S. A. (2018) 'Developments in mycotoxin analysis: an update for 2016-2017', *World Mycotoxin Journal,* 11(1), pp. 5-32.

Birch, J. R. and Racher, A. J. (2006) 'Antibody production', *Advanced Drug Delivery Reviews,* 58(5), pp. 671-685.

Blind, M. and Blank, M. (2015) 'Aptamer Selection Technology and Recent Advances', *Molecular Therapy - Nucleic Acids,* 4, pp. e223.

Bonwick, G. A. and Smith, C. J. (2004) 'Immunoassays: their history, development and current place in food science and technology', *International Journal of Food Science & Technology,* 39(8), pp. 817-827.

Boussebayle, A., Torka, D., Ollivaud, S., Braun, J., Bofill-Bosch, C., Dombrowski, M., Groher, F., Hamacher, K. and Suess, B. (2019) 'Next-level riboswitch development—implementation of Capture-SELEX facilitates identification of a new synthetic riboswitch', *Nucleic Acids Research,* 47(9), pp. 4883-4895.

Busman, M., Poling, S. M. and Maragos, C. M. (2011) 'Observation of T-2 toxin and HT-2 toxin glucosides from Fusarium sporotrichioides by liquid chromatography coupled to tandem mass spectrometry (LC-MS/MS)', *Toxins,* 3(12), pp. 1554-1568.

Callahan, B. J., McMurdie, P. J., Rosen, M. J., Han, A. W., Johnson, A. J. A. and Holmes, S. P. (2016) 'DADA2: High-resolution sample inference from Illumina amplicon data', *Nature Methods,* 13(7), pp. 581-583.

Cao, Y., Feng, T., Xu, J. and Xue, C. (2019) 'Recent advances of molecularly imprinted polymer-based sensors in the detection of food safety hazard factors', *Biosensors and Bioelectronics,* 141, pp. 111447.

EFSA Panel on Contaminants in the Food Chain. (2011) 'Scientific Opinion on the risks for animal and public health related to the presence of T-2 and HT-2 toxin in food and feed', *EFSA Journal,* 9(12), pp. 2481.

EFSA Panel on Contaminants in the Food Chain. (2014) 'Scientific Opinion on the risks for human and animal health related to the presence of modified forms of certain mycotoxins in food and feed', *EFSA Journal,* 12(12), pp. 3916.

Chen, P., Xiang, B., Shi, H., Yu, P., Song, Y. and Li, S. (2020) 'Recent advances on type A trichothecenes in food and feed: Analysis, prevalence, toxicity, and decontamination techniques', *Food Control,* 118, pp. 107371.

Chen, R., Kan, L., Duan, F., He, L., Wang, M., Cui, J., Zhang, Z. and Zhang, Z. (2021) 'Surface plasmon resonance aptasensor based on niobium carbide MXene quantum dots for nucleocapsid of SARS-CoV-2 detection', *Microchimica Acta,* 188(10), pp. 1-10.

Chen, X., Huang, Y., Duan, N., Wu, S., Xia, Y., Ma, X., Zhu, C., Jiang, Y. and Wang, Z. (2014) 'Screening and Identification of DNA Aptamers against T-2

Toxin Assisted by Graphene Oxide', *Journal of Agricultural and Food Chemistry,* 62(42), pp. 10368-10374.

Cho, M., Xiao, Y., Nie, J., Stewart, R., Csordas, A. T., Oh, S. S., Thomson, J. A. and Soh, H. T. (2010) 'Quantitative selection of DNA aptamers through microfluidic selection and high-throughput sequencing', *Proceedings of the National Academy of Sciences,* 107(35), pp. 15373-15378.

Cole, K.H. and Lupták, A., 2019. High-throughput methods in aptamer discovery and analysis. Methods in enzymology, 621, pp.329-346.

Crist, E., Mora, C. and Engelman, R. (2017) 'The interaction of human population, food production, and biodiversity protection', *Science,* 356(6335), pp. 260-264.

Crowther, J. R. (2009) *The ELISA guidebook.* Springer.

Darmostuk, M., Rimpelova, S., Gbelcova, H. and Ruml, T. (2015a) 'Current approaches in SELEX: An update to aptamer selection technology', *Biotechnology advances,* 33(6), pp. 1141-1161.

Darmostuk, M., Rimpelova, S., Gbelcova, H. and Ruml, T. (2015b) 'Current approaches in SELEX: An update to aptamer selection technology', *Biotechnology Advances,* 33(6, Part 2), pp. 1141-1161.

De Angelis, E., Monaci, L., Pascale, M. and Visconti, A. (2013) 'Fate of deoxynivalenol, T-2 and HT-2 toxins and their glucoside conjugates from flour to bread: An investigation by high-performance liquid chromatography high-resolution mass spectrometry', *Food Additives & Contaminants: Part A,* 30(2), pp. 345-355.

Di Marco Pisciottano, I., Imperato, C., Urbani, V., Guadagnuolo, G., Imbimbo, S., De Crescenzo, M., Soprano, V., Esposito, M. and Gallo, P. (2020) 'T-2 and HT-2 toxins in feed and food from Southern Italy, determined by LC-MS/MS after immunoaffinity clean-up', *Food Additives & Contaminants: Part B,* 13(4), pp. 275-283.

Dinolfo, M.I., Martínez, M., Castañares, E. and Arata, A.F., 2022. Fusarium in maize during harvest and storage: a review of species involved, mycotoxins, and management strategies to reduce contamination. European Journal of Plant Pathology, pp.1-16.

Drobysh, M., Ramanaviciene, A., Viter, R., Chen, C.-F., Samukaite-Bubniene, U., Ratautaite, V. and Ramanavicius, A. (2022) 'Biosensors for the Determination of SARS-CoV-2 Virus and Diagnosis of COVID-19 Infection', *International Journal of Molecular Sciences,* 23(2).

Duan, F., Zhang, S., Yang, L., Zhang, Z., He, L. and Wang, M. (2018) 'Bifunctional aptasensor based on novel two-dimensional nanocomposite of MoS2 quantum dots and g-C3N4 nanosheets decorated with chitosan-stabilized Au nanoparticles for selectively detecting prostate specific antigen', *Analytica Chimica Acta,* 1036, pp. 121-132.

Duan, N., Gong, W., Wu, S. and Wang, Z. (2017) 'An ssDNA library immobilized SELEX technique for selection of an aptamer against ractopamine', *Analytica Chimica Acta,* 961, pp. 100-105.

Ekwomadu, T. I., Akinola, S. A. and Mwanza, M. (2021) 'Fusarium Mycotoxins, Their Metabolites (Free, Emerging, and Masked), Food Safety Concerns, and Health Impacts', *International Journal of Environmental Research and Public Health,* 18(22).

El-Husseini, D. M., Sayour, A. E., Melzer, F., Mohamed, M. F., Neubauer, H. and Tammam, R. H. (2022) 'Generation and Selection of Specific Aptamers Targeting Brucella Species through an Enhanced Cell-SELEX Methodology', *International Journal of Molecular Sciences,* 23(11).

Ellington, A. D. and Szostak, J. W. (1990) 'In vitro selection of RNA molecules that bind specific ligands', *Nature,* 346(6287), pp. 818-822.

EuropeanCommission (2000) *White Paper on food safety*.

Famulok, M., Mayer, G. and Blind, M. (2000) 'Nucleic acid aptamers from selection in vitro to applications in vivo', *Accounts of Chemical research,* 33(9), pp. 591-599.

Felsenstein, J. (1985) 'Confidence limits on phylogenies: an approach using the bootstrap', *Evolution,* 39(4), pp. 783-791.

Ferreira, D., Barbosa, J., Sousa, D. A., Silva, C., Melo, L. D. R., Avci-Adali, M., Wendel, H. P. and Rodrigues, L. R. (2021) 'Selection of aptamers against triple negative breast cancer cells using high throughput sequencing', *Scientific Reports,* 11(1), pp. 1-15.

Filipe-Ribeiro, L., Cosme, F. and Nunes, F. M. (2020) 'New molecularly imprinted polymers for reducing negative volatile phenols in red wine with low impact on wine colour', *Food Research International,* 129, pp. 108855.

Fink-Gremmels, J. and van der Merwe, D. (2019) 'Mycotoxins in the food chain: contamination of foods of animal origin', *Chemical Hazards in Foods of Animal Origin*: Wageningen Academic Publishers, pp. 1190-1198.

Freire, L. and Sant'Ana, A. S. (2018) 'Modified mycotoxins: An updated review on their formation, detection, occurrence, and toxic effects', *Food and Chemical Toxicology,* 111, pp. 189-205.

Frutiger, A., Tanno, A., Hwu, S., Tiefenauer, R. F., Voros, J. and Nakatsuka, N. (2021) 'Nonspecific binding—fundamental concepts and consequences for biosensing applications', *Chemical Reviews,* 121(13), pp. 8095-8160.

Fumagalli, F., Ottoboni, M., Pinotti, L. and Cheli, F. (2021) 'Integrated Mycotoxin Management System in the Feed Supply Chain: Innovative Approaches', *Toxins,* 13(8).

Gao, S., Cheng, Y., Zhang, S., Zheng, X. and Wu, J. (2022) 'A biolayer interferometry-based, aptamer–antibody receptor pair biosensor for real-time, sensitive, and specific detection of the disease biomarker TNF-α', *Chemical Engineering Journal,* 433, pp. 133268.

Gehring, K. B. and Kirkpatrick, R. (2020) 'Hazard analysis and critical control points (HACCP)', *Food Safety Engineering*: Springer, pp. 191-204.

Goodwin, S., McPherson, J. D. and McCombie, W. R. (2016) 'Coming of age: ten years of next-generation sequencing technologies', *Nature Reviews Genetics,* 17(6), pp. 333-351.

Grove, J. F. (1993) 'Macrocyclic trichothecenes', *Natural Product Reports,* 10(5), pp. 429-448.

Guo, L., Xu, Y., Ferhan, A. R., Chen, G. and Kim, D.-H. (2013) 'Oriented gold nanoparticle aggregation for colorimetric sensors with surprisingly high analytical figures of merit', *Journal of the American Chemical Society,* 135(33), pp. 12338-12345.

Guo, X., Wen, F., Zheng, N., Luo, Q., Wang, H., Wang, H., Li, S. and Wang, J. (2014) 'Development of an ultrasensitive aptasensor for the detection of aflatoxin B1', *Biosensors and Bioelectronics,* 56, pp. 340-344.

Gómez-Caballero, A., Unceta, N., Goicolea, M. A. and Barrio, R. J. (2021) 'Plastic receptors developed by imprinting technology as smart polymers imitating natural behavior', *Reactive and Functional Polymers Volume Three*: Springer, pp. 69-116.

Hamula, C. L. A., Guthrie, J. W., Zhang, H., Li, X.-F. and Le, X. C. (2006) 'Selection and analytical applications of aptamers', *TrAC Trends in Analytical Chemistry,* 25(7), pp. 681-691.

Hassani, S., Akmal, M. R., Salek-Maghsoudi, A., Rahmani, S., Ganjali, M. R., Norouzi, P. and Abdollahi, M. (2018) 'Novel label-free electrochemical aptasensor for determination of Diazinon using gold nanoparticles-modified screen-printed gold electrode', *Biosensors and Bioelectronics,* 120, pp. 122-128.

Hock, B. (1997) 'Antibodies for immunosensors a review', *Analytica Chimica Acta,* 347(1-2), pp. 177-186.

Hohn, T. M. and Beremand, P. D. (1989) 'Isolation and nucleotide sequence of a sesquiterpene cyclase gene from the trichothecene-producing fungus Fusarium sporotrichioides', *Gene,* 79(1), pp. 131-138.

Hohn, T. M. and Vanmiddlesworth, F. (1986) 'Purification and characterization of the sesquiterpene cyclase trichodiene synthetase from Fusarium sporotrichioides', *Archives of Biochemistry and Biophysics,* 251(2), pp. 756-761.

Hoinka, J., Berezhnoy, A., Dao, P., Sauna, Z. E., Gilboa, E. and Przytycka, T. M. (2015) 'Large scale analysis of the mutational landscape in HT-SELEX improves aptamer discovery', *Nucleic Acids Research,* 43(12), pp. 5699-5707.

Hou, W., Shi, Z., Guo, Y., Sun, X. and Wang, X. (2017) 'An interdigital array microelectrode aptasensor based on multi-walled carbon nanotubes for detection of tetracycline', *Bioprocess and Biosystems Engineering,* 40(9), pp. 1419-1425.

Janik, E., Niemcewicz, M., Podogrocki, M., Ceremuga, M., Gorniak, L., Stela, M. and Bijak, M. (2021) 'The Existing Methods and Novel Approaches in Mycotoxins' Detection', *Molecules,* 26(13).

Ji, F., He, D., Olaniran, A. O., Mokoena, M. P., Xu, J. and Shi, J. (2019) 'Occurrence, toxicity, production and detection of Fusarium mycotoxin: a review', *Food Production, Processing and Nutrition,* 1(1), pp. 6.

Jiang, H., Guo, Q., Zhang, C., Sun, Z. and Weng, X. (2021) 'Microfluidic origami nano-aptasensor for peanut allergen Ara h1 detection', *Food Chemistry,* 365, pp. 130511.

Jing, L., Qin, M., Zhang, X., Song, Y., Zhang, J., Xia, X., Gao, K. and Han, Q. (2021) 'A novel borax-specific ssDNA aptamer screened by high-throughput SELEX and its colorimetric assay with aggregation of AuNPs', *Journal of Food Composition and Analysis,* 101, pp. 103947.

Juan, C., Ritieni, A. and Mañes, J. (2013) 'Occurrence of Fusarium mycotoxins in Italian cereal and cereal products from organic farming', *Food Chemistry,* 141(3), pp. 1747-1755.

Kang, K.-N. and Lee, Y.-S. (2013) 'RNA Aptamers: A Review of Recent Trends and Applications', in Zhong, J.-J. (ed.) *Future Trends in Biotechnology.* Berlin, Heidelberg: Springer Berlin Heidelberg, pp. 153-169.

Karimi Pur, M. R., Hosseini, M., Faridbod, F., Ganjali, M. R. and Hosseinkhani, S. (2018) 'Early detection of cell apoptosis by a cytochrome C label-Free electrochemiluminescence aptasensor', *Sensors and Actuators B: Chemical,* 257, pp. 87-95.

Kimura, M., Kaneko, I., Komiyama, M., Takatsuki, A., Koshino, H., Yoneyama, K. and Yamaguchi, I. (1998) 'Trichothecene 3-O-acetyltransferase protects both the producing organism and transformed yeast from related mycotoxins: cloning and characterization of Tri101', *Journal of Biological Chemistry,* 273(3), pp. 1654-1661.

Kohlberger, M. and Gadermaier, G. (2021) 'SELEX: Critical factors and optimization strategies for successful aptamer selection', *Biotechnology and Applied Biochemistry*.

Kolm, C., Cervenka, I., Aschl, U. J., Baumann, N., Jakwerth, S., Krska, R., Mach, R. L., Sommer, R., DeRosa, M. C., Kirschner, A. K. T., Farnleitner, A. H. and Reischer, G. H. (2020) 'DNA aptamers against bacterial cells can be efficiently selected by a SELEX process using state-of-the art qPCR and ultra-deep sequencing', *Scientific Reports,* 10(1), pp. 20917.

Komarova, N., Barkova, D. and Kuznetsov, A. (2020) 'Implementation of High-Throughput Sequencing (HTS) in Aptamer Selection Technology', *International Journal of Molecular Sciences,* 21(22).

Komarova, N. and Kuznetsov, A. (2019) 'Inside the Black Box: What Makes SELEX Better?', *Molecules,* 24(19).

Kotsiri, Z., Vidic, J. and Vantarakis, A. (2022) 'Applications of biosensors for bacteria and virus detection in food and water–A systematic review', *Journal of Environmental Sciences,* 111, pp. 367-379.

Krishna, V. D., Wu, K., Su, D., Cheeran, M. C. J., Wang, J.-P. and Perez, A. (2018) 'Nanotechnology: Review of concepts and potential application of sensing platforms in food safety', *Food Microbiology,* 75, pp. 47-54.

Köhler, G. and Milstein, C. (1975) 'Continuous cultures of fused cells secreting antibody of predefined specificity', *Nature,* 256(5517), pp. 495-497.

Lee, J.-H., Canny, M. D., De Erkenez, A., Krilleke, D., Ng, Y.-S., Shima, D. T., Pardi, A. and Jucker, F. (2005) 'A therapeutic aptamer inhibits angiogenesis by specifically targeting the heparin binding domain of VEGF165', *Proceedings of the National Academy of Sciences,* 102(52), pp. 18902-18907.

Leite, M., Freitas, A., Silva, A. S., Barbosa, J. and Ramos, F. (2021) 'Maize food chain and mycotoxins: A review on occurrence studies', *Trends in Food Science & Technology,* 115, pp. 307-331.

Lemoine, F., Domelevo Entfellner, J. B., Wilkinson, E., Correia, D., Dávila Felipe, M., De Oliveira, T. and Gascuel, O. (2018) 'Renewing Felsenstein's phylogenetic bootstrap in the era of big data', *Nature,* 556(7702), pp. 452-456.

Li, R., Wen, Y., Wang, F. and He, P. (2021a) 'Recent advances in immunoassays and biosensors for mycotoxins detection in feedstuffs and foods', *Journal of Animal Science and Biotechnology,* 12(1), pp. 1-19.

Li, R., Wen, Y., Wang, F. and He, P. (2021b) 'Recent advances in immunoassays and biosensors for mycotoxins detection in feedstuffs and foods', *Journal of Animal Science and Biotechnology,* 12(1), pp. 108.

Liland, K. H., Rukke, E.-O., Olsen, E. F. and Isaksson, T. (2011) 'Customized baseline correction', *Chemometrics and Intelligent Laboratory Systems,* 109(1), pp. 51-56.

Liu, B., Peng, J., Wu, Q., Zhao, Y., Shang, H. and Wang, S. (2022a) 'A novel screening on the specific peptide by molecular simulation and development of the electrochemical immunosensor for aflatoxin B1 in grains', *Food Chemistry,* 372, pp. 131322.

Liu, F., Zhang, C., Duan, Y., Ma, J., Wang, Y. and Chen, G. (2022b) 'In vitro selection and characterization of a DNA aptamer targeted to Prorocentrum minimum-A common harmful algae', *Science of The Total Environment*, pp. 154771.

Liu, J., Xie, G., Xiong, Q., Mu, D. and Xu, H. (2021) 'A simple and sensitive aptasensor with rolling circle amplification for viable Cronobacter sakazakii detection in powdered infant formula', *Journal of Dairy Science,* 104(12), pp. 12365-12374.

Liu, R., Zhang, F., Sang, Y., Katouzian, I., Jafari, S. M., Wang, X., Li, W., Wang, J. and Mohammadi, Z. (2022c) 'Screening, identification, and application of nucleic acid aptamers applied in food safety biosensing', *Trends in Food Science & Technology,* 123, pp. 355-375.

Lu, Q., Liu, X., Hou, J., Yuan, Q., Li, Y. and Chen, S. (2020) 'Selection of aptamers specific for DEHP based on ssDNA library immobilized SELEX and development of electrochemical impedance spectroscopy aptasensor', *Molecules,* 25(3), pp. 747.

Lv, M., Liu, Y., Geng, J., Kou, X., Xin, Z. and Yang, D. (2018) 'Engineering nanomaterials-based biosensors for food safety detection', *Biosensors and Bioelectronics,* 106, pp. 122-128.

Lyu, C., Khan, I. M. and Wang, Z. (2021) 'Capture-SELEX for aptamer selection: A short review', *Talanta,* 229, pp. 122274.

Magyar, D., Tischner, Z., Páldy, A., Kocsubé, S., Dancsházy, Z., Halász, Á. and Kredics, L. (2021) 'Impact of global megatrends on the spread of microscopic fungi in the Pannonian Biogeographical Region', *Fungal Biology Reviews,* 37, pp. 71-88.

Majdinasab, M., Badea, M. and Marty, J. L. (2022) 'Aptamer-Based Lateral Flow Assays: Current Trends in Clinical Diagnostic Rapid Tests', *Pharmaceuticals,* 15(1).

Mansouri, M., Fathi, F., Jalili, R., Shoeibie, S., Dastmalchi, S., Khataee, A. and Rashidi, M.-R. (2020) 'SPR enhanced DNA biosensor for sensitive detection of donkey meat adulteration', *Food Chemistry,* 331, pp. 127163.

Marin, S., Ramos, A. J., Cano-Sancho, G. and Sanchis, V. (2013) 'Mycotoxins: Occurrence, toxicology, and exposure assessment', *Food and Chemical Toxicology,* 60, pp. 218-237.

Martin, M. (2011) 'Cutadapt removes adapter sequences from high-throughput sequencing reads', *EMBnet. journal,* 17(1), pp. 10-12.

Marín, S., Freire, L., Femenias, A. and Sant'Ana, A. S. (2021) 'Use of predictive modelling as tool for prevention of fungal spoilage at different points of the food chain', *Current Opinion in Food Science,* 41, pp. 1-7.

McKeague, M., Bradley, C. R., Girolamo, A. D., Visconti, A., Miller, J. D. and DeRosa, M. C. (2010) 'Screening and initial binding assessment of fumonisin B1 aptamers', *International Journal of Molecular Sciences,* 11(12), pp. 4864-4881.

McKeague, M., De Girolamo, A., Valenzano, S., Pascale, M., Ruscito, A., Velu, R., Frost, N. R., Hill, K., Smith, M. and McConnell, E. M. (2015) 'Comprehensive analytical comparison of strategies used for small molecule aptamer evaluation', *Analytical chemistry,* 87(17), pp. 8608-8612.

McKeague, M. and DeRosa, M. C. (2012) 'Challenges and opportunities for small molecule aptamer development', *Journal of Nucleic Acids,* 2012.

Medina, A., Akbar, A., Baazeem, A., Rodriguez, A. and Magan, N. (2017) 'Climate change, food security and mycotoxins: Do we know enough?', *Fungal Biology Reviews,* 31(3), pp. 143-154.

Meneely, J. P., Ricci, F., van Egmond, H. P. and Elliott, C. T. (2011) 'Current methods of analysis for the determination of trichothecene mycotoxins in food', *TrAC Trends in Analytical Chemistry,* 30(2), pp. 192-203.

Meneely, J. P., Sulyok, M., Baumgartner, S., Krska, R. and Elliott, C. T. (2010a) 'A rapid optical immunoassay for the screening of T-2 and HT-2 toxin in cereals and maize-based baby food', *Talanta,* 81(1-2), pp. 630-636.

Meneely, J. P., Sulyok, M., Baumgartner, S., Krska, R. and Elliott, C. T. (2010b) 'A rapid optical immunoassay for the screening of T-2 and HT-2 toxin in cereals and maize-based baby food', *Talanta,* 81(1), pp. 630-636.

Molinelli, A., Grossalber, K., Führer, M., Baumgartner, S., Sulyok, M. and Krska, R. (2008) 'Development of Qualitative and Semiquantitative Immunoassay-Based Rapid Strip Tests for the Detection of T-2 Toxin in Wheat and Oat', *Journal of Agricultural and Food Chemistry,* 56(8), pp. 2589-2594.

Mondal, B., Ramlal, S., Lavu, P. S. and Kingston, J. (2018) 'Highly sensitive colorimetric biosensor for staphylococcal enterotoxin B by a label-free aptamer and gold nanoparticles', *Frontiers in Microbiology,* 9, pp. 179.

Moretti, A., Pascale, M. and Logrieco, A.F., 2019. Mycotoxin risks under a climate change scenario in Europe. Trends in food science & technology, 84, pp.38-40.

Mukherjee, S., Murata, A., Ishida, R., Sugai, A., Dohno, C., Hamada, M., Krishna, S. and Nakatani, K. (2022) 'HT-SELEX-based identification of binding pre-miRNA hairpin-motif for small molecules', *Molecular Therapy - Nucleic Acids,* 27, pp. 165-174.

Navani, N. K. and Li, Y. (2006) 'Nucleic acid aptamers and enzymes as sensors', *Current Opinion in Chemical Biology,* 10(3), pp. 272-281.

Ndossi, D. G., Frizzell, C., Tremoen, N. H., Fæste, C. K., Verhaegen, S., Dahl, E., Eriksen, G. S., Sørlie, M., Connolly, L. and Ropstad, E. (2012) 'An in vitro investigation of endocrine disrupting effects of trichothecenes deoxynivalenol (DON), T-2 and HT-2 toxins', *Toxicology Letters,* 214(3), pp. 268-278.

Nei, M. and Kumar, S. (2000) *Molecular evolution and phylogenetics.* Oxford University Press, USA.

Nguyen, B. H., Dai Tran, L., Do, Q. P., Le Nguyen, H., Tran, N. H. and Nguyen, P. X. (2013) 'Label-free detection of aflatoxin M1 with electrochemical Fe3O4/polyaniline-based aptasensor', *Materials Science and Engineering: C,* 33(4), pp. 2229-2234.

Nutiu, R. and Li, Y. (2003) 'Structure-switching signaling aptamers', *Journal of the American Chemical Society,* 125(16), pp. 4771-4778.

Ohsawa, K., Kasamatsu, T., Nagashima, J.-i., Hanawa, K., Kuwahara, M., Ozaki, H. and Sawai, H. (2008) 'Arginine-modified DNA aptamers that show enantioselective recognition of the dicarboxylic acid moiety of glutamic acid', *Analytical Sciences,* 24(1), pp. 167-172.

Oplatowska-Stachowiak, M., Kleintjens, T., Sajic, N., Haasnoot, W., Campbell, K., Elliott, C. T. and Salden, M. (2017) 'T-2 Toxin/HT-2 Toxin and Ochratoxin A ELISAs Development and In-House Validation in Food in Accordance with the Commission Regulation (EU) No 519/2014', *Toxins,* 9(12), pp. 388.

Osborne, S. E. and Ellington, A. D. (1997) 'Nucleic acid selection and the challenge of combinatorial chemistry', *Chemical Reviews,* 97(2), pp. 349-370.

Panasiuk, L., Jedziniak, P., Pietruszka, K., Piatkowska, M. and Bocian, L. (2019) 'Frequency and levels of regulated and emerging mycotoxins in silage in Poland', *Mycotoxin Research,* 35(1), pp. 17-25.

Paniel, N., Istamboulié, G., Triki, A., Lozano, C., Barthelmebs, L. and Noguer, T. (2017) 'Selection of DNA aptamers against penicillin G using Capture-SELEX for the development of an impedimetric sensor', *Talanta,* 162, pp. 232-240.

Patriarca, A. and Fernández Pinto, V. (2017) 'Prevalence of mycotoxins in foods and decontamination', *Current Opinion in Food Science,* 14, pp. 50-60.

Pattengale, N. D., Alipour, M., Bininda-Emonds, O. R. P., Moret, B. M. E. and Stamatakis, A. (2010) 'How many bootstrap replicates are necessary?', *Journal of Computational Biology,* 17(3), pp. 337-354.

Pereira, A. C., Pina, A. F., Sousa, D., Ferreira, D., Santos-Pereira, C., Rodrigues, J. L., Melo, L. D. R., Sales, G., Sousa, S. F. and Rodrigues, L. R. (2022) 'Identification of novel aptamers targeting cathepsin B-overexpressing prostate cancer cells', *Molecular Systems Design & Engineering*.

Perrone, G., Ferrara, M., Medina, A., Pascale, M. and Magan, N. (2020) 'Toxigenic fungi and mycotoxins in a climate change scenario: Ecology, genomics, distribution, prediction and prevention of the risk', *Microorganisms,* 8(10), pp. 1496.

Piccolo, K. (2021) 'Studying the Structure and Kinetics of Functional Nucleic Acids'.

Pieczka, I., Pongrácz, R., Bartholy, J. and Andre, K. S. (2018) 'Future temperature projections for Hungary based on RegCM4. 3 simulations using new Representative Concentration Pathways scenarios', *International Journal of Global Warming,* 15(3), pp. 277-292.

Polak-Śliwińska, M. and Paszczyk, B. (2021) 'Trichothecenes in Food and Feed, Relevance to Human and Animal Health and Methods of Detection: A Systematic Review', *Molecules,* 26(2).

PubChem (2022a) *[(4S,10R,11S)-11-acetyloxy-2-(acetyloxymethyl)-10-hydroxy-1,5-dimethylspiro[8-oxatricyclo[7.2.1.02,7]dodec-5-ene-12,2'-oxirane]-4-yl] 3-methylbutanoate*. Available at: https://www.ncbi.nlm.nih.gov/pubmed/ (Accessed).

PubChem (2022b) *HT-2 Toxin*. Available at: https://www.ncbi.nlm.nih.gov/pubmed/ (Accessed).

Raj, J., Farkaš, H., Jakovčević, Z., Medina, A., Magan, N., Čepela, R. and Vasiljević, M. (2022) 'Comparison of multiple mycotoxins in harvested maize samples in three years (2018–2020) in four continents', *Food Additives & Contaminants: Part A*, pp. 1-10.

Reid, R., Chatterjee, B., Das, S. J., Ghosh, S. and Sharma, T. K. (2020) 'Application of aptamers as molecular recognition elements in lateral flow assays', *Analytical Biochemistry,* 593, pp. 113574.

Rivas Casado, M., Parsons, D. J., Weightman, R. M., Magan, N. and Origgi, S. (2009) 'Modelling a two-dimensional spatial distribution of mycotoxin concentration in bulk commodities to design effective and efficient sample selection strategies', *Food Additives and Contaminants,* 26(9), pp. 1298-1305.

Roseanu, A., Jecu, L., Badea, M. and Evans, R.W., 2010. Mycotoxins: An overview on their quantification methods. Romanian Journal of Biochemistry, 47(1), pp.79-86.

Ruscito, A. and DeRosa, M. C. (2016) 'Small-Molecule Binding Aptamers: Selection Strategies, Characterization, and Applications', *Frontiers in Chemistry,* 4.

Rapid Alert System for Food and Feed (RASFF). (2021) *RASFF annual report 2020.*: Publications Office of the European Union [Website]. Available at: http://op.europa.eu/en/publication-detail/-/publication/2acefdec-0486-11ec-b5d3-01aa75ed71a1/language-en/format-PDF (Accessed).

Saitou, N. and Nei, M. (1987) 'The neighbor-joining method: a new method for reconstructing phylogenetic trees', *Molecular Biology and Evolution,* 4(4), pp. 406-425.

Sampson, T. (2003) 'Aptamers and SELEX: the technology', *World Patent Information,* 25(2), pp. 123-129.

Schuhmacher-Wolz, U., Heine, K. and Schneider, K. (2010) 'Report on toxicity data on trichothecene mycotoxins HT-2 and T-2 toxins', *EFSA Supporting Publications,* 7(7), pp. 65E.

Schütze, T., Wilhelm, B., Greiner, N., Braun, H., Peter, F., Mörl, M., Erdmann, V. A., Lehrach, H., Konthur, Z., Menger, M., Arndt, P. F. and Glökler, J. (2011) 'Probing the SELEX process with next-generation sequencing', *PloS One,* 6(12), pp. e29604-e29604.

Sharma, T. K., Bruno, J. G. and Dhiman, A. (2017) 'ABCs of DNA aptamer and related assay development', *Biotechnology Advances,* 35(2), pp. 275-301.

Shim, W.-B., Kim, M. J., Mun, H. and Kim, M.-G. (2014) 'An aptamer-based dipstick assay for the rapid and simple detection of aflatoxin B1', *Biosensors and Bioelectronics,* 62, pp. 288-294.

Spiga, F. M., Maietta, P. and Guiducci, C. (2015) 'More DNA–aptamers for small drugs: A capture–SELEX coupled with surface plasmon resonance and high-throughput sequencing', *ACS Combinatorial Science,* 17(5), pp. 326-333.

Stadler, D., Berthiller, F., Suman, M., Schuhmacher, R. and Krska, R. (2020) 'Novel analytical methods to study the fate of mycotoxins during thermal food processing', *Analytical and Bioanalytical Chemistry,* 412(1), pp. 9-16.

Stoltenburg, R., Nikolaus, N. and Strehlitz, B. (2012a) 'Capture-SELEX: selection of DNA aptamers for aminoglycoside antibiotics', *Journal of Analytical Methods in Chemistry,* 2012.

Stoltenburg, R., Nikolaus, N. and Strehlitz, B. (2012b) 'Capture-SELEX: Selection of DNA Aptamers for Aminoglycoside Antibiotics', *Journal of Analytical Methods in Chemistry,* 2012, pp. 415697.

Stoltenburg, R., Reinemann, C. and Strehlitz, B. (2005) 'FluMag-SELEX as an advantageous method for DNA aptamer selection', *Analytical and Bioanalytical Chemistry,* 383(1), pp. 83-91.

Sun, H. and Zu, Y. (2015) 'A Highlight of Recent Advances in Aptamer Technology and Its Application', *Molecules,* 20(7).

Sun, S., Zhao, R., Feng, S. and Xie, Y. (2018) 'Colorimetric zearalenone assay based on the use of an aptamer and of gold nanoparticles with peroxidase-like activity', *Microchimica Acta,* 185(12), pp. 535.

Tamura, K., Stecher, G. and Kumar, S. (2021) 'MEGA11: molecular evolutionary genetics analysis version 11', *Molecular Biology and Evolution,* 38(7), pp. 3022-3027.

Thipe, V. C., Bloebaum, P., Khoobchandani, M., Karikachery, A. R., Katti, K. K. and Katti, K. V. (2020) 'Green nanotechnology: Nanoformulations against toxigenic fungi to limit mycotoxin production', *Nanomycotoxicology*: Elsevier, pp. 155-188.

Tirado, M. C., Clarke, R., Jaykus, L. A., McQuatters-Gollop, A. and Frank, J. M. (2010) 'Climate change and food safety: A review', *Food Research International,* 43(7), pp. 1745-1765.

Toh, S. Y., Citartan, M., Gopinath, S. C. B. and Tang, T.-H. (2015) 'Aptamers as a replacement for antibodies in enzyme-linked immunosorbent assay', *Biosensors and Bioelectronics,* 64, pp. 392-403.

Tombelli, S., Minunni, M. and Mascini, M. (2005) 'Analytical applications of aptamers', *Biosensors and Bioelectronics,* 20(12), pp. 2424-2434.

Tuerk, C. and Gold, L. (1990) 'Systematic evolution of ligands by exponential enrichment: RNA ligands to bacteriophage T4 DNA polymerase', *Science,* 249(4968), pp. 505-510.

Twarużek, M., Skrzydlewski, P., Kosicki, R. and Grajewski, J. (2021) 'Mycotoxins survey in feed materials and feedingstuffs in years 2015–2020', *Toxicon,* 202, pp. 27-39.

Ueno, Y. (1984) 'Toxicological features of T-2 toxin and related trichothecenes', *Toxicological Sciences,* 4(2part2), pp. 124-132.

Verheecke-Vaessen, C., Diez-Gutierrez, L., Renaud, J., Sumarah, M., Medina, A. and Magan, N. (2019) 'Interacting climate change environmental factors effects on Fusarium langsethiae growth, expression of TRI genes and T-2/HT-2 mycotoxin production on oat-based media and in stored oats', *Fungal Biology,* 123(8), pp. 618-624.

Villa, C. C., Sánchez, L. T., Valencia, G. A., Ahmed, S. and Gutiérrez, T. J. (2021) 'Molecularly imprinted polymers for food applications: A review', *Trends in Food Science & Technology,* 111, pp. 642-669.

Villalonga, A., Pérez-Calabuig, A. M. and Villalonga, R. (2020) 'Electrochemical biosensors based on nucleic acid aptamers', *Analytical and Bioanalytical Chemistry,* 412(1), pp. 55-72.

Vivekananda, J. and Kiel, J. L. 2003. Methods and compositions for aptamers against anthrax. Google Patents.

Vivekananda, J. and Kiel, J. L. (2006) 'Anti-Francisella tularensis DNA aptamers detect tularemia antigen from different subspecies by Aptamer-Linked Immobilized Sorbent Assay', *Laboratory Investigation,* 86(6), pp. 610-618.

Wang, F.-B., Rong, Y., Fang, M., Yuan, J.-P., Peng, C.-W., Liu, S.-P. and Li, Y. (2013) 'Recognition and capture of metastatic hepatocellular carcinoma cells using aptamer-conjugated quantum dots and magnetic particles', *Biomaterials,* 34(15), pp. 3816-3827.

Wang, T., Chen, C., Larcher, L. M., Barrero, R. A. and Veedu, R. N. (2019) 'Three decades of nucleic acid aptamer technologies: Lessons learned, progress and opportunities on aptamer development', *Biotechnology Advances,* 37(1), pp. 28-50.

Wang, Y., Zhang, C., Wang, J. and Knopp, D. (2022) 'Recent Progress in Rapid Determination of Mycotoxins Based on Emerging Biorecognition Molecules: A Review', *Toxins,* 14(2).

Weigand, J. E. and Suess, B. (2009) 'Aptamers and riboswitches: perspectives in biotechnology', *Applied Microbiology and Biotechnology,* 85(2), pp. 229-236.

Wu, J., Ali, S., Ouyang, Q., Wang, L., Rong, Y. and Chen, Q. (2021) 'Highly specific and sensitive detection of aflatoxin B1 in food based on upconversion nanoparticles-black phosphorus nanosheets aptasensor', *Microchemical Journal,* 171, pp. 106847.

Wu, K., Ma, C., Zhao, H., Chen, M. and Deng, Z. (2019) 'Sensitive aptamer-based fluorescene assay for ochratoxin A based on RNase H signal amplification', *Food Chemistry,* 277, pp. 273-278.

Wu, Q., Qin, Z., Kuca, K., You, L., Zhao, Y., Liu, A., Musilek, K., Chrienova, Z., Nepovimova, E., Oleksak, P., Wu, W. and Wang, X. (2020) 'An update on T-2 toxin and its modified forms: metabolism, immunotoxicity mechanism, and human exposure assessment', *Archives of Toxicology,* 94(11), pp. 3645-3669.

Wu, S., Duan, N., Qiu, Y., Li, J. and Wang, Z. (2017) 'Colorimetric aptasensor for the detection of Salmonella enterica serovar typhimurium using ZnFe2O4-reduced graphene oxide nanostructures as an effective peroxidase mimetics', *International Journal of Food Microbiology,* 261, pp. 42-48.

Xia, R., Schaafsma, A. W., Wu, F. and Hooker, D. C. (2020) 'Impact of the improvements in Fusarium head blight and agronomic management on economics of winter wheat', *World Mycotoxin Journal,* 13(3), pp. 423-439.

Xie, M., Chen, Z., Zhao, F., Lin, Y., Zheng, S. and Han, S. (2022) 'Selection and Application of ssDNA Aptamers for Fluorescence Biosensing Detection of Malachite Green', *Foods,* 11(6).

Yang, C., Lates, V., Prieto-Simon, B., Marty, J.-L. and Yang, X. (2013) 'Rapid high-throughput analysis of ochratoxin A by the self-assembly of DNAzyme–aptamer conjugates in wine', *Talanta,* 116, pp. 520-526.

Yang, Y., Tang, Y., Wang, C., Liu, B. and Wu, Y. (2021) 'Selection and identification of a DNA aptamer for ultrasensitive and selective detection of λ-cyhalothrin residue in food', *Analytica Chimica Acta,* 1179, pp. 338837.

Yasgar, A., Jadhav, A., Simeonov, A. and Coussens, N. P. (2016) 'AlphaScreen-based assays: ultra-high-throughput screening for small-molecule inhibitors of challenging enzymes and protein-protein interactions', *High Throughput Screening*: Springer, pp. 77-98.

Ying, N., Wang, Y., Song, X., Yang, L., Qin, B., Wu, Y. and Fang, W. (2021) 'Lateral flow colorimetric biosensor for detection of Vibrio parahaemolyticus based on hybridization chain reaction and aptamer', *Microchimica Acta,* 188(11), pp. 1-9.

Yu, H., Alkhamis, O., Canoura, J., Liu, Y. and Xiao, Y. (2021) 'Advances and Challenges in Small-Molecule DNA Aptamer Isolation, Characterization, and Sensor Development', *Angewandte Chemie International Edition,* 60(31), pp. 16800-16823.

Zhang, F. and Liu, J. (2021) 'Label-Free Colorimetric Biosensors Based on Aptamers and Gold Nanoparticles: A Critical Review', *Analysis & Sensing,* 1(1), pp. 30-43.

Zhang, W., Wang, Y., Nan, M., Li, Y., Yun, J., Wang, Y. and Bi, Y. (2021) 'Novel colorimetric aptasensor based on unmodified gold nanoparticle and ssDNA for rapid and sensitive detection of T-2 toxin', *Food Chemistry,* 348, pp. 129128.

Zhang, X., Yang, G., Zhao, Y., Dai, X., Liu, W., Qu, F. and Huang, Y., 2023. Selection and Identification of an ssDNA Aptamer for Fibroblast Activation Protein. Molecules, 28(4), p.1682.

Zhong, H., Yu, C., Gao, R., Chen, J., Yu, Y., Geng, Y., Wen, Y. and He, J. (2019) 'A novel sandwich aptasensor for detecting T-2 toxin based on rGO-TEPA-Au@ Pt nanorods with a dual signal amplification strategy', *Biosensors and Bioelectronics,* 144, pp. 111635.

Zhu, W., Li, L., Zhou, Z., Yang, X., Hao, N., Guo, Y. and Wang, K. (2020) 'A colorimetric biosensor for simultaneous ochratoxin A and aflatoxins B1 detection in agricultural products', *Food Chemistry,* 319, pp. 126544.

Zuker, M. (2003) 'Mfold web server for nucleic acid folding and hybridization prediction', *Nucleic Acids Research,* 31(13), pp. 3406-3415.

Appendices

Appendix A

Apta20-01 checkerboard evaluation with HT-2.
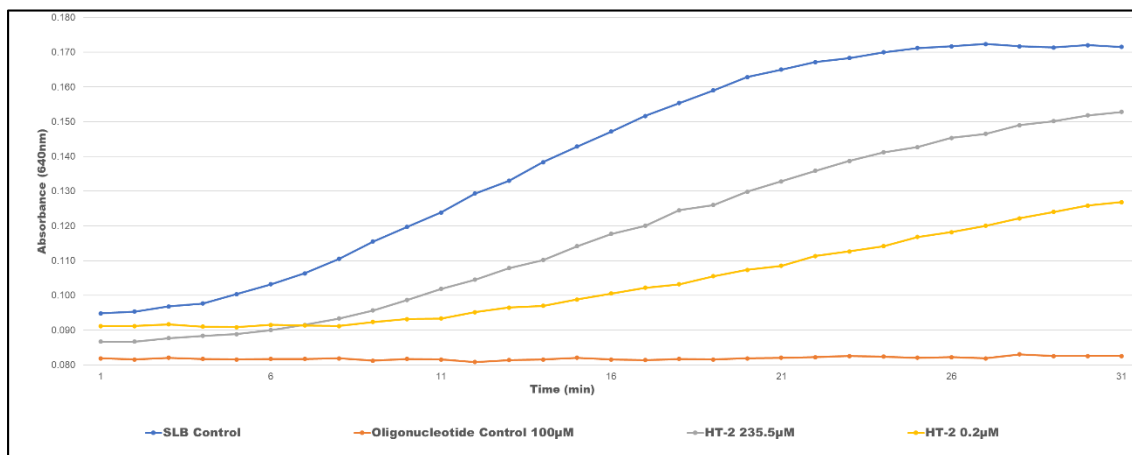
Figure 42 Absorbance curves (640nm) over time. Including SLB and oligonucleotide controls. Samples of Apta20-01 (100µM) incubated with 235.5µM and 0.2µM HT-2.
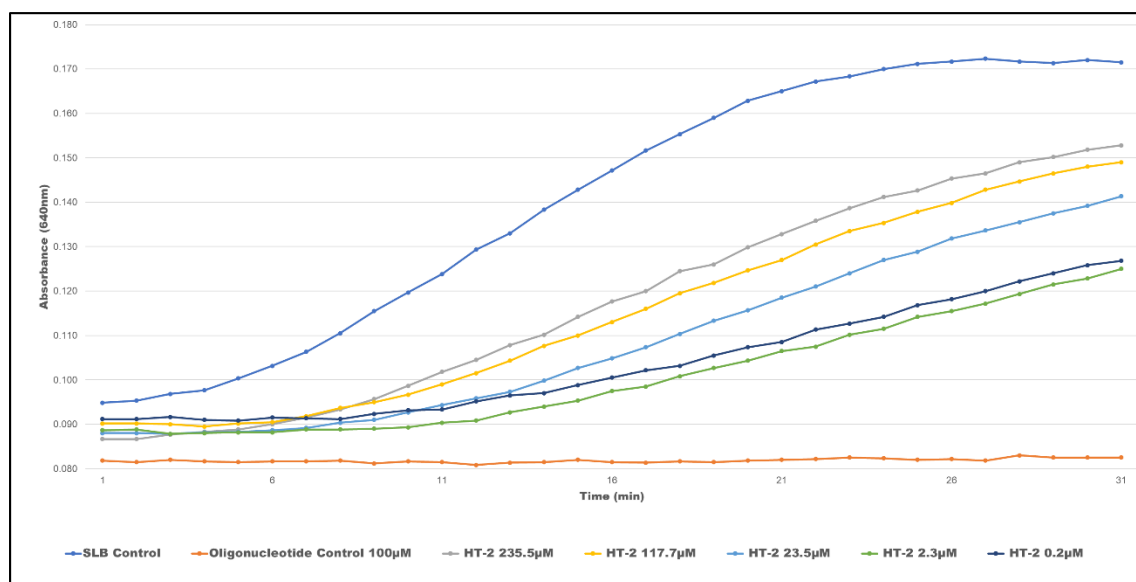
Figure 43 Absorbance curves (640nm) over time. Including SLB and oligonucleotide controls. Samples of Apta20-01(100µM) incubated with 235.5µM, 117.7µM, 23.5µM, 2.3µM and 0.2µM HT-2.
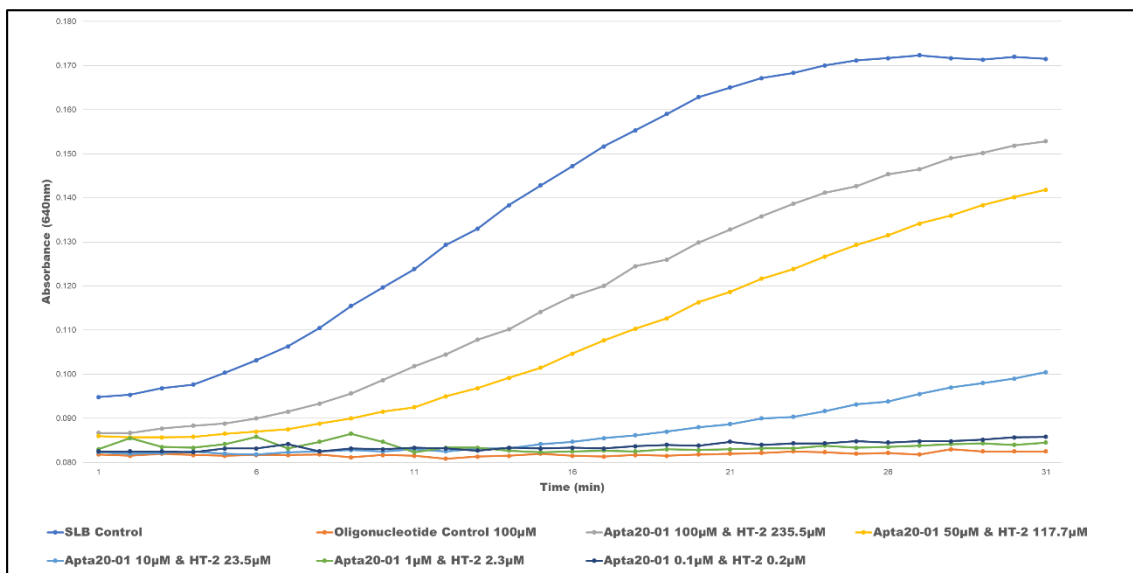
Figure 44 Absorbance curves (640nm) over time. Including SLB and oligonucleotide controls Samples of Apta20-01(100µM, 50µM, 10µM, 1µM, 0.1µM) incubated with 235.5µM, 117.7µM, 23.5µM, 2.3µM and 0.2µM HT-2 showing varying aggregation of AuNPs.
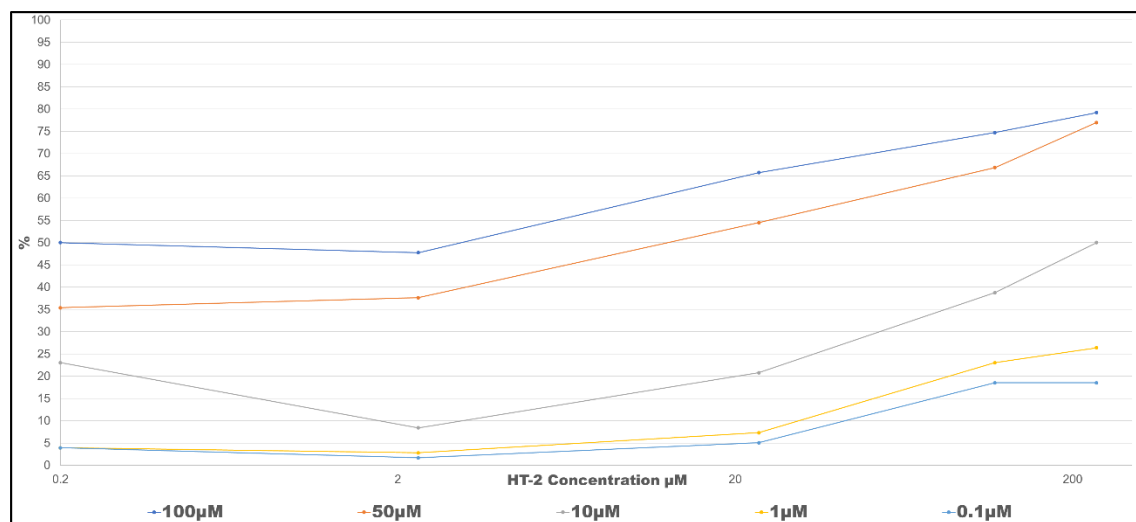
Figure 45 Calibration curve of % maximum absorbance values with baseline corrections of Apta20-01 at 100µM, 50µM, 10µM, 1µM and 0.1µM incubated with 235.5µM, 117.7µM, 23.5µM, 2.3µM and 0.2µM HT-2.

195

Appendix B

Apta20-02 checkerboard evaluation with T-2.
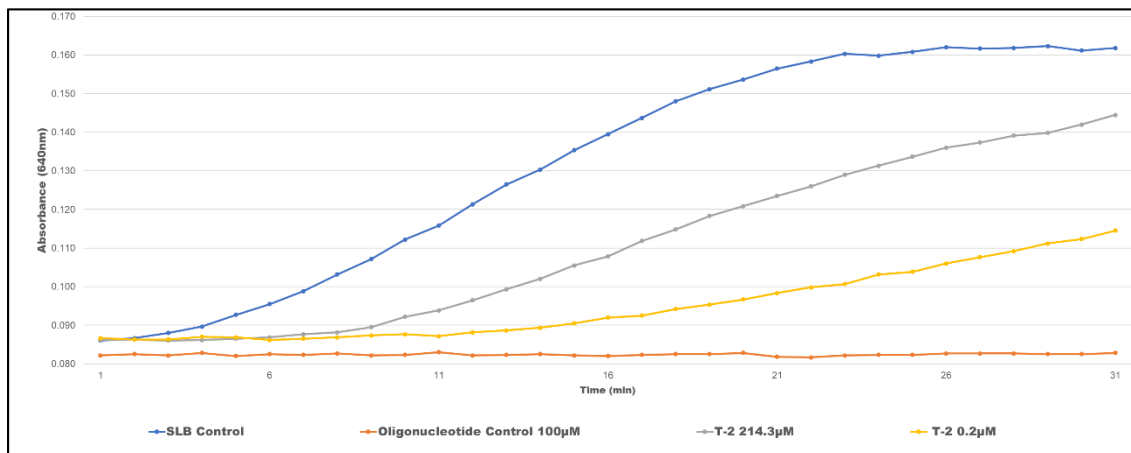
Figure 46 Absorbance curves (640nm) over time. Including SLB and oligonucleotide controls. Samples of Apta20-02 (100µM) incubated with 214.3µM and 0.2µM T-2.
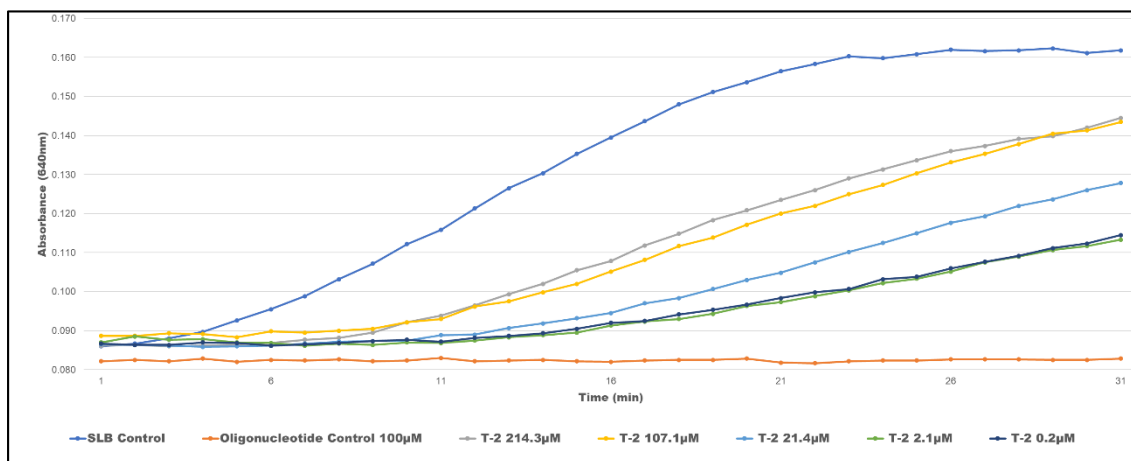
Figure 47 Absorbance curves (640nm) over time. Including SLB and oligonucleotide controls. Samples of Apta20-02(100µM) incubated with 214.3µM, 107.1µM, 21.4µM, 2.1µM and 0.2µM T-2.
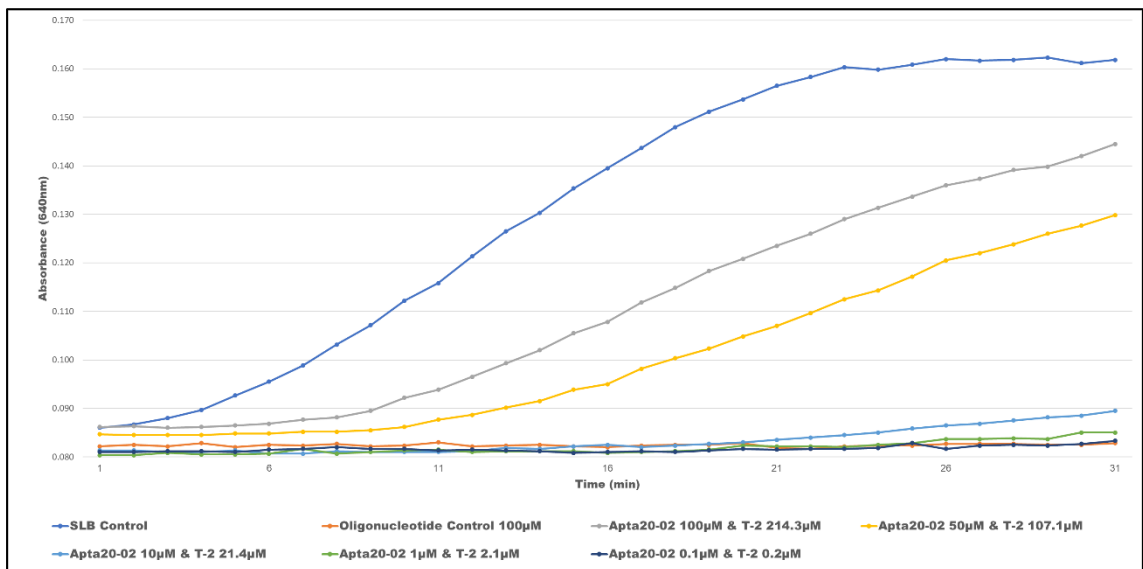
Figure 48 Absorbance curves (640nm) over time. Including SLB and oligonucleotide controls Samples of Apta20-02(100μM, 50μM, 10μM, 1μM, 0.1μM) incubated with 214.3μM, 107.1μM, 21.4μM, 2.1μM and 0.2μM T-2 showing varying aggregation of AuNPs.
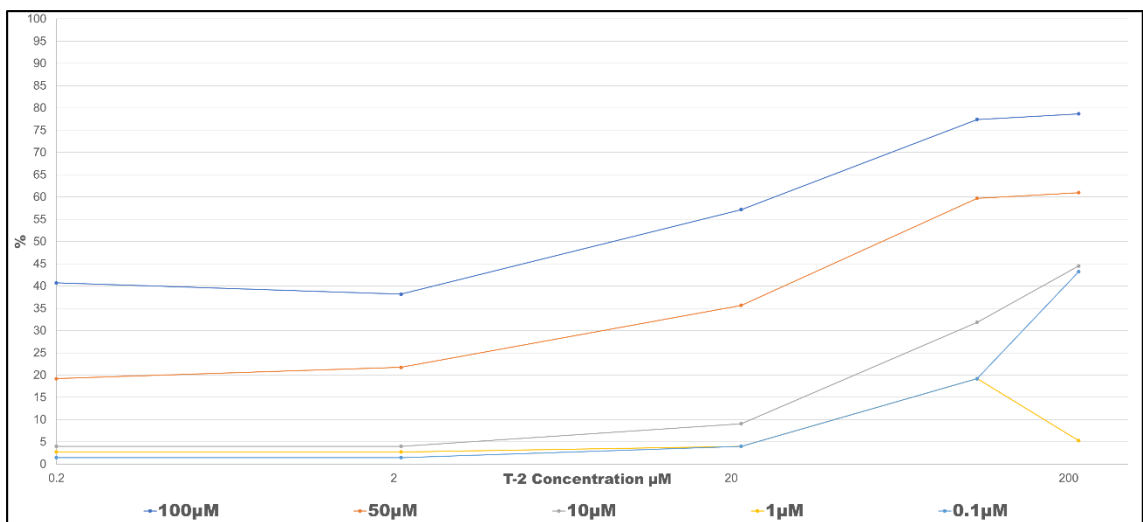
Figure 49 Calibration curve of % maximum absorbance values with baseline corrections of Apta20-02 at 100μM, 50μM, 10μM, 1μM and 0.1μM incubated with 214.3μM, 107.1μM, 21.4μM, 2.1μM and 0.2μM T-2.

197

Appendix C

Apta20-02 checkerboard evaluation with HT-2.
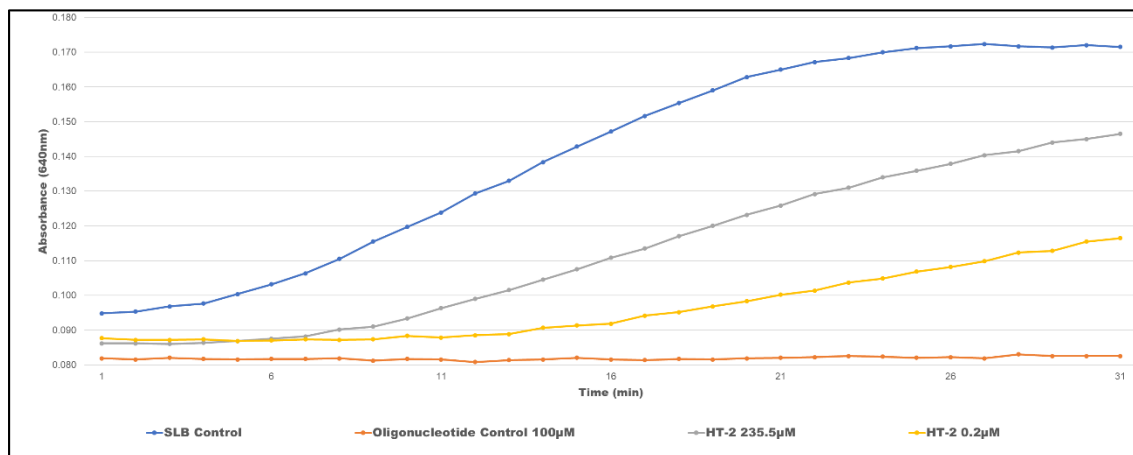
Figure 51 Absorbance curves (640nm) over time. Including SLB and oligonucleotide controls. Samples of Apta20-02 (100µM) incubated with 235.5µM and 0.2µM HT-2.
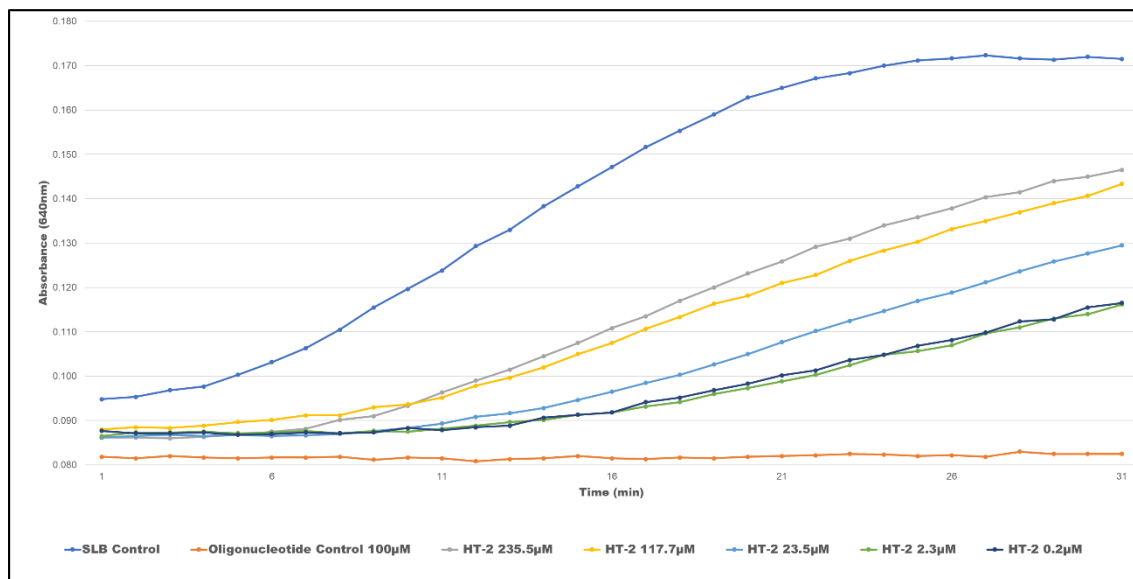
Figure 50 Absorbance curves (640nm) over time. Including SLB and oligonucleotide controls. Samples of Apta20-02(100µM) incubated with 235.5µM, 117.7µM, 23.5µM, 2.3µM and 0.2µM HT-2.
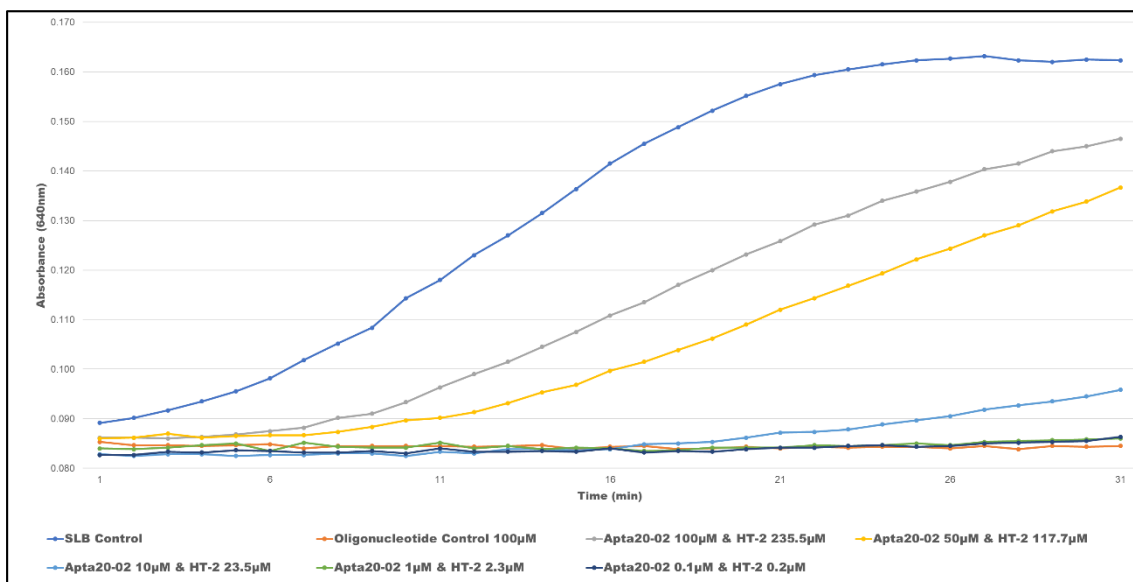
Figure 52 Absorbance curves (640nm) over time. Including SLB and oligonucleotide controls Samples of Apta20-02(100µM, 50µM, 10µM, 1µM, 0.1µM) incubated with 235.5µM, 117.7µM, 23.5µM, 2.3µM and 0.2µM HT-2 showing varying aggregation of AuNPs.
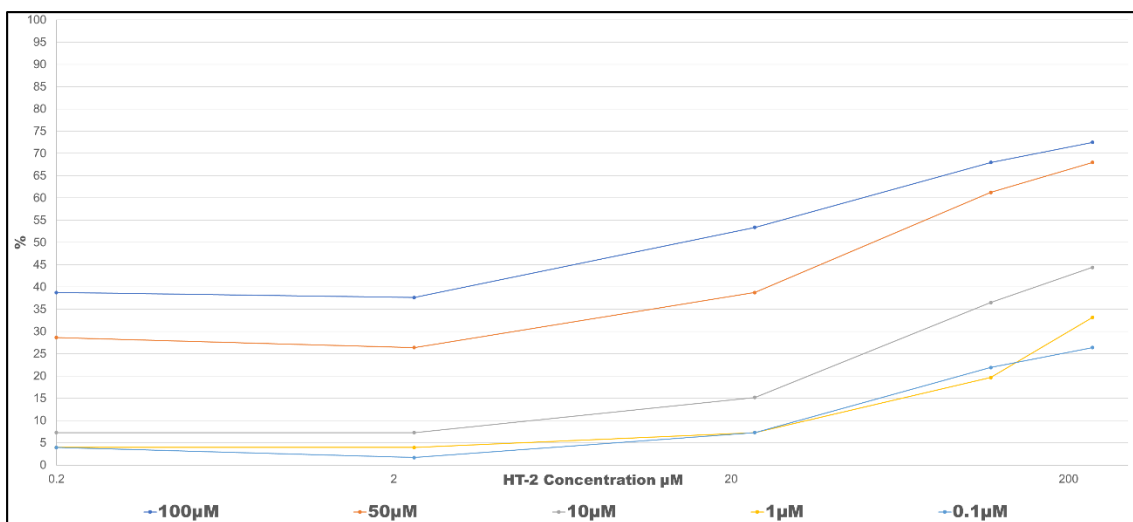
Figure 53 Calibration curve of % maximum absorbance values with baseline corrections of Apta20-02 at 100µM, 50µM, 10µM, 1µM and 0.1µM incubated with 235.5µM, 117.7µM, 23.5µM, 2.3µM and 0.2µM HT-2.

Appendix D

Apta20-04 checkerboard evaluation with T-2.
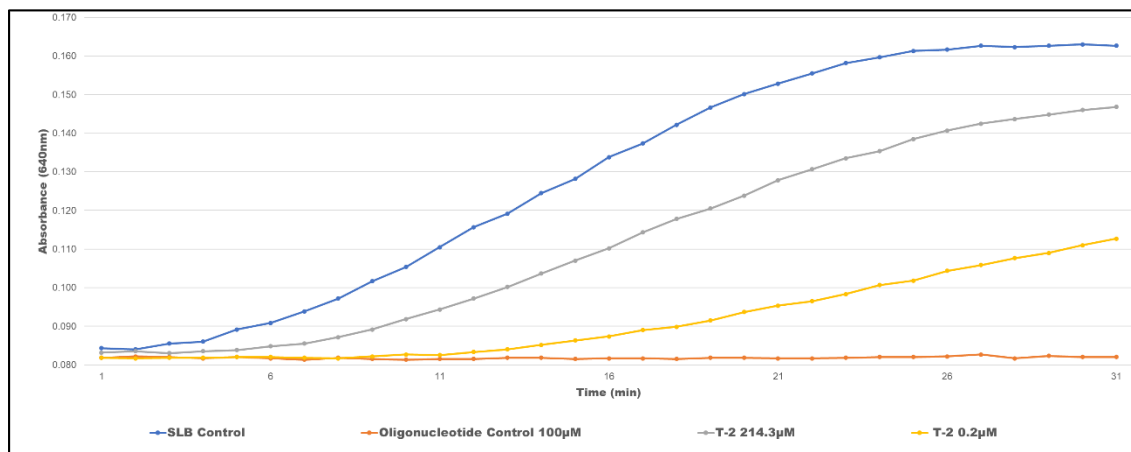
Figure 54 Absorbance curves (640nm) over time. Including SLB and oligonucleotide controls. Samples of Apta20-04 (100µM) incubated with 214.3µM and 0.2µM T-2.
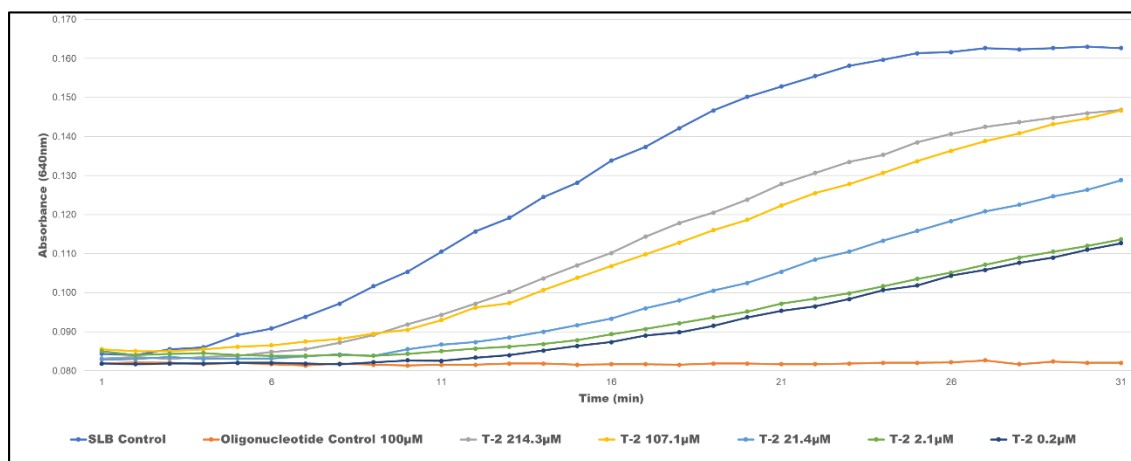
Figure 55 Absorbance curves (640nm) over time. Including SLB and oligonucleotide controls. Samples of Apta20-04(100µM) incubated with 214.3µM, 107.1µM, 21.4µM, 2.1µM and 0.2µM T-2.
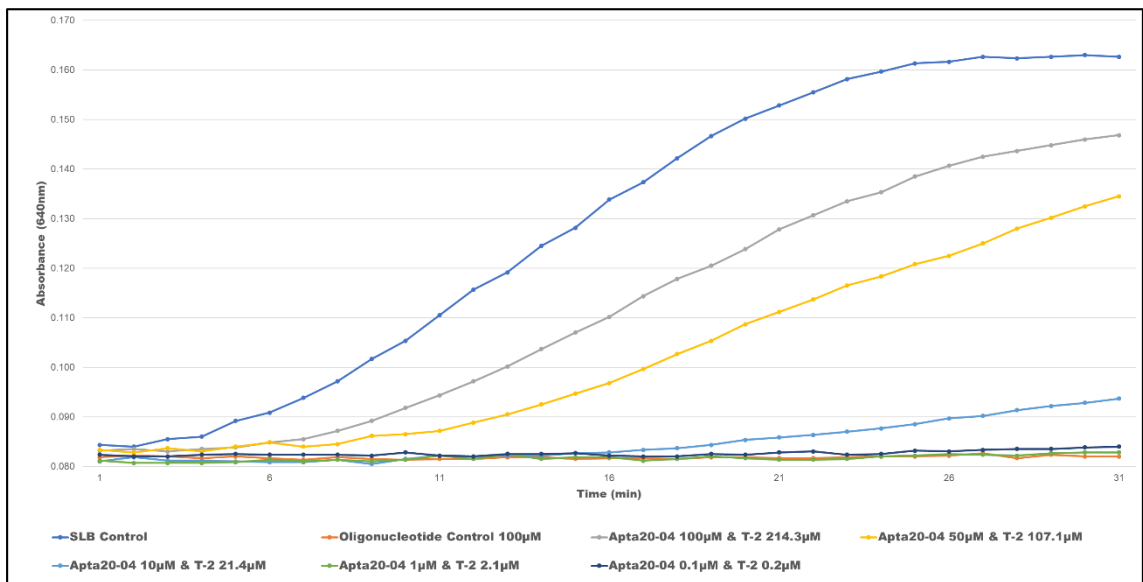
Figure 56 Absorbance curves (640nm) over time. Including SLB and oligonucleotide controls Samples of Apta20-04(100μM, 50μM, 10μM, 1μM, 0.1μM) incubated with 214.3μM, 107.1μM, 21.4μM, 2.1μM and 0.2μM T-2 showing varying aggregation of AuNPs.
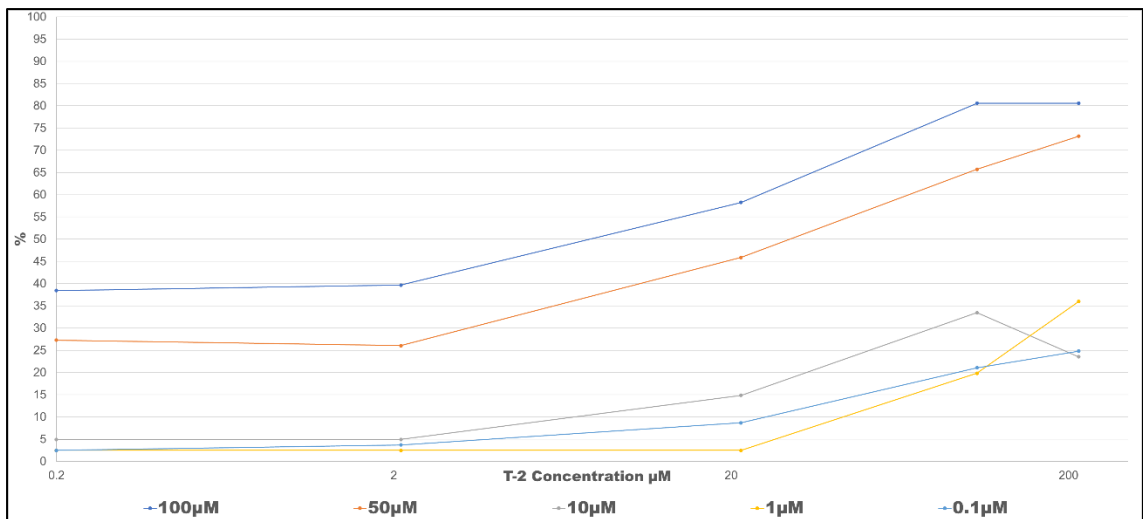
Figure 57 Calibration curve of % maximum absorbance values with baseline corrections of Apta20-04 at 100μM, 50μM, 10μM, 1μM and 0.1μM incubated with 214.3μM, 107.1μM, 21.4μM, 2.1μM and 0.2μM T-2.

Appendix E

Apta20-04 checkerboard evaluation with HT-2.
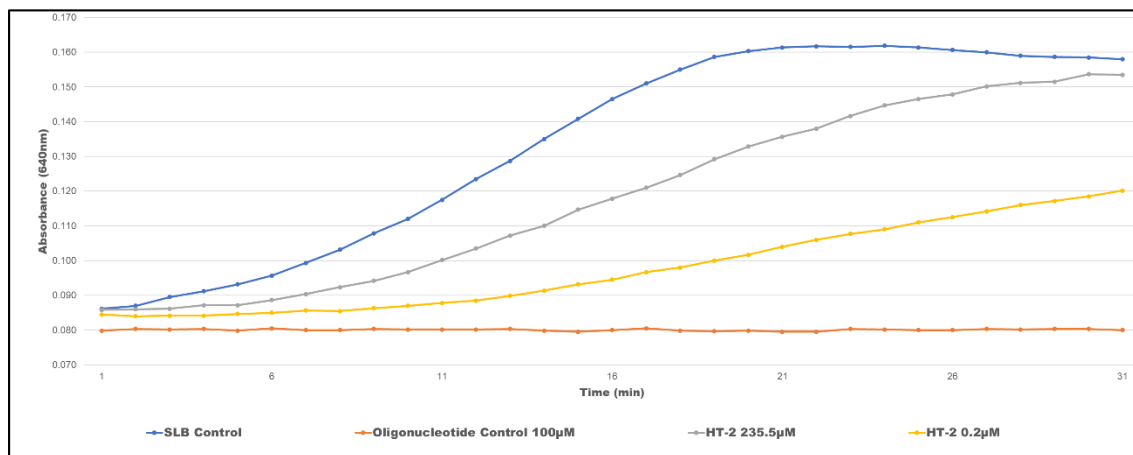
Figure 58 Absorbance curves (640nm) over time. Including SLB and oligonucleotide controls. Samples of Apta20-04 (100µM) incubated with 235.5µM and 0.2µM HT-2.
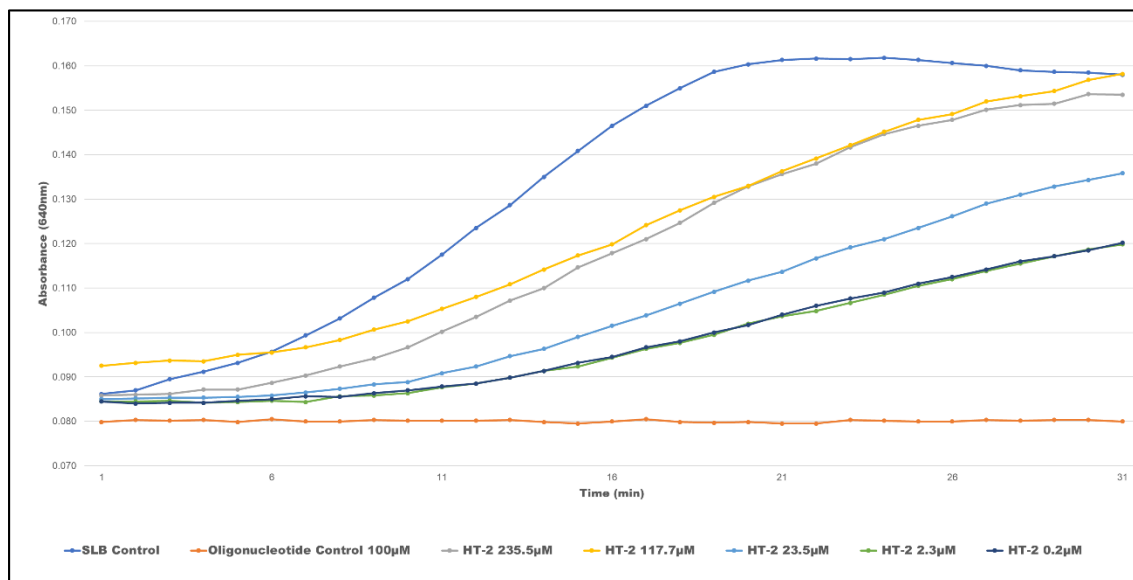
Figure 59 Absorbance curves (640nm) over time. Including SLB and oligonucleotide controls. Samples of Apta20-04(100µM) incubated with 235.5µM, 117.7µM, 23.5µM, 2.3µM and 0.2µM HT-2.
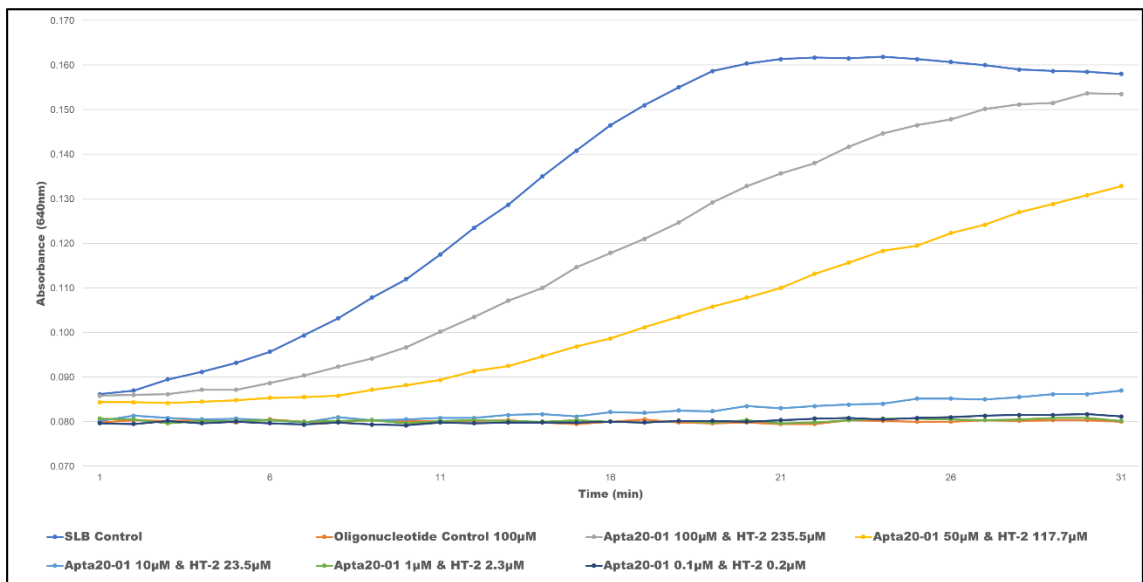
Figure 60 Absorbance curves (640nm) over time. Including SLB and oligonucleotide controls Samples of Apta20-04(100μM, 50μM, 10μM, 1μM, 0.1μM) incubated with 235.5μM, 117.7μM, 23.5μM, 2.3μM and 0.2μM HT-2 showing varying aggregation of AuNPs.
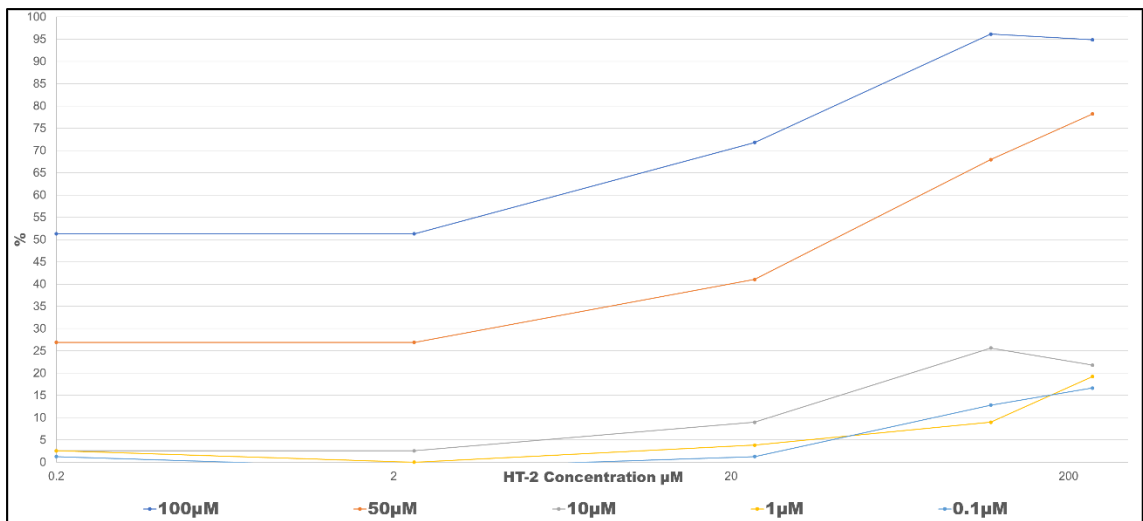
Figure 61 Calibration curve of % maximum absorbance values with baseline corrections of Apta20-04 at 100μM, 50μM, 10μM, 1μM and 0.1μM incubated with 235.5μM, 117.7μM, 23.5μM, 2.3μM and 0.2μM HT-2.

Appendix F

Apta20-57 checkerboard evaluation with T-2.
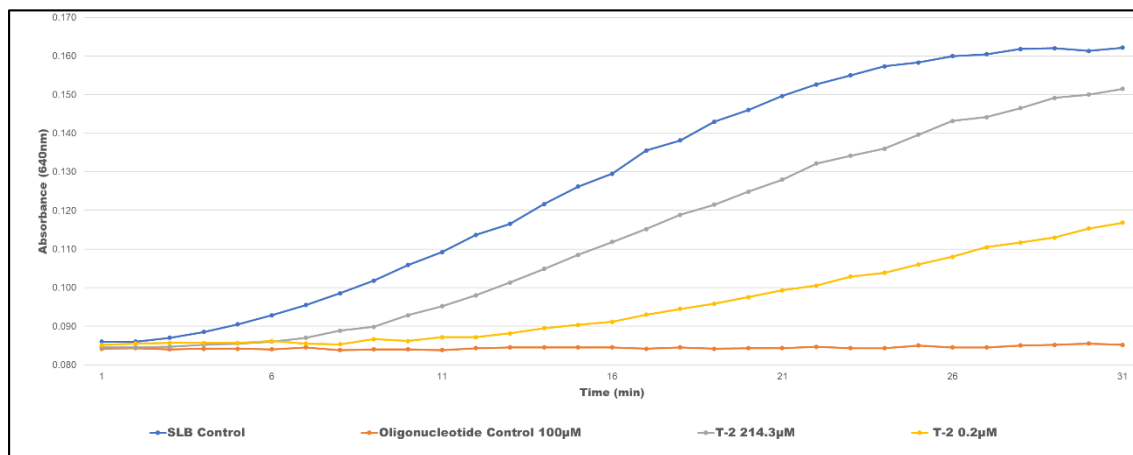
Figure 62 Absorbance curves (640nm) over time. Including SLB and oligonucleotide controls. Samples of Apta20-57 (100µM) incubated with 214.3µM and 0.2µM T-2.
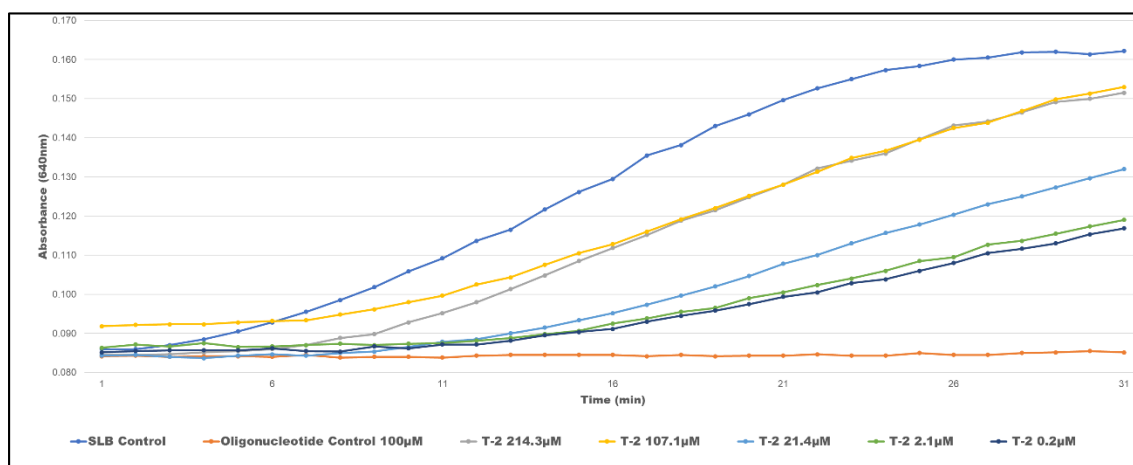
Figure 63 Absorbance curves (640nm) over time. Including SLB and oligonucleotide controls. Samples of Apta20-57(100µM) incubated with 214.3µM, 107.1µM, 21.4µM, 2.1µM and 0.2µM T-2.
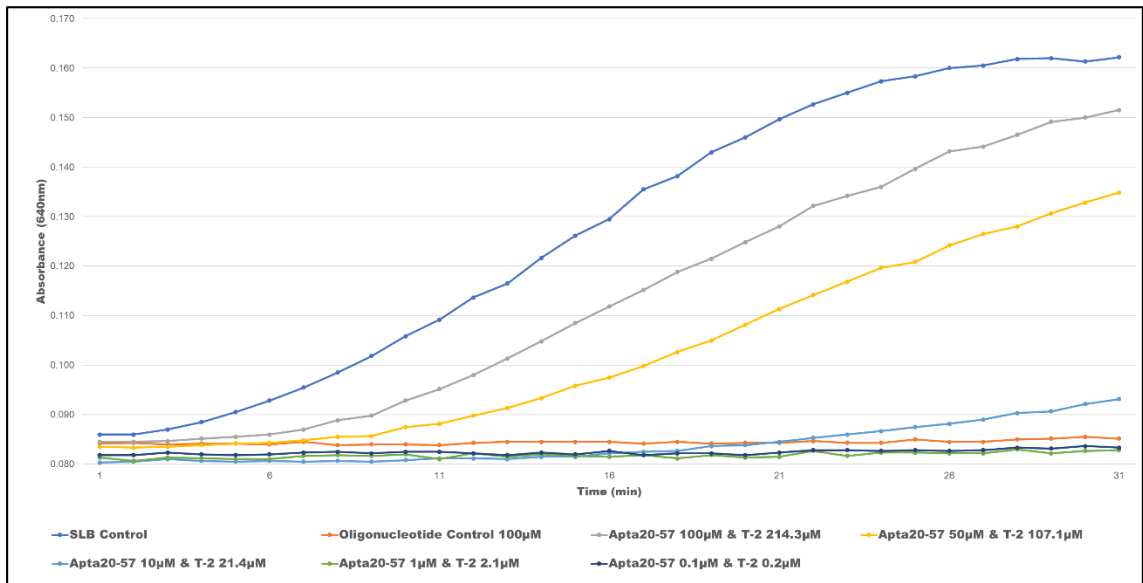
Figure 64 Absorbance curves (640nm) over time. Including SLB and oligonucleotide controls Samples of Apta20-57(100µM, 50µM, 10µM, 1µM, 0.1µM) incubated with 214.3µM, 107.1µM, 21.4µM, 2.1µM and 0.2µM T-2 showing varying aggregation of AuNPs.
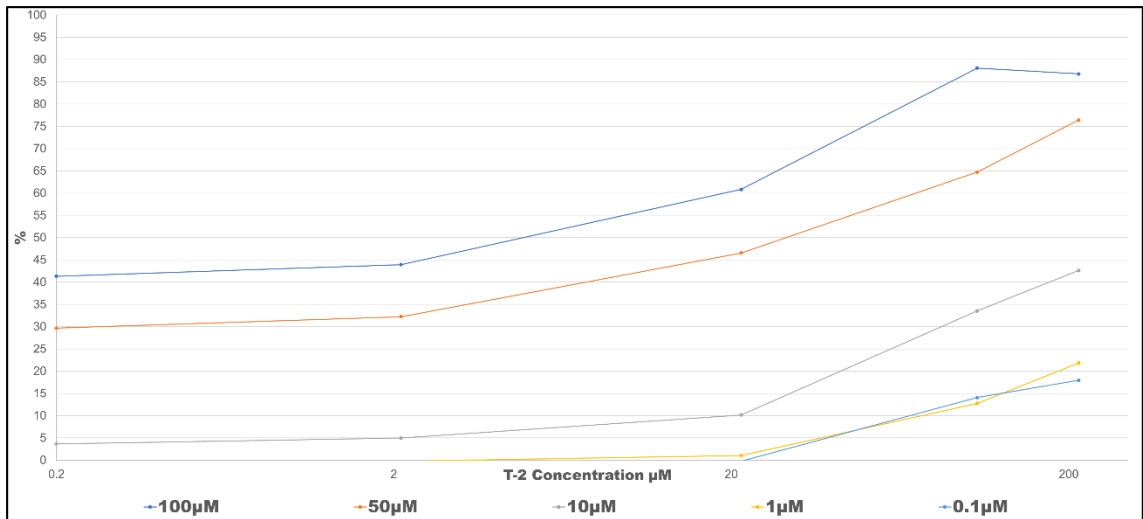
Figure 65 Calibration curve of % maximum absorbance values with baseline corrections of Apta20-57 at 100µM, 50µM, 10µM, 1µM and 0.1µM incubated with 214.3µM, 107.1µM, 21.4µM, 2.1µM and 0.2µM T-2.

Apta20-57 checkerboard evaluation with HT-2.
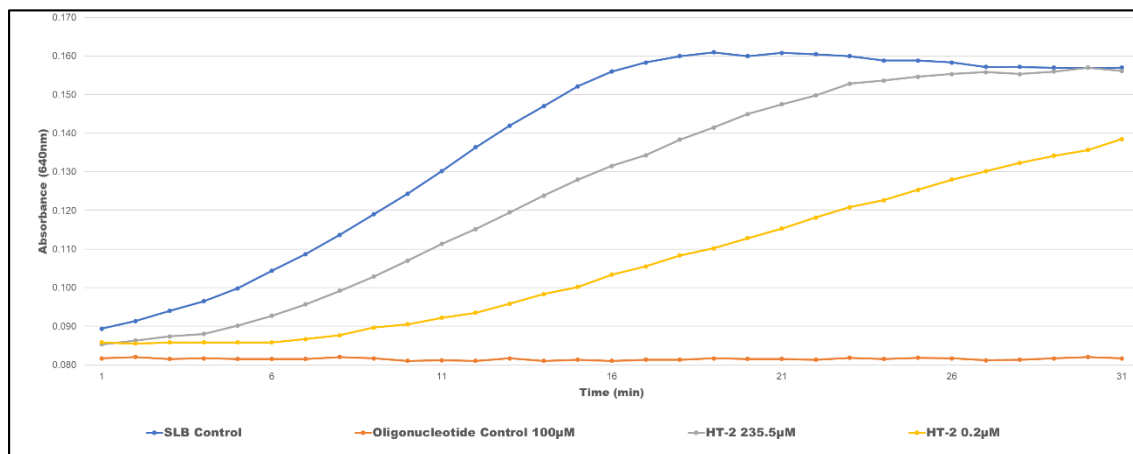
Figure 66 Absorbance curves (640nm) over time. Including SLB and oligonucleotide controls. Samples of Apta20-57 (100µM) incubated with 235.5µM and 0.2µM HT-2.
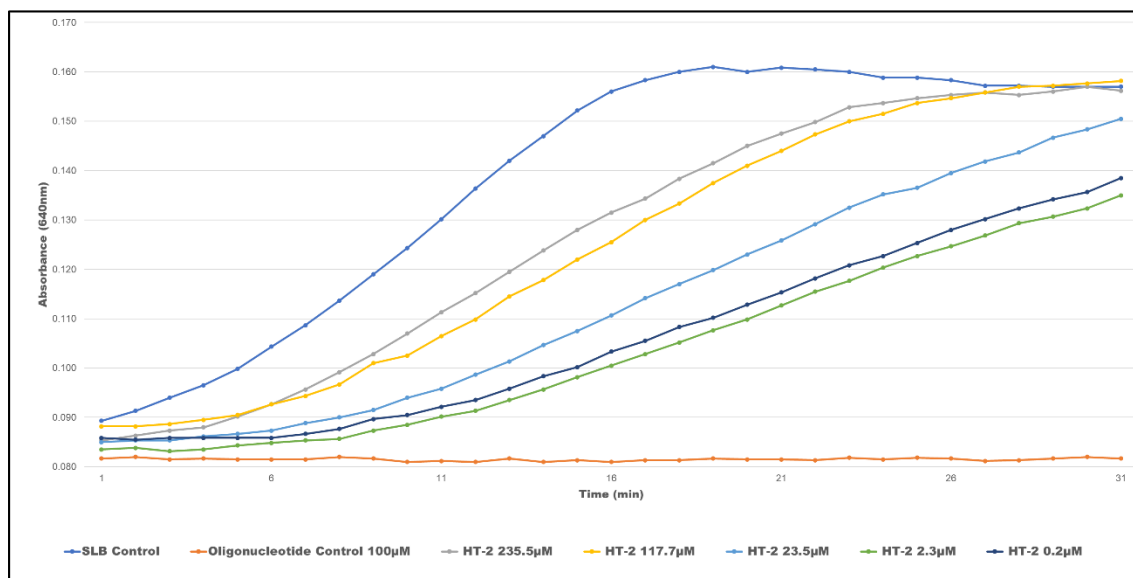
Figure 67 Absorbance curves (640nm) over time. Including SLB and oligonucleotide controls. Samples of Apta20-57(100µM) incubated with 235.5µM, 117.7µM, 23.5µM, 2.3µM and 0.2µM HT-2.
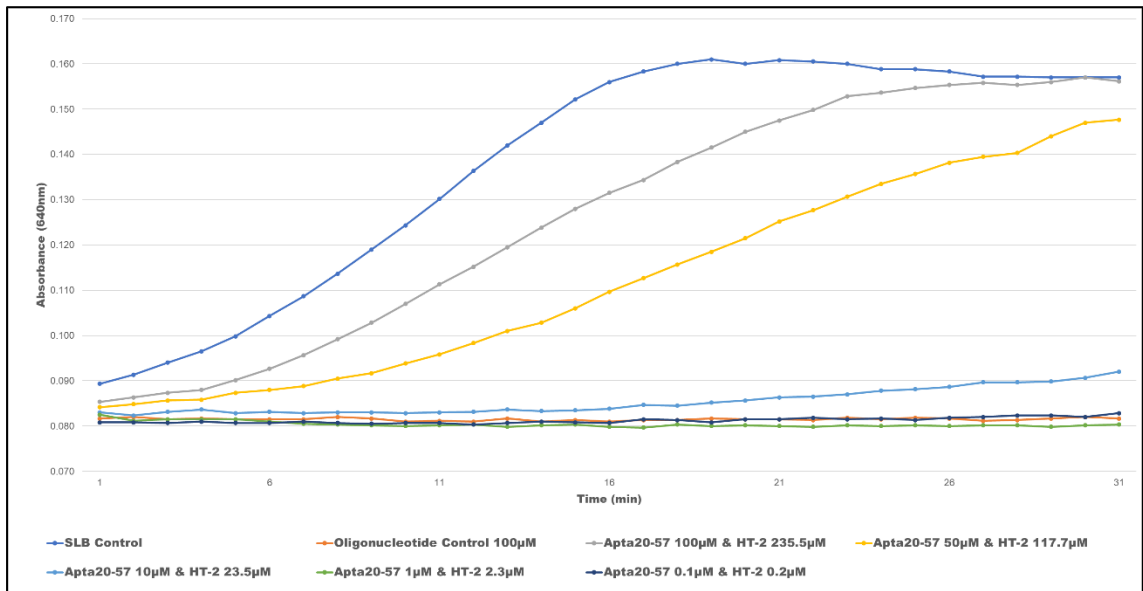
Figure 68 Absorbance curves (640nm) over time. Including SLB and oligonucleotide controls Samples of Apta20-57(100μM, 50μM, 10μM, 1μM, 0.1μM) incubated with 235.5μM, 117.7μM, 23.5μM, 2.3μM and 0.2μM HT-2 showing varying aggregation of AuNPs.
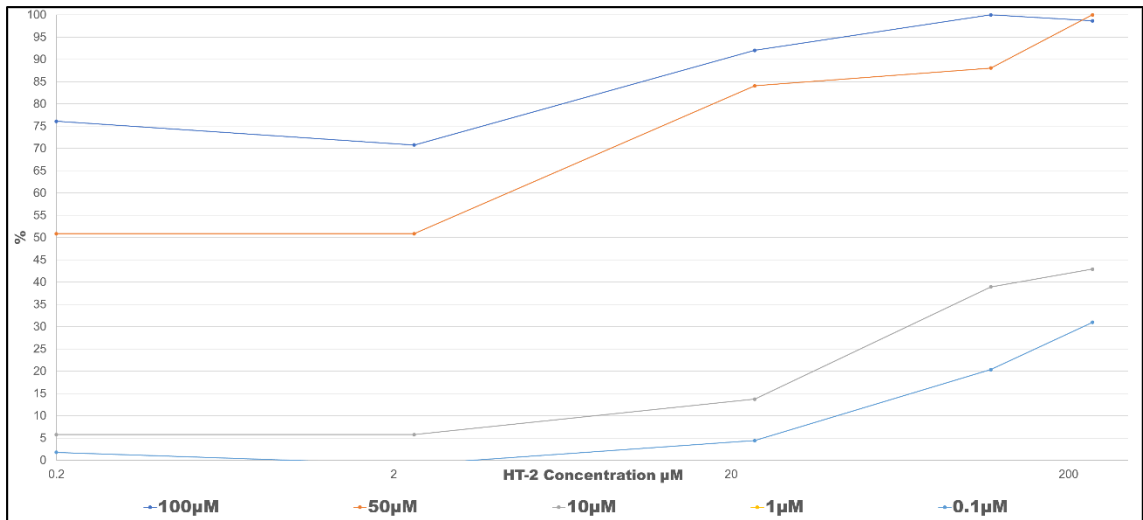
Figure 69 Calibration curve of % maximum absorbance values with baseline corrections of Apta20-57 at 100μM, 50μM, 10μM, 1μM and 0.1μM incubated with 235.5μM, 117.7μM, 23.5μM, 2.3μM and 0.2μM HT-2.

207

Apta20-90 checkerboard evaluation with T-2.
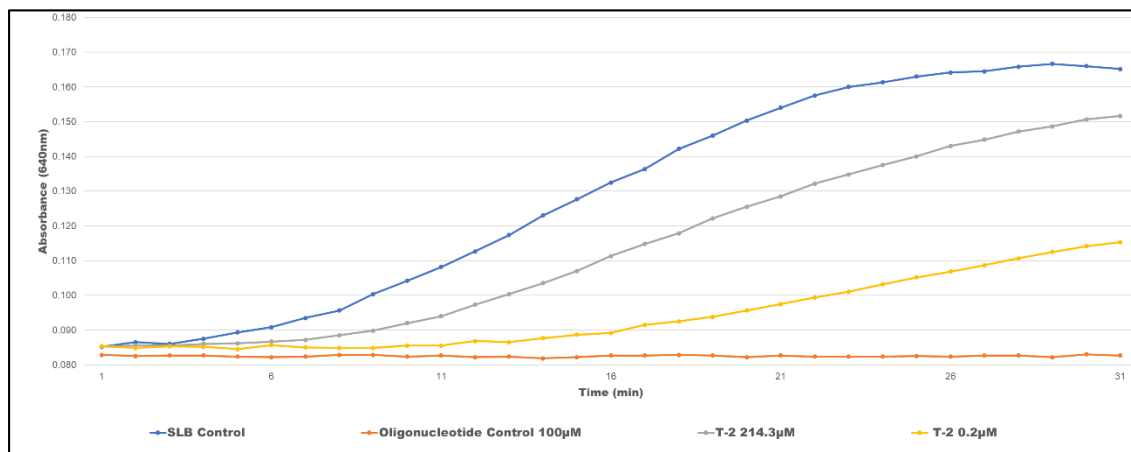
Figure 70 Absorbance curves (640nm) over time. Including SLB and oligonucleotide controls. Samples of Apta20-90 (100µM) incubated with 214.3µM and 0.2µM T-2.
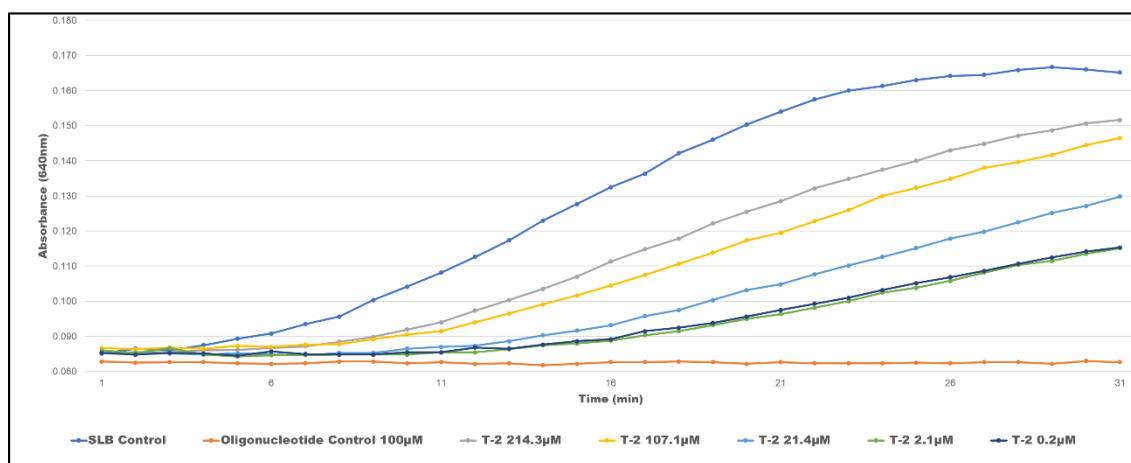
Figure 71 Absorbance curves (640nm) over time. Including SLB and oligonucleotide controls. Samples of Apta20-90(100µM) incubated with 214.3µM, 107.1µM, 21.4µM, 2.1µM and 0.2µM T-2.
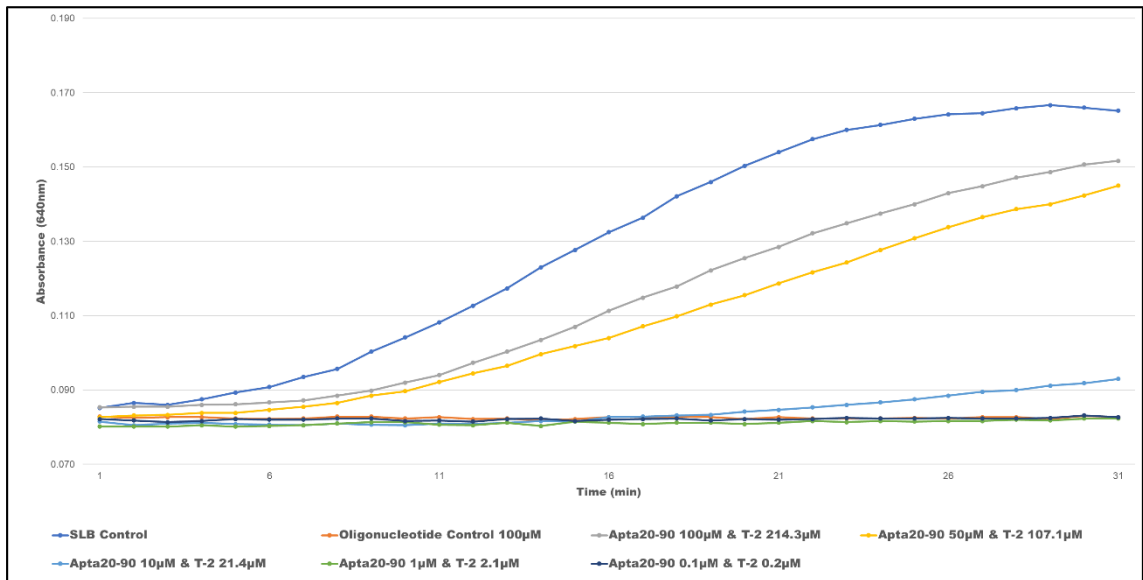
Figure 72 Absorbance curves (640nm) over time. Including SLB and oligonucleotide controls Samples of Apta20-90(100µM, 50µM, 10µM, 1µM, 0.1µM) incubated with 214.3µM, 107.1µM, 21.4µM, 2.1µM and 0.2µM T-2 showing varying aggregation of AuNPs.
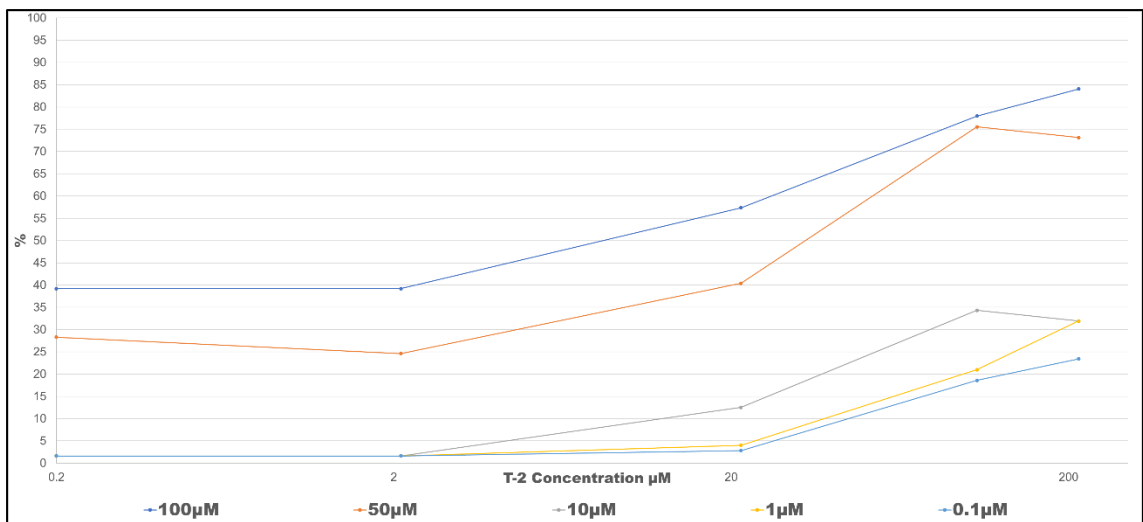
Figure 73 Calibration curve of % maximum absorbance values with baseline corrections of Apta20-90 at 100µM, 50µM, 10µM, 1µM and 0.1µM incubated with 214.3µM, 107.1µM, 21.4µM, 2.1µM and 0.2µM T-2.

Appendix I

Apta20-90 checkerboard evaluation with HT-2.
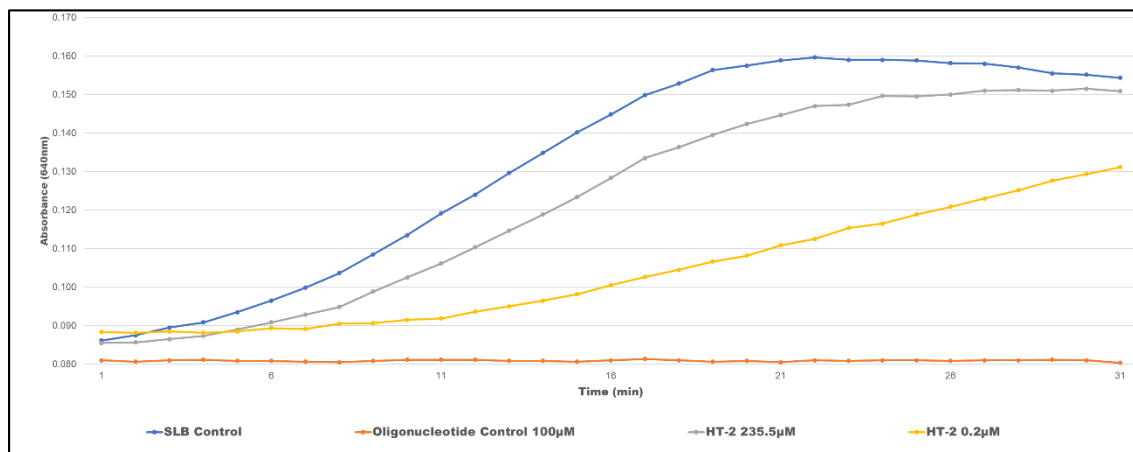
Figure 74 Absorbance curves (640nm) over time. Including SLB and oligonucleotide controls. Samples of Apta20-90 (100µM) incubated with 235.5µM and 0.2µM HT-2.
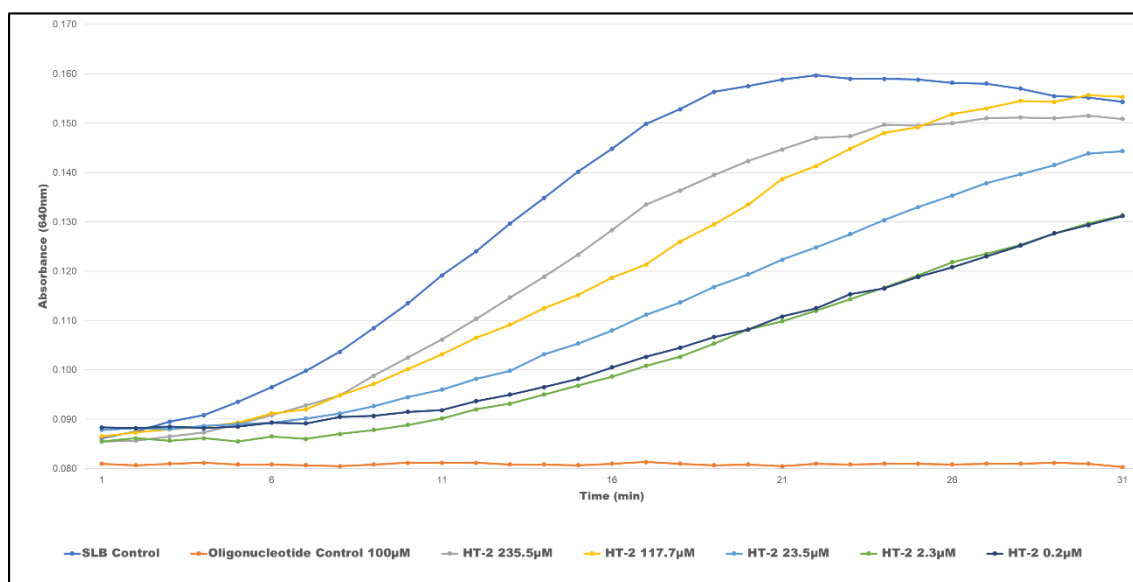
Figure 75 Absorbance curves (640nm) over time. Including SLB and oligonucleotide controls. Samples of Apta20-90(100µM) incubated with 235.5µM, 117.7µM, 23.5µM, 2.3µM and 0.2µM HT-2.
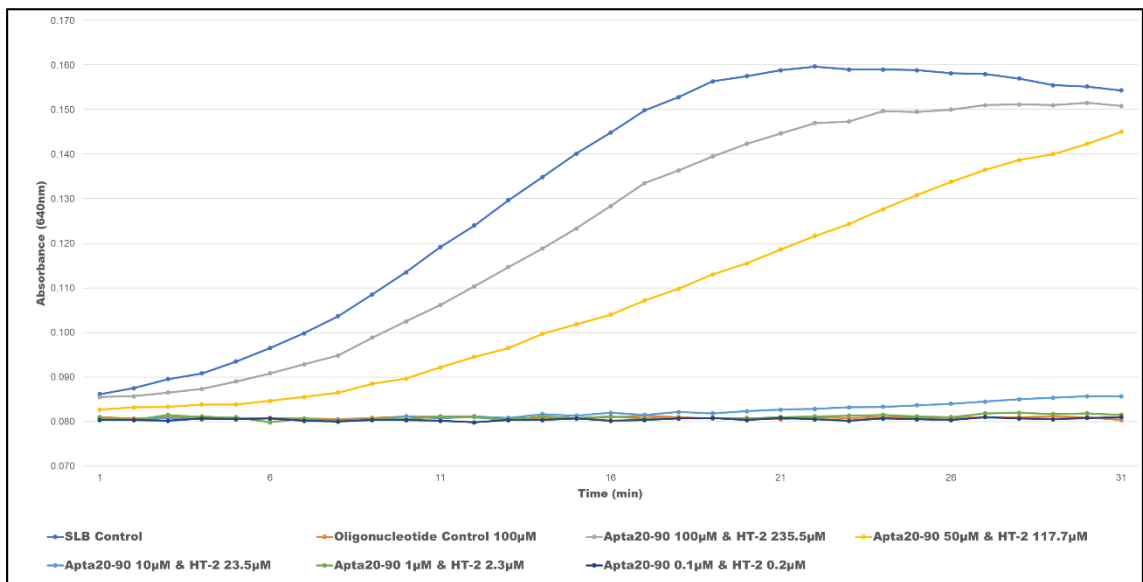
Figure 76 Absorbance curves (640nm) over time. Including SLB and oligonucleotide controls Samples of Apta20-90(100µM, 50µM, 10µM, 1µM, 0.1µM) incubated with 235.5µM, 117.7µM, 23.5µM, 2.3µM and 0.2µM HT-2 showing varying aggregation of AuNPs.
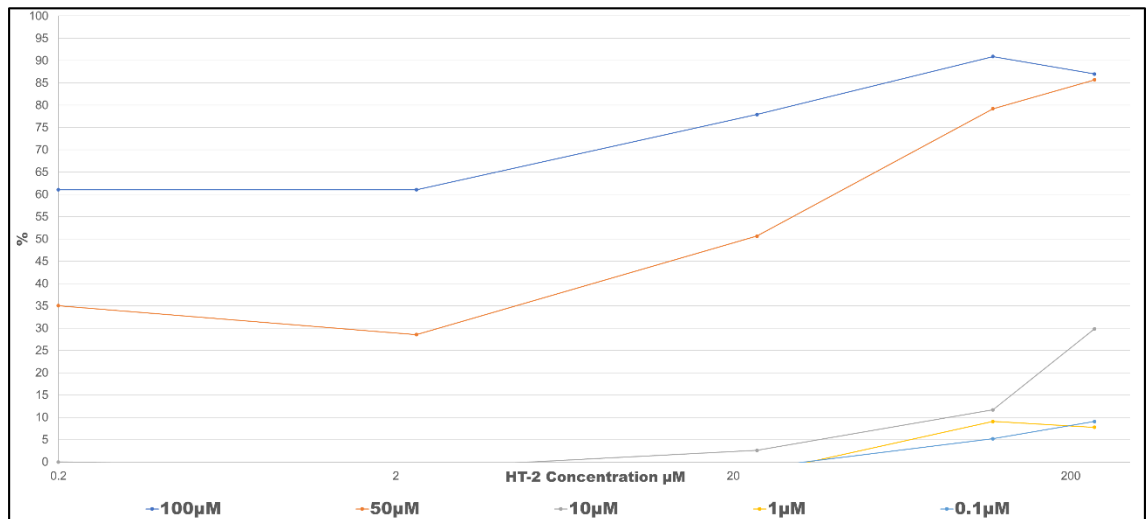
Figure 77 Calibration curve of % maximum absorbance values with baseline corrections of Apta20-90 at 100µM, 50µM, 10µM, 1µM and 0.1µM incubated with 235.5µM, 117.7µM, 23.5µM, 2.3µM and 0.2µM HT-2.

211

Appendix J

Apta20-100 checkerboard evaluation with T-2.
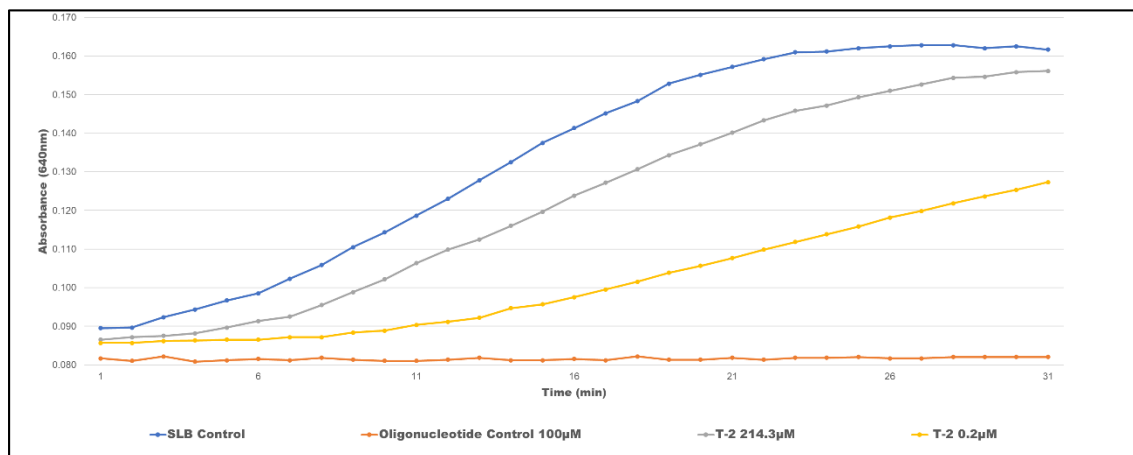
Figure 78 Absorbance curves (640nm) over time. Including SLB and oligonucleotide controls. Samples of Apta20-100 (100µM) incubated with 214.3µM and 0.2µM T-2.
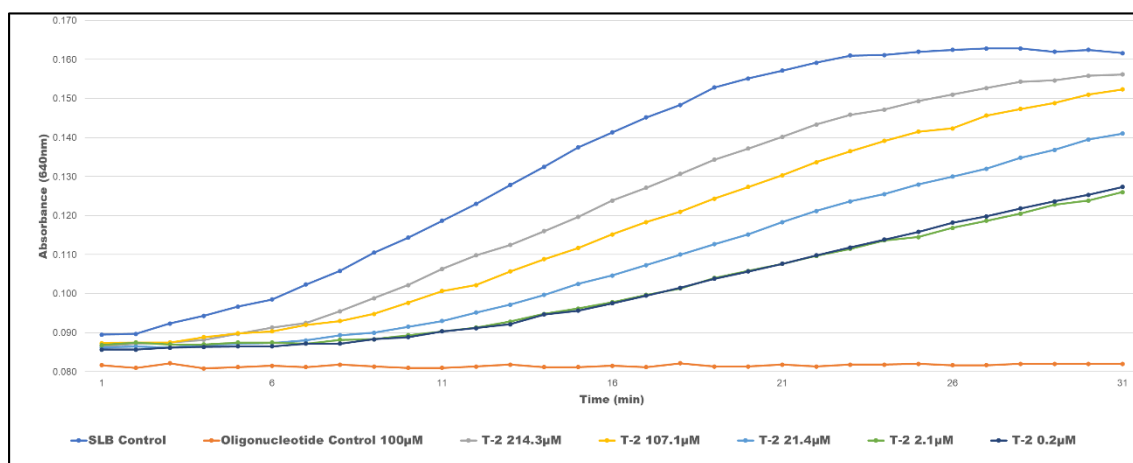
Figure 79 Absorbance curves (640nm) over time. Including SLB and oligonucleotide controls. Samples of Apta20-100(100µM) incubated with 214.3µM, 107.1µM, 21.4µM, 2.1µM and 0.2µM T-2.
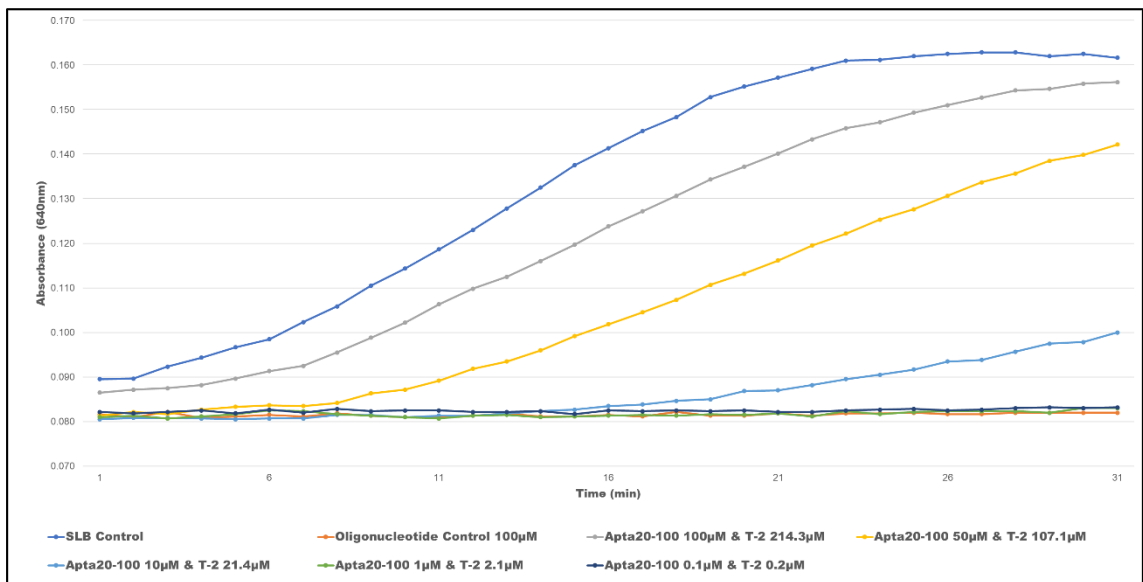
Figure 80 Absorbance curves (640nm) over time. Including SLB and oligonucleotide controls Samples of Apta20-100(100µM, 50µM, 10µM, 1µM, 0.1µM) incubated with 214.3µM, 107.1µM, 21.4µM, 2.1µM and 0.2µM T-2 showing varying aggregation of AuNPs.
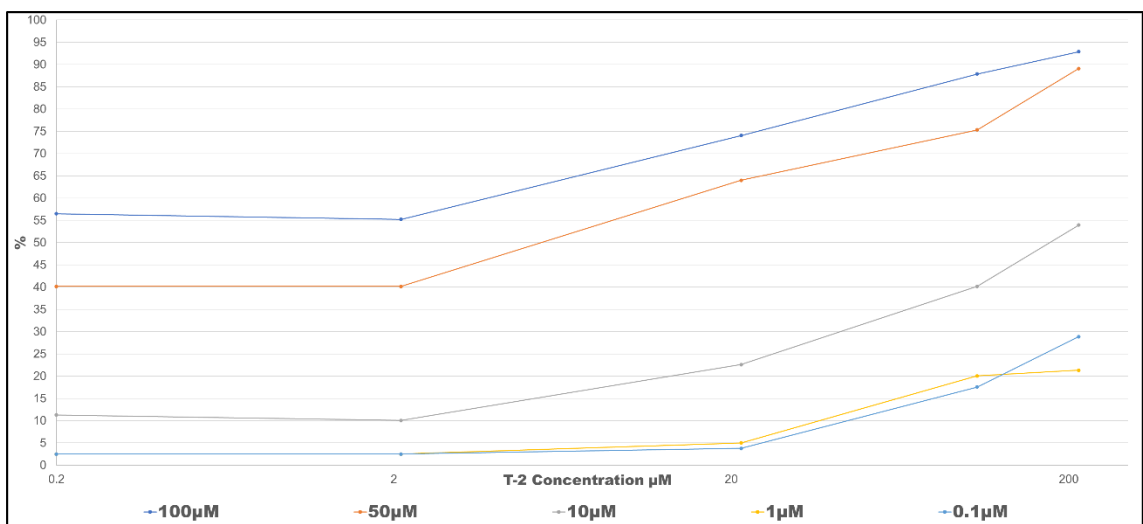
Figure 81 Calibration curve of % maximum absorbance values with baseline corrections of Apta20-100 at 100µM, 50µM, 10µM, 1µM and 0.1µM incubated with 214.3µM, 107.1µM, 21.4µM, 2.1µM and 0.2µM T-2.

213

Appendix K

Apta20-100 checkerboard evaluation with HT-2.
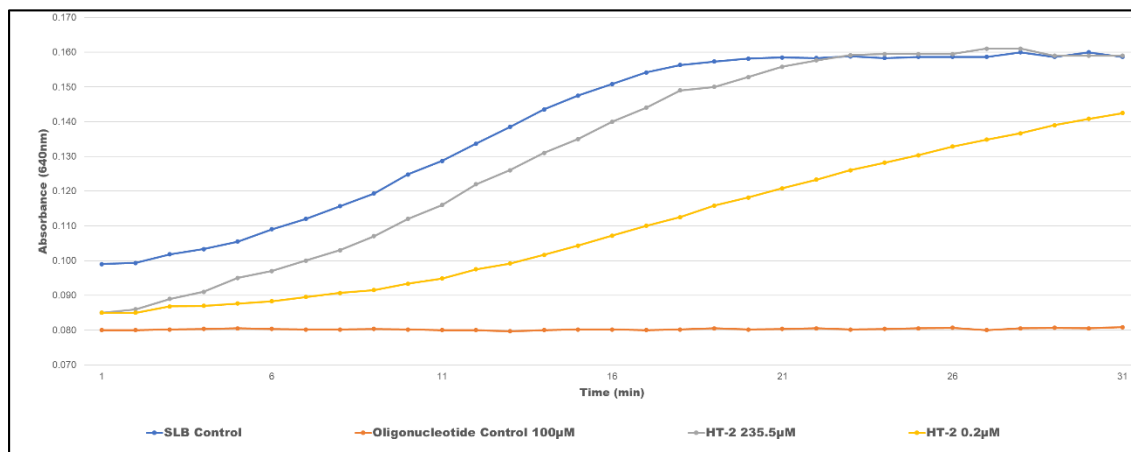
Figure 82 Absorbance curves (640nm) over time. Including SLB and oligonucleotide controls. Samples of Apta20-100 (100µM) incubated with 235.5µM and 0.2µM HT-2.
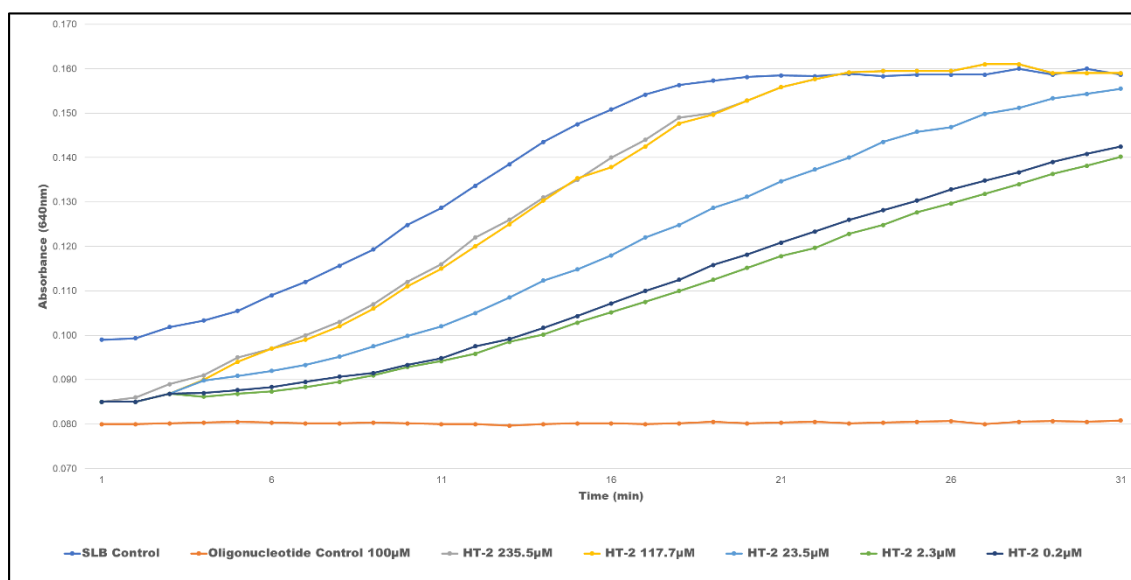
Figure 83 Absorbance curves (640nm) over time. Including SLB**Figure 84** Calibration curve of % maximum absorbance values with baseline corrections of Apta20-100 at 100µM, 50µM, 10µM, 1µM and 0.1µM incubated with 235.5µM, 117.7µM, 23.5µM, 2.3µM and 0.2µM HT-2.
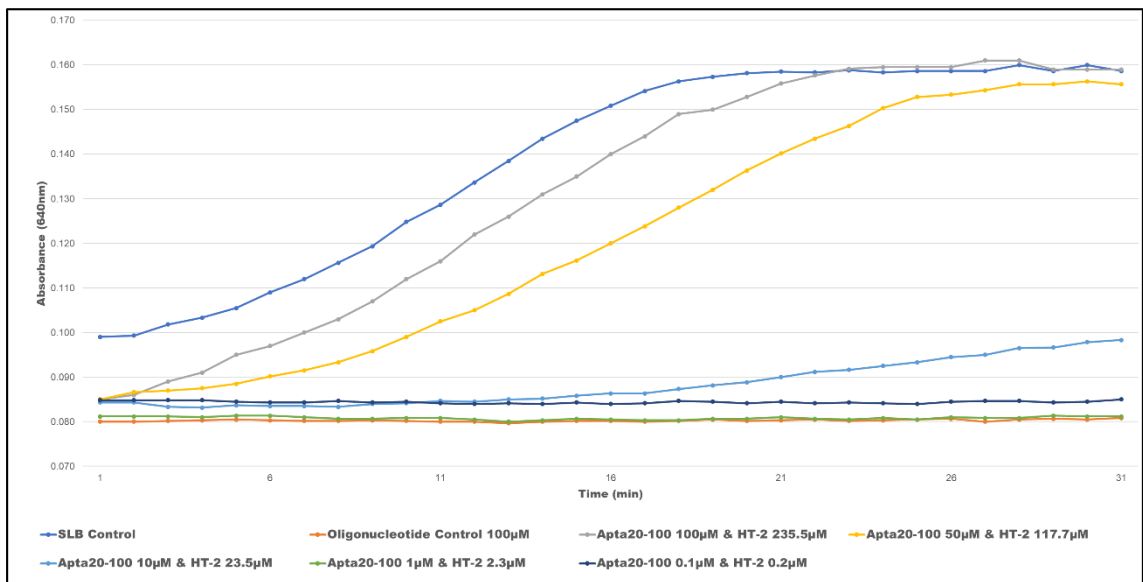
Figure 85 Absorbance curves (640nm) over time. Including SLB and oligonucleotide controls Samples of Apta20-100(100µM, 50µM, 10µM, 1µM, 0.1µM) incubated with 235.5µM, 117.7µM, 23.5µM, 2.3µM and 0.2µM HT-2 showing varying aggregation of AuNPs.
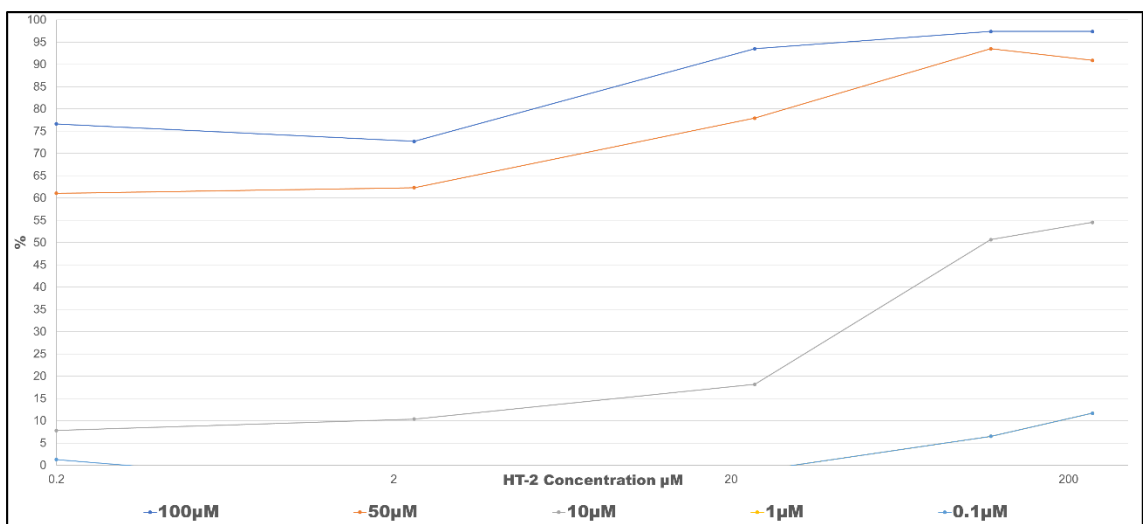
Figure 86 Calibration curve of % maximum absorbance values with baseline corrections of Apta20-100 at 100µM, 50µM, 10µM, 1µM and 0.1µM incubated with 235.5µM, 117.7µM, 23.5µM, 2.3µM and 0.2µM HT-2.

215